Mechanisms of foregut development and malformations

Adonis Ioannides

A thesis submitted for the degree of Doctor of Philosophy in the University of London

2005

Institute of Child Health
University College London
30 Guilford Street
London
WC1N 1EH

ProQuest LLC
789 East Eisenhower Parkway
P.O. Box 1346
Ann Arbor, MI 48106-1346

To Marilena, Estela and Isabella

ACKNOWLEDGEMENTS

This project could not have been possible without the help of three people. Professor Andy Copp has shown formidable commitment and true enthusiasm for the work, always finding time from his extremely busy schedule to discuss the experiments and their implications, as well as teach experimental techniques at the benchside. Professor Lewis Spitz ignited my interest in the study of the science of oesophageal atresia and tracheo-oesophageal malformations and has, throughout the work, kept in touch with the development of the project, always providing guidance based on his immense experience in the field. Dr Deborah Henderson's contribution has been central to this work. She essentially provided quality control by being constructively critical, ensuring the work would stand up to scientific scrutiny. She also taught me laboratory techniques and supervised the work closely. I am grateful to all the members of the Neural Development Unit for the useful tips on laboratory matters and specifically Patricia Ybot-Gonzales, Vicky Reed and Jenny Murdoch. I would also like to thank my Consultants at my clinical placements for allowing me the time and the opportunity to finish writing the thesis and specifically Ahmed Said for his contribution in that respect. Most importantly, I would like to thank my wife Marilena for her unwavering support, my daughters, Estela and Isabella, for making it all worthwhile and my parents, Savvas and Zoe for their guidance. Finally, I would like to thank the Wellcome Trust and the Medical Research Council for funding the work and making it all possible.

ABSTRACT

Oesophageal atresia (OA) and tracheo-oesophageal fistula (TOF) are important human malformations of the foregut, the development of which is poorly understood. In this thesis, the mechanisms that underlie the development of OA/TOF, as well as normal tracheo-oesophageal development, were investigated. The rat model of OA/TOF, based on exposure of embryos to the anticancer agent Adriamycin, was adapted to the mouse in order to allow more in depth study of the cellular and molecular events that underlie the malformations. The Adriamycin-treated mouse was shown to have persistence of an undivided foregut at E11.5, in contrast to saline controls in which the foregut was in the process of separating into a ventral structure (trachea) and a dorsal structure (oesophagus). This failure of tracheo-oesophageal separation was also a feature of the *Sonic hedgehog* (*Shh*) null mutant mouse. The study of the respiratory marker Nkx2.1 confirmed that the foregut normally divides along the dorsoventral boundary of respiratory/ gastrointestinal specification and that the fundamental defect in both the Adriamycin-treated and *Shh* null mutant mice is persistence of an undivided foregut in which both the respiratory and gastrointestinal lineages are represented, with a preservation of the dorsoventral pattern of expression of that marker. The study of expression of *Shh* showed this to have a dorsoventral pattern that was closely related to the separation boundary and which changed as separation progressed. Moreover, this dorsoventral expression pattern was disturbed in those Adriamycin-treated embryos that had failed to separate the trachea and oesophagus. The process of tracheo-oesophageal separation was also found to be associated with a distinct pattern of programmed cell death (PCD) in the dorsal foregut and at the dorsoventral boundary. PCD cells were present before any morphological evidence of separation, suggesting a possible role for

PCD in controlling the separation process. When a PCD inhibitor was applied to an *in vitro,* whole embryo, culture system, the process of tracheo-oesophageal separation was arrested, suggesting that PCD is a requirement and not just a consequence of separation.

ABBREVIATIONS

ABC = avidin-biotin peroxidase complex

Aip = anterior intestinal portal

BCIP = 5-bromo-4-chloro-3-indoyl-phosphate

cDNA = complementary deoxyribonucleic acid

Cip = caudal intestinal portal

DAB = diaminobenzadine tetrahydrochloride

DEPC = diethylpyrocarbonate

DIG = Digoxygenin

DMEM = Dulbecco's Modified Eagles Medium

DMSO = dimethyl sulphoxide

DNA = deoxyribonucleic acid

DPX = dextropropoxyphene

E = embryonic day

EDTA = ethylenediamine-tetra-acetic acid

FCS = fetal calf serum

HCl = hydrochloric acid

IMS = industrial methylated spirits

JPEG = Joint Photographic Experts Group

LiCl = lithium chloride

MilliQ = ultrapure-deionised water

MilliRO = deionised water

mRNA = messenger RNA

NBT = 4-nitroblue tetrazolium chloride

OA = oesophageal atresia

PBS = phosphate buffered saline

PCD = programmed cell death

PFA = paraformaldehyde

RNA = ribonucleic acid

Rnase = ribonuclease

SDS = sodium dodecyl sulphate

Shh = sonic hedgehog

SSC = sodium chloride/ sodium citrate buffer

TBS-TX = Tris buffered saline/Triton-X100

TESPA = 3-aminopropyltriethoxy silane

TOF = tracheo-oesophageal fistula

TUNEL = TdT-mediated dUTP nick end labelling

zVAD-fmk = benyloxycarbonyl-valine-alanine-aspartate fluoromethylketone

TABLE OF CONTENTS

LIST OF TABLES

LIST OF FIGURES

CHAPTER 1 – GENERAL INTRODUCTION

1.1 – DEVELOPMENT OF THE FOREGUT AND ITS DERIVATIVES

1.1.1 – Gastrulation

Gastrulation is the process by which the cells of the early embryo are allocated to the three principal germ layers: ectoderm, mesoderm and endoderm. The ectoderm gives rise to the skin and central nervous system, the mesoderm to muscle, bone and blood and the endoderm to the digestive tract and a variety of other organs. These endodermally-derived structures include organs associated with the digestive tract such as the liver and pancreas and others that serve a diverse range of functions such as the respiratory tract, thyroid gland, thymus and the tympanic cavities. Gastrulation takes place during the third week of development of the human embryo. The cells of the three germ layers are derived from the totipotent cells of the epiblast. The ectoderm is derived from epiblast cells that do not migrate. The mesoderm and definitive endoderm are derived from epiblast cells that migrate through the primitive streak, a midline structure in the epiblast at the posterior end of the bilaminar germ disc (Fig. 1.1a,b). Mapping of cells passing through the primitive streak has shown that cells of the definitive endoderm are derived from the anterior primitive streak (Lawson et al., 1991). Following their migration, these cells displace the cells of the visceral endoderm (hypoblast) (Lin et al., 1994). The visceral endoderm forms the yolk sac and does not contribute to the development of the gut, apart from some limited regions at the extreme anterior end and extreme posterior end of the foregut. The migration of epiblast cells through the primitive streak has been shown to be dependant on FGF receptor-1 (FGFR1) function in the mouse. Embryos lacking FGFR1 function have defects in the endoderm and anterior mesoderm (Ciruna et al., 1997).

1.1.2 – Specification of the definitive endoderm

The mechanisms that underlie the specification of endodermal fate are not well understood. One important question that needs to be addressed is the temporal relationship between the migration through the primitive streak and endodermal specification. It is possible that the fate of epiblast cells is determined before migration. Fate mapping studies showing that anterior primitive streak cells contribute to the endoderm are consistent with this hypothesis (Lawson et al., 1991; Lawson et al., 1986). Furthermore, the transcription factor and endodermal marker *Hnf3β* is expressed in epiblast cells at the anterior tip of the primitive streak at the very early primitive streak stage (Ang et al., 1993). Alternatively, epiblast cells might become specified during their migration through a specific part of the primitive streak. This theory is supported by the observation that some epiblast cells start expressing *Fgf3* as they exit the primitive streak and become committed to a mesodermal fate (Niswander & Martin, 1992). It is even possible that cells acquire their fate only after their migration. The molecular signals involved in the specification process are not well understood. Studies in frogs have identified a signaling pathway involving the genes *Mixer* and *(Sox)17α/β* that can drive endoderm formation (Henry & Melton, 1998; Hudson et al., 1997). It has been shown that *Mixer* function is required for the expression of *(Sox)17α/β* which in turn mediate an activin-induced endoderm differentiation pathway. In the zebrafish, embryos that have a loss-of-function mutation for the locus *casanova* do not form a gut tube and lack any endodermal differentiation with absence of expression of early endodermal markers (Alexander et al., 1999). There is, however, no evidence of a role for these genes in mice or other higher vertebrates. Certain growth factors, including members of the *Fgf* family, have been associated with primitive streak formation and patterning in higher vertebrate embryos, but not with endodermal specification itself.

1.1.3 – General endodermal patterning

Following gastrulation, but before the flat sheet of definitive endoderm has folded to form the gut tube, the process of endoderm patterning takes place. The result of this process is the establishment of an anteroposterior axis in the endoderm, in line with a similar axis in the other two germ layers. The anteroposterior axis of the embryo has already been established by the formation of the primitive streak at its caudal end. The migration of cells through the primitive streak initiates endodermal anteroposterior patterning, as those that first migrate through the streak contribute to the anterior endoderm, whereas later migrating cells are directed towards the posterior endoderm (Lawson & Pedersen, 1987). Anteroposterior patterning of the endoderm is reflected in differential gene expression, with the establishment of anteroposterior boundaries for certain factors. Anterior endodermal markers include *Hesx1* (Thomas & Beddington, 1996) and *Otx1* (Rhinn et al., 1998), whereas posterior markers include *Cdx2* (Beck et al., 1995) and *IFABP*. The exact mechanisms that underlie this differential expression are poorly understood, but one possibility is that it relies on signals from the adjacent, already specified, mesoderm and ectoderm. There is also evidence that factors expressed in the early (visceral) endoderm have an indirect effect on patterning of the definitive endoderm by influencing gene expression on adjacent endoderm. Lineage tracing studies have demonstrated that the anterior marker *Hesx1* is first expressed in the anterior primitive endoderm before the onset of gastrulation. These cells are replaced by migrating epiblast cells during gastrulation and the cells of the definitive anterior endoderm also express *Hesx1*. The anterior pattern may be relayed from primitive to definitive endoderm by the adjacent anterior neuroectoderm, which also expresses *Hesx1* (Thomas & Beddington, 1996).

1.1.4 – Formation of the gut tube from a sheet of cells

A series of morphogenetic movements converts the flat endodermal layer into the primitive gut tube. In the mouse and chicken embryos, this process involves the formation of two crescent-shaped folds at the anterior and posterior tips of the embryo, known as the anterior intestinal portal (Aip) and caudal intestinal portal (Cip) (Fig. 1.1c). The Aip moves posteriorly, whereas the Cip moves anteriorly, with the two folds meeting at the yolk stalk, which provides an entrance into the yolk sac. Embryonic turning, which is the process in which a change of embryo configuration brings the anterior and posterior tips of the embryo closer together, leads to the convergence of the two portals (Fig. 1.1c). Embryonic turning is a feature of mouse development and does not occur in the chicken. The folding of the endoderm in a lateral to ventral direction also contributes to formation of the primitive gut tube (Fig. 1.1d). The processes of lateral to ventral and rostral-to-caudal folding of the gut have a bearing on the establishment of a dorsoventral (DV) axis in the gut tube. The cells of the anterior endoderm contribute to the ventral gut rostral to the yolk sac whereas the cells of the posterior endoderm contribute to the ventral gut caudal to the yolk sac. The dorsal part of the gut tube is derived from the original midline endoderm. The transcription factor *GATA4*, which is expressed in the endoderm and mesoderm of the Aip and the endoderm of the yolk sac, plays an important role in embryonic folding with *GATA4-/-* embryos displaying severe disruption of the ventral body pattern as a result of failure of both lateral-to-ventral and rostral-to-caudal folding (Molkentin et al., 1997; Kuo et al., 1997). Bone morphogenetic proteins (Bmps) 2,4,5 and 7 are also expressed in the Aip and contribute to ventral convergence and ventral closure.

Fig. 1.1 The formation of the endodermal cell layer and gut tube

Schematic representations of gastrulation (a,b) and embryonic folding (c,d). **(*a*)** The primitive streak (Ps) is a midline structure that appears in the epiblast (Eb) at the caudal end of the bilaminar germ disc. It comprises the primitive groove (Pg) and a depression at its rostral end, the primitive pit (Pp). **(*b*)** The bilaminar germ disc is seen in cross section at the level of the primitive streak as indicated by the dotted line in (*a*). During gastrulation, epiblast cells migrate through the primitive streak and either displace the original cells of the hyboblast (Hb) in the midline to form the definitive endoderm (double arrowheads) or occupy the space between the two original germ layers (arrowheads) to form the mesoderm. **(*c*)** The formation of the gut tube involves the development of two crescent-shaped folds in the endoderm at the two ends of the embryo. The anterior intestinal portal (Aip) grows posteriorly and caudal intestinal portal (Cip) moves anteriorly (double arrowheads). In the mouse, Aip and Cip movements are minimised by the dorsal concavity of the embryo. The two endodermal folds meet at the yolk stalk (Ys), which leads into the yolk sac. Embryonic turning (arrows) contributes to the convergence of the two endodermal folds. Following this rostrocaudal folding, the anterior endoderm will come to represent the ventral endoderm rostral to the yolk sac (orange line) and the posterior endoderm the ventral endoderm caudal to the yolk sac (green line). **(*d*)** Seen in cross section, lateral to ventral endodermal folding (arrows) also contributes to the formation of the gut tube. As a result of this folding, the original midline endoderm (blue lines) will from the dorsal endoderm. En – endoderm, A – anterior, P – posterior, V – ventral, D - dorsal

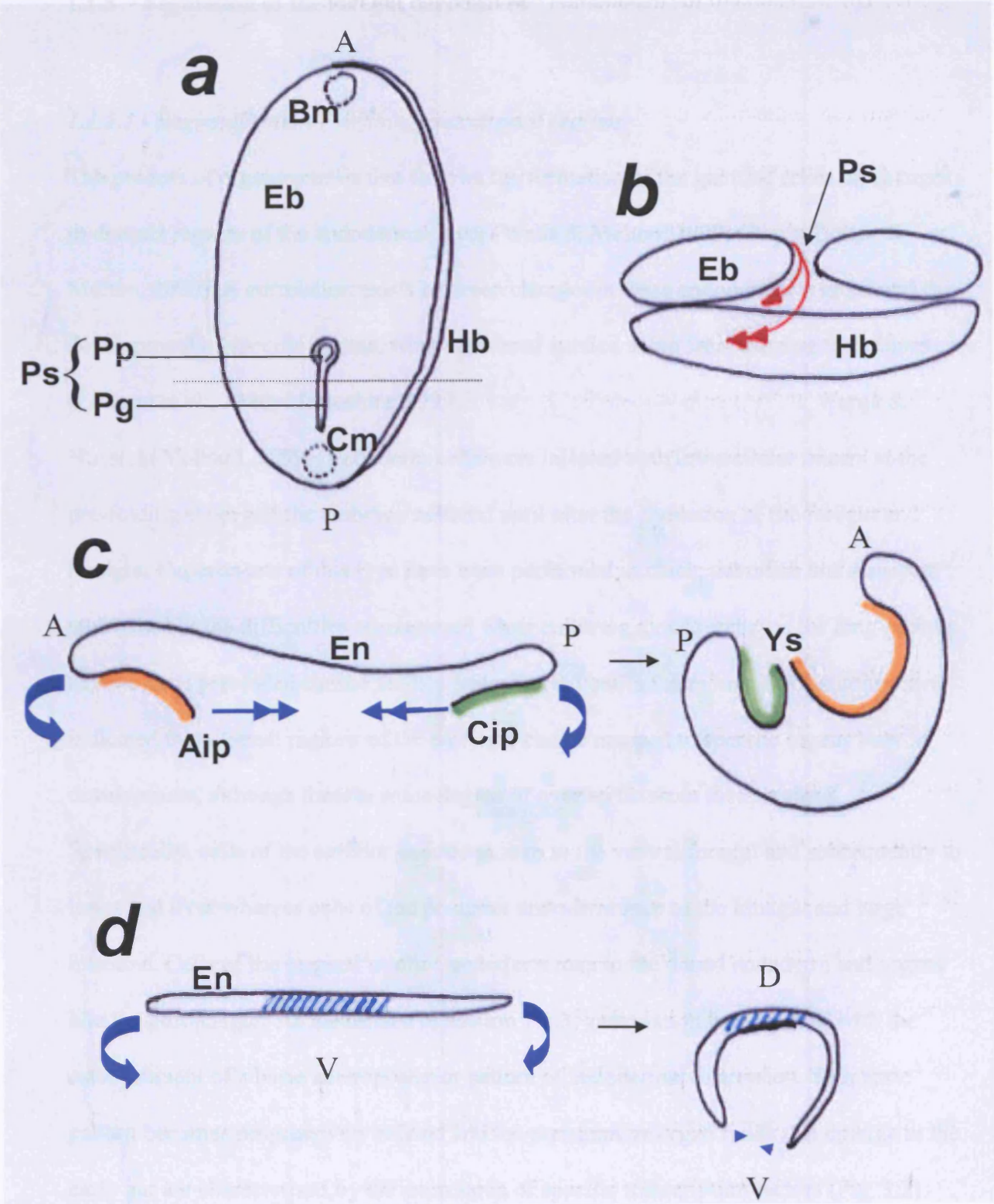
a
A
Bm
Eb
Hb
Ps
Pp
Pg
Cm
P
b
Ps
Eb
Hb
c
A
En
P
Aip
Cip
P
Ys
A
d
En
V
D
V

1.1.5 – Formation of the foregut derivatives

1.1.5.1 - Regionalisation – defining endodermal regions

The process of organogenesis that follows the formation of the gut tube relies on changes in distinct regions of the endodermal layer (Wells & Melton, 1999; Grapin-Botton & Melton, 2000). A correlation exists between changes in these endodermal regions and the development of specific organs, which has been studied using fate-mapping techniques (Lawson et al., 1986; Matsushita, 1999; Warga & Nusslein-Volhard, 1999). Endoderm cells were injected with intracellular tracers at the pre-folding stage and the embryos cultured until after the formation of the foregut and hindgut. Experiments of this type have been performed in chick, zebrafish and *Xenopus* embryos, but the difficulties encountered when culturing mouse embryos for long periods of time have precluded similar studies being carried out in the mouse. Such studies have indicated that distinct regions of the early gut can be mapped to specific organs later in development, although there is some degree of overlap between these regions. Specifically, cells of the anterior endoderm map to the ventral foregut and subsequently to lungs and liver whereas cells of the posterior endoderm map to the hindgut and large intestine. Cells of the original midline endoderm map to the dorsal endoderm and organs like the oesophagus. As mentioned in section 1.1.3, gastrulation is associated with the establishment of a basic anteroposterior pattern of endodermal expression. This basic pattern becomes progressively refined and the presumptive organ fields that emerge in the early gut are characterised by the expression of specific transcription factors (Fig. 1.2).

Fig. 1.2 Derivatives of the foregut endoderm and regional expression of transcription factors in the endoderm

Schematic representation of the foregut and its derivatives. The foregut endoderm gives rise to the pharynx (Ph), oesophagus (Oe), stomach (St) and duodenum (Du). In addition to these parts of the gastrointestinal tract, a number of organs bud off the main gut tube. Organ budding and cytodifferentiation are associated with region-specific expression of endodermal transcription factors. In the pharynx, the thyroid gland (Thr) develops from a ventral midline evagination before assuming its position in the neck. Thyroid development is associated with expression of *Nkx2.1* (*Ttf1*) and *Foxe1* (*Ttf2*). The pharyngeal pouches (Php) are paired, lateral evaginations of the pharyngeal endoderm and give rise to the external auditory canal (1^{st}), tonsils (2^{nd}), inferior parathyroid and thymus (Thm) (3^{rd}), superior parathyroid (4^{th}) and ultimobranchial body (5^{th}). The thyroid gland and the derivatives of pouches 3 to 5 lose their original connection to the gut tube as shown by the dotted lines. The development of these pouch derivatives is associated with the expression of *Pax9* and *Hoxa3* with *Pax1* being an additional thymus-specific marker. The respiratory system comprising the trachea (Tr), bronchial structures (Br) and lungs (Lu) is associated with the expression of *Nkx2.1*, *Irx1* and *Irx2*. The liver (Li) and pancreas (Pa) also maintain their connection to the gut tube and are associated with expression of *Hex1* and *Hnf6* (liver) and *Hes1, Pdx1* and *Hlxb9* (pancreas). There is some anteroposterior overlap in gut tube expression of transcription factors. The oesophagus is associated with *Sox2* expression, the stomach with expression of *Sox2*, *GATA4* and *Tcf4* and the duodenum with expression of *Tcf4* and *Pdx1*.

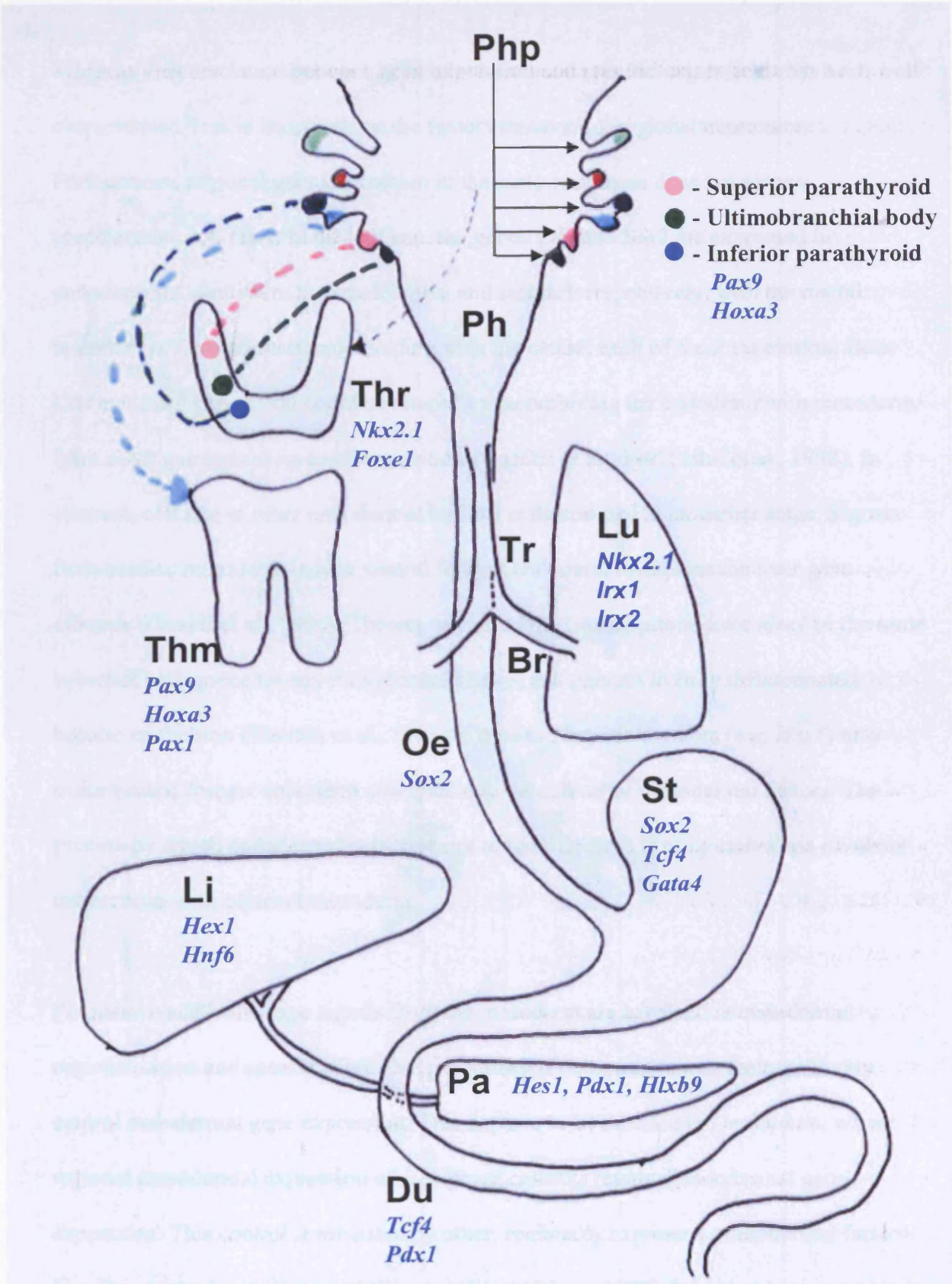
Php
- Superior parathyroid
- Ultimobranchial body
- Inferior parathyroid
Pax9
Hoxa3
Ph
Thr
Nkx2.1
Foxe1
Tr
Lu
Nkx2.1
Irx1
Irx2
Thm
Pax9
Hoxa3
Pax1
Br
Oe
Sox2
St
Sox2
Tcf4
Gata4
Li
Hex1
Hnf6
Pa
Hes1, Pdx1, Hlxb9
Du
Tcf4
Pdx1

Whereas the correlation between gene expression and specific organ fields has been well characterised, less is known about the factors that control regional expression. Furthermore, regional gene expression in the early endoderm does not always predetermine cell fates. In the chicken, the genes *Cdx* and *Sox2* are expressed in endoderm that will form the small bowel and stomach respectively, with the rostral boundary of *Cdx* expression coinciding with the caudal limit of *Sox2* expression. Both *Cdx* and *Sox2* expression could be altered by recombining the endoderm with mesoderm from other gut regions up to embryonic day 4 (Ishii et al., 1997; Ishii et al., 1998). In contrast, cell fate in other endodermal regions is determined at an earlier stage. Signals from cardiac mesoderm induce ventral foregut endoderm to express the liver gene *albumin* (Gualdi et al., 1996). The expression of the transcription factor *Hex1* in the same subset of cells precedes any mesodermal signals and persists in fully differentiated hepatic epithelium (Thomas et al., 1998). These pre-hepatic markers (e.g. *Hex1*) may make ventral foregut endoderm susceptible to the effects of mesodermal factors. The process by which endodermal cells commit to specific fates is progressive and involves interactions with adjacent mesoderm.

Permissive and instructive signals from the mesoderm are involved in endodermal regionalisation and specification. One possibility is that mesodermal factors directly control endodermal gene expression. This appears to be the case in *Drosophila*, where regional mesodermal expression of *Hox* genes controls regional endodermal gene expression. This control is mediated by other, regionally expressed, mesodermal factors like Decapentaplegic (Dpp) and Wingless (Wg) (Bienz, 1997). It has not been possible to demonstrate a similar pattern in vertebrate embryos, even though *Hox* genes are known to have anteroposterior patterns of expression in all three germ layers (Bilder & Scott,

1998). There is evidence that endodermal factors like *Shh* control mesodermal expression of some *Hox* genes (Roberts et al., 1998). Some *Hox* genes expressed in the endoderm share anteroposterior expression boundaries with some organ specific endodermal signals like the pancreatic specific *Pdx1*. It is also possible that factors that originate in the endoderm themselves provide positional information for gene expression in neighbouring endodermal cells.

1.1.5.2 - Organ budding

Regionalisation and early gut tube patterning are followed by a process of cytodifferentiation of the gut endoderm. This morphological differentiation leads to the development of the columnar epithelium that will line the gastrointestinal tract.
In addition to giving rise to the gastrointestinal epithelium, the gut endoderm will form a number of diverse organs that will bud off the main gut tube. The organs derived from the foregut include the thyroid and parathyroid glands, the thymus and ultimobranchial body (the precursor of the calcitonin-producing cells of the thyroid), the respiratory system, the external auditory canal, the pancreas, liver and gall bladder.

The first sign of development of these organs is localised thickening of the epithelium. The thyroid, respiratory system, liver and gallbladder all originate from subsets of ventral endodermal cells whereas the pancreas has a dorsal origin. In contrast, the auditory canal, thymus, parathyroids and the ultimobranchial body are derived from the endoderm of lateral evaginations of the foregut in the region of the pharynx known as pharyngeal pouches. The organs can either become completely separated from the main gut tube (thyroid, thymus, parathyroids, ultimobranchial body) or maintain a connection (respiratory system, liver, gallbladder and pancreas). As described in section 1.1.5.1,

epithelial thickening and the emergence of organ buds are associated with the expression of genes that are specific for that organ. Whereas the precise signals that control the expression of these genes or the budding process itself are not well understood, these organ specific factors are required for the budding process to proceed. The transcription factor *Nkx2.1* is expressed in the thyroid and respiratory primordia and a loss of function mutation in this gene results in agenesis of the thyroid gland and profound respiratory hypoplasia (Minoo, 2000; Yuan et al., 2000; Minoo et al., 1999). Similarly, mutation in the paired box gene *Pax 9*, which is expressed in the endoderm of the pharyngeal pouches, leads to agenesis of pharyngeal pouch derivatives (Peters et al., 1998). Expression of the transcription factor *Pdx1* in the dorsal foregut endoderm is also required for the development of the dorsal pancreatic bud (Wilding & Gannon, 2004; Edlund, 1998).

1.1.5.3 - Definitive organogenesis

Following the specification of organ forming fields and the emergence of organ buds, definitive organogenesis is the result of a complex choreography of cellular processes including cell proliferation, cell death and variations in cell adhesion and cell mobility. Cell proliferation contributes to organ development in two ways. Firstly, general cellular proliferation is responsible for the overall growth of an organ. For example, mice with a loss of function mutation for genes controlling epithelial cell proliferation in the liver (e.g. hepatocyte growth factor) exhibit a normally specified and differentiated liver which is, however, significantly smaller in size (Zaret, 1998). As is the case with endodermal field specification, epithelial/ mesenchymal interactions play a central role in the control of cell proliferation. Examples include the mitogenic effect of the secreted endodermal factor Shh on the lung mesenchyme, and the effect of growth factors such as fibroblast

growth factors (FGF) and epidermal growth factors (EGF) on epithelial cell proliferation. Furthermore, factors originating in the endoderm also have an effect on the proliferation of endodermal cells. An example is the pancreatic transcription factor Pdx1 which controls the proliferation of pancreatic endocrine cells (Wilding & Gannon, 2004). Loss of function mutations in *Pdx1* leads to arrest of pancreatic development at a very early stage (Ahlgren et al., 1996).

Cell proliferation also plays a role in shaping the developing organs, with differential cell proliferation in different subsets of endodermal cells. An example is provided by the process of branching morphogenesis in the developing lung buds during which the epithelium at the tips of the lung buds grows at a higher rate than the rest of the endoderm. The result of this is lengthening of the bronchial structures and the establishment of an elaborate conducting system (Goldin et al., 1984; Goldin & Wessells, 1979; Bellusci et al., 1997a; Bellusci et al., 1997b).

Programmed cell death plays an important role in organ development (Jacobson et al., 1997). It contributes to sculpting as demonstrated by the elimination of cells between the developing digits (Milligan et al., 1995), the hollowing out of solid structures to create a lumen (Coucouvanis & Martin, 1995) and in the invagination and fusion of epithelial sheets (Cuervo et al., 2002). It is also involved in deleting vestigial structures, adjusting cell numbers (Barde, 1989) and eliminating abnormal cells (Clarke et al., 1993).

Cell movement and the rearrangement of cellular architecture is central to the development of many endodermal organs and in particular to the development of the

endodermal glands. The ability of cells to become associated and adhere to other neighbouring cells is known as cell adhesion and plays a role in many developmental processes. Cell adhesion is mediated by molecules that are expressed on the cell surface and which establish interactions with similar molecules on neighbouring cells. The cadherins are an important family of cell adhesion molecules. Specifically, the epidermal cadherin (E-cadherin) is expressed on the surface of all budding endodermal cells suggesting that it plays a role in the budding process (Levi et al., 1991; Thiery et al., 1984). Another process involved in organ formation is the establishment of a pattern of attractive and repulsive cues that direct growth and branching. One such mesenchymal factor is Fgf10 which provides attractive cues to proliferating epithelial cells .

1.1.5.4 - Differentiation of organ-specific cell types within the developing organ buds

Cellular differentiation in developing endodermal organs is a gradual process, with cellular differentiation markers being expressed early in endodermal regionalisation and a gradual commitment of cells to a specific fate according to reciprocal interactions with surrounding cells. Gene inactivation studies have demonstrated the role of specific factors within organ forming fields. For example, inactivation of *Pax8* leads to failure of development of the thyroxine producing follicular cells of the thyroid, which are a specific subset of the cells of the thyroid (Kang et al., 2001). On the other hand, inactivation of the respiratory-specific transcription factor *Nkx2.1* leads to failure of development of all pulmonary cell types (Yuan et al., 2000; Minoo et al., 1999). Interestingly, *Nkx2.1*, which is expressed in the entire respiratory primordium at early stages of development (E9 in the mouse), gradually becomes restricted to a specific subset of pulmonary cells (type II pneumocytes) (Minoo et al., 1999). This probably suggests that the cells within an organ-forming field are initially pluripotent and become

gradually specified to a specific role. The signals that dictate this transition, as well as the changes in the receptiveness of endodermal cells to these signals, are not well understood. Available evidence suggests that these signals originate in the mesenchyme. In the case of the pancreas, which consists of both endocrine and exocrine cell populations, it has been shown that inactivation of the mesenchymal factor *Isl1* leads to failure of exocrine development (Apelqvist et al., 1997). Finally, as is the case with most epithelial mesenchymal interactions, the endoderm also plays a role in mesodermal specification, with the secreted endodermal glycoprotein Shh controlling muscular differentiation in the cells of the mesoderm that are arranged around the gut epithelium.

1.2 – DEVELOPMENT OF THE TRACHEA AND THE OESOPHAGUS

1.2.1 – The morphology of respiratory development

Development of the respiratory system begins in the mouse on embryonic day (E) 9.5 (day 19 in the human) with the appearance of the laryngo-tracheal groove (the primordium of the subglottic larynx and trachea) in the ventral floor of the anterior foregut, just caudal to the level of the pharynx (Ten Have-Opbroek, 1981). During a period of rapid longitudinal growth of the foregut, the ventral trachea becomes separated from the dorsal oesophagus, with the separation process starting at the caudal end of the groove and proceeding in a cranial direction. The precise mode of separation of the trachea from the oesophagus remains controversial; is it primarily a process of division of the foregut into trachea and oesophagus or a process of active tracheal outgrowth (Fig. 1.3)? Tracheal and bronchopulmonary development should be regarded as distinct, but concurrent aspects of the development of the respiratory system. The initial foregut evagination at the laryngotracheal groove represents the tracheal primordium, but soon after its appearance, a bifurcation appears at its caudal end and the two primitive bronchopulmonary buds appear and start growing in a ventro-caudal direction. These buds are the primordia of the two lungs and the two primary bronchi. From that point onwards, pulmonary development can be largely viewed as a process of progressive lengthening and branching of the primitive bronchopulmonary buds (Warburton et al., 2000). Traditionally, the process of branching morphogenesis has been divided into five stages (Have-Opbroek, 1981). The embryonic stage (26 days to 6 weeks in the human) comprises, as well as the emergence of the two primary bronchopulmonary buds, further stages of branching which produce the secondary bronchopulmonary buds (5^{th} week in the human) and the tertiary bronchopulmonary buds (6^{th} week in the human). The

secondary buds will yield the lung lobes and the tertiary ones the bronchopulmonary segments. During the pseudoglandular stage of pulmonary development (6-16 weeks in the human), there are 14 more stages of branching that result in the formation of small branches known as terminal bronchioles. The canalicular stage (16-28 weeks in the human) is characterised by the division of the terminal bronchioles into at least two respiratory bronchioles and the beginning of the development of the respiratory vasculature with increasing vascularisation of the mesenchyme that surrounds the developing respiratory structures. During the saccular stage (28-36 weeks), the respiratory bronchioles divide further to yield terminal sacs. Finally, during the alveolar stage (36 weeks to term), the alveoli become increasingly mature.

1.2.2 – Controversial aspects of tracheo-oesophageal development

Despite intense interest in the mechanisms of lung development, the events underlying the morphogenesis of the anterior respiratory structures have been the subject of continuing debate. In broad terms, there have been two contrasting theories to explain how the respiratory foregut, anterior to the point of origin of the bronchopulmonary buds, separates from the gastrointestinal (oesophageal) foregut. One theory suggests that there is active growth of a mesenchymal septum which develops in the coronal plane and as a result separates the foregut lumen into ventral (respiratory) and dorsal (gastrointestinal) structures (Fig. 1.3a,b) (Arey, 1966; Gray & Scandalakis, 1972). This theory postulates that the septum is formed by opposing epithelio-mesenchymal ridges that grow medially and meet in the midline, resulting in separation (Fig. 1.3c). Furthermore, the septum has been described as ascending, with the separation first being established distally, at the level of the bronchopulmonary buds. Direct evidence of septum formation has, however, been lacking, casting doubt on this theory and most studies of tracheo-oesophageal

development have failed to identify such a structure (Zaw-Tun, 1982; O'Rahilly & Muller, 1984; Kluth et al., 1987). Other theories support the notion of fusion of the lateral foregut walls that results in separation of the trachea from the oesophagus. Separation progresses in a caudo-rostral direction but does not involve the development of a septum (Qi & Beasley, 2000; Duan et al., 2003).

An alternative theory suggests that the respiratory system develops as a result of rapid outgrowth from the original foregut tube (Sasaki et al., 2001a). This would be in keeping with the mode of development of other foregut derivatives, both midline and lateral. For example, the thyroid, thymus and parathyroid glands all bud off the foregut and rapidly grow away from it, eventually losing their original connection to it. The outgrowth theory is also consistent with the accepted pattern of rapid longitudinal growth at the distal tips of the developing bronchopulmonary structures. Applied to the trachea, this theory suggests that the tracheal primordium buds off the ventral foregut and remains a separate structure from the foregut during the subsequent stages of development. This has been likened to the way a column of water forms after a tap is switched on (the so-called tap and water theory) (Fig. 1.3d,e).

A third theory, has been formulated by a group in Germany which combines elements of both main theories and uses scanning electron microscope images of chick embryos to suggest that tracheo-oesophageal separation is the result of the development of foregut folds (Kluth & Fiegel, 2003; Kluth et al., 1987). This theory describes three foregut folds: anterocranial or laryngeal, dorsal or pharyngo-oesophageal and inferior or tracheo-oesophageal (Fig. 1.3f,g). The paired laryngeal and single tracheo-oesophageal folds

Fig. 1.3 Models of tracheo-oesophageal separation

Schematic representation of the foregut illustrating theories of tracheo-oesophageal separation. Sagittal sections of the foregut (Fo) in *a, b, d, e, f* and *g* and transverse section in *c* at levels indicated in *a* and *b*. ***(a-c)*** One theory suggests that the foregut initially elongates as an undivided structure having a ventral (tracheal) and a dorsal (oesophageal) components (dotted line demarcates components in *a* and *b*). This theory suggests that the foregut then separates into the trachea (Tr) and oesophagus (Oe) as a result of the growth, in the coronal plane, of lateral mesenchymal ridges (arrowheads in *c*) which fuse to form a mesenchymal septum. Separation initially occurs at the level of the origin of the lung buds (Lb) and progresses in a rostral direction (arrows in *a* and *b*). A parallel theory supports the caudo-rostral progression of separation although it postulates that the lateral walls collapse and fuse, resulting in separation. This theory rejects the development of a septum ***(d,e)*** Another theory considers the respiratory diverticulum (Rd) to appear as a ventral evagination from the foregut with the two lung buds (Lb) at its caudal limit. It has been postulated that the trachea becomes separated from the oesophagus as a result of rapid downward growth (arrow in e) of the respiratory diverticulum. According to this theory, the trachea is never part of an undivided foregut and this model has been likened to a column of water following the switching on of a tap (tap and water theory). ***(f,g)*** The paired laryngeal (L) and single inferior (I) folds define the tracheo-oesophageal space (Tos). Subsequent approximation (arrows) of these folds defines the separate trachea and oesophagus. The dorsal (D) fold marks the boundary between the pharynx and oesophagus.

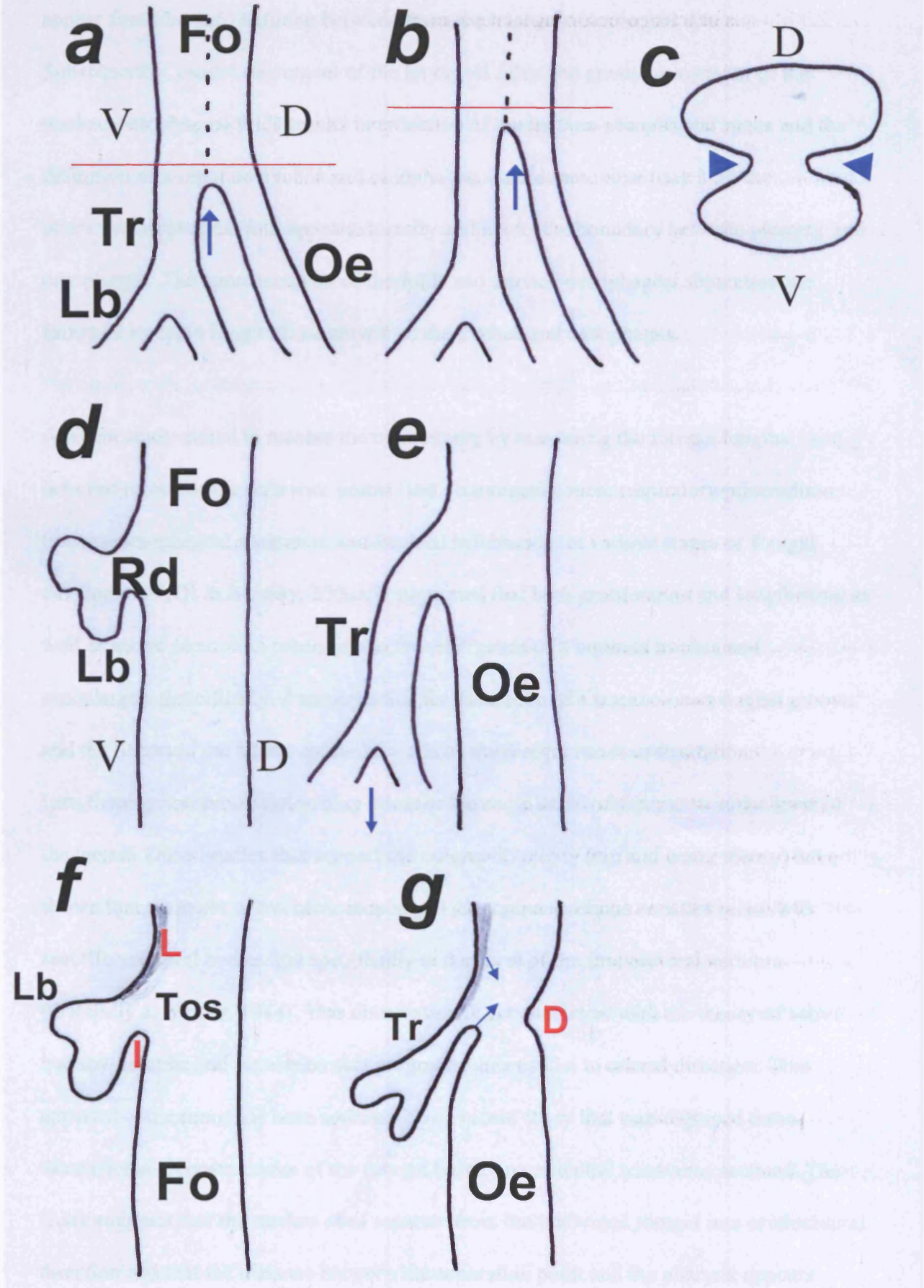
a
Fo
V
D
Tr
Oe
Lb
b
c
D
V
d
Fo
Rd
Lb
V
D
e
Tr
Oe
f
L
Lb
Tos
I
Fo
g
Tr
D
Oe

appear first (day 2.5) defining between them the tracheo-oesophageal space. Subsequently, caudal movement of the laryngeal folds and cranial movement of the tracheo-oesophageal folds results in reduction of the tracheo-oesophageal space and the definition of a separate trachea and oesophagus. At the same time (day 3.5), the pharyngo-oesphageal fold appears dorsally and marks the boundary between pharynx and oesophagus. The approximation of the folds and tracheo-oesophageal separation are followed by rapid longitudinal growth of the trachea and oesophagus.

A recent study aimed to resolve the controversy by measuring the foregut lengths between reproducible reference points (last pharyngeal pouch, respiratory primordium, tracheo-oesophageal separation and tracheal bifurcation) at various stages of foregut development (Qi & Beasley, 2000). It suggested that both proliferation and lengthening as well as active separation contribute to the emergence of a separate trachea and oesophagus. Specifically, it suggests that the formation of a tracheo-oesophageal groove and the fusion of the lateral epithelial walls of the foregut result in separation. Lengthening and proliferation play a role in the completion of separation at the level of the larynx. Other studies that support the outgrowth theory (tap and water theory) have shown that the point of tracheo-oesophageal divergence remains constant relative to specific vertebral bodies and specifically at the level of the first cervical vertebra (O'Rahilly & Muller, 1984). This observation is not consistent with the theory of active tracheo-oesophageal separation that progresses in a caudal to cranial direction. This apparent conundrum has been addressed by a recent study that uses digitised three-dimensional reconstructions of the foregut based on sequential transverse sections. The study suggests that the trachea does separate from the undivided foregut in a caudocranial direction and that the distance between the separation point and the pharynx appears

constant as a result of the ongoing lengthening of the cranial foregut (Williams et al., 2003).

1.2.3 – Molecular aspects of tracheo-oesophageal development

1.2.3.1 - Mechanisms of respiratory field specification

The process that directs the positioning and establishment of the lung primordium in the ventral foregut is less well understood than the subsequent processes of branching morphogenesis and cytodifferentiation of the pulmonary epithelium. A number of studies have identified the homeodomain transcription factor *Nkx2.1* as an early respiratory marker expressed in the ventral, prospective-respiratory epithelium of the foregut. Although it is the earliest detected marker of respiratory specification, *Nkx2.1* is not likely to be required for the initial specification of the respiratory primordium. Mouse embryos that carry a homozygous targeted disruption of the *Nkx2.1* locus do develop respiratory structures although they are very rudimentary, with pulmonary branching morphogenesis being severely disrupted (Yuan et al., 2000; Minoo et al., 1999). These observations indicate the critical role of *Nkx2.1* in respiratory development, but rule out a requirement of this transcription factor for respiratory specification.

The upstream events that control the timing and the anteroposterior and dorsoventral positioning of the *Nkx2.1*- positive domain are not well understood. Studies of the development of the hepatic and pancreatic endoderm have thrown up possible clues as to the induction/ regulation of *Nkx2.1* and respiratory-specific expression. Posterior foregut endoderm, destined for hepatopancreatic development, expresses *Nkx2.1* when recombined with cardiac mesoderm in culture, demonstrating a role for cardiac mesoderm

in inducing this respiratory epithelial marker (Deutsch et al., 2001). A more recent study of lung bud formation in the chicken embryo has identified specific mesodermal factors that may play role in respiratory specification. Expression of *Tbx4*, a member of the T-box transcription factor gene family, in the mesoderm correlates closely, both temporally and spatially, with the anteroposterior regionalisation of the respiratory primordium within the foregut (Sakiyama et al., 2003). Gene expression studies demonstrate that the posterior boundaries of *Tbx4* and *Nkx2.1* are identical. Furthermore, ectopic expression of *Tbx4* was shown to induce ectopic *Nkx2.1* expression albeit only in the ventral foregut endoderm. This would suggest that *Tbx4* contributes to the specification of the *Nkx2.1* domain in the ventral foregut endoderm. However, the initiation of *Nkx2.1* expression may be under the control of a different system as ventral *Nkx2.1* expression precedes that of *Tbx4*. The action of *Tbx4* could be mediated by *Fgf10*, as *Tbx4* defines an *Fgf10* mesodermal expression domain during early respiratory development. Interestingly, *Fgf10* null mutants develop a trachea but lack any subsequent pulmonary branching morphogenesis (Sekine et al., 1999).

Other factors potentially involved in the specification of the lung primordium include the mesodermally expressed *Gli* family of transcription factors. Double homozygous $Gli2^{-/-}$; $Gli3^{-/-}$ embryos completely fail to develop respiratory structures and show a reduction in the endodermal expression of *Hnf3β* (Motoyama et al., 1998). The gene *Sonic hedgehog* (*Shh*), which encodes an important signaling molecule with multiple morphogenetic roles in the developing embryo, is also specifically expressed in the ventral foregut endoderm as early as E9.5 when the laryngotracheal groove is formed (Litingtung et al., 1998). In the foregut, the *Shh* signal is thought to be mediated through the transmembrane receptor *Patched* (*Ptch*) and the *Gli* family of transcription factors and the *Shh* transduction

pathway is highly conserved between drosophila and mouse (Platt et al., 1997; Litingtung et al., 1998; Muller & Basler, 2000; Methot & Basler, 2001). The upstream factors that control the ventral expression of *Shh* are not known. The proximity of the shh-producing notochord to the foregut makes it a good candidate for a source of inductive signals although there is no evidence that it is involved in respiratory specification. The mechanisms of pancreatic specification provide an interesting analogy. In this case, it has been shown that the default expression pattern of the early foregut is of dorsal *Shh* expression which is inhibited by activin originating from the notochord (Kim et al., 2000; Hebrok et al., 1998). In contrast, ventral *Shh* expression is induced by ventral mesodermal factors and is likely to involve the *Fgf* pathway (Deutsch et al., 2001).

1.2.3.2 – Epithelial-mesenchymal interactions in the respiratory foregut

The morphogenetic events that follow the specification of the respiratory primordium constitute two separate processes. The first is the morphogenesis of the primary respiratory bud that leads to the development of the anterior respiratory structures (larynx and trachea). The second is the progressive elongation and branching of the primitive bronchopulmonary buds, a process known as branching morphogenesis, that leads to the development of an elaborate bronchial network and the alveoli. These two processes are heavily dependent on a signaling crosstalk between the endoderm and mesoderm.

Little is known about the molecular events that underlie tracheal development. The factors that have so far been implicated in this process are the transcription factor *Nkx2.1* in the endoderm and the growth factors *Fgf10* and *Tbx4* in the mesoderm. Loss of function of *Nkx2.1* leads to the development of a common tracheo-oesophageal channel and grossly abnormal bronchopulmonary structures (Li et al., 2000a; Minoo et

al., 1999; Yuan et al., 2000). A disturbance in the normal *Nkx2.1* expression pattern, caused by ectopic *Tbx4* and *Fgf10* expression, leads to ectopic lung bud formation as well as failure of tracheo-oesophageal septation and separation (Sakiyama et al., 2003).

Branching morphogenesis is dependant on epithelial-mesenchymal interactions involving peptide growth factors, transcription factors and extracellular matrix proteins and their receptors (Costa et al., 2001). The most important epithelial factors are BMP-4, PDGF, Shh and Nkx2.1. Loss of function of *Shh* or *Nkx2.1* in mutant embryos, leads to severe disruption in the development of distal lung (Minoo et al., 1999; Litingtung et al., 1998; Yuan et al., 2000). The key mesenchymal mediator of lung development is the FGF signaling pathway. Development of distal lung structures is completely dependant on this pathway and failure of formation of structures distal to the mainstem bronchi is seen in embryos with targeted disruption of *Fgf-10* (Sekine et al., 1999). Transcription factors of the *Hox* family and the *Gli* family also play crucial roles in branching and epithelial differentiation (Motoyama et al., 1998; Aubin et al., 1997; Grindley et al., 1997). The FGF and PDGF signaling pathways play an important role in the development of the alveoli (Bostrom et al., 2002; Bostrom et al., 1996; Weinstein et al., 1998). Pulmonary cell specification is also dependant on *Nkx2.1* as it activates promoters of lung-specific surfactant protein genes such as *Sp-B* and, as a result, controls development of alveolar type II cells (Minoo et al., 1999).

1.3 – MALFORMATIONS OF THE TRACHEA AND THE OESOPHAGUS

1.3.1 – Types of human tracheo-oesophageal malformations

Malformations of the trachea and the oesophagus are best studied together because the developmental processes involved are closely associated (as described in section 2.1), even though the two structures belong to different systems (respiratory and gastrointestinal). The commonest types of tracheo-oesophageal malformations are grouped under the umbrella terms oesophageal atresia and tracheo-oesophageal fistula (OA/TOF) and occur in about 1 in 2500 to 3000 live births (Ashcraft & Holder, 1969). The grouping together of these malformations as OA/TOF is rather arbitrary but they broadly involve a combination of discontinuity of the oesophagus (atresia) and abnormal tracheo-oesophageal communication (fistula). Of the five main types of OA/TOF, by far the commonest is the association of atresia of the proximal oesophagus with a fistula between the trachea and the distal oesophagus and stomach (Fig. 1.4a-e). Arguably, the OA/TOF group should also include the exceedingly rare malformations characterized by atresia of the trachea associated with tracheo-oesophageal fistula. Other, less well-defined groups of tracheo-oesophageal malformations include tracheal and oesophageal stenoses and the presence of oesophageal webs, although some of these malformations could be considered under the atresia heading. Laryngotracheo-oesophageal clefts are a rare group of malformations characterized by a variable degree of continuity between the ventral respiratory structures and the dorsal gastrointestinal structures (Wolfson et al., 1984). In the mildest form, the cleft involves only the subglottic larynx and the oesophagus whereas at the other end of the spectrum it extends distally beyond the tracheal carina and into the main bronchi (Fig. 1.4f).

Fig. 1.4 Main types of human tracheo-oesophageal malformations

Schematic representation of the main types of human tracheo-oesophageal malformations. (***a-e***) These five types of malformations are grouped together under the term oesophageal atresia and tracheo-oesophageal fistula (OA/TOF). (***a***) The commonest type (about 85% of OA/TOF) is the association of atresia of the proximal oesophagus (Oe) (arrowhead in *a*) with an abnormal fistulous connection (Fi) between the trachea (Tr) and the distal oesophagus. The origin of the fistula is usually from the area of the tracheal bifurcation into the two bronchi (Br). (***b***) An additional fistula exists between the atretic proximal oesophagus and the trachea (arrowhead in *b*). (***c***) Only a proximal tracheo-oesophageal fistula exists and the distal oesophagus is blind ending (arrowhead in *c*). (***d***) Oesophageal atresia without tracheo-oesophageal fistula. In this type of defect, the gap between the two blind ends of the oesophagus is usually long. (***e***) The oesophagus is not atretic and there is a fistula between the trachea and the oesophagus (arrowhead in *e*). This type of OA/TOF is also known as H-type fistula because of its appearance. The length and position of the fistula vary. (***f***) Tracheo-oesophageal cleft is characterised by a communication between the posterior aspect of the trachea and the anterior aspect of the oesophagus (dotted line). The communication is of variable length and can extend from the larynx in the mildest form to the main bronchi in the most severe form.

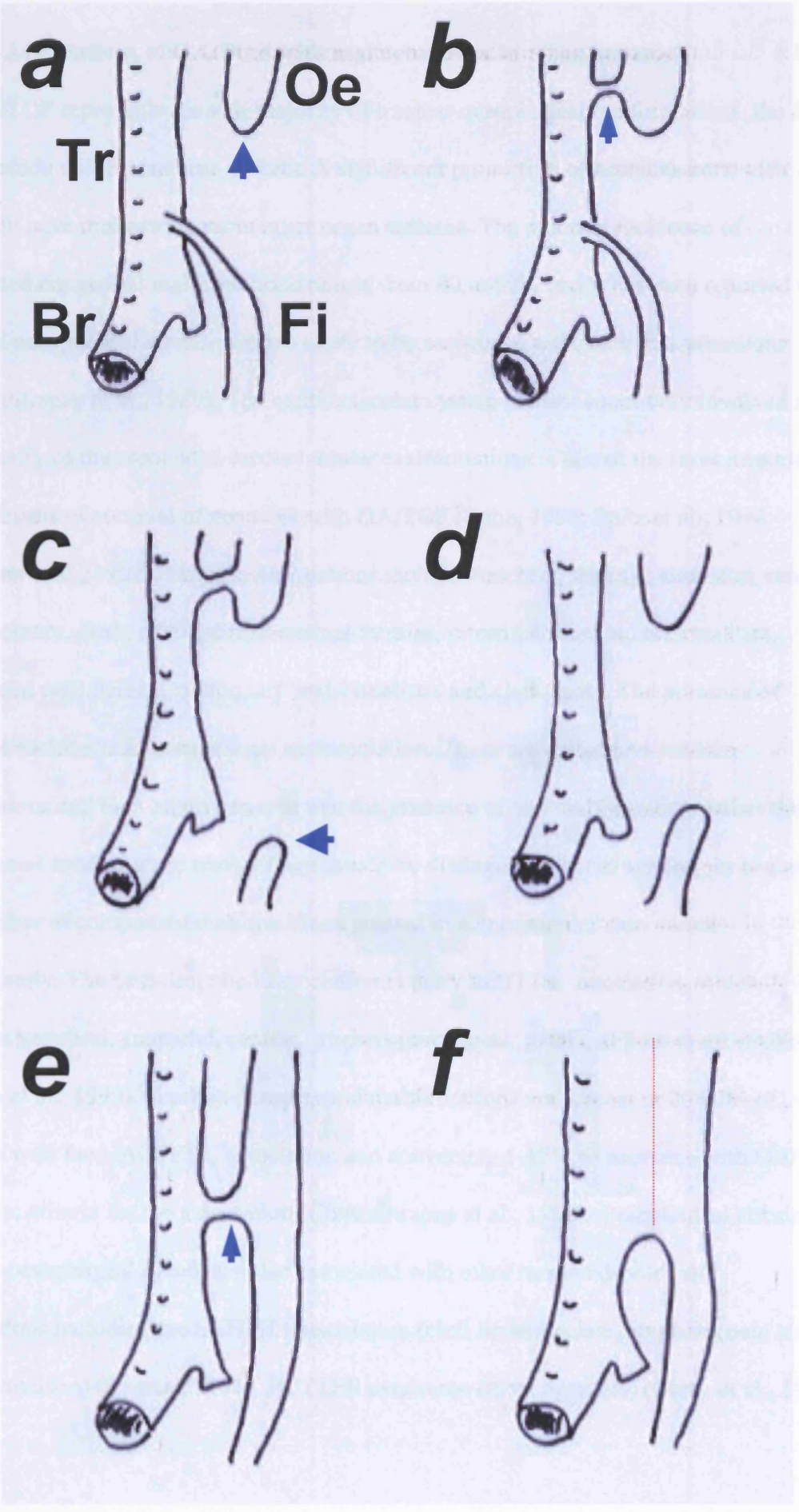
a
Oe
Tr
Br
Fi
b
c
d
e
f

1.3.2 – Associations of OA/TOF with malformations in other systems

As OA/TOF represents the vast majority of tracheo-oesophageal malformations, the focus of this study will be on these defects. A significant proportion of neonates born with OA/TOF have malformations in other organ systems. The reported incidence of associated congenital malformations ranges from 40 to 60% and it has been reported that isolated oesophageal atresia is more likely to be associated with such malformations (Chittmittrapap et al., 1989). The cardiovascular system is most commonly involved and the severity of the associated cardiovascular malformations is one of the most important determinants of survival of neonates with OA/TOF (Spitz, 1996; Spitz et al., 1994; Iuchtman et al., 1992). Other malformations include vertebral, skeletal, anorectal, renal, genitourinary, limb, other gastrointestinal atresias, intestinal rotation abnormalities, abdominal wall defects, pulmonary malformations and cleft palate. The presence of multiple malformations represents an association. These are called non-random associations and their significance is that the presence of one malformation makes the presence of another more likely. They should be distinguished from syndromes because the number of component malformations present in any particular case varies significantly. The best-described association is the VACTERL association, which includes vertebral, anorectal, cardiac, tracheo-esophageal, renal and limb malformations (Brown et al., 1999). Tracheo-oesophageal malformations are present in 20-67% of patients with the VACTERL association and conversely 5-17% of neonates with OA/TOF fulfill the criteria for the association (Chittmittrapap et al., 1989). Oesophageal atresia and tracheo-oesophageal fistula are also associated with other rare syndromes and associations including the SCHISIS association (cleft lip and palate, omphalocoele and hypogenitalism) (Czeizel, 1981), POTTER syndrome (renal agenesis) (Curry et al., 1984)

and the CHARGE association (Coloboma, heart defects, choanal atresia, renal, genitourinary and ear malformations) association (Koletzko & Majewski, 1984).

1.3.3 – Aetiology of tracheo-oesophageal malformations

The aetiology of OA/TOF is likely to be multifactorial and remains unknown. The overwhelming majority of cases are sporadic/ non-syndromic, although a small number within this non-familial group are associated with chromosomal abnormalities. Familial/ syndromic cases of OA/TOF are very rare, representing less than 1% of the total.

In the case of sporadic/ non-syndromic OA/TOF, the likely cause is an insult that occurs during the narrow gestational window of tracheo-oesophageal organogenesis. This is illustrated in the reported cases of human OA/TOF that are associated with maternal intake of chemotherapeutic agents as is the case with the thioamide Methimazole (Clementi et al., 1999). That said, the nature of the insult in the vast majority of sporadic cases remains ill defined and may be a non-specific event such as a threatened abortion. Twin pregnancy may also disturb organogenesis and OA/TOF is 2 to 3 times more common in twins (Orford et al., 2000). Genetic susceptibility could also be involved as illustrated by the few reported cases of non-syndromic OA/TOF occurring in multiple members of the same family (Kashuk & Lilly, 1983; Lipson & Berry, 1984; Van Staey et al., 1984). The overall risk of non-syndromic OA/TOF in a sibling of an affected child is about 1%.

The presence of associated malformations in other organ-systems could provide clues as to the possible aetiology of OA/TOF. These malformations occur in distinct patterns, known as non-random associations, as described above. The pattern of these non-random

associations is likely to be dictated by the timing of a possible insult that affects multiple morphogenetic events. The insult could act by transiently disturbing a specific developmental signalling pathway. In the mouse, loss of function mutations for genes of the *Shh* pathway lead to a spectrum of anomalies that is similar to those of VACTERL, implicating the pathway in the embryogenesis of the malformations (Kim et al., 2001). In the human, the evidence is less conclusive with the *SHH* and *PATCHED-1* (*PTC-1*) mutations leading to holoprosencephaly, a malformation not associated with OA/TOF (Ming et al., 2002; Ming et al., 1998; Roessler et al., 1996). Tracheo-oesophageal fistula and other features of VACTERL have however been described in patients with a mutation of *GLI3* (Kang et al., 1997), a gene participating in the *SHH* signalling pathway.

Chromosomal abnormalities such as trisomies (18 and 21) (Beasley et al., 1997) and deletions (22q11 and 17q22q23.3) (Digilio et al., 1999; Marsh et al., 2000) are known to be associated with OA/TOF and have been reported in up to 6% of patients who have associated malformations in other systems (Brunner & Winter, 1991). The presence of many of the features of the non-random associations described above in cases of chromosomal deletions (e.g. 22q11) has led to the study of all chromosomal aberrations in search of a genetic region that is likely to be involved in OA/TOF susceptibility. No such region has been identified linked to chromosomal abnormalities (Brewer et al., 1998). The recent development of comparative genomic hybridisation (CGH) using microarray technology enables the detection of cytogenetically invisible microdeletions (Oostlander et al., 2004). It will be very interesting to apply this technology to a panel of patients' DNA with OA/TOF to determine whether genetic loss is common in this group of malformations.

Finally, familial/syndromic OA/TOF is very rare. A well-studied example is Feingold syndrome (oculodigitoesophagoduodenal syndrome) which is a rare autosomal dominant disorder that includes oesophageal atresia (Courtens et al., 1997; Feingold et al., 1997). Studies of affected families have localised the defect to chromosome 2 (2p23-p24) and have shown that haploinsufficiency of a gene or genes in that region is associated with syndromic OA/TOF (Celli et al., 2000). Further characterisation of the genes involved could contribute to the study of the molecular basis of OA/TOF.

1.3.4 – Clinical history, prognosis and management

The evolution of surgical techniques and of neonatal intensive care has resulted in the survival of the vast majority of neonates with OA/TOF. The mortality still associated with OA/TOF can be largely attributed to the presence of malformations in other organ systems. In this respect, the most important are cardiac malformations that have been shown to be, together with low birth weight, the most important predictors of mortality (Spitz, 1996; Spitz et al., 1994; Spitz, 1993; Iuchtman et al., 1992). The management of OA/TOF is surgical and the aim is to establish oesophageal continuity either primarily or in a staged procedure. In the presence of other malformations, the aim is also surgical correction of the malformations. Although OA/TOF repair is relatively straight forward, infants with repaired OA/TOF continue to suffer morbidity associated either with abnormal oesophageal function or respiratory dysfunction (Brown et al., 1999; Romeo et al., 1987; Biller et al., 1987; Chetcuti et al., 1992; Robertson et al., 1995; Somppi et al., 1998; Koivusalo et al., 2005). These residual problems are attributed either to primary defects in the oesophagus, trachea or lungs or are secondary to events early in life such as aspiration pneumonia (LeSouef et al., 1987).

1.3.5 – Animal models of tracheo-oesophageal malformations

1.3.5.1 - The history of animal models

In recent years, congenital malformations have become one of the leading causes of neonatal mortality in the Western world . This can be explained by the dramatic decrease in the number of deaths caused by neonatal infection as a result of effective antibiotic treatment and the general improvement in the care of extremely low birth weight babies in neonatal units. In contrast, mortality rates for several major congenital malformations remain unacceptably high. The mortality data are even worse when rates of intrauterine death are taken into account. This reflects the lack of progress in understanding the embryological basis of malformations or in turning this improving knowledge into preventive therapies (Kluth & Lambrecht, 1997a).

This is particularly true in the case of OA/TOF. Although very significant progress has been made in recent years in the clinical management of these malformations, there is still significant morbidity and even mortality, especially in the presence of associated malformations (e.g. heart). The detailed embryological events that underlie the development of OA/TOF are not well understood. One reason is the lack of any significant number of human embryos with OA/TOF that are available for study at the appropriate stages of gestation; it should be pointed out that tracheo-oesophageal development takes place in the 3rd and 4th weeks of gestation. Furthermore, there are no satisfactory alternative techniques for the study of these defects, such as *in vitro* culture models or computer generated three dimensional reconstructions.

In view of these shortcomings, the development of a reliable and reproducible animal model of these malformations has been a goal of paediatric surgical researchers for decades. A number of mechanical techniques were initially used to produce tracheo-oesophageal malformations. Rabbit and sheep foetuses were operated *in utero* and had their oesophagus ligated, but this did little more than to offer a model for the study of some aspects the pathophysiology of oesophageal atresia (Trahair et al., 1995; Wesson et al., 1984). A model that was based on causing malformations by inducing hyperflexion of chick embryos met with limited success (Kleckner et al., 1984). The major drawback of these approaches was that they assumed a mechanistic embryological basis for tracheo-oesophageal malformations and certainly ignored any cellular and molecular aspects of the aetiology of these anomalies. Moreover, none of these techniques attempted to understand OA/TOF in terms of an aberration of normal tracheo-oesophageal development. Depleting vitamin A or riboflavin from the diet of pregnant rats caused tracheo-oesophageal malformations including OA/TOF, but these were not consistent (WILSON et al., 1953; KALTER & WARKANY, 1957). The study of the effect of teratogenic agents on embryo development appeared more promising. In 1978, Thompson et al, described a number of malformations, including OA/TOF, in rat and rabbit foetuses exposed in utero to the anticancer agent Adriamycin (doxorubicin hydrochloride) (Thompson et al., 1978). This observation was not followed up until 20 years later when Diez-Pardo et al (1996) described in detail the first reproducible model of tracheo-oesophageal malformations based on exposure to this particular teratogenic agent.

1.3.5.2 - The Adriamycin rat model

Adriamycin is an anthracycline antibiotic used in anticancer chemotherapy. Its action is based on its ability to enter the nucleus of cells and intercalate into DNA, interfering with DNA replication and transcription. It also has mutagenic properties and interferes with the function of the cell membrane and other cell organelles. Diez-Pardo et al (1996) found that daily intraperitoneal injections of pregnant rats with 1.75 mg/ kg body weight of Adriamycin from E6 to E9 produced tracheo-oesophageal malformations in 45% of the exposed embryos. Subsequent studies confirmed the reproducibility of the model either at the same dose (Possogel et al., 1998a)or at slightly higher doses (2 and 2.2 mg/ kg) (Merei et al., 1997a; Merei et al., 1998a; Crisera et al., 1999a). Subsequent modifications of the model were aimed at reducing the exposure of embryos to Adriamycin by manipulating days of injection, while at the same time maintaining the reproducibility of the malformations. Injections on days 8 and 9 only, were associated with reduced embryo mortality whereas the frequency of malformations was not significantly altered (41%) (Qi et al., 1996).

The great advantage of the Adriamycin rat model is the close phenotypic similarity between the rat and human malformations. The commonest type of human malformation (oesophageal atresia with distal tracheo-oesophageal fistula) is also the commonest type of experimental defect (Ashcraft & Holder, 1969). This similarity validates the model and makes it extremely useful for the study of faulty organogenesis. Furthermore, Adriamycin-treated rat embryos exhibit malformations in other systems, in addition to OA/TOF. The spectrum of associated malformations in the model is similar to the VACTERL association seen in humans (Merei et al., 1999), although the frequency and severity of the rat-associated malformations is greater. These include vertebral, radial and

other skeletal (Kotsios et al., 1998; Merei et al., 1998; Xia et al., 1999a; Abu-Hijleh et al., 2000; Kolker et al., 2000), anorectal (Liu & Hutson, 2000), cardiovascular (Qi et al., 1997a; Otten et al., 2000), tracheo-bronchial (*other than OA/TOF*) (Qi et al., 1997b; Xia et al., 1999b) and renal tract (Temelcos & Hutson, 2004a; Temelcos & Hutson, 2004b; Merei et al., 2001) malformations. Foregut malformations in the Adriamycin-treated have been also associated with disturbance in the development of organs with neural crest contribution. These associated defects include cardiovascular, thymic and parathyroid malformations, as well as abnormal development of the parafollicular cells of the thyroid.(Otten et al., 2000; Martinez et al., 2004)

The association between tracheo-oesophageal malformations and malformations of the notochord has been studied in detail. Notochordal malformations include thickening and hypertrophy, abnormal position of the notochord in relation to the foregut and bifurcation and presence of abnormal branches (Qi & Beasley, 1999; Possoegel et al., 1999; Williams et al., 2001; Vleesch, V et al., 2002; Gillick et al., 2003; Mortell et al., 2004). The adherence of either an abnormal, ventrally position ectopic notochord, or a ventral branch of a notochordal bifurcation to the foregut has been seen as evidence that the notochord is involved in the embryogenesis of tracheo-oesophageal malformations by exerting traction on the developing foregut (Williams et al., 2001; Qi & Beasley, 1999). Apart from the mechanical effects of an abnormal notochord on the developing foregut, the persistence of *Shh* expression in the abnormal notochord branches has formed the basis for molecular explanations for the embryogenesis of tracheo-oesophageal malformations (Gillick et al., 2003; Mortell et al., 2004).

The analysis of the rat model has contributed significantly to our understanding of the embryogenesis of tracheo-oesophageal malformations. A number of theories have been put forward which themselves reflect the theories of normal development. One of these theories assumes that normal tracheal development and tracheo-oesophageal separation is the result of rapid longitudinal growth of the tracheal primordium away from the foregut. According to this theory, tracheo-oesophageal malformations are fundamentally caused by a failure of tracheal growth, the result of which is a compensatory overgrowth of the undivided foregut with the bronchopulmonary buds originating directly from the foregut (Fig. 1.5a,b) (Possogel et al., 1998a; Merei et al., 1997b; Sasaki et al., 2001a; Merei et al., 1998a). According to a second theory, normal development depends on an active separation process that divides the foregut into a ventral trachea and a dorsal oesophagus and it is this process that fails (Fig. 1.5c,d) (Qi & Beasley, 2000; Williams et al., 2003). Interestingly, both these theories share one important point. Atresia of the proximal oesophagus is not part of the initial malformation. Both theories suggest that the atretic oesophagus is a result of late rearrangement of the cranial foregut resulting in a blind ending structure in the dorsal mesenchyme. According to both theories, the tracheo-oesophageal fistula represents the primitive foregut distal to the origin of the bronchopulmonary buds, which connects the undivided foregut to the stomach. The near term arrangement is completed by trachealisation of the undivided foregut. A third theory is in sharp contrast with the two described above. It proposes that the oesophagus does initially develop as a separate structure which then becomes atretic secondary to an, as yet undetermined, event. According to this theory, the tracheo-oesophageal fistula grows from the trachea at the level of the lung buds and reconnects with the stomach in order to re-establish the continuity of the gastrointestinal tract (Fig. 1.5e,f) (Crisera et al., 1999a; Crisera et al., 2000a). None of the theories described above are based on experimental

Fig. 1.5 Theories on the development of oesophageal atresia and tracheo-oesophageal fistula

Schematic representations (sagittal sections) of the foregut illustrating the theories to explain the faulty organogenesis in oesophageal atresia (OA) and tracheo-oesophageal fistula (TOF). ***(a,b)*** In the first theory, the respiratory diverticulum (Rd) fails to elongate resulting in failure of the trachea to grow (tracheal agenesis) in contrast to the lung buds that develop normally. The overall growth and elongation of the foregut continues with the bronchial structures originating directly from the foregut. At a later stage, the foregut rostral to the bronchi assumes tracheal (Tr) histological characteristics whereas the foregut distal to the bronchial origin connects to the stomach and is described as the fistula (Fi). The upper atretic oesophagus (Ao) results from rearrangement of the anterior foregut (arrow in *b*). ***(c,d)*** In the second theory, the process of tracheo-oesophageal separation becomes arrested (arrows in *c* and *d*). If the failure is partial, a small length of oesophagus (Oe) does separate from the trachea. Following the arrest of separation, the undivided foregut assumes the histological characteristics of trachea whereas the initially separated oesophagus becomes the fistula that connects the trachea to the stomach. The upper atretic oesophagus forms, as in the first theory, by late rearrangement of the anterior foregut. ***(e,f)*** In contrast to the first two theories, the third postulates that normal tracheo-oesophageal separation does take place. An insult to the embryo (possibly ischaemic) results in loss of part of the oesophagus (dotted line in *f*) resulting in an atretic upper oesophageal pouch. The development of the fistula from the trachea (arrow in *f*) compensates for the oesophageal loss by reconnecting to the stomach. This theory suggests that the fistula is a structure of respiratory origin.

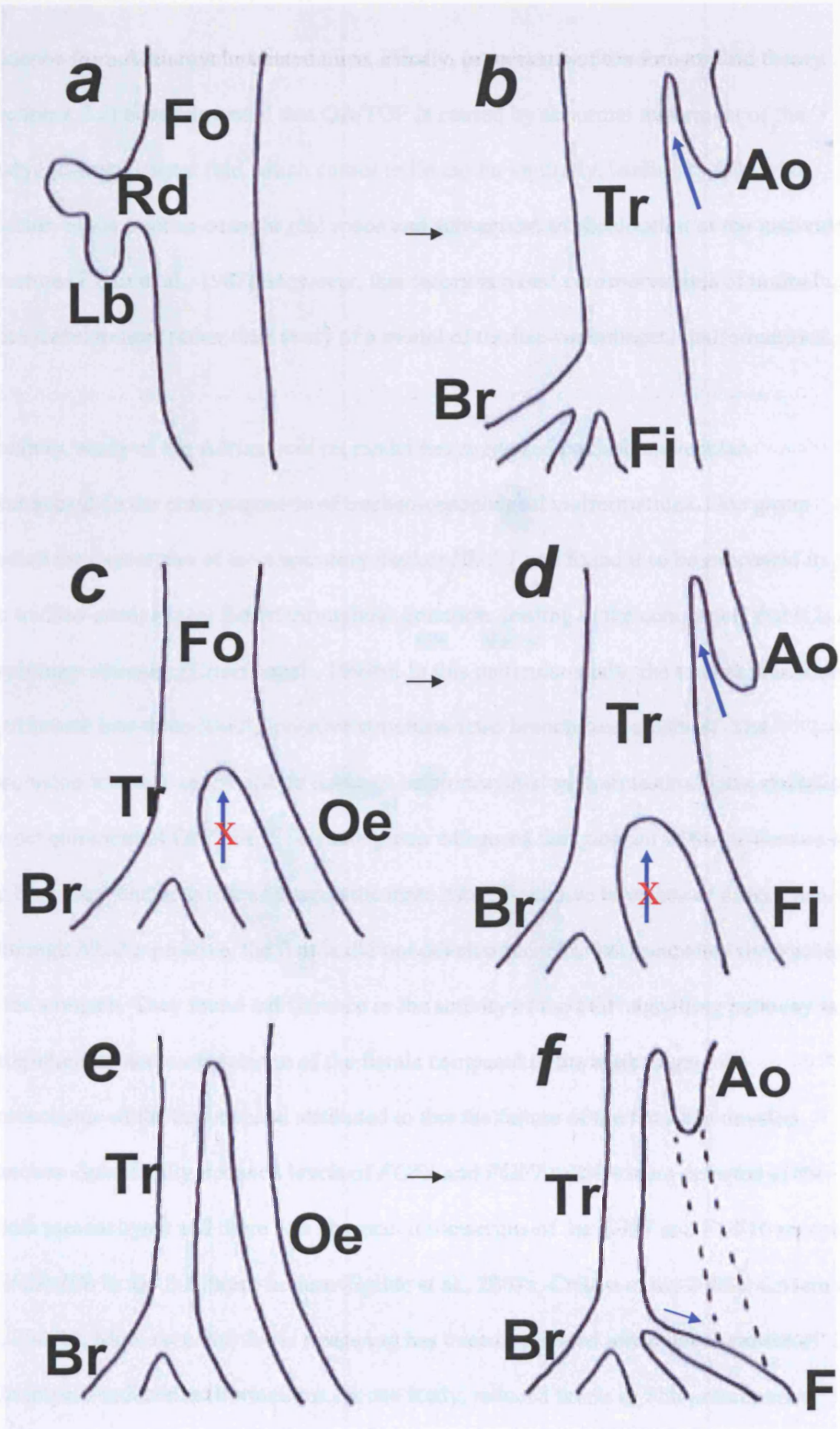
a
Fo
Rd
Lb
b
Tr
Ao
Br
Fi
c
Fo
Tr
Oe
Br
d
Ao
Tr
Br
Fi
e
Tr
Oe
Br
f
Ao
Tr
Br
Fi

evidence from Adriamycin-treated mice. Finally, proponents of the foregut fold theory (*section 1.2.2*) have suggested that OA/TOF is caused by abnormal movement of the pharyngo-oesophageal fold which comes to lie too far ventrally, leading to failure of division of the tracheo-oesophageal space and subsequent trachealisation of the undivided structure (Kluth et al., 1987). However, this theory is based on observations of normal chick development rather than study of a model of tracheo-oesophageal malformations.

Recently, study of the Adriamycin rat model has suggested possible molecular mechanisms in the embryogenesis of tracheo-oesophageal malformations. One group studied the expression of the respiratory marker *Nkx2.1* and found it to be expressed in the tracheo-oesophageal fistula throughout gestation, leading to the conclusion that it is a respiratory structure (Crisera et al., 1999b). In this particular study, the trachea was found to trifurcate into three *Nkx2.1*-positive structures (two bronchi and a fistula). The conclusion was that an imbalance between respiratory and gastrointestinal fates underlies the development of OA/TOF. The same group addressed the question of the difference in the branching characteristics between the three *Nkx2.1*-positive branches of the trachea. Although *Nkx2.1*-positive, the fistula did not develop branches but connected the trachea to the stomach. They found a difference in the activity of the FGF signalling pathway in the epithelium and mesenchyme of the fistula compared to the epithelium and mesenchyme of the bronchi and attributed to this the failure of the fistula to develop branches. Specifically, reduced levels of *FGF1* and *FGF7* mRNA were detected in the fistula mesenchyme and there was absence of transcripts of the FGF7 and FGF10 receptor *FGF2R-IIIb* in the fistula epithelium (Spilde et al., 2003a; Crisera et al., 2000a; Crisera et al., 2000b). More recently, *Sonic hedgehog* has been implicated in the development of Adriamycin-induced malformations. In one study, reduced levels of Shh protein have

been found in the foregut of Adriamycin-treated embryos developing OA/TOF (Arsic et al., 2003). In another, reduced levels of *Gli-2* (a key member of the *Shh* signalling cascade) mRNA have been found in the mesenchyme of the fistula (Spilde et al., 2003b). Another study reported a disturbance in the spatial pattern of *Shh* expression in the foregut of Adriamycin-treated embryos, showing failure of downregulation of *Shh* at the site of tracheo-oesophageal separation, although these findings were poorly illustrated in the associated paper (Orford et al., 2001a). A recent study of human neonates with OA/TOF has shown that Shh protein is absent from the epithelium of the fistula but present in the epithelium of the atretic oesophagus (Spilde et al., 2003c). Despite these findings, the role of *Shh* in the development of Adriamycin-induced tracheo-oesophageal malformations remains unclear.

1.3.5.3 - Genetic mouse models

Loss of function mutations in foregut patterning genes have been generated in mice in order to study the role of these genes in development. The developmental defects caused by these mutations include tracheo-oesophageal malformations. Although the tracheo-oesophageal phenotype differs from that described in the rat, these defects represent a unique opportunity to gain an insight into the molecular mechanisms that underlie the development of tracheo-oesophageal malformations in contrast to the Adriamycin model, whose molecular basis is unknown and could include a multitude of molecular effects. The genes whose mutation yields foregut defects include those associated with the *Shh* pathway.

Sonic hedgehog (*Shh*) null mutant embryos are grossly abnormal, in keeping with the key role of this secreted glycoprotein in a number of developmental processes (Riddle et al.,

1993; Johnson et al., 1994; Roelink et al., 1995; Marigo et al., 1996; Litingtung et al., 1998; Chuong et al., 2000). These embryos have major forebrain malformations (holoprosencephaly), severely curtailed limb development and significant cardiovascular malformations (Chiang et al., 1996). In the foregut, the literature describes an abnormal tracheo-oesophageal development with the trachea and oesophagus having separate lumens but being very closely juxtaposed (Litingtung et al., 1998; Pepicelli et al., 1998). The description of the caudal foregut in *Shh*$^{-/-}$ embryos includes a communication between the lungs and the stomach, and an atresia of the oesophagus, although these phenotypic arrangements are not illustrated in detail (Litingtung et al., 1998). What is clear, however, is that the lungs themselves are abnormal, consisting of dilated sacs with reduced branching (Litingtung et al., 1998). The foregut phenotype of the double mutant: *Gli2*$^{-/-}$*Gli3*$^{+/-}$ is better defined. There is an undivided foregut ending in a trifurcation of two lung buds and a fistula to the stomach and the lungs are fused with significantly reduced epithelial branching (Motoyama et al., 1998). Both the *Shh*$^{-/-}$ and *Gli2*$^{-/-}$*Gli3*$^{+/-}$ embryos have malformations in other organ-systems. A number of these conform to the VACTERL association supporting the involvement of the *Shh* pathway in its embryogenesis (Kim et al., 2001). An almost identical foregut phenotype to the *Gli2*$^{-/-}$ *Gli3*$^{+/-}$ mutants is produced by a loss of function mutation of the transcription factor and respiratory marker *Nkx2.1*, which is not a member of the *Shh* pathway (Yuan et al., 2000; Minoo et al., 1999). In these embryos, there is failure of tracheo-oesophageal septation and an undivided oesophagotrachea connects the pharynx to the stomach. The bronchi originate from this undivided tube and the lungs are markedly hypoplastic. Finally, haploinsufficiency of *Foxf1* (also known as *FREAC1* or *HFH8*), a transcriptional target of *Shh* also causes tracheo-oesophageal malformations including oesophageal atresia and

tracheo-oesophageal fistula as well as lung hypoplasia and fusion of the lung lobes (Mahlapuu et al., 2001a).

1.4 – AIMS OF THE THESIS

Despite intense clinical interest in oesophageal atresia (OA) and tracheo-oesophageal fistula (TOF), the abnormal embryogenesis that underlies the development of these foregut malformations remains controversial. This can be largely attributed to the incomplete understanding of normal tracheo-oesophageal development, at both gross morphological and cellular and molecular levels.

The overall aim of this work was to study the mechanisms of normal tracheo-oesophageal development and the underlying cellular and molecular events in the context of foregut morphogenesis and to understand how disturbance of these mechanisms can lead to the development of tracheo-oesophageal malformations.

The initial specific aims of the study were

1. To develop an Adriamycin-based mouse model of tracheo-oesophageal malformations
2. To study and compare at the morphological level, normal mouse tracheo-oesophageal development and abnormal organogenesis in both the Adriamycin-treated and *Sonic hedgehog* mouse models of tracheo-oesophageal malformations.
3. Given that the molecular disturbance in the *Shh* model of tracheo-oesophageal malformations is known (loss of *Shh* function), I aimed to study the role of *Shh* in normal tracheo-oesophageal development and in the development of the Adriamycin-induced malformations.

In Chapter 3, normal tracheo-oesophageal morphology was studied in saline-treated CBA/Ca embryos and abnormal tracheo-oesophageal morphology in Adriamycin-treated

CBA/ Ca and homozygous mutant (*Shh*$^{-/-}$) embryos. Then, in Chapter 4, dorsoventral separation of the foregut along the boundary of respiratory specification was studied both in normal and abnormal development. Next, in Chapter 5, the role of *Shh* in foregut development and tracheo-oesophageal separation was studied in the saline-treated and Adriamycin-treated CBA/Ca embryos. Having identified tracheo-oesophageal separation as a fundamental process in the development of the anterior foregut, the roles of programmed cell death and cell proliferation were studied in Chapter 6. Finally, in Chapter 7, the hypothesis that programmed cell death is a requirement for tracheo-oesophageal separation, was tested using an *in vitro* culture system of foregut development.

CHAPTER 2 – MATERIALS AND METHODS

2.1 – GENERAL CONSIDERATIONS

All chemicals used were obtained from Sigma-Aldrich unless stated otherwise. All experiments were carried out at room temperature unless stated otherwise.

2.2 – MAINTENANCE OF MOUSE COLONIES

2.2.1 – Mouse strains

The inbred CBA/Ca mouse (Harlan, UK) was used as the 'normal' strain. A colony of heterozygous *Shh*$^{+/-}$ mice (Chiang et al., 1996) was established in our laboratory. Embryos homozygous for the loss of function mutation for *Shh* were generated by mating heterozygous mice. Homozygous embryo generation largely followed Mendelian ratios (25%). Genotyping for breeding purposes was as described in Chiang et al. (1996).

2.2.2 – Colony conditions

Mice were housed in an established animal facility according to Home Office regulation, with an alternating light/ dark cycle of 16 and 8 hours respectively.

2.2.3 – Embryo generation from timed pregnancies

Mice were mated overnight and the females were checked in the morning for the presence of a copulation plug. The presence of such a plug was taken as evidence of pregnancy and the female was taken to a different cage and started on a special pregnancy diet. The day

of discovery of a copulation plug was regarded as day 0 of gestation and 12:00 (midday) was designated as E0.5.

2.3 – TERATOGENIC MANIPULATION OF PREGNANT MICE

2.3.1 – The teratogenic agent

Adriamycin (doxorubicin hydrochloride) is an anthracycline antibiotic that has been extensively used in anticancer chemotherapy (Arcamone et al., 1969; Bonadonna et al., 1969). During extensive animal testing, multiple teratogenic and other toxic effects of the agent have been described, including damage to the cell membrane, generalised restriction of growth, mutagenic effects and interference with the processes of DNA replication and transcription (Ross et al., 1978). Adriamycin was obtained from Pharmacia & Upjohn (UK), in vials containing 5 ml of a 2 mg/ml solution (10 mg of Adriamycin) which were diluted with normal saline to a working concentration according to the required dose for injection: 0.4 mg/ml for the 4 mg/kg body weight dose, 0.3 mg/ml for the 3 mg/kg dose, 0.2 mg/ml for the 2 mg/kg dose etc etc. The vials were stored at 4 ^{o}C and, once the seal was breached in order to dilute the agent, it was used within two weeks.

Due to the known toxic effects of Adriamycin, stringent safety regulations were followed during usage or when exposure was possible. It was stored was in a designated fridge. Whenever the solution was handled, the user wore safety goggles, face mask and gloves, and work on the agent was carried out in an extraction hood. Any material that became soiled with Adriamycin (e.g. tissue paper) was disposed of in a double yellow bag, before being incinerated. Within the animal facility, mice that were administered Adriamycin

were kept in separate cages that were clearly marked and were not handled by laboratory staff other than for changing food and water supplies. At the end of the experiment, the carcasses of Adriamycin-treated mice were disposed off separately in clearly labeled bags before incineration. It was the responsibility of the license holder to dispose of the bedding of the cage in double yellow bag, as well as to wash the cage by hand before normal machine washing.

2.3.2 – Administration of agent

Adriamycin was administered to pregnant mice on days 7.5 and 8.5 of gestation by an intraperitoneal injection at a dose of 2, 3, 3.5, 4, 4.5, 5 or 6 mg/kg body weight. The working Adriamycin solution used for each dose ensured that the mice received the same volume of solution per body weight irrespective of the dose used. The mice were subsequently monitored for any signs of ill health and the license holder was contacted immediately if such signs developed. In this case, the animal was humanely killed by cervical dislocation and disposed of appropriately.

2.4 – EMBRYO HARVEST AND PROCESSING

2.4.1 – Timing of harvest

Pregnant mice were sacrificed between 12:00 and 13:00 so that embryos from different litters were of comparable gestation. None of the injected mice were allowed to proceed to term, with the embryos harvested at E17.5 and E18.5 used as 'near-term' substitutes for the study of development at term.

2.4.2 – Techniques of harvesting

The mice were killed by cervical dislocation. The abdomen was then cleaned with alcohol and access was gained to the peritoneal cavity by tenting the lower abdominal wall with forceps and cutting through with scissors. From that initial access point, a slightly curved, transverse incision was fashioned across the lower abdominal wall. The uterine horns were readily identified and each was separated from the corresponding ovary. Each horn was dissected free, having been put under tension, and finally the attachment of the two horns at the cervix was divided and the uterus removed from the abdominal cavity. This was immediately transferred into a dish containing 10% fetal calf serum (FCS) diluted in Dulbecco's Modified Eagle Medium (DMEM/ Gibco BRL)) where remaining pieces of fat and other tissue were removed. No further dissection was performed at this stage and the uterus was transferred in the FCS/DMEM solution to the dissection room for further manipulation under a dissecting microscope.

2.4.3 – Dissection of conceptuses

Under a dissecting microscope, two sharp dissecting forceps (watchmaker's no 5) were used to split the uterine wall at the end of each uterine horn. Once the initial opening was made, the forceps were again used to extend the opening along the length of each horn, taking particular care not to damage the conceptuses. Once the uterine wall was opened, each conceptus was gently pushed free into the medium using the blunt edge of the forceps. The conceptuses were then transferred to fresh medium (FCS/DMEM) for continuing dissection. The decidua and amniotic cavity were opened and the umbilical vessels severed in order to free the embryo. Any residual pieces of amniotic membrane were carefully removed. The embryos were then carefully transferred, using pipettes,

through three different ice cold phosphate buffered saline (PBS) solutions to be washed free of blood and other debris and in order to be assessed for growth and development.

2.4.4 – Assessment of embryos

The embryos were first assessed for any gross morphological abnormalities. If any were present, the embryos were photographed (section 2.10.1). The developmental stage of the embryos was then determined by counting somite pairs. This was done by first identifying the limb buds and taking the first somite beyond the fore limb bud to be somite 11 and the first somite beyond the hind limb bud to be somite 27. The total number of somites were then counted on from those reference points. The determination of somite number could only be accurately achieved up to E12.5. The size (and by implication the growth) of embryos was assessed by measuring the crown-rump length using an eyepiece graticule at constant magnification.

2.4.5 – Embryo fixation and embedding

Following the three PBS washes, the embryos were processed and fixed appropriately depending on their subsequent use. Embryos solely intended for histological analysis were fixed in Bouin's fixative. These embryos were kept in Bouin's at 4 ^{o}C until they were ready for embedding. Embryos that were intended for any other use, including *in situ* hybridisation and immunohistochemistry, were fixed with 4% paraformaldehyde (PFA) in PBS. The length of the fixation period depended on the embryo size. Embryos at E9.5 and 10.5 were fixed for 24 hours whilst bigger embryos were maintained in fixative for 48 hours. At the end of the fixation period, the embryos were taken through three PBS washes and were dehydrated through a series of ethanol solutions (30%, 50%, 70%, 85%, 95%, and 100% in DEPC-H_20) for 30 minutes each. The dehydration process could be

stopped when the embryos were in the 70% ethanol solution and the embryos could then be stored at 4 ^{o}C to continue the process at a later date. Following the 100% ethanol, embryos were taken through one 15 minute wash with 50% ethanol in Histoclear (National Diagnostics) and two 15 minute washes in Histoclear. They were then put for 20 minutes in a 55 ^{o}C oven in 50% Histoclear in wax and then taken through two 30 minute paraffin wax (Raymond Lamb) solutions in the oven before being embedded in paraffin wax. Embryos at E11.5 or older were embedded using plastic moulds whereas smaller embryos were embedded in glass moulds using a dissecting microscope to ensure the appropriate orientation. Alternatively, embryos that were destined for use in whole-mount *in situ* hybridisation experiments were dehydrated using methanol rather than ethanol. Following the three PBS washes, these embryos were processed through four 30 minute washes (25%, 50%, 75% and 100% methanol) and were then stored in 100% methanol at -20 ^{o}C until their intended use.

An alternative embedding protocol was used for embryos that had been stained after a whole-mount *in situ* hybridisation experiment. If vibratome sectioning of these embryos was required (section 2.6.4), these embryos were embedded using a special vibratome embedding mixture. This was prepared by dissolving 4.5 g of gelatin in 800 ml of PBS and adding 270 g of albumin and 180 g of sucrose to the solution. The mix was then aliquoted in 20 ml tubes and stored at -20 ^{o}C. The embryos to be embedded were equilibrated with the mix and placed on the side of the embedding mould. The final embedding mixture was prepared by diluting 25% glutaraldehyde 1/10 in the original mix. The final mix was stirred vigorously and the embryos orientated in the solution. The embryo orientation had to be carried out quickly as the solution set within approximately

one minute. The blocks were kept at 4 °C for one hour and could then be cut or stored by wrapping in clingfilm or by removing from mould and placing in sterile PBS at 4 °C.

2.5 – WHOLE EMBRYO CULTURE

2.5.1 – Preparation of rat serum

Rat serum was used as a key component of the culture medium. It was prepared from blood obtained from old, male rats. The animals were anaesthetised by being placed in a dessicator containing ether. Anaesthesia was maintained by placing a paper cone, containing ether-soaked tissue paper, over the animal's head during dissection. The abdominal wall was cleaned using 70% industrial methylated spirit (IMS) and the abdomen opened using a midline incision. The aorta was identified in the retroperitoneum and the blood was removed from the aorta using a 10-ml syringe until the animal died of exanguination. The blood was then centrifuged at 3500 g for 5 minutes. This resulted in pelleting of the red blood cells and the formation of a fibrin clot in the supernatant. The fibrin clot was squeezed using sterile forceps and the solution centrifuged again. The serum in the supernatant was then pooled from different tubes and centrifuged again to remove any remaining red cells. The serum was then heat inactivated at 56 °C for 30 minutes and then aliquoted into 5-ml tubes and stored at –20 °C until required.

2.5.2 – Embryo harvest

The embryos for culture were harvested on E10.5 between 12:00 and 13:00. All dissection instruments were cleaned with 70% IMS. After killing the pregnant mice by cervical dislocation, the uterus was exposed with a curved, transverse, lower abdominal

incision as described in section 2.4.2. From that point onwards, the technique for harvesting embryos for culture was modified from that described in section 2.4.2 as follows. Each uterine horn was separately freed from the associated ovary and cleaned from fat before being held with tension away from the abdomen, still attached to the cervix. The tension allowed opening of the uterine wall using fine, iridectomy scissors without damaging the conceptuses. After making a small initial opening at the end of the uterine horn, the uterine wall was opened along the length of the horn by inserting the tip of one blade into that opening and moving the blade towards the cervix. Damage to the underlying conceptuses was avoided by maintaining the horn under tension and the tip of the blade pointing away from the conceptus. Once the entire length of the uterine horn was opened, the conceptuses were teased off the uterus using the blunt edge of a forceps blade and transferred into prewarmed (at 37 $^{\circ}$C) 10% FCS (in DMEM) in order to be transported to the dissection room for further dissection under the microscope.

2.5.3 – Microscopic dissection

Subsequent dissection took place in freshly prepared explanting solution (Table 2.1) under a dissecting microscope. Using fine dissecting forceps, the decidua was carefully removed, followed by the fine Reichert's membrane to expose the yolk sac. A hole was then made in the yolk sac, near its junction with the placenta, towards the caudal end of the embryo. Continuing to use the forceps, the tear in the yolk sac was extended along the equator of the conceptus. This extension was made by picking up the free edge of the yolk sac with forceps and pulling in opposing directions. In this way, the risk of severing major yolk sac blood vessels was reduced. The yolk sac was opened for about three quarters of its circumference so that the embryo could be exteriorised. The yolk sac was then tucked under the caudal end of the embryo. Finally, the embryo was fully

exteriorised by removing the fine amniotic membrane, that is adherent to the embryo, by careful dissection (Cockroft, 1990).

2.5.4 – Culture conditions

2.5.4.1 - Preparation of the culture medium

The embryos were cultured in 25% rat serum diluted in freshly prepared culture solution (Table 2.1). Before use, the thawed rat serum was filtered using a 0.45 μm filter. Each embryo was cultured in individual culture tubes in 2.5 ml of culture medium. For some embryos, either 10 μl of dimethylsulphoxide (DMSO) or 10 μl of 50 mM z-vad-FMK in DMSO (giving a final z-vad-FMK concentration of 200 μM), were added to the culture medium.

2.5.4.2 - Culture technique

The culture medium was prepared in special culture tubes (Nunc 10 ml plastic tubes) before the final stage of embryo dissection and equilibrated in the culture incubator at 37 °C. Before being placed in the incubator, the medium was pre-oxygenated as follows. Forty per cent oxygen (5% CO_2, 55% N_2) was delivered for two minutes using a glass pipette the tip of which was kept away from the wall of the tube and the surface of the medium. This gave enough flow so that it did not create bubbles in the medium, but ruffled the surface of the media continuously. The aim of this was to saturate the tube with the oxygen/ CO_2 mixture. In order to minimise gas leaks, grease was applied to the top of the tube, and during subsequent gassings the tube top was only minimally displaced to allow introduction of the glass pipette. This method of gassing was used during all subsequent gassings in the presence of the embryos. Following dissection, the

Table 2.1 Composition of explanting and culture solutions

Reagent	Explanting solution g/l	Culture solution g/l
NaCl	6.9	6.9
KCl	0.3	0.3
$MgSO_4.7H_2O$	0.1	0.1
$MgCl_2.6H_2O$	0.05	0.05
$NaH_2 PO_4.H_2O$	0.1	0.1
$CaCl_2.2H_2O$	0.27	0.27
$NaHCO_3$ *	0.5	2
Glucose *	1.5	2

* The solution was prepared and autoclaved before the addition of the glucose and the sodium bicarbonate. When either solution was required, the appropriate amounts of the two reagents were added to the autoclaved solution and the resulting solution was filtered through a 0.45 μm filter.

embryos were carefully transferred using a pipette into the prewarmed medium and gassed again. They were then placed onto rotating rollers in the incubator (at 38 °C) and gassed again at 6 and at 16 hours.

2.5.4.3 - Embryo assessment

During dissection, embryos were discarded if major yolk sac blood vessels were damaged, leading to significant haemorrhage and exsanguination. Embryos were included in the culture experiment if they satisfied the following criteria at the time of dissection and at the first check at 30 minutes after the beginning of the culture: (i) the presence of a

regular and vigorous heartbeat with a minimum rate of 60 beats per minute and (ii) the presence of blood flow in the umbilical, head and neck vessels. The same criteria were used in the final assessment at 18 hours in order to determine which embryos would be included in the experimental analysis. Embryos failing either criterion were discarded without analysis. Those that showed milder signs of ill health at the final assessment, for example a mild degree of oedema, but which satisfied criteria (i) and (ii) above, were judged to be alive and were included in the study.

2.6 – EMBRYO SECTIONING

2.6.1 – Equipment used

An Optech instruments model HM 330 rotary microtome was used to section wax embedded embryos. For sectioning whole-mount *in situ* hybridisation embryos, a Vibratome 1000 from Technical Products International was used.

2.6.2 – Preparation of slides

Glass slides were coated with 3-aminopropyltriethoxysilane (TESPA) before use in order to improve adherence of tissue sections. Slides were placed in racks and immersed for10 seconds in of 8% TESPA in acetone. This was followed by two 10 second washes in acetone before washing in MilliRo water and drying overnight in a 30 °C oven. The following day, the slides were removed from the racks, put back in their container and stored at 4 °C. Newly TESPA-coated slides were used within two months or were recoated for maximal effect. If the slides were required for ISH, then the glass jars used for the TESPA-coating as well as the racks loaded with the slides were baked first in a 180 °C oven for four hours. In this case, the water used for the slide preparation was

DEPC treated (0.5-1 ml DEPC per litre of MilliQ water). The DEPC/water solution was allowed to settle overnight before autoclaving. After TESPA coating, the slides were kept in their racks, wrapped in aluminium foil, until used.

2.6.3 – Sectioning technique

For the majority of embryos, only the relevant parts of the embryo were sectioned and analysed. Thickness of sections varied between 5 and 10 micrometres and sequences of sections were transferred onto slides with water that had been prewarmed on a hot-plate (25 °C). As soon as the wax wrinkles disappeared, the water was drained using a pipette and any excess moisture was removed with tissue. The slides were then placed onto a drying rack and placed in a 30 °C oven overnight. Following the drying period, they were wrapped and stored at room temperature.

2.6.4 – Obtaining vibratome sections

This was used to obtain sections from embryos in whole-mount *in situ* hybridisation experiments, which had been embedded in vibratome mix as described in section 2.4.5. The embryo blocks were trimmed so that their base was larger than their height to optimise sectioning, then positioned in the mounting tray using superglue and the mounting tray was filled with sterile PBS. Thirty to fifty μm sections were then cut, transferred onto glass slides and mounted with 50% glycerol/PBT. The slides were subsequently stored in flat slide holders at 4 °C and were regularly assessed for evidence of drying up and the glycerol/PBT solution was replenished.

2.7 – STAINING TECHNIQUES

2.7.1 – Haematoxylin & eosin staining

Haematoxylin & eosin (H&E), which stains both the nucleus and the cytoplasm, was used for general histology. Paraffin sections were dewaxed in Histoclear for 10 minutes and then rehydrated through a series of 30 second washes with IMS solutions (100%, 95%, and 70%) and a rinse in MilliRo water. They were then immersed in Ehrlich's haematoxylin (DPH) for 2.5 minutes and rinsed again in MilliRo water until the sections appeared blue. After rinsing under running tap water for five minutes, excess haematoxylin was removed by quickly dipping in acid alcohol solution (1% HCl in 70% ethanol) before immersion in tap water until the sections turned blue again and then staining in 1% eosin (Raymond Lamb) for two minutes. The slides were finally rinsed under running tap water until the water ran clear and then were dehydrated through a series of 30 second IMS washes (70%, 95%, and 100%). After being placed in Histoclear for another ten minutes, sections were mounted using dextropropoxyphene (DPX, Fisher Scientific) medium and air dried.

2.7.2 – Methyl Green staining

This is a nuclear stain and was used to counterstain sections from immunohistochemistry experiments. Following completion of staining with 3,3-diaminobenzidine tetrahydrochloride (DAB), sections were washed twice in water and placed in methyl green for ten minutes. They were then taken through three water washes (10, 10 and 30 seconds respectively) and taken through three rinses of butanol (BDH) (10, 10 and 30 seconds respectively) before finally being taken through two changes of Histoclear (30

seconds and 5 minutes respectively). They were then mounted using DPX mounting medium and allowed to air dry in an extraction hood.

2.7.3 – Periodic Acid Schiff (PAS) staining

This histochemical stain stains mucopolysaccharides a deep magenta colour. Sections were dewaxed in Histoclear for five minutes and then rehydrated through a series of IMS solutions (100%, 95% and 70%) for 30 seconds each. They were then rinsed with water and placed in the Periodic Acid solution for 10 minutes. They were then rinsed with MilliRo water, placed under tap water for one minute and then rinsed once again with MilliRo water. They were then placed in Schiff's reagent (pararosaniline HCl 1%, sodium bisulfite 4% in HCl) for twenty minutes, rinsed in MilliRo water and washed under tap water for another five minutes. They were then counterstained with Mayer's haematoxylin for one minute, washed under tap water for five minutes and then dehydrated through an IMS series (70%, 95% and 100%) for 30 seconds each. They were then placed in Histoclear for five minutes and mounted as described above

2.8 – IMMUNOHISTOCHEMISTRY

2.8.1 – General principles

Paraffin sections were pre-treated with Declere (Cell Marque Corp, USA) in order to enhance the exposure of epitope sites as well as for the purpose of dewaxing. The slides were immersed in Declere, diluted 1 to 20 with distilled water, and placed in the microwave (*at medium*) for 20 minutes. At the halfway point, the slides were checked to ensure that they were still well covered by the Declere solution. At that point, fresh diluted Declere solution was placed separately in the microwave and allowed to boil. At

the end of the 20 minutes, the slides were transferred to the fresh Declere solution and allowed to cool down to room temperature for 15 minutes. They were then taken through two quick water washes and three washes in Tris-buffered-saline-Triton X-100 buffer (TBS-TX: 50 mM Tris HCl pH 7.5, 150 mM NaCl, 0.5% Triton X-100 in water; the first two for ten seconds, third for five minutes) and then treated with 0.6% H_2O_2 (in 0.05 M Tris-HCl) for 7.5 minutes. Following three more TBS-TX washes, the slides were incubated for an hour in 10% fetal calf serum (in TBS-TX) at room temperature before overnight exposure to the primary antibody at 4°C. The primary antibody was diluted appropriately (Table 2.2) using 1% FCS (in TBS-TX) and 80 µl of the diluted antibody was applied to each slide. Parafilm was used to ensure adequate spread of the antibody and to prevent drying of the slides. The slides were then placed in a humid container. The following day the slides were taken through three TBS-TX washes, the diluted secondary antibody was applied in an identical manner as for the primary antibody and a two hour incubation was performed at room temperature. They were then washed with TBS-TX and developed using ABComplex and DAB. The ABComplex was prepared 30 minutes before the intended use and 6 drops were applied to each slide which were then placed in a moist environment without parafilm for 30 minutes. DAB was prepared, filtered with a 0.45 µm millipore filter and applied to the slides. In order to optimise staining, the development of one of the slides was monitored under the microscope. The duration of DAB staining ranged from 15 to 30 minutes according to the antibody and no further specific staining could be achieved after that because of enzyme kinetics. Non-specific staining appeared beyond that time point and this was avoided. Sections were counterstained with methyl green, dehydrated and mounted in DPX mounting medium, as described in section 2.7.2.

2.8.2 – Antibodies used

The antibodies used and their dilutions are shown in Table 2.2.

Table 2.2 Antibody details

Primary antibody	Source	Immunogen type	Dilution	Secondary antibody	Source	Dilution
Nkx2.1	NeoMarkers MS-699-P1	Mouse monoclonal IgG_1	1:100	Biotinylated Rabbit Anti-Mouse	DAKO E0354	1:400
Hnf3β	DSHB* 4C7	Mouse monoclonal IgG_1	1:100	Biotinylated Rabbit Anti-Mouse	DAKO E0354	1:400
Shh	Santa Cruz N19	Goat polyclonal IgG	1:200	Biotinylated Rabbit Anti-goat	DAKO	1:250
Caspase 3	Cell Signaling 9661S	Rabbit polyclonal IgG	1:1000	Biotinylated Goat Anti-Rabbit	DAKO E0432	1:250
Phospho-histone H3	Upstate 06-570	Rabbit polyclonal IgG	1:200	Biotinylated Goat Anti-Rabbit	DAKO E0432	1:400

*- Developmental Studies Hybridoma Bank

2.9 – IN SITU HYBRIDISATION

2.9.1 – Preparation of gene probes

2.9.1.1 - Transformation of bacteria

Competent *Escherichia coli* (*E. Coli*) cells were used for transformation with circular plasmids containing a cDNA of interest. Competent cells were taken from –80 °C and thawed on ice. For each plasmid, 50 µl aliquots of competent cells were gently pipetted into premarked plastic tubes and kept on ice for 45 minutes. The tubes were then placed in a water bath at 42 °C for 45 seconds and then chilled on ice for two minutes. LB broth (500 µl) was added to each tube and they were placed on a shaker for 90 minutes. At the end of this period, 200 µl of cells were placed on LB agar plates and spread with a loop. The plates were placed in a 37 °C oven overnight.

2.9.1.2 - Isolation of plasmid DNA/ DNA purification

Agar plates containing bacterial colonies were removed from the 37 °C oven, wrapped in clingfilm and placed at 4 °C until use. Fresh LB broth was prepared to which 1 µl/ml of ampicillin was added. Universal containers were marked (three for each plasmid) and 5 ml of the LB broth/ ampicillin mix was added to each container. The agar plates were then inspected and isolated colonies were identified on the plate. The colonies were touched using an autoclaved pipette tip and the tip was then placed into the LB broth mix. The containers were then placed in a shaker, at 37 °C overnight. The next morning, 1.5 ml of LB-broth was taken from each universal and placed into separate Eppendorf tubes. Cells were pelleted by centrifugation for two minutes at 10000 g. Plasmid was then isolated using the Promega Wizard plasmid isolation kit according to the manufacturer's

instructions. Briefly, excess fluid was discarded and the Eppendorfs were refilled with 1.5 ml of LB-broth and centrifuged again. All excess fluid was pipetted off to leave the pellet at the bottom of the tube. The pellets were resuspended using 200 µl of cell resuspension solution and cells were then lysed using 200 µl of cell lysis solution. The tubes were gently inverted four times to mix cells and solution. Neutralisation solution (200 µl) was added and the tubes were again inverted several times to achieve adequate mixing. The purpose of this step is to denature the bacterial chromosomal DNA and proteins, producing a white precipitate. The lysate was then centrifuged for five minutes at 10000 g in order to pellet the bacterial chromosomal DNA and leave the plasmid DNA in solution. In order to purify plasmid DNA, the plunger was removed from a 2.5-ml syringe (one syringe per lysate) and the syringe attached to a microcolumn. One millilitre of DNA purification resin, together with the clear lysate from the previous step, were added to each syringe. The plunger was then reintroduced onto the syringe and the resin/lysate mix was pushed through the microcolumn. The syringe was removed from the microcolumn and the plunger was removed from the syringe. Two ml of column wash solution (containing ethanol) was introduced into the syringe, the plunger was reintroduced, the syringe was reattached to the microcolumn and the wash solution was pushed through the microcolumn. The microcolumn was then removed from the syringe, attached to an Eppendorf microcentrifuge tube and centrifuged at 10000 g for two minutes. The microcolumn was then transferred to a new microcentrifuge tube and the DNA was eluted from the column by adding 50 µl of sterile water to it, waiting for one minute and then centrifuging the tube at 10000 g for twenty seconds. The microcolumn was then removed and discarded and the Eppendorf tubes containing the eluted plasmid DNA were stored at –20 °C until use.

2.9.1.3 - Digestion of plasmid DNA

Once plasmid DNA had been isolated, it was checked for the presence of the required DNA insert using restriction endonucleases that cleave the DNA at specific sites. Two microlitres of plasmid were mixed with 1 µl of endonuclease, 2 µl of buffer and 15 µl of sterile water and kept at 37 °C for 90 minutes. The solution was then electrophoresed through a 1% agarose gel to confirm the presence of the appropriate DNA fragment. Once the presence of the expected insert site was confirmed, a large scale digestion was carried out in order to prepare enough linearised plasmid to allow preparation of labelled probes for *in situ* hybridisation. Twenty microlitres of plasmid, 5 µl of the appropriate endonuclease, 20 µl of the appropriate buffer and 155 µl of sterile water were incubated in a 37 °C waterbath for three hours, purified by precipitating with 400 µl of ethanol and 10 µl of sodium acetate and stored at – 20 °C overnight. Before precipitation, the success of linearisation was checked by gel electrophoresis. Before proceeding to synthesis of the probe, the DNA was resuspended and tested again for integrity of the DNA. It should be noted that from this point onwards, only DEPC-treated solutions and pre-packed pipette tips were used to avoid contamination by RNA-ases. The samples were centrifuged at 13000 g for 15 minutes (4 °C), the pellet was washed with 200 µl of freshly made 70% ethanol and centrifuged again at 13000 g for 5 minutes. The excess fluid was removed with a pipette and the pellet was air dried for 10 minutes, resuspended in 20 µl of DEPC-water and stored at -20 °C until use. Before freezing, 2 µl of each sample was run on a 1% agarose gel.

2.9.1.4 - Synthesis of digoxigenin(DIG)-labelled RNA probes

Synthesis of the labeled RNA probe was carried out using a Boehringer-Mannheim DIG-labeling kit. One microlitre of linearised plasmid DNA was mixed with 2 µl of DIG RNA

labeling mix, 2 µl of 10x transcription buffer, 1 µl of RNAase inhibitor, 2 µl of the appropriate RNA polymerase and 12 µl of DEPC-water and incubated at 37 °C for two hours. The result was checked by running 1 µl of the DIG-labeled RNA transcript on a 1% agarose gel. The amount of probe synthesised was estimated by comparing the brightness of the RNA and DNA bands on the electrophoresis gel. The transcription reaction was stopped using 2 µl of EDTA solution (pH 8.0) and precipitated using 2.5 µl of 4 M LiCl and 75 µl of ethanol, pre-chilled at – 20 °C. The probe was then stored at – 20 °C overnight. The labelled probe was then resuspended by centrifuging at 13000 g (4 °C) for 15 minutes, washing with 200 µl of 70% ethanol and recentrifuging for 5 minutes at 13000 (4 °C). The pellet was air dried for 5 minutes before dissolving in 100 µl of DEPC-water. The probe was either used straight away in the *in situ* hybridisation experiment or kept at – 20 °C for further use.

2.9.2 – Whole-mount *in situ* hybridisation

In situ hybridisation on whole embryos was performed as already described (Copp et al, 1999) with minor modifications.

2.9.2.1 - Embryo pre-treatment and hybridisation

The embryos to be used in this experiment had been stored in 100% methanol at – 20 °C. Storage in methanol is essential for the prevention of gas bubble formation during the subsequent use of hydrogen peroxide. The embryos were rehydrated by taking them through a series of washes in 75%, 50% and 25% methanol in PBT (0.1% Tween-20 in PBS) followed by two washes with PBT. The rehydration process was carried out with the embryos on ice on a slow rocker. The embryos were then bleached with 6% hydrogen peroxide in PBT for one hour. This was followed by three washes with PBT. Embryos

were then treated with proteinase K (5 μg/ml in PBT) in order to digest protein and unmask RNA sites. Exposure to proteinase K was for 10 minutes for the E11.5 embryos and for 7 minutes for the E10.5 embryos. The embryos were then washed in glycine (2 mg/ml in PBT) to inactivate proteinase K followed by two quick PBT washes. They were then refixed in glutaraldehyde (0.2% in PFA) for 20 minutes followed by two PBT washes. The embryos were then transferred to 2 ml microtubes and 0.5 ml of prehybridisation mix (50% formamide, 5x SSC pH 4.5, 1% SDS, 50 μg/ml yeast RNA, 50 μg/ml heparin) was added to each tube. The embryos were incubated in the prehybridisation mix for two hours at 70 °C. After the prehybridisation stage, the embryos were stored at -20 °C until further use or used immediately for the *in situ* hybridisation procedure. Otherwise, the prehybridisation mix was removed and replaced with 0.5 ml of hybridisation mix which was made by adding 10 μl of digoxygenin-labelled RNA probe to 0.5 ml of freshly made prehybridisation mix (1 μg/ml concentration of probe). The embryos were incubated in a 70 °C water bath overnight.

2.9.2.2 - Post-hybridisation

The embryos were transferred to bigger polystyrene tubes and most of the hybridisation mix was pipetted off. The embryos were washed twice (20 minutes each) at 70 °C with wash solution I (50% formamide, 5x SSC, 1% SDS) and twice (20 minutes each) at 65 °C with wash solution II (50% formamide, 2x SSC pH 4.5). This was followed by three five minute washes at room temperature with TBST working solution. The TBST solution was prepared as follows: 40 g of NaCl, 1 g of KCl, 125 ml of 1M Tris pH 7.5 were added to 500 ml of water and then autoclaved to make 10x TBST solution. Then 50 ml of 10x TBST, 5 ml of Tween-20, 0.2 g of Levamisol were mixed and made up to 500 ml with water to make the TBST working solution. The embryos were preblocked with 10%

sheep serum in TBST for 90 minutes at room temperature. The antibody solution was prepared concurrently. A tube of embryo powder was thawed. This had been previously prepared as follows: Ten litters of E12.5 CD1 mouse embryos were homogenised in PBS, diluted by 20% in ice-cold acetone and incubated on ice for 30 minutes. The solution was then centrifuged at 10000 g for two hours, the supernatant was removed, the pellet was washed with ice-cold acetone and centrifuged again. The pellet was then spread and ground into a very fine powder on a sheet of filter paper and allowed to air dry. The powder was then stored in an air-tight tube at – 20 °C. TBST solution was added to the thawed embryo powder. The amount of TBST solution required was 5 ml per tube of embryos used in the experiment The solution was heated at 70 °C for 30 minutes and 25 µl of sheep serum and 1.5 µl of anti-digoxygenin antibody per embryo tube were added to it. The solution was kept on ice and shaken gently for 60 minutes to allow for adequate preabsorption of the antibody. The solution was centrifuged at 3000 g for 10 minutes and the supernatant was filtered using a 0.45 µm filter. The antibody was added to the embryo tubes (3 ml per tube) and the tubes were placed on a slow rocker at 4 °C for one to three days.

2.9.2.3 - Post-antibody development

The embryos were taken through three five-minute TBST washes followed by five one-hour TBST washes and left rocking overnight at room temperature. The next day the embryos were taken through four ten-minute NTMT (0.1M NaCl, 0.1M Tris HCl pH 9.5, 0.05M $MgCl_2$, 0.1% Tween-20, 0.02 g/ 50 ml of Levamisol) washes. They were then transferred to glass tubes and 18 µl of NBT solution was added per ml of NTMT. The tubes were wrapped in foil, placed in a light box and left to rock gently at room temperature. The embryos were checked for colour development initially every half an

hour. When colour development was considered adequate (staining of areas of established gene expression and before background staining appeared), the reaction was stopped by washing the embryos twice with PBT. The embryos were stored in PBT solution with the addition of thimerizole (0.02%) to prevent fungal growth at 4 °C in the dark. The embryos could then be embedded in albumin/gelatin mixture (section 2.4.5) and sectioned on a vibratome for further analysis (section 2.6.4).

2.9.3 – *In situ* hybridisation on sections

In situ hybridisation on paraffin embedded sections was performed using digoxygenin-labelled riboprobes for *Shh* and *Ptch*, as previously described (Breitschopf et al., 1992) with minor modifications.

2.9.3.1 - Pre-hybridisation treatment

Slides bearing wax-embedded embryo sections were de-waxed by immersion in two ten-minute Histoclear washes followed by two three-minute washes with ethanol. The sections were then rehydrated by taking them through two-minute washes with 90%, 70% and 50% IMS and then through one two-minute wash with freshly prepared PBS. The slides were then placed in freshly prepared 4% PFA in a fume hood for 20 minutes and then taken through two two-minute PBS washes. The slides were then exposed to 20 μg/ml proteinase K for eight minutes and then taken through two two-minute PBS washes. They were then placed back in the 4% PFA solution in the fume hood for a further five minutes, followed by two more PBS washes. The slides were then placed in 0.1M triethanolamine solution in the presence of a stirrer in a fume hood and acetic anhydride (0.25%) was drizzled over the sections. The purpose of this step is twofold: first to stop proteinase K activity and second to prevent non-specific electrostatic binding

of the probe to the sections by masking positive charges on the sections. This step was followed by two more PBS washes and the sections were dehydrated through the same alcohol series and allowed to air dry.

Hybridisation mix was prepared as for the whole-mount experiment (section 2.9.2.1) with the addition of 1 µl/ml of RNAguard and 0.5 mg/ml of tRNA. The complete hybridisation mix was applied to the slides (80 µl per slide) and the slides were covered with fresh coverslips. The rack was then placed in a light tight box in the presence of tissue paper soaked in 50% formamide in 2x SSC. The boxes were sealed with tape and nescofilm and double bagged to preserve moisture before being placed in a 65 °C oven overnight. At all times, the slides were kept horizontal.

2.9.3.2 - Post-hybridisation

The coverslips were gently washed off the slides by placing the rack in 2x SSC solution at 65 °C. The slides were then washed twice (20 minutes each) in 50% formamide in 2xSSC, twice (30 minutes each) in 2x SSC and twice (30 minute each) in 0.2x SSC at 65 °C. The purpose of these steps was to remove non-specific RNA binding. At the end of this series of washes, the slides were allowed to cool down to room temperature.

2.9.3.3 - Antibody detection

The slides were then put in a buffer (B1) solution (0.1M Tris HCl, 0.15M NaCl pH 7.6) for two minutes and then blocked with 10% FCS in B1 in a humid chamber for 60 minutes. The blocking solution was then drained and 300 µl of anti-digoxygenin antibody was applied to each slide. The sections were then covered with nescofilm coverslips. The antibody dilution was 1:1000 in 2% FCS in B1 buffer. The slides were left in a humid

chamber at 4 °C overnight. The next day, the slides were taken through three three-minute B1 washes and then two equilibrating ten-minute B2 (0.1M tris HCl pH 9.5, 0.1M NaCl, 0.05M $MgCl_2$) washes. The developing reagent was then prepared in a light-protected container: 18 µl of NBT/BCIP (Boehringer-Mannheim) was added per ml of B2 buffer, and then 0.5 ml of this solution applied to each slide. The reaction was stopped with tap water when the characteristic bluish staining appeared. The sections were then dehydrated through an IMS series, taken through two ten-minute Histoclear washes and mounted using Vectra mount. This mounting medium was used instead of DPX because it caused minimal fading of the staining.

2.10 – PHOTOGRAPHY AND IMAGE PROCESSING

2.10.1 – Photography of whole embryos

Embryos were photographed using a camera attached to the stereo-microscope (Zeiss SV11). The negatives were scanned (Filmscan 1800, Microtec scanner) and the images stored as JPEG files.

2.10.2 – Digital photography and image analysis

A Zeiss Progres digital camera, attached to a Zeiss Axiophot II microscope was used to capture digital images which were imported and processed using Adobe Photoshop 5.2 software. Image parameters, such as brightness, contrast and colour balance were adjusted in order to achieve optimal visualisation of the image, without altering its nature or content.

2.11 – DATA ANALYSIS AND STATISTICS

2.11.1 – Graph creation

All data were represented by vertical box plots prepared using Sigmaplot (version 4.01) software. Vertical boxes with error bars define the median, 10^{th}, 25^{th}, 75^{th} and 90^{th} percentile values and all outlying values are represented by dots. This type of graph was used throughout the thesis unless specified, and was chosen in preference to mean +/- standard error plots because of the lack of normality in some of the data.

2.11.2 – Statistical analysis

Statistical analysis was performed using Sigmastat (version 1.0) software. The tests used were the unpaired t test (where data were normal) or the Mann-Whitney test (if normality failed) when comparing two groups of data. The chi square analysis of contingency tables was used to determine significant association between two different parameters. Alternatively, if there were fewer than five expected observations in any cell of a 2x2 contingency table, the Fisher exact test was used. A p value smaller than 0.05 was considered significant. Allowance for multiple comparisons using the same set of data (protection of α level) was made by requiring the value of the test statistic (e.g. student's t) corresponding to 0.05/No. tests to be excluded in order to achieve significance at p=0.05.

CHAPTER 3 – MOUSE MODELS OF TRACHEO-OESOPHAGEAL MALFORMATIONS

3.1 – INTRODUCTION

The close phenotypic similarity between the tracheo-oesophageal malformations in the Adriamycin-rat model and the human malformations, have made the model a useful tool in the study of the abnormal embryogenesis that underlies these defects.

Despite its obvious advantages, however, the Adriamycin rat model has an inherent problem. Although the laboratory rat has, for many years, played a significant role in efforts to improve our understanding of human biology, the study of the rat genome is only at its preliminary stages (Hancock, 2004). The relative paucity of molecular probes and markers available for the rat compared to the mouse has meant that, despite extensive morphological analysis of the model, little progress has been made in deciphering the complex molecular mechanisms that underlie tracheo-oesophageal malformations. This problem has been compounded by the fact that all genetic models of foregut malformations have been described in the mouse. On the other hand, the global loss of function of a gene, as seen in the genetic models, leads to extensive foregut defects and is unlikely to be a very good representation of the embryological events that lead to specific tracheo-oesophageal malformations in humans. In that respect, the rat model is a much better research tool.

These considerations suggested the need to adapt the Adriamycin model to the mouse.

Moreover, the value of such an adaptation would be greatly increased if the abnormal organogenesis in the Adriamycin model could be studied in close conjunction with that in the genetic models of tracheo-oesophageal malformations. The *Shh* null mutant mouse embryo would be a good candidate for such a parallel study. It has been described as having foregut malformations, including OA/TOF and the role of *Shh* in mouse biology has been extensively studied in a number of organ systems. However, the review of the published literature does not lead to a clear understanding of the foregut morphology in the *Shh* null embryos. For this reason, further clarification and detailed description of the tracheo-oesophageal morphology in the mutant embryos would be desirable.

This chapter describes the development of an Adriamycin mouse model of tracheo-oesophageal malformations based on the work on the rat model as well as preliminary work on the effect of Adriamycin on mouse embryos. Aspects of normal tracheo-oesophageal development that are still a matter of debate are also addressed. Furthermore, the tracheo-oesophageal morphology in the *Shh* null embryos is described and comparisons are made with the Adriamycin-treated mouse embryos.

3.2 – RESULTS

3.2.1 – The Adriamycin mouse model of tracheo-oesophageal malformations

3.2.1.1 - Normal tracheo-oesophageal development in the mouse

Stages of tracheo-oesophageal separation

In the CBA/Ca strain (a commonly used inbred strain of mouse), there is no evidence of the respiratory primordium at E9.5 (15-20 somite stage) (Fig. 3.1a&c insets). In the pharyngeal foregut, an epithelial thickening in the ventral midline denotes the position of the thyroid primordium and the epithelium of the laterally placed pharyngeal pouches is also prominent (Fig. 3.1a inset). The foregut maintains a wide configuration. Further caudally, the ventral hepatic diverticulum denotes the junction between the foregut and midgut (Fig. 3.1c inset). By about E10 (20-25 somite stage), a ventral evagination has appeared in the floor of the post-pharyngeal foregut and is known as the laryngotracheal groove. The groove is the primordium of the infraglottic larynx and trachea. At the caudal end of this groove, the primitive lung buds are seen growing in a ventrolateral direction and will form the future bronchi and lungs. By E10.5 (25-30 somite stage), during a period of rapid longitudinal growth, the prospective trachea has gained significant length but is still part of an undivided foregut (Fig. 3.1a,b). At its cranial end, the laryngotracheal groove persists (Fig. 3.1a). At its caudal end, the primitive lung buds continue to grow and have started to separate from the main foregut tube (Fig. 3.1c). By E11 (30-35 somite stage), the ventral trachea has started to separate from the dorsal oesophagus. This separation starts at the level of the lung buds. In the meantime, the

Fig. 3.1 Tracheo-oesophageal development in the CBA/Ca mouse (E9.5 – E12.5)

Diagrams of early tracheo-oesophageal development (cranial to top, caudal to bottom; dorsal to right, ventral to left) and transverse sections stained with haematoxylin and eosin, through E10.5 (*a, b, c*), E11.5 (*d, e, f*) and E12.5 (*g, h, i*) saline treated embryos. Sections correspond to the levels indicated in the schematic representations of the foregut. Insets in (*a*) and (*c*) are from corresponding levels from an E9.5 embryo. ***(a ,b, c)*** At E9.5, in the pharyngeal foregut, epithelial thickening denotes the position of the thyroid primordium in the ventral midline (black arrowhead, inset in *a*) and the primordia of the pharyngeal pouches (blue arrowhead, inset in *a*). The foregut maintains the wide configuration of the pharynx as far caudal as the junction with the midgut, where a ventral evagination (black arrowhead, inset in *c*) denotes the hepatic diverticulum (level of pericardio-peritoneal canals, blue arrowhead in *c*). At E10.5, the laryngotracheal groove (Lt) is a ventral evagination of the foregut (Fo) appearing at the caudal limit of the pharynx. It represents the primordium of the subglottic larynx and trachea. At the caudal end of the groove the primitive lung buds (Lb) are seen growing in a ventrolateral direction. At this stage, the respiratory foregut remains undivided. ***(d, e, f)*** By E11.5, the laryngotracheal groove can still be identified at the cranial end whilst at the caudal end the foregut has started to separate into a ventral trachea (Tr) and a dorsal oesophagus (Oe). The separation process (arrows in e) starts at the level of the lung buds and proceeds in a cranial direction. At its caudal end, the trachea is seen to bifurcate into the two bronchi (Br) that have developed from the lung buds. ***(g, h, i)*** By E12.5, only the cranial-most part of the laryngotracheal groove can be seen to be continuous with the lumen of the pharyngeal foregut (Ph) and has yet to separate from it. Just caudal to that level, the separation process has reached the larynx (La). Ao, aorta; At, atrium; s, atrial septum. Scale bars, 100 μm.

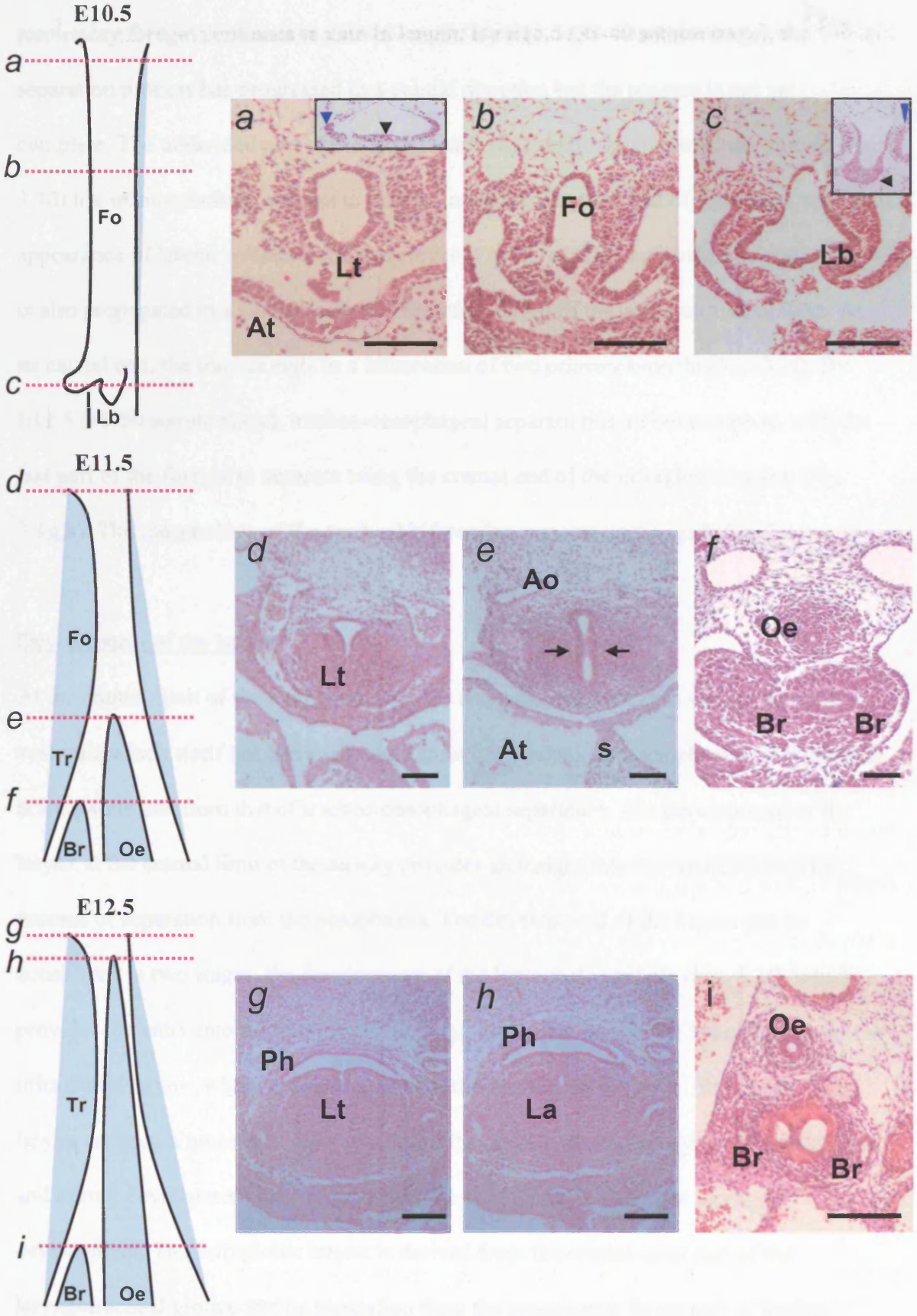
E10.5
a
b
c
Fo
Lb
a
Lt
At
b
Fo
c
Lb
E11.5
d
Fo
e
Tr
f
Br
Oe
d
Lt
e
Ao
At
s
f
Oe
Br
Br
E12.5
g
h
Tr
i
Br
Oe
g
Ph
Lt
h
Ph
La
i
Oe
Br
Br

respiratory foregut continues to gain in length. By E11.5 (35-40 somite stage), the separation process has progressed in a cranial direction but the process is not yet complete. The undivided part of the foregut still features the laryngotracheal groove (Fig. 3.1d) but its morphology appears to change just cranial to the level of separation with the appearance of lateral epithelial folds or ridges (Fig. 3.1e). The appearance of these ridges is also propagated in a caudal to cranial direction ahead of the process of separation. At its caudal end, the trachea ends in a bifurcation of two primary bronchi (Fig. 3.1f). By E12.5 (45-50 somite stage), tracheo-oesophageal separation is all but complete, with the last part of the foregut to separate being the cranial end of the infraglottic larynx (Fig. 3.1g,h). The morphology of the tracheal bifurcation remains unchanged (Fig. 3.1i).

Development of the larynx

At the cranial limit of the laryngotrachea, the entry into the airway is via the laryngeal vestibule which itself has to be separated from the pharynx and oesophagus. This process is a separate one from that of tracheo-oesophageal separation. The development of the larynx at the cranial limit of the airway provides an insight into the completion of the process of separation from the oesophagus. The development of the larynx can be considered in two stages: the development of the laryngeal vestibule (Fig. 3.2f), which provides the entry into the airway, and supraglottic larynx on the one hand and that of the infraglottic larynx, which is continuous with the trachea, on the other. Both parts of the larynx undergo a process of separation from the dorsally placed pharynx and oesophagus and during development their lumens become continuous to complete laryngeal development. The infraglottic larynx is derived from the cranial-most part of the laryngotracheal groove and its separation from the oesophagus forms part of tracheo-

Fig. 3.2 Stages of normal laryngeal development

Sagittal section (*a*) of an E15.5 embryo and transverse sections (*b-f*) from the level of the larynx in E12.5 (*b, c, d*), E13.5 (*e*) and E15.5 (*f*) embryos. All sections stained with Haematoxylin & Eosin. Approximate level of the transverse sections is shown by the dotted line in (*a*). At E12.5 (*b, c, d*), the sections are taken from progressively more caudal levels. **(*a*)** The process of separation of the trachea (Tr) from the oesophagus (Oe) has been completed. As a result of this process, the infraglottic larynx, which is found at the cranial limit of the trachea, also separates from the oesophagus (arrow in a). **(*b*)** Between E12 and E12.5, the entrance into the airway is defined by the development of the epiglottic (E) and two arytenoid (A) swellings in the pharyngeal mesoderm. **(*c*)** The fusion of the two arytenoid cartilages in the midline defines a triangular space between the three swellings known as the cecum (C) and a midline mesodermal prominence, the laryngeal lamina (L). **(*d*)** Just caudal to that level, the laryngeal lamina transiently obliterates the foregut lumen. **(*e*)** By E13.5, the fused epithelial surfaces forming the laryngeal lamina have started to separate from each other revealing the laryngeal lumen (arrow) in order to bring the larynx into continuity with the trachea. **(*f*)** The process of laminar separation is completed by E15.5 with the laryngeal vestibule (Lv) being continuous with the trachea. m, manubrium; h, heart; Ph, pharyngeal foregut. Scale bar, 100 μm

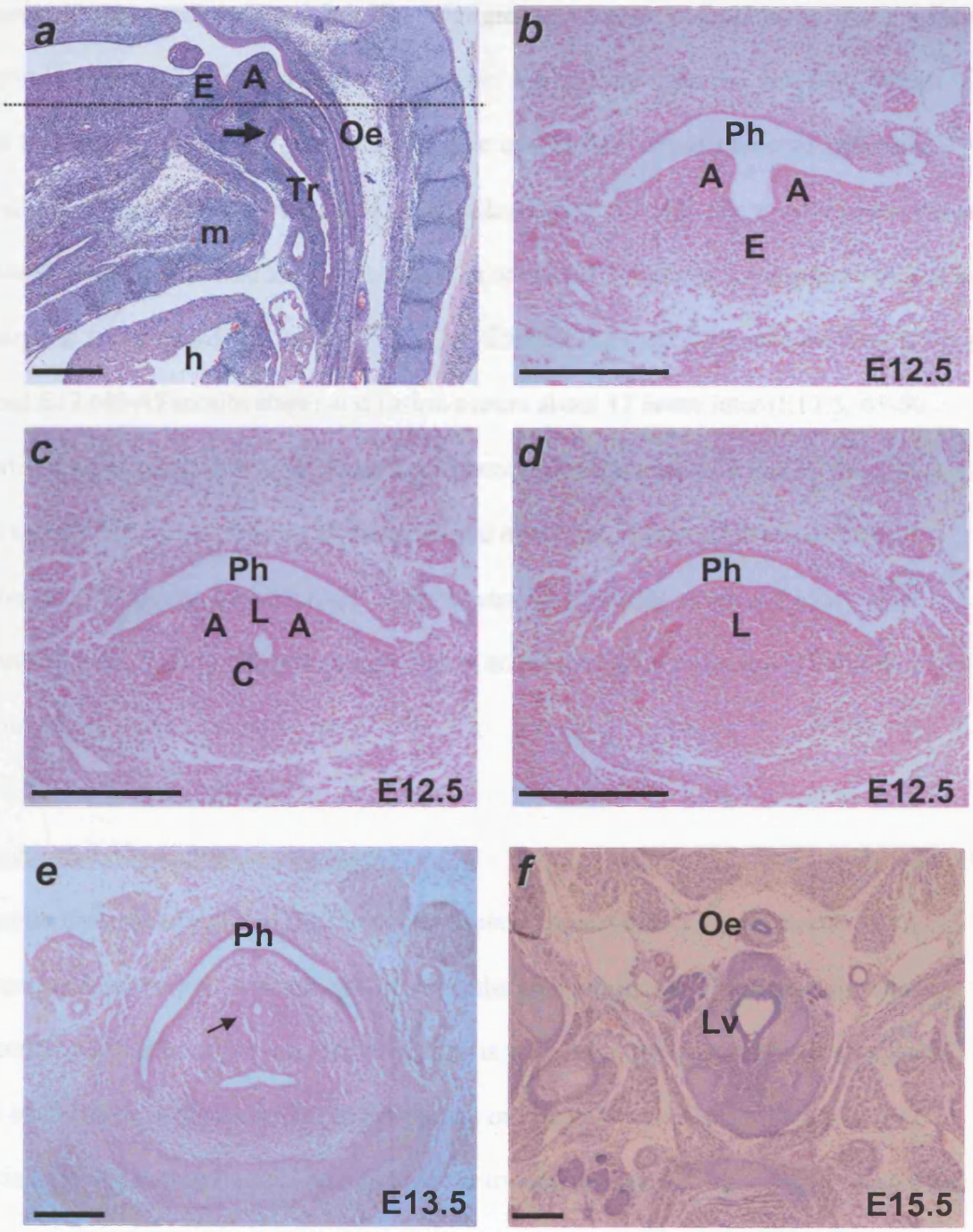
a
E
A
Oe
Tr
m
h
b
Ph
A
A
E
E12.5
c
Ph
A
L
A
C
E12.5
d
Ph
L
E12.5
e
Ph
E13.5
f
Oe
Lv
E15.5

oesophageal separation (Fig. 3.2a). The laryngeal vestibule is defined by the development of three swellings in the pharyngeal mesoderm: the midline epiglottic swelling, which will form the epiglottis and guard the entrance into the airway, and the two arytenoid swellings, which will form the arytenoid cartilages (Fig. 3.2a,b). The arytenoid swellings grow towards the midline and fuse to form an epithelial lamina and by doing so define a triangular space called the cecum (Fig. 3.2c). The development of these swellings starts at about E12 (40-45 somite stage) and fusion occurs about 12 hours later (E12.5, 45-50 somite stage). The lumen of the cecum will become continuous with that of the infraglottic larynx and trachea as the laryngeal epithelial lamina, which transiently obliterates the lumen of the foregut, starts to separate, thereby forming the laryngeal vestibule (Fig. 3.2d-f). This process begins at about the E13.5 stage and is completed by about E15.5.

Length analysis of foregut components

Despite in depth analysis of the molecular aspects of respiratory development (bronchopulmonary morphogenesis in particular) the mechanisms by which the trachea becomes a separate organ from the oesophagus after originating from the foregut, have not been fully established either in the human or in any other organism. My aim was initially to use morphological data in order to try and resolve the controversy of whether the trachea develops by rapid outgrowth from the foregut or grows initially as part of an undivided foregut and then separates from it. To do this, the length of the trachea was measured during progressive stages of development between E10.5 and E12.5 and the length of the tracheal portion that remained undivided, and that which was separated, were recorded. In order to standardize the measurements, the cranial and caudal limits of

the trachea were identified and used when counting the number of sections of known thickness (Fig. 3.3).

The limits were identified as follows: the cranial limit was the cranial-most region of the laryngotracheal groove, which ultimately forms the subglottic part of the larynx. By definition, this segment includes a small portion that is not strictly trachea, but the subglottic larynx shares its origin with the trachea from the laryngotracheal groove and separates from the foregut together with the trachea. Therefore, it was included in the length measurements. At early stages of development (E10.5 and E11.5), this cranial point is clearly identifiable as the ventral outgrowth of the laryngotracheal groove whereas at E12.5, this point was taken as the caudal limit of the laryngeal epithelial lamina (Fig 3.1a,d,g). The caudal limit of the trachea was easily identified as the point at which the trachea bifurcates into the two bronchi or bronchopulmonary buds (Fig 3.1f,i). In the case of E10.5 embryos, where the trachea is not yet a separate structure, the two lung buds emerge from the caudal end of the prospective trachea and this level was used as the caudal limit of the measurements. In addition to the cranial and caudal limits, the point of separation of the trachea from the foregut (point where the undivided trachea becomes divided) is very easily identifiable (Fig 3.1e,h).

Analysis of these data reveals that at E10.5, in CBA/Ca mice, the whole trachea is undivided (Fig. 3.3). By E11.5, tracheo-oesophageal separation has started at the caudal end of the oesophagotrachea and is proceeding but has not yet been completed. The total length of the trachea has increased significantly ($p<0.0001$) but the length of the undivided segment is significantly shorter than the length of the E10.5 undivided trachea/foregut ($p<0.0001$). This decrease supports the hypothesis that the trachea

Fig. 3.3 Analysis of foregut lengths: undivided versus divided segments of the foregut during normal development

Box plots summarise length data according to gestation. The numbers above the vertical boxes denote the number of embryos examined for each gestation. The lengths were calculated by counting the number of sections of known thickness between the levels indicated by the dotted lines on the schematic representations (not to scale) below the graph. Representative transverse sections for each level and each gestation are shown in Fig.1. The plot demonstrates the shift from the predominance of the undivided segment at E10.5, when the entire respiratory foregut is undivided, towards predominance of the divided segment at E12.5. By E11.5, the length of the undivided segment has significantly decreased (compared to E10.5, $p<0.0001$) and is significantly shorter than that of the divided segment ($p<0.0001$). The total foregut length (sum of the undivided and divided values) increases significantly with gestational age ($p<0.0001$).

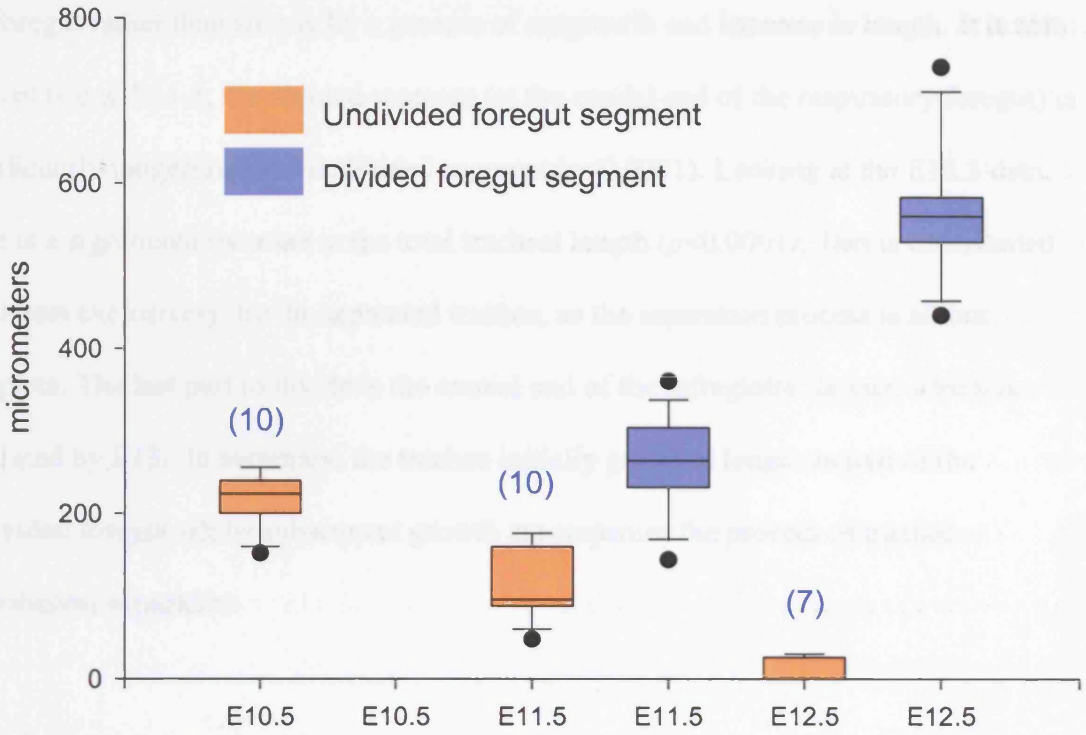
800
600
400
200
0
micrometers
Undivided foregut segment
Divided foregut segment
(10)
(10)
(7)
E10.5
E10.5
E11.5
E11.5
E12.5
E12.5

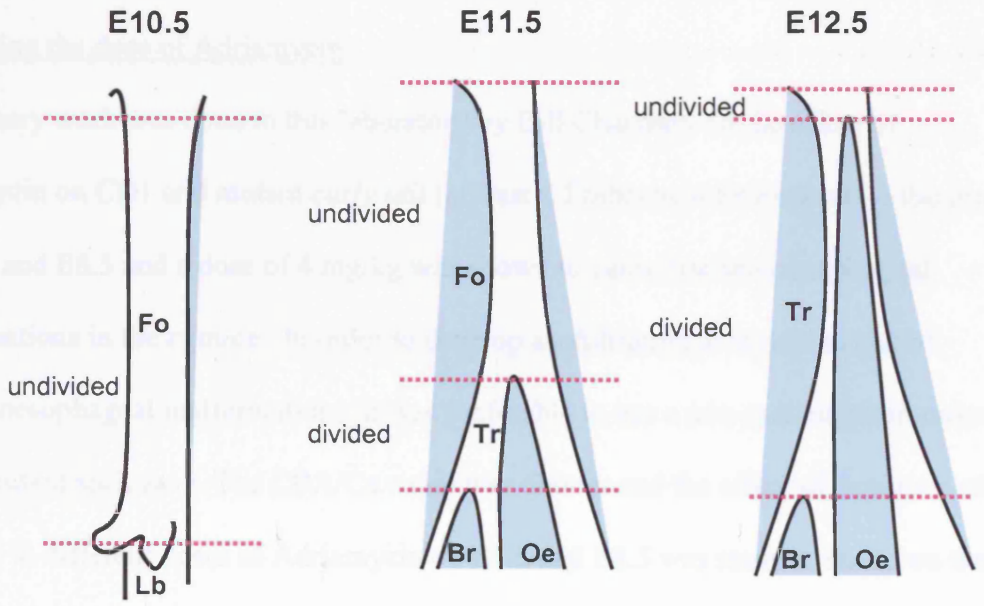
E10.5
E11.5
E12.5
Fo
undivided
Lb
undivided
Fo
divided
Tr
Br
Oe
undivided
divided
Tr
Br
Oe

becomes a separate structure by a process of separation of the prospective trachea from the foregut rather than simply by a process of outgrowth and increase in length. It is also evident that at E11.5, the divided segment (at the caudal end of the respiratory foregut) is significantly longer than the undivided segment ($p<0.0001$). Looking at the E12.5 data, there is a significant increase in the total tracheal length ($p<0.0001$). This is contributed to, almost exclusively, by the separated trachea, as the separation process is all but complete. The last part to divide is the cranial end of the infraglottic larynx, which is separated by E13. In summary, the trachea initially grows in length as part of the undivided foregut whilst subsequent growth accompanies the process of tracheo-oesophageal separation

3.2.1.2 - Establishing the Adriamycin mouse model

Optimising the dose of Adriamycin

Preliminary work was done in this laboratory by Bill Chaudhry on the effect of Adriamycin on CD1 and mutant *curly tail* (*ct*) mice. Embryos were exposed to the drug on E7.5 and E8.5 and a dose of 4 mg/kg was shown to cause tracheo-oesophageal malformations in the *ct* mice. In order to develop an Adriamycin mouse model of tracheo-oesophageal malformations, it was preferable to use a non-mutant strain rather than a mutant such as *ct*. The CBA/Ca strain was chosen and the effect of exposure of the embryos to different doses of Adriamycin on E7.5 and E8.5 was studied. Based on the dose of Adriamycin used in the rat experiments (1.75 mg/kg) and that used by Bill Chaudhry in the mouse experiments (4 mg/kg), doses between 2 and 6 mg/ kg were assessed in terms of the number of dead or resorbed embryos, the development of tracheo-oesophageal malformations and the association of these malformations with

Table 3.1 Adriamycin dose-response experiment, with dosing at E7.5 and E8.5

Adriamycin dose, mg/kg	Embryos (litters)	Resorbed embryos (%)	Tracheo-oesophageal defects (%) *	Lung defects (%)*
2	33 (3)	0 (0)	0 (0)	0 (0)
3	102 (12)	4 (4)	0 (0)	0 (0)
3.5	27 (3)	1 (4)	0 (0)	0 (0)
4	95 (14)	3 (3)	37 (40)	0 (0)
4.5	66 (9)	2 (3)	27 (42)	6 (9)
5	63 (9)	13 (21)	25 (50)	15 (30)
6	22 (4)	13 (59)	5 (56)	5 (56)

* percentage of live embryos

maldevelopment of the lungs. The results of the dose-response experiment are shown in Table 3.1. None of the embryos treated with 2, 3 or 3.5 mg/kg of Adriamycin had tracheo-oesophageal or lung malformations. Malformations of the tracheo-oesophagus were common at doses of 4 mg/kg and above, while malformations of the lungs were observed in embryos exposed to 4.5, 5 and 6 mg/kg of Adriamycin. The frequency of resorption rose markedly from 5 mg/kg upwards. Since 4 mg/kg was associated with tracheo-oesophageal defects but not lung defects, this dose was chosen as the optimal level for all subsequent analyses.

Mice treated with 4 mg/kg of Adriamycin on E7.5 and E8.5 were next examined in more detail with respect to litter size, and the growth characteristics and spectrum of abnormalities found in embryos at different gestational ages. The numbers of live embryos in saline-treated and Adriamycin-treated litters showed no statistically

Table 3.2 Mean numbers of live embryos in saline-treated and Adriamycin-treated (4 mg/kg) pregnancies analysed on different days of gestation [υ =]

	Mean number of live embryos per litter (number of litters)						
	E10.5	E11.5	E12.5	E13.5	E15.5	E17.5/ E18.5	Overall Mean
Saline	6.9 (11)	7.3 (6)	6.6 (7)	8 (4)	7 (3)	7.3 (3)	7.29 (34)
Adriamycin	6.8 (13)	6.8 (19)	5.4 (8)	5.8 (9)	8.5 (4)	7.3 (6)	6.86 (59)*

[υ] All mice dosed at E7.5 and E8.5

[=] Includes litters that were harvested but not subjected to sectioning and phenotypical analysis

- The difference between the two groups is not statistically significant (unpaired t test, p=0.345)

significant difference between the two groups (Table 3.2) and the figures for individual gestations do not suggest progressive loss of Adriamycin-treated embryos as pregnancy progresses. The crown-rump (CR) length and somite number data of embryos treated with the 4 mg/kg dose compared to control embryos are summarised in Figure 3.4. Crown-rump lengths were similar between the two groups at E9.5, E10.5 and E11.5 whereas Adriamycin-treated embryos were significantly smaller at E12.5, E13.5 and E15.5 (p<0.01). Saline–treated embryos were significantly more advanced in terms of somite number at E10.5 (median 28 versus 27, p< 0.01) but there was no significant difference between the two groups at E11.5 (median 39). Overall, these results suggest that Adriamycin at 4 mg/kg does not inhibit the progression of embryonic development but has a delaying effect on embryonic growth. Table 3.3 summarises the results of morphological and histological examination of 170 Adriamycin-treated and 85 saline-treated control mouse embryos and fetuses at various gestational ages. Overall, foregut

Fig. 3.4 Crown-rump (CR) length and somite number in saline- and Adriamycin-treated embryos (4 mg/kg)

Box plots summarising crown-rump (CR) lengths (a) and somite numbers (b) according to gestational age at which embryos analysed (all dosing on E7.5 and E8.5). The numbers above the vertical boxes denote the number of embryos examined for each gestation. Asterisks (*) indicate statistically significant difference between saline and Adriamycin-treated groups using the unpaired t-test and the Mann-Whitney Rank Sum test. The numbers above the vertical boxes denote the number of embryos in each group. ***(a)*** Adriamycin-treated embryos have a closely similar crown-rump length to saline-treated controls at E9.5, E10.5 and E11.5 whereas they are significantly smaller at E12.5, E13.5 and E15.5 ($p< 0.01$). ***(b)*** There is a statistically significant difference ($P< 0.01$) in the number of somites between saline-treated (median= 28) and Adriamycin-treated embryos (median= 27) at E10.5, whereas there is no difference at E11.5, when both groups have a median somite number of 39.

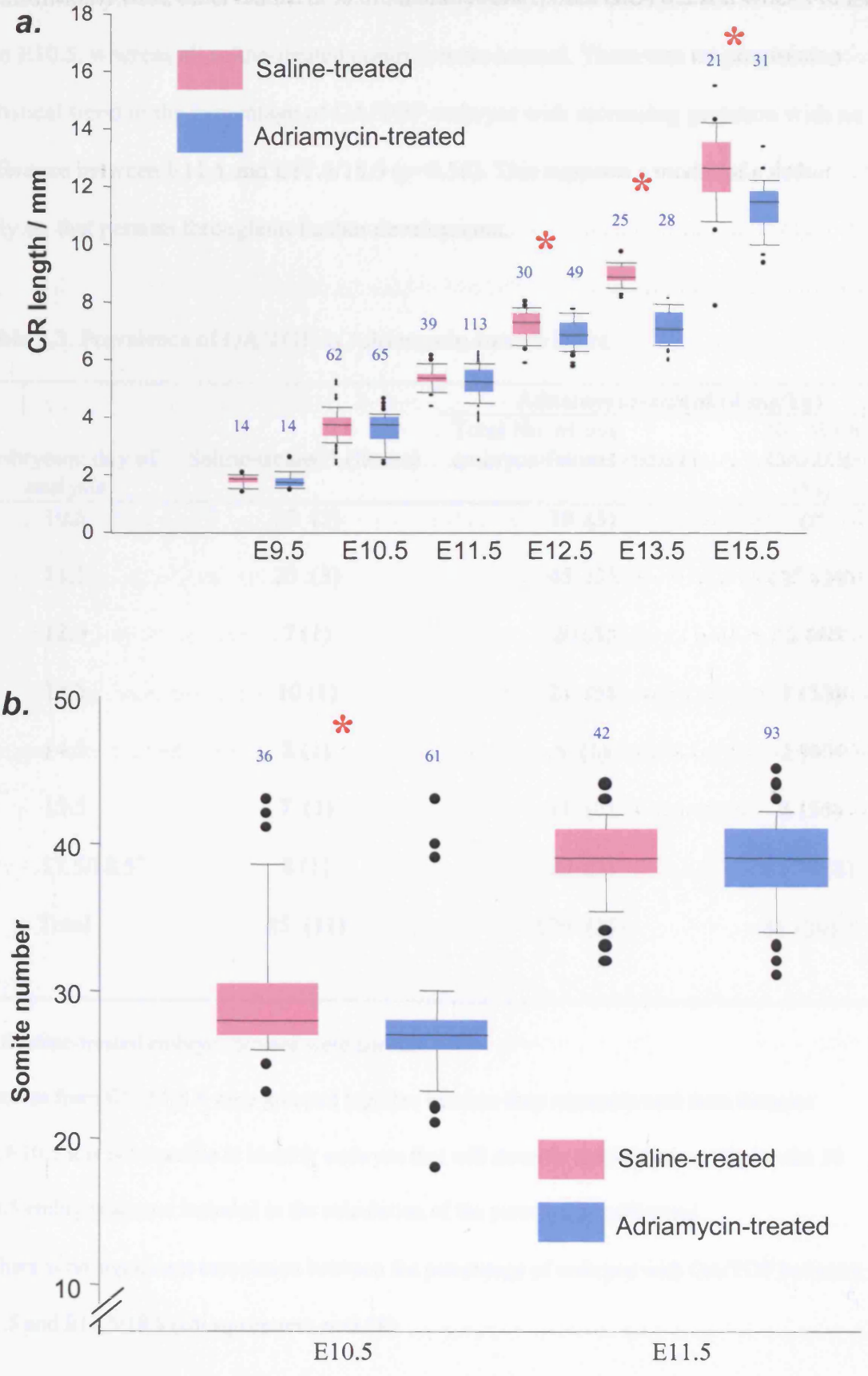
a.
CR length / mm
Saline-treated
Adriamycin-treated
14
14
62
65
39
113
30
49
25
28
21
31
E9.5
E10.5
E11.5
E12.5
E13.5
E15.5
b.
Somite number
36
61
42
93
Saline-treated
Adriamycin-treated
E10.5
E11.5

malformations were observed in 39 % of Adriamycin-exposed embryos and fetuses older than E10.5, whereas all saline-treated controls were normal. There was no progressive statistical trend in the percentage of OA/TOF embryos with increasing gestation with no difference between E11.5 and E17.5/18.5 (p=0.58). This supports a model of a defect early on that persists throughout further development.

Table 3.3. Prevalence of OA/TOF in Adriamycin-treated litters

		Adriamycin-treated (4 mg/kg)	
Embryonic day of analysis	Saline-treated* (litters)	Total No. of live embryos/fetuses (litters)	No. With OA/TOF (%)
10.5	22 (3)	39 (5)	0[υ]
11.5	23 (3)	45 (7)	13[♣] (29)
12.5	7 (1)	20 (3)	12 (60)
13.5	10 (1)	21 (5)	7 (33)
14.5	8 (1)	5 (1)	2 (40)
15.5	7 (1)	11 (2)	6 (55)
17.5/18.5[=]	8 (1)	29 (4)	11[♣] (38)
Total	85 (11)	170 (27)	51 (39) [υ]

* All saline-treated embryos/fetuses were normal

[=] Fetuses from E17.5/18.5 were grouped together because they represent near term foetuses

[υ] At E10.5 it is not possible to identify embryos that will develop malformations. Hence the 39 E10.5 embryos are not included in the calculation of the percentage malformed

[♣] There is no significant association between the percentage of embryos with OA/TOF between E11.5 and E17.5/18.5 (chi square test, p=0.58)

Aberrations of tracheo-oesophageal development

At E10.5, foregut anatomy is comparable between Adriamycin-treated and control embryos. The laryngo-tracheal groove arises as an outpouching from the ventral aspect of the pharyngeal foregut, at the level where its luminal diameter narrows significantly (Fig 3.5a,b). At this point in development, the trachea is not a separate structure from the oesophagus. Indeed, the bronchial buds can be seen arising from the main foregut tube at the caudal end of the laryngo-tracheal groove (Fig. 3.5c,d). Tracheo-oesophageal development diverges from normal by E11.5 in a proportion of Adriamycin-treated embryos. Separation of trachea and oesophagus is under way by this stage in control embryos and proceeds in a cranial direction, starting at the level of the lung buds (Fig. 3.6c,d). In contrast, 13 out of 45 Adriamycin-treated embryos at E11.5 exhibited an undivided foregut (Fig. 3.6g,h). In 12 of these embryos, the oesophago-trachea gives rise to a fistula to the stomach, which either originates from a rostral position relative to the emergence of the bronchi or else arises as part of a trifurcation, at the level of origin of the bronchi. Tracheo-oesophageal malformations in embryos of all gestations conformed to one of these basic phenotypes (Figs. 3.7&8) with the exception of a single E12.5 embryo in which the fistula originated from one of the main bronchi and became atretic before connecting to the gastrointestinal tract (Table 3.4). Adriamycin-treated near term fetuses, at E17.5 and E18.5, exhibited a small globular stomach connected to the TOF (11 out of 29 studied, Fig. 3.8f).

The classic OA/TOF malformation was seen in two embryos, which exhibited an upper oesophagus as a dorsal outpouching from the undivided foregut. In these embryos, the pattern of separation of the proximal oesophagus from the ventral trachea was distinctly abnormal compared to saline-control embryos (Fig. 3.9d). The atretic upper oesophagus

Fig. 3.5 Saline and Adriamycin-treated embryos are morphologically indistinguishable at E10.5

Transverse sections stained with haematoxylin & eosin, through E10.5 saline-treated (*a, c*) and Adriamycin-treated (*b, d*) embryos. Sections *a* and *b* are at the level of the laryngotracheal groove (Lt) just caudal to the pharyngeal foregut. Sections *c* and *d* are from the caudal end of the groove at the level of emergence of the lung buds (Lb). ***(a, b)*** The development of the ventral evagination, that forms the laryngotracheal primordium, from the post pharyngeal foregut is morphologically comparable between saline controls and Adriamycin-treated experimental embryos. ***(c, d)*** The development of the lung (or bronchopulmonary) buds from the caudal end of the laryngotracheal groove does not appear to be disturbed in Adriamycin-treated embryos with the two groups being morphologically indistinguishable. Scale bar, 100 μm

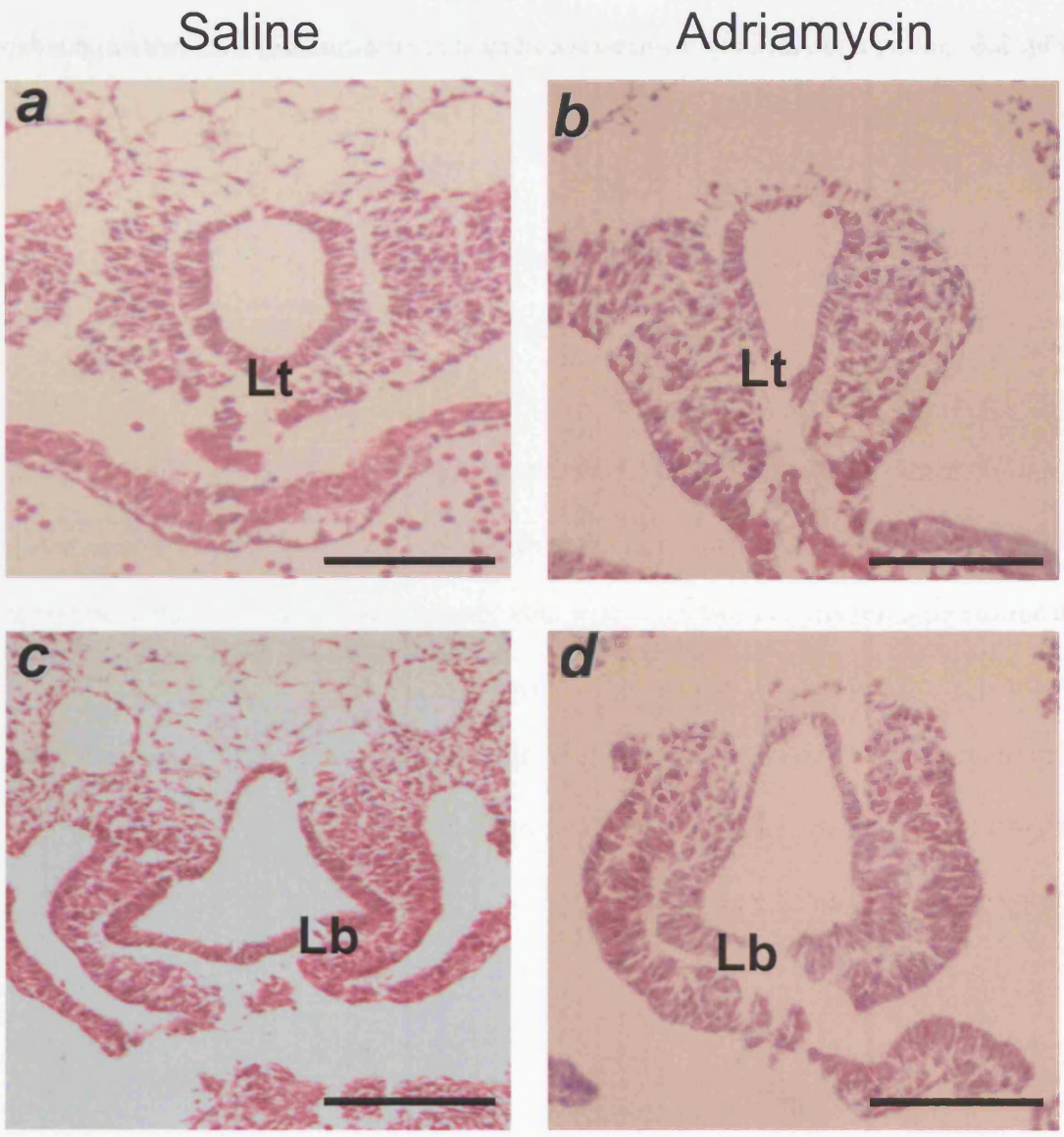
Saline
Adriamycin
a
Lt
b
Lt
c
Lb
d
Lb

Fig. 3.6 Failure of separation of oesophagus and trachea during development of OA/TOF in Adriamycin-treated embryos.

Transverse sections, stained with haematoxylin and eosin, through E11.5 saline-treated (*a,b,c,d*) and Adriamycin-treated (*e,f,g,h*) embryos. Sections *a* to *d* and *e* to *h* are from increasingly caudal levels. Sections *d* and *h* are taken from the level of the atrial septum. ***(a,b,e,f)*** Appearance of the laryngo-tracheal groove (Lt) is comparable between saline and Adriamycin-treated embryos. ***(c,d,g,h)*** Further caudally, saline-treated embryos undergo separation of the ventral trachea (Tr) from the dorsal oesophagus (Oe) whereas, in Adriamycin treated embryos, a common oesophago-trachea (Oet) persists. In *c*, tracheo-oesophageal separation is associated with the appearance of lateral epithelial ridges (arrows). Ao, aorta; h, heart. Scale bars, 100 μm.

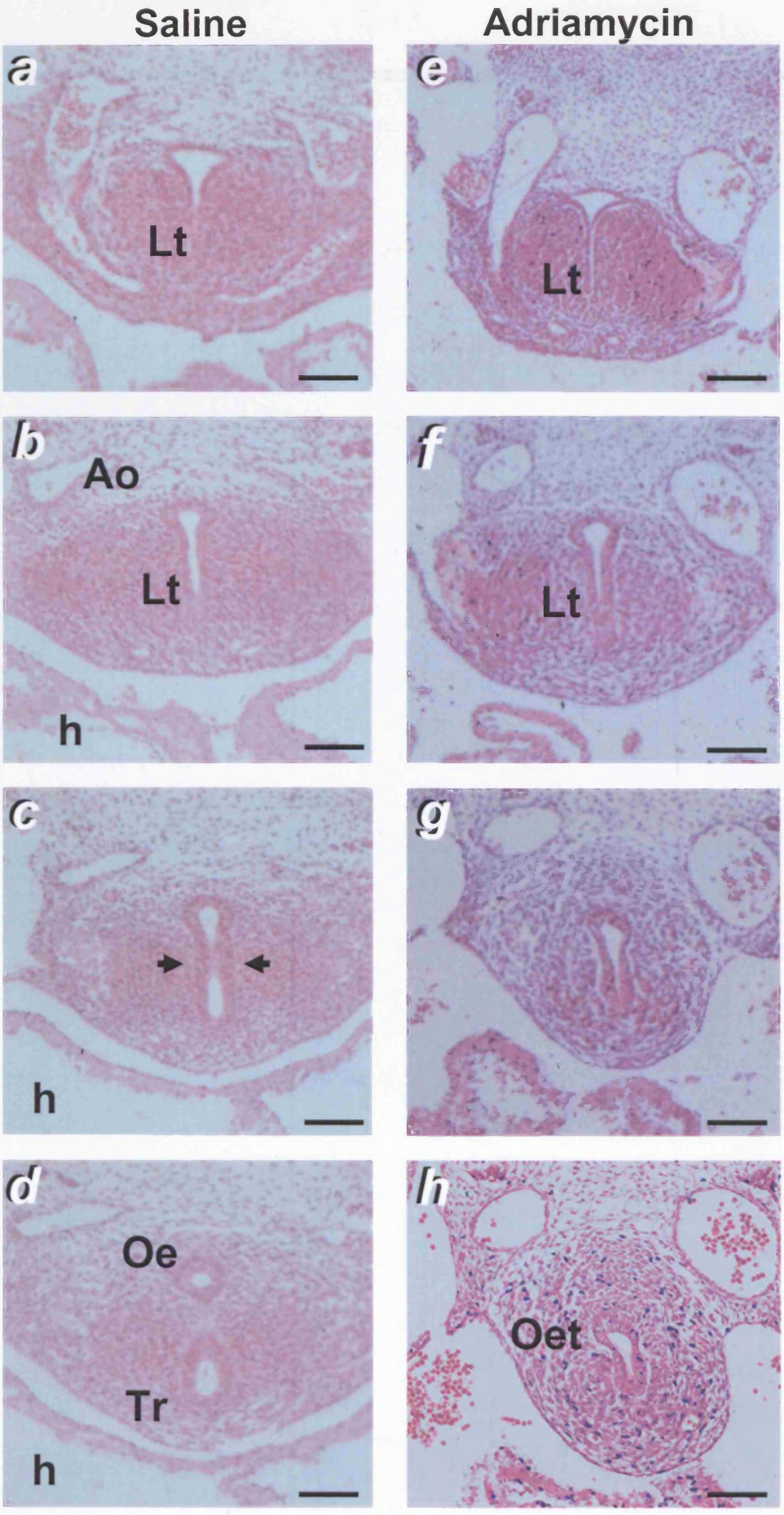
Saline
Adriamycin
a
Lt
e
Lt
b
Ao
Lt
h
f
Lt
c
h
g
d
Oe
Tr
h
h
Oet

Fig. 3.7 Variable level of origin of the tracheo-oesophageal fistula in Adriamycin-treated embryos.

Transverse sections, stained with haematoxylin and eosin, from an E15.5 saline treated embryo (*a,c*) and from two E15.5 Adriamycin-treated embryos (*b* and *d*). Sections are at the level of the manubrium sterni and clavicles (*a,b*) and at the level of the cardiac outflow tract (*c,d*). The Adriamycin-treated embryo in **(*b*)** demonstrates a high origin of the fistula (arrow) from the undivided oesophago-trachea (Oet). At a similar level, a saline-treated embryo **(*a*)** exhibits a separate trachea (Tr) and oesophagus (Oe). In **(*d*)**, a second Adriamycin-treated embryo exhibits a lower level fistula originating at the level of emergence of the main bronchi (arrowheads), thereby forming a trifurcation (arrow). At the same level, the saline-treated embryo **(*c*)** shows an undivided trachea distinct from the oesophagus. In sections slightly caudal to this level, the trachea of the control embryo bifurcates to form the main bronchi (inset). Ao- aorta. Scale bar, 200 μm.

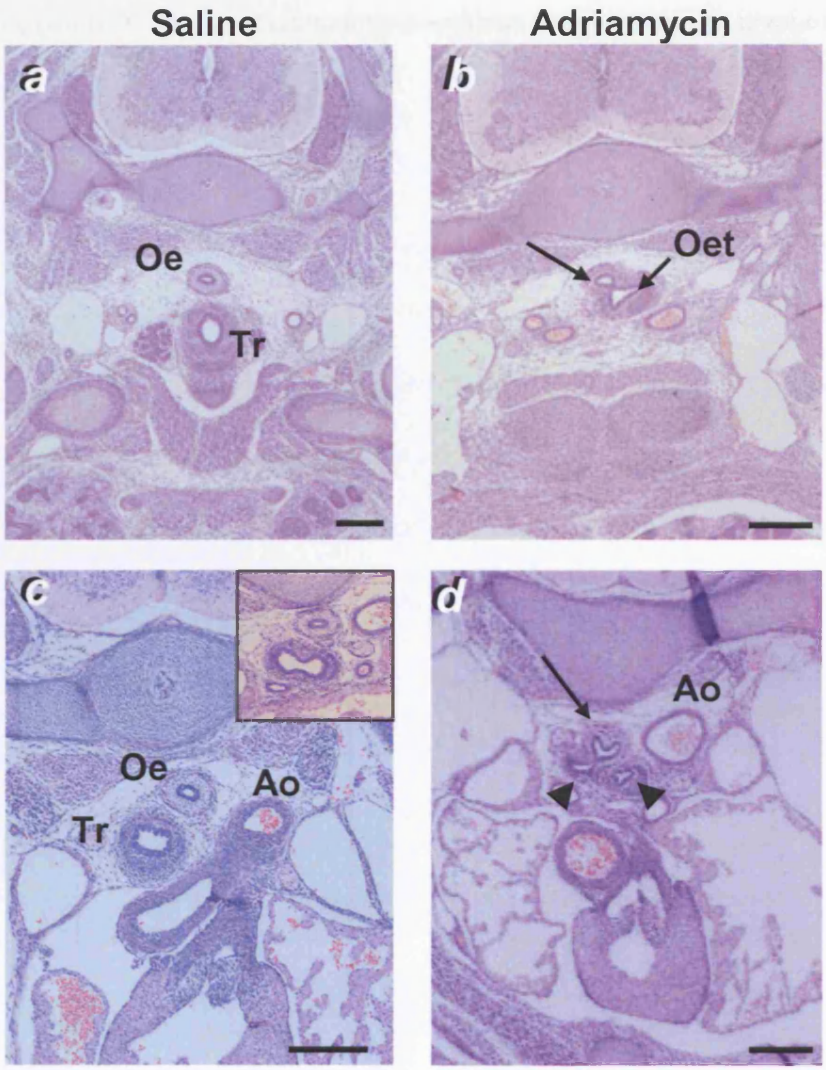
Saline
Adriamycin
a
Oe
Tr
b
Oet
c
Oe
Ao
Tr
d
Ao

Fig. 3.8 The oesophagotrachea in late gestation and near-term embryos/fetuses.

Sagittal (*a,b*) and transverse (*c,d*) sections stained with haematoxylin & eosin through E15.5 saline- (*a,c*) and Adriamycin-treated (*b,d*) embryos. The level of the transverse sections in *c* and *d* approximately corresponds to the level of the dotted lines in *a* and *b* (level of clavicular heads and thoracic inlet). Dissected anterior foregut structures from E18.5 saline- (*e*) and Adriamycin-treated (*f*) embryos. In the saline-treated embryos (***a,c***), the oesophagus (Oe) and trachea (Tr) are separate structures in contrast to the Adriamycin-treated embryos (***b,d***) that have an undivided oesophagotrachea (Oet) at the same level. The fistula comes off the oesophagotrachea at about the level of the cardiac outflow tract (arrow in *b*). (***e,f***) The fistula (Fi) forms a trifurcation with the main bronchi (arrow in *f*) and connects to a small, globular stomach (St). h - heart, Th- thyroid gland, Cl - clavicle, Sal - salivary glands, Lu - lungs. Scale bar, 200μm.

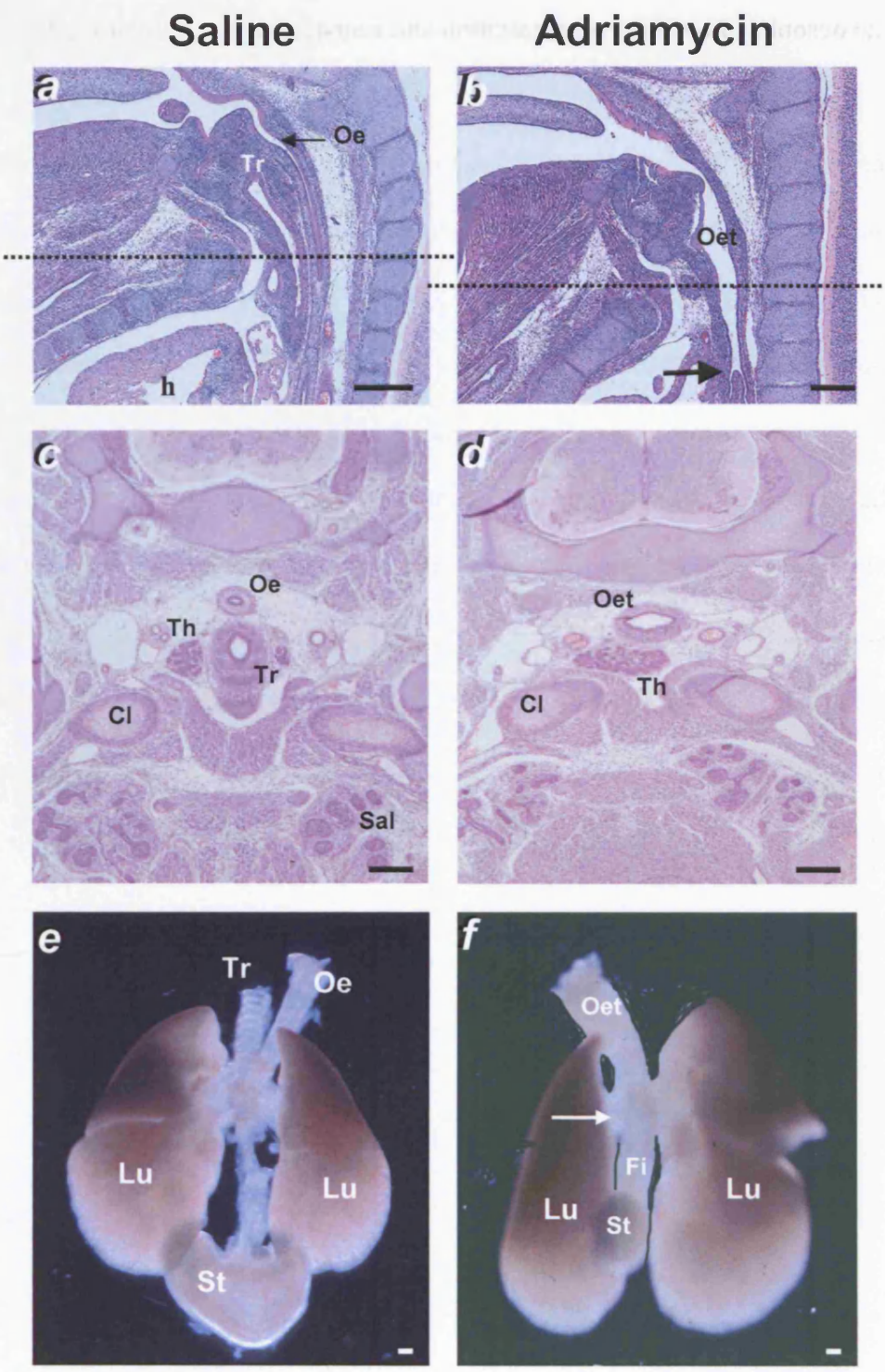
Saline
Adriamycin
a
Oe
Tr
h
b
Oet
c
Oe
Th
Tr
Cl
Sal
d
Oet
Th
Cl
e
Tr
Oe
Lu
Lu
St
f
Oet
Fi
Lu
Lu
St

Fig.3.9 A rare case of oesophageal atresia in an Adriamycin-treated embryo.

Transverse sections, stained with haematoxylin and eosin, through E12.5 saline-treated (*a,c,e*) and Adriamycin-treated *(b,d,f)* embryos. Sections are from the level of the thyroid in *a* and *b* and the atrial septum in *c* to *f*. **(*a,b*)** Development of the laryngotracheal groove (Lt) is comparable between the saline- and Adriamycin-treated embryo. **(*c,d*)** Normal tracheo-oesophageal separation in (*c*) contrasts with an undivided foregut in the Adriamycin treated embryo (arrow in *d*). At a slightly more caudal level, the oesophagus becomes a separate structure for a short distance (inset in *d*). In (***e***) the normally separated oesophagus (Oe) is patent whereas the oesophagus in the Adriamycin-treated embryo has become atretic (asterisk in ***f***). Tr - trachea. Scale bar, 100 μm.

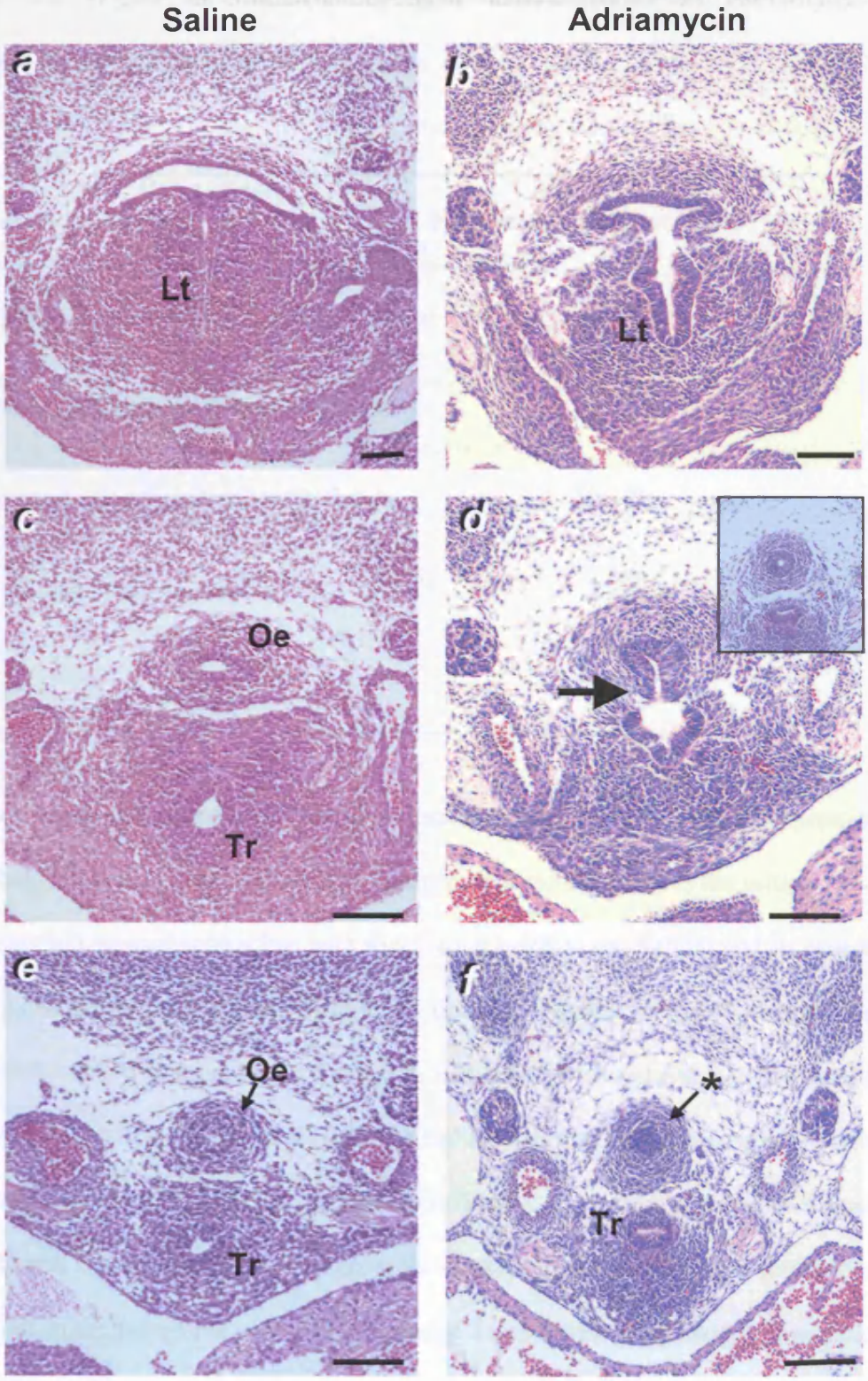
Saline
Adriamycin
a
Lt
b
Lt
c
Oe
Tr
d
e
Oe
Tr
f
*
Tr

Table 3.4. Types of tracheo-oesophageal malformations in Adriamycin-treated embryos/fetuses (all gestations)

Type of malformation	Number of embryos/fetuses (%)
Oesophagotrachea with trifurcation	36 (70)
Oesophagotrachea with proximal fistula	11 (22)
Proximal oesophageal atresia with fistula	2 (4)
Other (absent or atretic fistula)	2 (4)
Total	51

lacked a lumen and ended blindly in the dorsal mesenchyme (Fig 3.9f). This proximal oesophageal atresia phenotype would appear to be a modification of the initial malformation (oesophagotrachea with trifurcation or proximal fistula) and its presence can only be determined in embryos at E12.5 or older. The types of tracheo-oesophageal malformations are summarised in Table 3.4. Adriamycin-treated embryos/foetuses that had separated their trachea and oesophagus had normal tracheo-oesophageal morphology. It should be noted that in all Adriamycin-treated embryos, including those with tracheo-oesophageal malformations, the fusion of the arytenoid swellings and the formation of the laryngeal epithelial lamina proceeded normally. Lung development and segmentation was also normal.

Foregut length analysis was used to supplement the observations described above. At E11.5, about 60% of Adriamycin-treated embryos were morphologically comparable to controls. In contrast, affected Adriamycin-treated embryos had significantly different ratios of divided/ undivided foregut length. Within this group, there were two types of embryos. In one type, the respiratory foregut remained undivided along its entire length. In the second type, there was a divided segment but this was significantly shorter than in control embryos, whereas the undivided segment was significantly longer compared to controls (data for both types combined are shown in Fig. 3.10). The total length of the respiratory foregut in affected Adriamycin-treated embryos (both types) was comparable to control embryos (Fig. 3.11). At E12.5, the foregut at this gestation in control embryos is almost entirely divided. In contrast, a proportion of Adriamycin-treated embryos had a foregut that was entirely undivided or had a short divided segment (Fig. 3.10). Again, the total length of the foregut was comparable to control embryos (Fig. 3.11). These observations suggest that the growth in length of the respiratory foregut in affected Adriamycin-treated embryos is not disturbed, and supports the idea that there is interference with the separation process itself.

Effect of Adriamycin on other organ systems

Malformations observed in other systems are summarised in Table 3.5. Embryos were examined for abnormalities of the notochord, thymus and cardiovascular system. Malformations of the notochord were found in 20 out of 104 embryos at E10.5-E12.5. Of 25 embryos with demonstrable foregut malformations (E11.5/12.5), 10 had notochord defects. Conversely, out of 13 embryos with abnormal notochords, 10 had tracheo-oesophageal malformations. The association between tracheo-oesophageal malformations and notochordal defects was statistically significant (chi square test; p=0.0041). The

Fig. 3.10 Disturbance in the length of undivided versus divided foregut segments in affected Adriamycin-treated embryos

Box plots summarise length data. The numbers above the vertical boxes denote the number of embryos examined for each gestation. The lengths were calculated by counting the number of sections of known thickness between defined levels as indicated by the dotted lines on the schematic representations in Fig. 3. The saline-treated control data is shown in this figure for purposes of comparison (already shown in Fig. 3). The pattern in affected Adriamycin-treated embryos sharply contrasts with the arrangement in saline-treated control embryos. At both gestations (E11.5 and E12.5), the foregut remains largely undivided. It should be noted that Adriamycin-treated embryos with disturbed tracheo-oesophageal separation conform to two main patterns; the majority fail completely to separate the trachea from the oesophagus whilst in a small number a limited degree of separation takes place, with the tracheo-oesophageal fistula originating from a rostral position relative to the lung buds. This variation between embryos accounts for the outlying values seen in box plot representing the E12.5 divided segment.

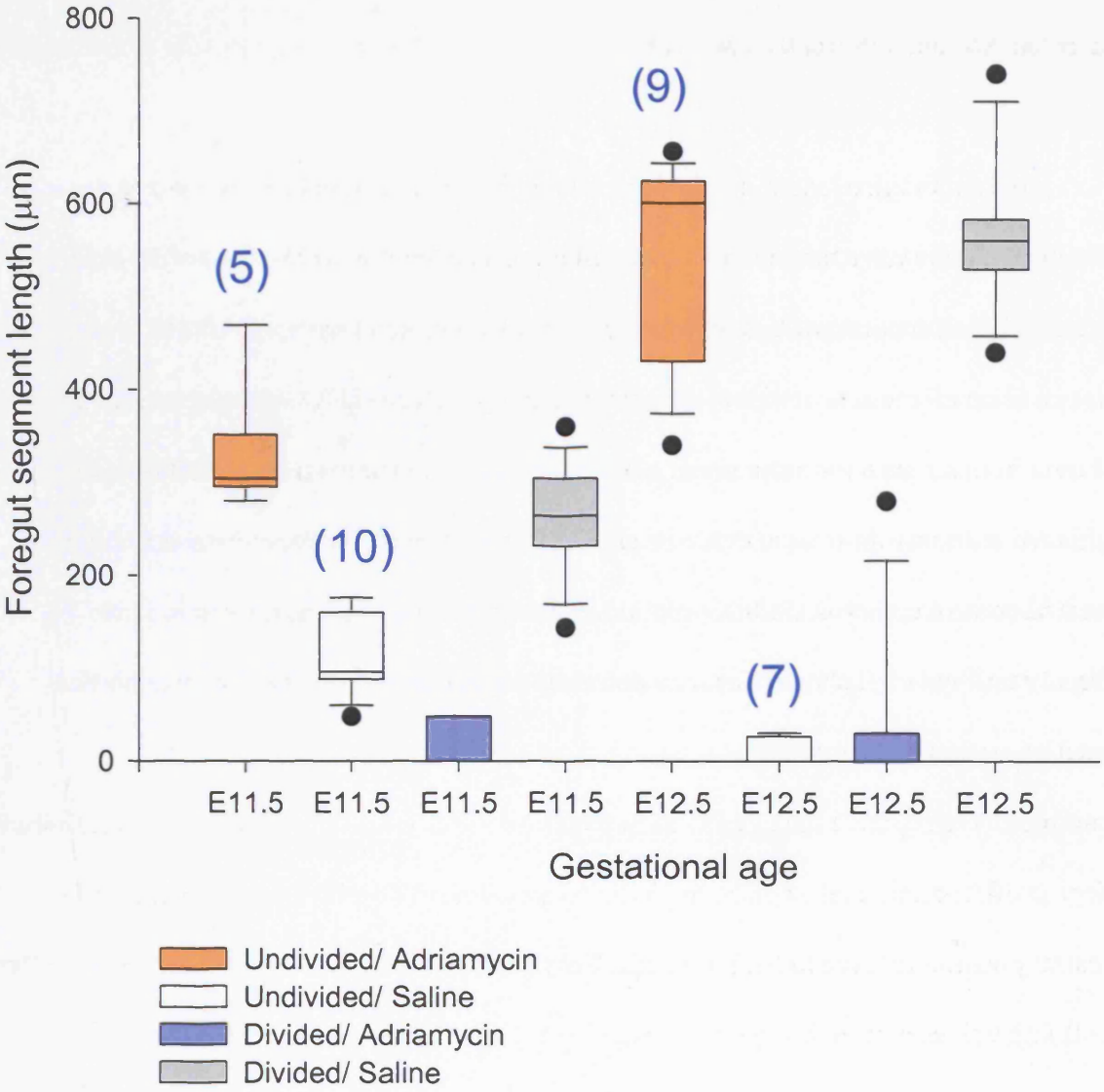
800
600
400
200
0
Foregut segment length (μm)
(5)
(10)
(9)
(7)
E11.5
E11.5
E11.5
E11.5
E12.5
E12.5
E12.5
E12.5
Gestational age
Undivided/ Adriamycin
Undivided/ Saline
Divided/ Adriamycin
Divided/ Saline

Fig. 3.11 Comparing foregut growth in control and affected Adriamycin-treated embryos: total length of the respiratory foregut does not differ between saline controls and affected Adriamycin-treated embryos

Box plots summarise length data. The numbers above the vertical boxes denote the number of embryos examined for each gestation. The lengths were calculated by counting the number of sections of known thickness between defined levels as indicated by the dotted lines on the schematic representations in Fig. 3. Total lengths are the sums of undivided and divided segments. For each gestation, the total length of foregut in control and Adriamycin-treated embryos did not differ significantly (unpaired t-test; $p > 0.05$). The overall growth in length of the respiratory foregut appears to be unaffected by the administration of Adriamycin.

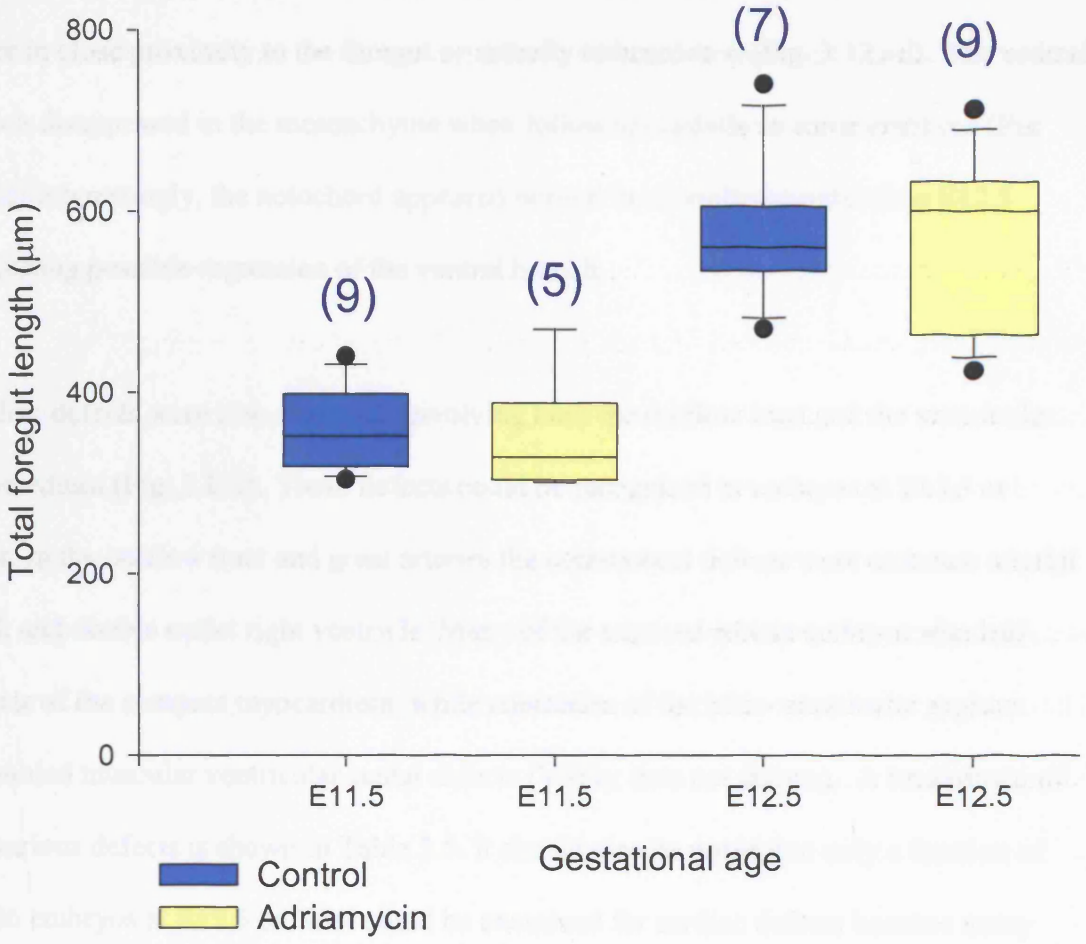
800
600
400
200
0
Total foregut length (µm)
(9)
(5)
(7)
(9)
E11.5
E11.5
E12.5
E12.5
Gestational age
Control
Adriamycin

notochord appeared either abnormally thickened or duplicated with the ventral branch either in close proximity to the foregut or actually tethered to it (Fig. 3.12a-d). The ventral branch disappeared in the mesenchyme when followed caudally in some embryos (Fig 3.12d).Interestingly, the notochord appeared normal in all embryos older than E12.5 suggesting possible regression of the ventral branch.

Cardiac defects were also observed, involving both the outflow tract and the ventricular myocardium (Fig. 3.12f). These defects could be recognised in embryos at E13.5 or older. In the outflow tract and great arteries the commonest defects were common arterial trunk and double outlet right ventricle. Many of the exposed mouse embryos also had defects of the compact myocardium, while anomalies of the inter- ventricular septum resembled muscular ventricular septal defects (VSDs; data not shown). A breakdown of the various defects is shown in Table 3.5. It should also be noted that only a fraction of the 66 embryos at E13.5 or older could be examined for cardiac defects because many were dissected rather than sectioned, or appropriate sections to illustrate cardiac or great vessel anatomy were not available.

Bilateral or unilateral absence of the thymic rudiments was the commonest associated malformation (Fig. 3.12h). It could only be detected in embryos at E13.5 or older, as this is the gestation at which the thymic primordium's origin from the ventral aspect of the third pharyngeal pouch can be readily detected. Thymic agenesis affected 49 of 57 examined embryos including all embryos with tracheo-oesophageal malformations. It should be noted that not all 66 embryos of the relevant gestations could be examined for the presence of thymic malformations as some of the embryos at later gestations were dissected rather than sectioned.

Fig. 3.12 Malformations in other organ systems of Adriamycin-treated embryos.

(*a-d*) Transverse sections at the level of the pharynx, through an E12.5 Adriamycin-treated embryo; stained with H&E. (*e,f*) Transverse sections at the level of the cardiac outflow tract through an E15.5 saline-treated (*e*) and Adriamycin-treated embryo (*f*); stained with H& E. (*g,h*) Transverse sections at the level of the manubrium sterni (m) through an E14.5 saline-treated (*g*) and Adriamycin-treated (*h*) embryo; stained with H&E. ***(a-d)*** The ventral branch of the divided notochord appears to regress in the mesenchyme in the most caudal section (arrow in *d*).***(e,f)*** The normal septation of the outflow tract into aorta (Ao) and pulmonary trunk (Pu) (*e*) contrasts with the undivided common arterial trunk in the Adriamycin-treated embryo (arrow in *f*). ***(g,h)*** The left thymic rudiment (Th) has not developed in this Adriamycin-treated E14.5 embryo (*h*) in contrast to the saline-treated embryo (*g*) in which the thymic rudiments appear on either side of the trachea (Tr). At, atria; Oe, oesophagus. Scale bar, 200 μm.

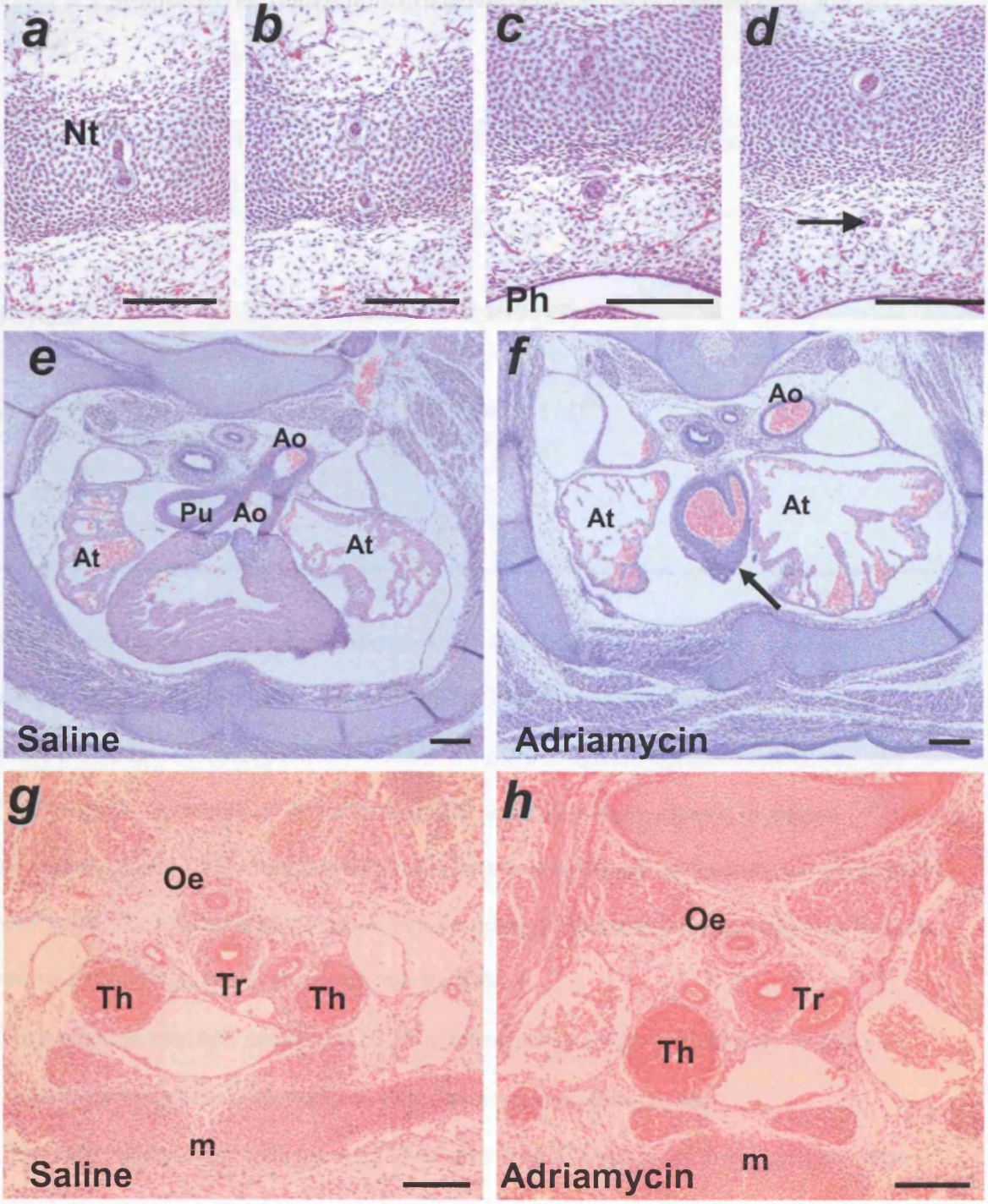
a
Nt
b
c
Ph
d
e
Ao
Pu
Ao
At
At
Saline
f
Ao
At
At
Adriamycin
g
Oe
Th
Tr
Th
m
Saline
h
Oe
Tr
Th
m
Adriamycin

Table 3.5. Associated malformations in Adriamycin-treated (4 mg/kg) embryos and fetuses

Organ/ System affected	Ratio of abnormal embryos (%)
Notochord*	20/104 (19)
Thymus$^{\Phi}$	49/57 (87)
Cardiovascular$^{\Sigma}$	26/35 (74)$^{\Omega}$
✓ Ventricular septal defects	24/35
✓ Common arterial trunk	15/35
✓ Double outlet right ventricle	6/35
✓ Overriding aorta	3/35

* This ratio includes embryos only between E10.5 and E12.5. The breakdown according to gestation is 7/39 for E10.5, 8/45 for E11.5 and 5/20 for E12.5. Considering only gestations at which the tracheo-oesophageal malformations are morphologically demonstrable (E11.5 and E12.5) then 10/13 embryos (77%) with abnormal notochords had tracheo-oesophageal malformations and 10/25 embryos (40%) with tracheo-oesophageal malformations had abnormal notochords. The association between tracheo-oesophageal malformations and notochordal defects was statistically significant (chi square test; p=0.0041)

$^{\Phi}$ This ratio includes only embryos at E13.5 or older (not all embryos of these gestations were available for analysis as some embryos were dissected and not sectioned)

$^{\Sigma}$ This ratio includes only embryos at E13.5 or older (not all embryos of these gestations were suitable for cardiac analysis as they were either not sectioned or the specific cardiac sections were either unavailable or insufficient for analysis)

$^{\Omega}$ Some embryos had more than one cardiac defect present

3.2.2 – The *Shh*$^{-/-}$ model

3.2.2.1 - General growth patterns of the Shh$^{-/-}$ *null embryo*

Despite reports in the literature that homozygous mutant fetuses survive until term, *Shh*$^{-/-}$ embryos / foetuses were found to be under-represented in litters from E12.5 onwards, with none at all in the single litter obtained at E15.5 (Table 3.6). The difference in the percentage of *Shh*$^{-/-}$ embryos was significant between E10.5/E11.5 litters on the one hand and E12.5/E13.5 litters on the other. The homozygous null embryos, which have cardiac malformations, start exhibiting evidence of cardiac insufficiency at about day E12.5, and by E14.5 they are extremely oedematous. It is probable that the late embryonic lethality is associated with severe cardiac failure. The homozygous null embryos do not appear to be developmentally delayed, based on development of the somites (Fig. 3.13), whereas they are significantly growth retarded compared to both heterozygous and wild type embryos, a discrepancy that becomes evident from E10.5 onwards (Fig. 13, $p<0.0001$). It is worth noting that compared to CBA/Ca mice, *Shh* embryos of all genotypes are more developmentally advanced at the same point in gestation (i.e. at same chronological age) in terms of their somite numbers. The difference is about 6 somites, which correlates with roughly 12 hours of development. Heterozygous embryos are morphologically indistinguishable from wild type embryos throughout gestation whereas homozygous null embryos can be readily distinguished on the basis of their grossly abnormal morphology, in particular forebrain defects (holoprosencephaly) and short limbs (Fig. 3.14a).

Fig. 3.13 Development and growth of embryos of different *Shh* genotypes

Box plots summarise data for somite numbers (*a*) and crown-rump length (*b*). **(*a*)** There is no statistically significant difference in somite numbers between $Shh^{-/-}$ embryos and their pooled heterozygous and wild type littermates in somite numbers at either E10.5 or E11.5. This suggests that general development in homozygous null embryos is comparable to the morphologically normal embryos, up to E11.5. **(*b*)** The crown-rump length of $Shh^{-/-}$ embryos is significantly shorter than that of their pooled heterozygous and wild type littermates ($p<0.0001$) at both E10.5 and E11.5. This suggests that homozygous null embryos are growth retarded.

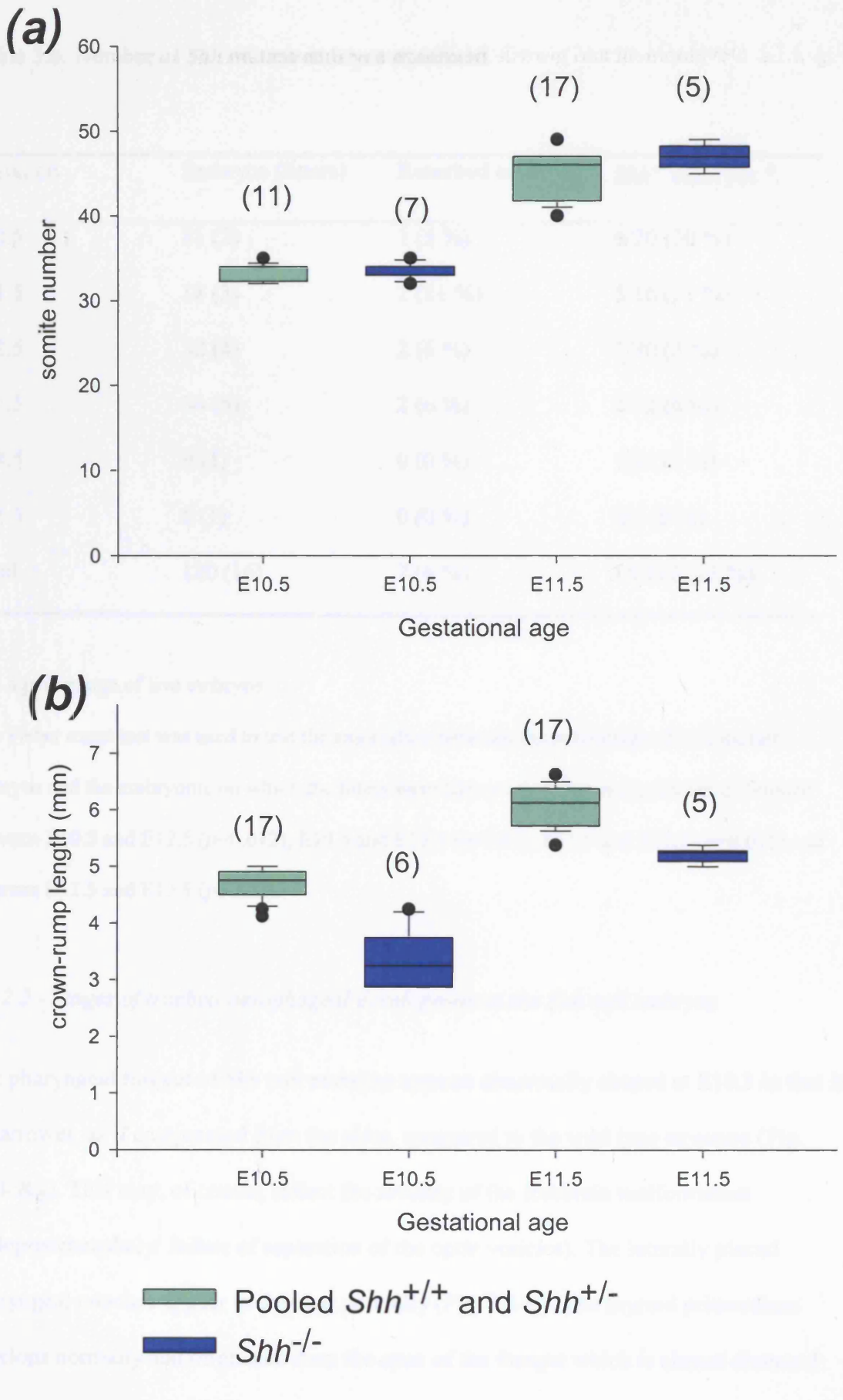
(a)
somite number
60
50
40
30
20
10
0
(11)
(7)
(17)
(5)
E10.5
E10.5
E11.5
E11.5
Gestational age
(b)
crown-rump length (mm)
7
6
5
4
3
2
1
0
(17)
(6)
(17)
(5)
E10.5
E10.5
E11.5
E11.5
Gestational age
Pooled Shh+/+ and Shh+/-
Shh-/-

Table 3.6. Number of *Shh* mutant embryos examined

Gestation	Embryos (litters)	Resorbed embryos	*Shh*$^{-/-}$ embryos *
E10.5	21 (2)	1 (5 %)	6/20 (30 %)
E11.5	18 (3)	2 (11 %)	5/16 (31 %)
E12.5	32 (4)	2 (6 %)	1/30 (3 %)
E13.5	34 (5)	2 (6 %)	2/32 (6 %)
E14.5	9 (1)	0 (0 %)	1/9 (11 %)
E15.5	6 (1)	0 (0 %)	0/6 (0 %)
Total	120 (16)	7 (6 %)	15/113 (13 %)

* as a percentage of live embryos

The Fisher exact test was used to test the association between the percentage of null mutant embryos and the embryonic on which the litters were harvested. There is significant difference between E10.5 and E12.5 (p=0.012), E10.5 and E13.5 (p=0.04), E11.5 and E12.5 (p=0.015) and between E11.5 and E13.5 (p=0.03).

3.2.2.2 - Stages of tracheo-oesophageal development in the Shh null embryos

The pharyngeal foregut of *Shh* null embryos appears abnormally shaped at E10.5 in that it is narrower, as if compressed from the sides, compared to the wild type structure (Fig. 3.14c&g). This may, of course, reflect the severity of the forebrain malformation (holoprosencephaly/ failure of separation of the optic vesicles). The laterally placed pharyngeal pouches appear to develop normally (Fig. 3.14c). The thyroid primordium develops normally and originates from the apex of the foregut which is almost diamond shaped, rather than ventro-dorsally flat (Fig. 3.14c).

Fig. 3.14 Foregut anatomy in the E10.5 *Shh* null embryo

A *Shh* null embryo at E10.5 (*a*), a schematic representation of the foregut (*b*) and transverse sections, stained with H&E, from an E10.5 $Shh^{-/-}$ embryo taken from the levels indicated in the diagram (*c-f*) and from corresponding levels from a control embryo (pooled $Shh^{+/+}$ / $Shh^{+/-}$ embryos) (*g-l*). **(*a*)** Homozygous null embryos are readily distinguishable by the narrow, undivided forebrain (arrow in *a*), fused optic vesicle, short limbs (Li) and enlarged heart (h). **(*c-l*)** The pharyngeal foregut (Ph) in $Shh^{-/-}$ embryos is diamond shaped (*c*), in contrast to the flat shape of control embryos (*g*). Development of the thyroid primordium (Th) and the pharyngeal pouches (Pp & arrow in *c*) is comparable between null mutant and control embryos. In $Shh^{-/-}$ embryos, the thyroid primordium develops from the ventral aspect of the foregut and the pharyngeal pouch derivatives (arrow in *c*) develop normally from the lateral aspects of the 'diamond'. The post-pharyngeal foregut (Fo) in $Shh^{-/-}$ embryos remains undivided and its lumen narrows significantly (*d*) before widening again at the level of the lung buds (Lb) in (*e*). In sharp contrast, the foregut in control embryos exhibits the characteristic folds (arrowheads in *h*) and more caudally divides into an oesophagus (Oe) and a trachea (Tr) in (*i*). Further caudally in control embryos (*k*), the trachea divides into two normal lung buds. (*f,l*) The post-lung bud foregut in $Shh^{-/-}$ embryos joins what appears to be a morphologically normal stomach (St) in a way comparable to control embryos. Scale bars, 1 mm for *a* and 100 μm for *c-l*

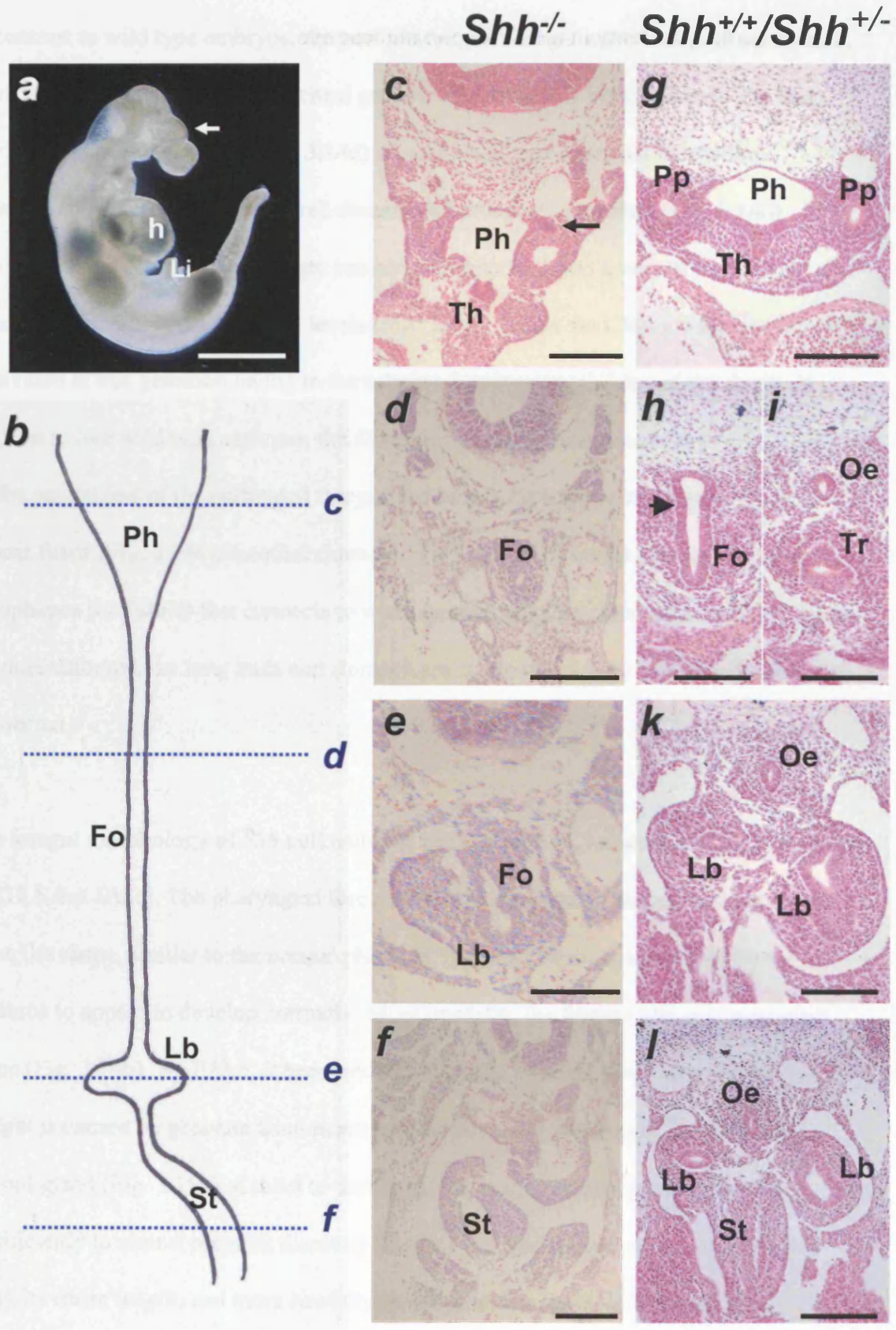
Shh-/-
Shh+/+/Shh+/-
a
h
Li
b
c
Ph
d
Fo
Lb
e
St
f
c
Ph
Th
g
Pp
Ph
Pp
Th
d
Fo
h
Fo
i
Oe
Tr
e
Fo
Lb
k
Oe
Lb
Lb
f
St
l
Oe
Lb
Lb
St

In contrast to wild type embryos, the post pharyngeal foregut narrows significantly and there is no identifiable laryngotracheal groove. The foregut is very narrow without an obvious prospective trachea (Fig. 3.14d) whereas wild type embryos exhibit the characteristic lateral folds and a well demarcated prospective trachea (Fig. 3.14h). In $Shh^{+/+}$ embryos at E10.5, the foregut has already separated into a ventral trachea and a dorsal oesophagus at more caudal levels (Fig. 3.14i), unlike the CBA/Ca foregut which is undivided at this gestation owing to the relative developmental delay of the strain. In contrast to *Shh* wild type embryos, the *Shh* null foregut remains undivided (Fig. 3.14d). At the caudal end of the undivided foregut, the lung buds emerge ventrolaterally but appear fused (Fig. 3.14e). Another characteristic is the short length of post lung bud oesophagus (or fistula) that connects to what appears to be a normal stomach (Fig. 3.14f). In some embryos, the lung buds and stomach are so close that they appear to be directly connected.

The foregut morphology of *Shh* null embryos changes at E11.5 and maintains its features at E12.5 and E13.5. The pharyngeal foregut remains abnormally shaped but assumes a more flat shape, similar to the normal pharynx. The pharyngeal pouch derivatives continue to appear to develop normally. More caudally, the foregut assumes a crescent shape (Fig. 3.15b). By E13.5, it becomes clear that the crescent shape of the pharyngeal foregut is caused by pressure from mesodermal thickening/swelling at the level of the thyroid gland (Fig. 3.15b). Caudal to that level, the foregut lumen narrows down significantly to almost pinpoint diameter (Fig. 3.15c). The foregut remains undivided along its entire length, and more caudally, starts to widen again until it ends in a trifurcation of two fused bronchopulmonary buds and a distal oesophagus/ fistula that leads to the stomach (Fig. 3.15d). The bronchopulmonary buds fail to separate and by

Fig. 3.15 Foregut anatomy in the E13.5 *Shh* null embryo

Schematic representation of the foregut in the E13.5 *Shh* homozygous null embryo (*a*) and transverse sections, stained with H&E, through E13.5 null embryos taken at the levels indicated on the diagram. (***b-f***) The pharyngeal foregut (Ph) has a crescent-like shape, which appears to be the result of a ventral mesodermal thickening (arrow in *b*). The post-pharyngeal foregut (Fo) has a pinpoint diameter (arrow in *c*) and widens caudally just cranial to the level of the lung buds (Lb). The foregut remains undivided between the pharynx and the lung buds and ends in a trifurcation of two lung buds and a fistula (Fi) to the stomach (*d*). The lung buds are fused and the developing bronchopulmonary structures are very rudimentary consisting of unbranched spaces (*d*). The fistula arises dorsally and also narrows down as it lies adjacent to the liver (*e*) (Li). The fistula (arrow in *f*) connects to the stomach (St) which appears morphologically normal. Scale bar, 200 μm

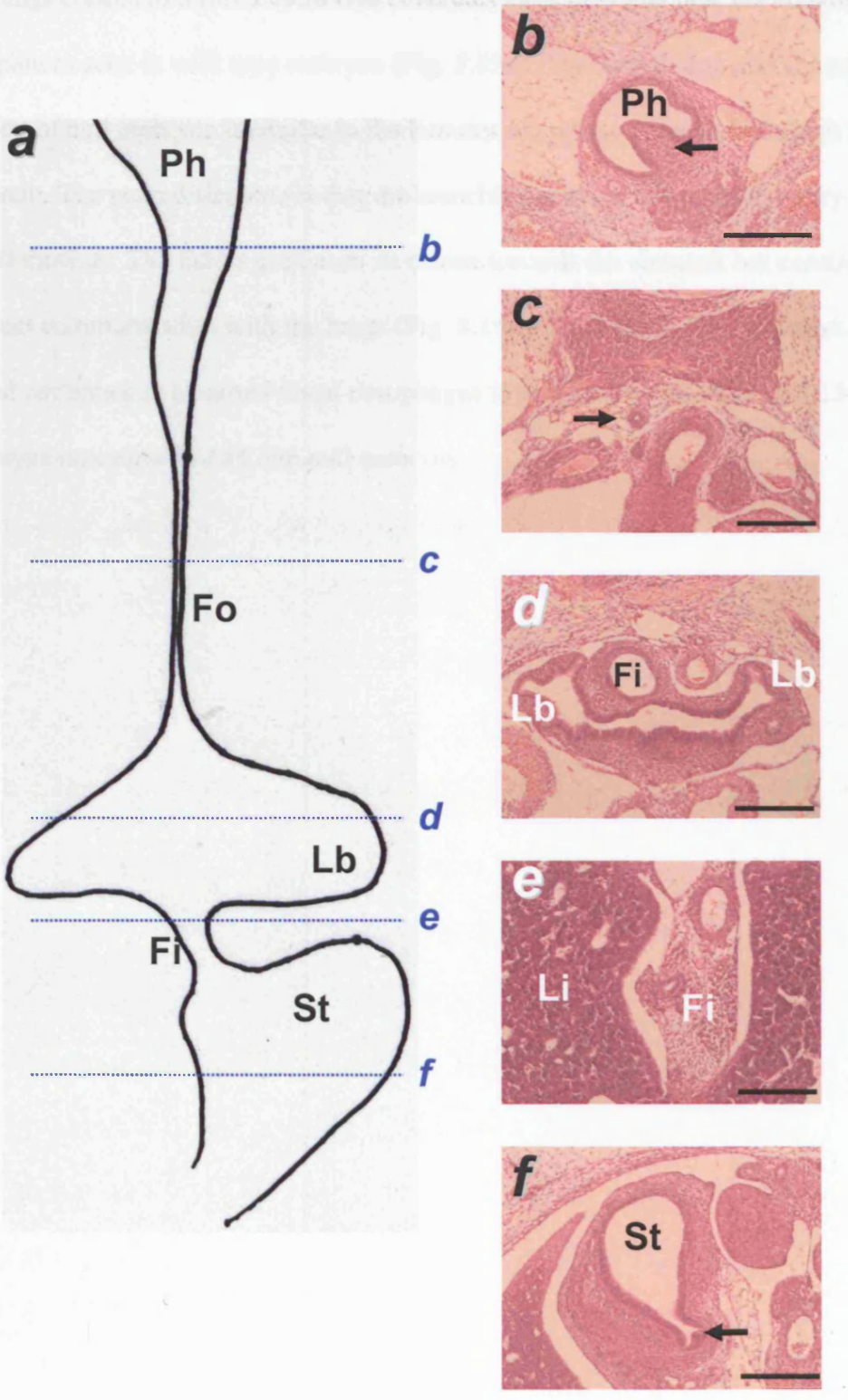
a
Ph
b
c
Fo
d
Lb
e
Fi
St
f
b
Ph
c
d
Fi
Lb
Lb
e
Li
Fi
f
St

E13.5 the lungs consist of a fused collection of dilated structures that lack the elaborate branching pattern seen in wild type embryos (Fig. 3.15d). The lung fusion and abnormal segmentation of null embryos is similar to the features of embryos treated with high doses of Adriamycin. The main difference is that the branching is much more rudimentary in the Shh null mutants. The fistula continues its course towards the stomach but continues to be in direct communication with the lungs (Fig. 3.15d). It eventually loses contact with the lung and continues as a narrow distal oesophagus towards the stomach (Fig. 3.15e,f). This phenotype is common to all *Shh* null embryos.

3.3 – DISCUSSION

3.3.1 – Importance of the Adriamycin mouse model of OA/TOF

The Adriamycin rat model of oesophageal atresia and tracheo-oesophageal fistula has been extensively studied since it was first described in 1996 (Diez-Pardo et al., 1996). The majority of the work on this model has focused on analysis of the morphology of the tracheo-oesophageal defects and the malformations observed in other organ systems. A number of theories have been put forward to explain the faulty organogenesis in the model but there has been little progress in understanding the cellular and molecular events that underlie these malformations. This lack of progress is understandable as the availability of molecular probes and genetically modified strains for the rat is significantly limited compared to the mouse. Yet, the Adriamycin rat model has provided a reproducible and reliable model of tracheo-oesophageal malformations, the phenotype of which closely parallels that of the human defects (Diez-Pardo et al., 1996; Crisera et al., 1999a; Merei et al., 1998c; Merei et al., 1997b). The adaptation of the Adriamycin model to the mouse provides extensive opportunities to study the molecular mechanisms that underlie these malformations and also allows direct comparison between developmental processes in the teratogenic and genetic models. Furthermore, this combined approach may contribute to our understanding of the cellular/molecular mechanisms that underlie normal development, which are not themselves well understood.

3.3.2 – Resolving the controversy of normal tracheo-oesophageal development

The controversy about the mechanisms that underlie normal tracheo-oeosphageal development is longstanding and one that has not yet been fully resolved. It is remarkable

that we have significant knowledge of the transcriptional control of pulmonary development, yet there is still a debate about the basic concept of how the trachea develops and separates from the oesophagus. The present detailed analysis of the stages of normal tracheo-oesophageal development in the CBA/Ca mouse was an integral part of the characterisation of the mouse model. Moreover, it contributes towards a resolution of the controversy regarding the mechanisms of normal development.

Historically, the two most prominent theories have been the so-called "tap water" theory (Sasaki et al., 2001b) and the theory of the ascending septum (Gray & Scandalakis, 1972). The former supports the notion that the trachea, with the two lung buds at its caudal end, simply grows caudally away from the foregut, from which it originates and, as a result, becomes separated from the oesophagus. The "ascending septum" theory supports the notion that the foregut is divided into a ventral trachea and a dorsal oesophagus by a septum that grows in a cranial direction. A variation of the septum theory suggests that the lateral walls of the foregut collapse and fuse, resulting in separation without the actual formation of an epitheliomesenchymal septum (Qi & Beasley, 2000; Williams et al., 2003). My data suggest that tracheo-oesophageal development involves elements of both theories. Following the appearance of the laryngotracheal groove in the narrowed, post-pharyngeal foregut at about E10 in the mouse, the foregut grows in length for approximately another 24 hours with no evidence of separation. At about that time, the trachea starts appearing as a separate structure at its caudal end, at the level of the lung buds. From that point onwards, the separated trachea increases significantly in length and by E11.5, the divided segment is longer than the undivided one. Tracheal growth is likely to contribute to the lengthening of the separated trachea, although it is important to bear in mind that during this period the entire foregut continues to grow in length. Yet, at the

same time, the absolute length of the undivided segment decreases significantly between E10.5 and E11.5 and virtually disappears by E12.5. These observations suggest that there is an active separation process that is responsible for separating the originally undivided foregut whilst active growth of the various foregut components continues. Even if we assume that the rate of longitudinal growth of the respiratory structures is far greater than that of the rest of the foregut, a specific separation process is still required to account for these changes in lengths.

3.3.3 – The early defect in the Adriamycin model

Analysis of the Adriamycin mouse model (4 mg/kg) suggests that the early events within the developing foregut are not overtly disturbed in embryos destined to develop OA/TOF. The development of the laryngotracheal groove, and the appearance of lung buds from its caudal end, appear to proceed normally in Adriamycin-treated embryos. Development in treated embryos first diverges morphologically from that in controls between E10.5 and E11.5 when the foregut fails to divide into a distinct dorsal oesophagus and ventral trachea. It should be noted that this onset of abnormalities occurs more than 48 hours after the second dose of the teratogenic agent, at E8.5. The findings suggest that this failure of foregut division, with persistence of an oesophagotrachea, is fundamental to the embryogenesis of OA/TOF in the Adriamycin-treated mouse. Failure of foregut division can be total, in which case the oesophagotrachea ends in a trifurcation, or it can be partial, with a more proximal emergence of the fistula; in such embryos, the fistula and trachea are separate structures for a short distance. With regards to the nature of this early anomaly, analysis of the foregut length data suggest that disturbance of overall foregut growth is not a factor in Adriamycin-treated embryos as the total foregut length is comparable between affected experimental and control embryos. It appears that what is

disturbed is the process of separation, resulting in the undivided segment contributing the whole or the majority of the foregut length. It should of course be pointed out that an assessment of growth with the use of markers of mitosis or proliferation would be required to address this question more accurately.

Analysis of the early events in the Adriamycin mouse model appears to reject an alternative theory put forward by researchers working on the rat model. It has been suggested that the primary defect is atresia and loss of continuity of the oesophagus with the development of an abnormal communication (fistula) between the trachea and the distal oesophagus/ stomach (Crisera et al., 1999a). This theory assumes that tracheo-oesophageal separation has already taken place and that the separated oesophagus then becomes atretic. This notion is contradicted by my data which suggest that, at the earliest possible point, the foregut can be seen as having failed to separate. Recent evidence that the tracheo-oesophageal fistula can be shown to be discontinuous from the stomach in some embryos (in the rat model) (Spilde et al., 2002a), could perhaps be explained by my observation that the fistula in the mouse model can itself be atretic and not communicate with the stomach whilst the fundamental defect remains the failure of tracheo-oesophageal separation.

3.3.4 – Specificity of the Adriamycin-generated defects

A general problem with teratogenic models is that it is often difficult to identify the specific effect on cellular function that produces the resulting phenotype. Adriamycin interferes with a number of cellular processes including DNA synthesis and cell replication (Ross et al., 1978). Crown-rump length data suggest that Adriamycin does have a growth retarding effect, but that this is only significant after E12.5. Adriamycin-

treated embryos appear to grow normally in the initial period after exposure, during the time of tracheo-oesophageal separation (E10.5-12). Analysis of somite numbers at E10.5 suggests that Adriamycin-treated embryos are slightly developmentally delayed (27 versus 28 somites), but this effect disappears by E11.5. It is difficult to draw firm conclusions from these data, but it appears that growth and development in Adriamycin-treated embryos are not grossly disturbed during the early period of foregut patterning. On the other hand, even small developmental perturbations in critical time windows can have significant phenotypic consequences. On balance, however, the Adriamycin effect appears to be a specific one, affecting tracheo-oesophageal separation and other morphogenetic processes (e.g. heart development).

Adriamycin appears to be a useful tool for the study of abnormal tracheo-oesophageal separation. It interferes with the process, but at the dose used in this study (4 mg/kg) does not seem to interfere with other related developmental events at either end of the respiratory foregut, such as pulmonary and laryngeal development. At the caudal end of the trachea, lung development is undisturbed, as is the development of the entry into the larynx at the cranial end of the laryngotrachea. Adriamycin specifically disturbs the tracheo-oesophageal separation process. The effect of Adriamycin on other organ systems is likely to be related to the timing of exposure to the teratogenic insult. This could account for the multiple associated malformations, reported in the Adriamycin-treated rat, which largely conforms to the VACTERL association (Merei et al., 1999; Beasley et al., 2000; Millar et al., 2001).

The association between OA/TOF and notochordal malformations in the Adriamycin-treated rat has been studied in detail (Possoegel et al., 1999; Qi & Beasley, 1999;

Vleesch, V et al., 2002; Gillick et al., 2003; Merei, 2004). Abnormalites of the notochord have also been linked to the development of midgut and other intestinal atresias (Gillick et al., 2002a; Merei, 2004). The close association between defects of the notochord and tracheo-oesophageal malformations makes it possible that the abnormal notochord somehow disturbs foregut development. The actual tethering of the ventral branches of the notochord to the foregut provides a mechanistic interpretation of such disruption (Qi & Beasley, 1999; Williams et al., 2001; Vleesch, V et al., 2002). Conversely, it has been suggested that compensatory overgrowth of the foregut during embryogenesis of OA/TOF causes abnormal bending of the tethered notochord (Merei et al., 1998). Others have questioned the cause-effect association between the two malformations as either of them can be seen in isolation (Possoegel et al., 1999). The role of the notochord as a source of important developmental signals (Kim et al., 1997) provides an alternative, molecular explanation for the association between abnormalities of the notochord and foregut. The conservation of *Shh* expression in the abnormally positioned notochord could underlie the development of tracheo-oesophageal malformations (Gillick et al., 2003; Mortell et al., 2004). The findings, in the present study of the Adriamycin-treated mouse, of abnormally divided and positioned notochords, sometimes tethered to the foregut, are consistent with the studies in the Adriamycin-treated rat. Furthermore, the association of notochordal defects and tracheo-oesophageal malformations is statistically significant (Table 5). The role of the abnormal notochord as an ectopic source of Shh is discussed in depth in Chapter 5.

3.3.5 – The late rearrangement of the tracheo-oesophageal phenotype

An atretic upper oesophagus is an infrequent finding in the Adriamycin mouse model. Considering that all abnormal E11.5 embryos share the phenotype of an undivided

foregut without a distinct oesophagus, one could hypothesise that a short, atretic oesophagus, seen at E12.5 in two embryos, develops as a result of rearrangement of the proximal oesophagotrachea rather than by atresia of a normally separated oesophagus. This is consistent with the finding that the proximal atretic oesophagus is also abnormal at its cranial end, where it separates from the pharynx. This hypothesis is supported by evidence from the Adriamycin rat model that has a higher prevalence of proximal OA. In one report (Possogel et al., 1998), 9 out of 10 Adriamycin-exposed embryos at E12 had an undivided oesophagotrachea, which developed into proximal OA with distal TOF in all 9 by E13. In another study in the rat, the proximal oesophageal pouch first appeared as a dorsal outpouching from the cranial foregut on E15, well after the completion of tracheo-oesophageal separation (Beasley et al., 2004). This confirmed that the development of the proximal oesophagus in OA/TOF is a separate developmental process. The higher prevalence of proximal (OA) in the rat model could perhaps be explained by a species difference in the way the foregut adapts to failure of separation. An alternative explanation is that the Adriamycin effect on foregut development in the rat differs from that in the mouse, as the requirement for a significantly higher dose in the mouse would suggest (4 mg/kg versus 1.75 mg/kg in the rat).

The majority of late gestation or near-term affected Adriamycin-treated mouse fetuses have a persistently undivided or partially undivided oesophagotrachea with no evidence of the so-called upper oesophageal pouch. In fact, the near term phenotype of the majority of Adriamycin-treated fetuses resembles a rare human malformation known as laryngotracheo-oesophageal cleft. According to the classification of these malformations (Holder, 1993), in type III cleft there is a communication between the laryngotrachea and the oesophagus that extends into the trachea whereas in type IV cleft the communication

extends all the way to the tracheal bifurcation. Based on this classification, the mouse phenotype of the oesophagotrachea and trifurcation or proximal fistula could be characterised as type IV or type III clefts respectively (see General Introduction). This phenotypic analysis would suggest that OA/TOF and laryngotracheo-oesophageal clefts are closely related embryologically and indeed share the same fundamental anomaly. According to this theory, all OA/TOFs start as clefts that are subsequently modified by rearrangement of the proximal foregut.

If we compare the Adriamycin rat and mouse models, there is obviously a phenotypic difference. The rat malformations resemble closely the human anomalies. On the other hand, the mouse malformations resemble the rare forms of human tracheo-oesophageal defects. The key, however, is that the two models have almost identical early malformations. Based on this similarity, the mouse model can be used to study the fundamental defects that underlie the majority of tracheo-oesophageal malformations.

3.3.6 – Fundamental defect in the *Shh* mutant

The foregut malformations in the *Shh* mutant mouse embryos have been previously described (Litingtung et al., 1998), although a review of the relevant literature reveals a lack of clarity in the description of the phenotypic arrangements at the caudal end of the trachea. Authors state that the lumen of the trachea/oesophagus, or even the lungs, is in direct contact with that of the stomach and call this oesophageal atresia and tracheo-oesophageal fistula. Atresia of the oesophagus is certainly not demonstrated and the nature of the fistulous connection between the trachea and the stomach/ distal oesophagus is not well illustrated or explained. Furthermore, the description of the cranial foregut

contradicts the present findings, by suggesting that the trachea and oesophagus have separate lumens but never completely separate, with their walls in close apposition. My analysis offers a more straightforward interpretation of the tracheo-oesophageal development in the *Shh* mutant. Contrary to previous reports, I found that the trachea and oesophagus failed to separate in all embryos examined. The undivided oesophagotrachea gave rise to the lungs, which are themselves grossly abnormal. The oesophagotrachea/lungs are themselves connected to the stomach by a short 'fistula' which probably corresponds to the previous description of the lungs being 'continuous with the stomach' (Litingtung et al., 1998).

Hence, the tracheo-oesophageal phenotype of both the Adriamycin-treated and *Shh* mutant embryos is similar and essentially comprises an undivided oesophagotrachea and an abnormal communication (fistula) of this undivided structure to the stomach. Further clarification and analysis of the proximal foregut (pharyngeal) anatomy in the *Shh* mutant is required, as this was not analysed in detail in the present study.

3.3.7 – Importance of a comparative analysis of the Adriamycin and *Shh* models

One of the reasons for adapting the Adriamycin model from the rat to the mouse was the availability of mouse genetic models of tracheo-oesophageal malformations. The advantage of this approach is as follows: first, the tracheo-oeosphageal phenotype produced by Adriamycin closely resembles human malformations. Second, the analysis of the molecular mechanisms that underlie the abnormal tracheo-oesophageal development in the Adriamycin-treated mouse will benefit from a direct, stage by stage, comparison with an equivalent mouse model in which the tracheo-oesophageal malformations can be attributed to a precise genetic perturbation (loss of function mutation). The close

phenotypic similarity between the Adriamycin and *Shh* models is a significant finding. It would suggest that both the action of the teratogenic agent and the loss of function mutation of *Shh*, lead to a similar failure in the physical separation of the trachea and oesophagus. This similarity does not, of course, mean that Adriamycin acts by directly (or indirectly) disturbing the function of *Shh*, although this is a possibility. More importantly, it focuses attention on the specific process of tracheo-oesophageal separation as fundamental to the pathogenesis of tracheo-oesophageal malformations. Furthermore, it allows us to create testable hypotheses for the possible mode of action of Adriamycin. Such hypotheses are elaborated and tested in subsequent chapters of this thesis.

3.4 - SUMMARY

The Adriamycin model of tracheo-oesophageal malformations was described in the rat whereas genetic models exist in the mouse. In order to study the molecular basis of these malformations, the Adriamycin model was adapted to the mouse. Analysis of the length of foregut segments suggests that during normal mouse development, the trachea grows initially as part of an undivided foregut and later becomes separated from the dorsal oesophagus with the separation process starting at the level of the lung buds and proceeding in a cranial direction. In the Adriamycin-treated mouse embryos, tracheo-oesophageal development is disturbed with the fundamental anomaly being a total or partial failure of the process of tracheo-oesophageal separation. Adriamycin, at the dose used for detailed analysis in this study, does not interfere with development at either end of the trachea (larynx and lungs) suggesting that its action specifically disturbs the tracheo-oesophageal separation process. The foregut of *Shh* null mutant embryos also fails to develop a separate trachea and oesophagus. These observations suggest that both the teratogen and the loss of gene function interfere with the same fundamental process during tracheo-oesophageal development.

CHAPTER 4 – DEVELOPMENT OF THE RESPIRATORY ENDODERM

4.1 - INTRODUCTION

The findings of the previous chapter suggested that normal tracheo-oesophageal development involves an active process of separation between the ventral, respiratory and the dorsal, gastrointestinal parts of the anterior foregut. Failure of this process of separation seems certain to underlie the development of tracheo-oesophageal malformations in both Adriamycin-treated and the homozygous *Shh* null mutant mouse embryos. However, the findings of the previous chapter comprised entirely an analysis of morphological data. It is important to extend this analysis to ask whether the process of tracheo-oesophageal separation leads to segregation of molecularly defined cell populations (i.e. respiratory and gastrointestinal) within the developing foregut. It is moreover crucial to distinguish between models of abnormal morphogenesis in which either both cell fates are represented in the undivided foregut, or whether failure of separation results from the failure of either of the main cellular elements (respiratory or gastrointestinal) to develop. Theories attributing tracheo-oesophageal malformations to an imbalance of fates within the foregut have been formulated for the Adriamycin-rat model. On the one hand, it has been suggested that the respiratory element is deficient resulting in the lung buds arising directly from the primitive foregut in the absence of a normal trachea (Merei et al., 1998a; Merei et al., 1997b; Possogel et al., 1998a). The same theory postulates secondary trachealisation of the primitive foregut. On the other hand, it has been suggested that following normal development of the two elements, there is loss of the gastrointestinal element between the proximal oesophagus and the stomach (primary oesophageal atresia) (Crisera et al., 1999a).

In order to resolve these conflicting theories, I reasoned that it would be important to study endodermal and respiratory development in both normal and abnormal tracheo-oesophageal development. In this chapter, therefore, I have studied expression of the endodermal marker *Hnf3β* and that of the respiratory marker *Nkx2.1*. The aim was to establish whether the effect of Adriamycin, or the loss of function of *Shh*, were mediated by, or associated with, interference with the molecular specification and development of the respiratory endoderm.

4.2 – RESULTS

4.2.1 – Expression of the endodermal marker Hnf3β

During normal mouse development, expression of the winged helix transcription factor *Hnf3β* is detected at the onset of gastrulation (about E6.5) in the anterior portion of the primitive streak (Ang et al., 1993). Its expression persists in the developing neural tube and the definitive endoderm (Fig 4.1a), structures derived from the mouse equivalent of Hensen's node. Endodermal expression is detected in both the foregut endoderm and the various foregut derivatives including the pharyngeal pouches, the hepatic diverticulum and the respiratory diverticulum . At E10.5, Hnf3β is detected in the postpharyngeal foregut and the endoderm of the ventral evagination representing the respiratory diverticulum and the primitive lung buds . As the trachea begins to separate from the oesophagus (E11.5), both structures maintain strong Hnf3β expression At E12.5, Hnf3β expression is maintained in the trachea, oesophagus, developing bronchopulmonary structures and other endoermally-derived organs, for example the liver, as shown by its detection in hepatocytes (Fig. 4.1a). In summary, Hnf3β expression is consistent with that of a factor that is involved in both the establishment and the maintenance of the endodermal lineage.

Exposure to Adriamycin does not disturb the expression of Hnf3β. Adriamycin-treated embryos had expression patterns closely similar to controls irrespective of whether they were morphologically normal or had tracheo-oesophageal malformations. At E10.5, all Adriamycin-treated embryos have uniform Hnf3β expression in the endoderm of the undivided foregut. From E11.5 onwards, embryos that fail to separate the trachea from the oesophagus have an undivided foregut with Hnf3β expression in both the ventral and

Fig. 4.1 The transcription factor Hnf3β is uniformly expressed in the foregut endoderm.

Immunohistochemistry for Hnf3β on transverse sections from saline-treated (*a*) and Adriamycin-treated (*b,c*) E12.5 embryos. **(*a*)** At low magnification, Hnf3β is seen in the floor plate of the neural tube (Fp), the oesophagus (Oe), the lung buds (Lu) and the hepatocytes (hp - *weak staining*). **(*b*)** The common oesophagotrachea (Oet) of Adriamycin-treated embryos is uniformly stained in both dorsal and ventral parts. **(*c*)** At the level of the trifurcation, both the lung buds (arrowheads) and the prospective fistula (arrow) are positive for Hnf3β. Adr - Adriamycin. Scale bar, 120 μm.

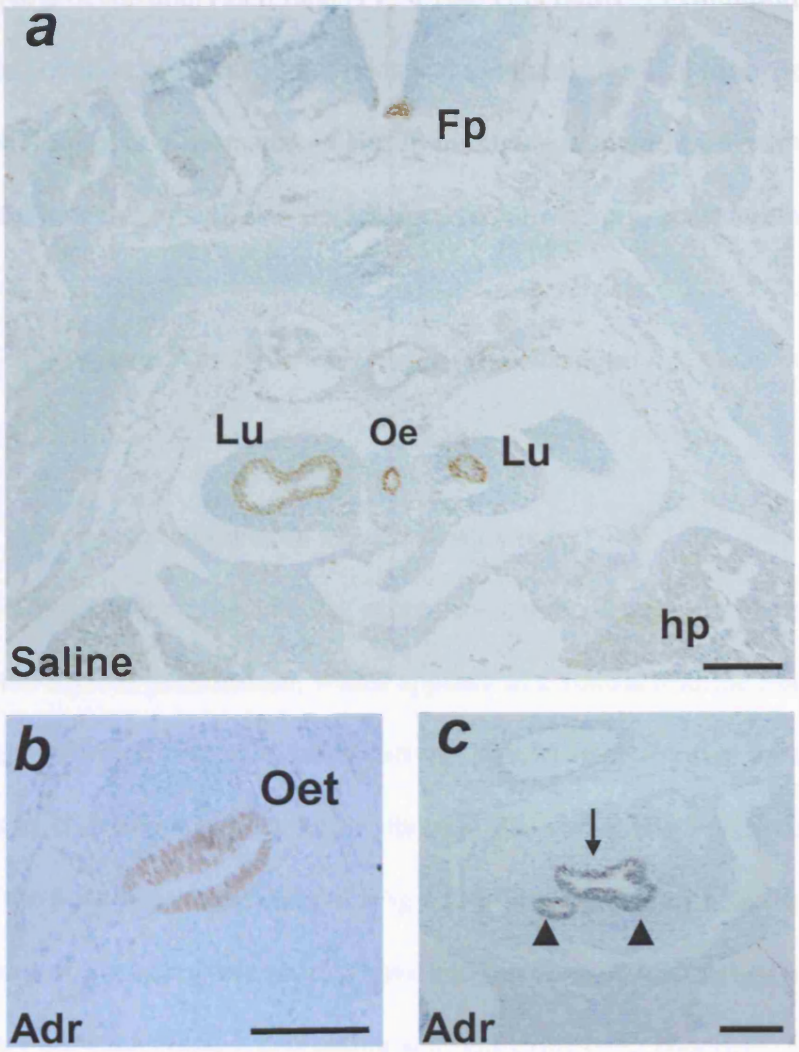
a
Fp
Lu
Oe
Lu
hp
Saline
b
Oet
Adr
c
Adr

dorsal parts of the undivided tube (Fig 4.1b). This uniform expression persists all the way to the trifurcation of the two lung buds and the fistula with all three branches being positive (Fig 4.1c). Expression of Hnf3β in other endodermal derivatives and the floor plate of the neural tube is also undisturbed in Adriamycin-treated embryos (*not shown*).

4.2.2 – The role of *Nkx2.1* in respiratory development

4.2.2.1 - Expression patterns in normal development

In E9.5 CBA/Ca embryos, Nkx2.1 expression can be detected in ventral areas of the brain and in the thyroid primordium, which appears as a ventral midline thickening in the pharyngeal foregut (Fig 4.2a, inset). Strong Nkx2.1 expression in the thyroid primordium persists at 10.5 (Fig 4.2a). By E10.5, there is also strong Nkx2.1 expression in the ventral part of the post pharyngeal foregut (Fig 4.2c). The transcription factor is expressed in the endoderm of the laryngotracheal groove and the prospective trachea with a well-defined boundary between Nkx2.1 expressing and non-expressing endoderm (Fig 4.2c). At the caudal end of the prospective trachea, the two lung buds are also strongly positive for Nkx2.1 and have actually started to bud off the foregut (Fig 4.2e). This arrangement persists at E11.5, with Nkx2.1 expression being restricted to the prospective respiratory epithelium (Fig 4.3a,d,e). by this stage, tracheo-oesophageal separation has started at the level of the lung buds and is progressing cranially. The separated trachea is strongly Nkx2.1-positive in contrast to the dorsal oesophagus that is entirely negative (Fig 4.3g,h). At more cranial levels, the still undivided foregut maintains the dorsoventral pattern seen in the E10.5 foregut (Fig 4.3d,e). At levels just cranial to the separation front, the foregut that is about to undergo separation appears to invaginate along the dorsoventral boundary demarcated by Nkx2.1 expression (Fig 4.3d,e). In order to demonstrate that dorsoventral

Nkx2.1 expression corresponds to the pattern of respiratory differentiation of the foregut endoderm, I used a histochemical technique that stains proteoglycans produced by respiratory cells at this stage (Periodic Acid Schiff, PAS). The results show that Nkx2.1 expression corresponds well with functional cellular differentiation within the developing foregut (Fig 4.3b,e,h,l). Strong Nkx2.1 expression is maintained at E12.5, during the period of completion of tracheo-oesophageal separation (Fig 4.4). Branching morphogenesis of the lungs is progressing and the bronchopulmonary tissues are strongly Nkx2.1- positive (Fig 4.4g). The trachea remains strongly Nkx2.1-positive in sharp contrast to the oesophagus that is negative (Fig. 4.4c,e). At this stage, laryngeal development is in progress and Nkx2.1 expression is seen in parts of the developing larynx. Specifically, it is expressed in the rostral-most part of the laryngotracheal groove, the precursor of the subglottic larynx (Fig. 4.4a). From E14.5 onwards, the pattern described above has started to change; Nkx2.1 expression in the proximal respiratory structures (larynx and trachea) has started to be downregulated whilst strong expression is maintained in the developing lungs (Fig 4.5). Interestingly, in the anterior foregut, the thyroid adjacent to the trachea maintains a strong Nkx2.1 signal (Fig 4.5). This pattern persists towards term with expression becoming virtually restricted to the lungs.

4.2.2.2 - Expression patterns in the Adriamycin mouse model

As seen from the analysis of the morphological data, the early developmental events within the anterior foregut are not overtly disturbed by Adriamycin treatment. Examination of Nkx2.1 expression confirms this finding. At E9.5, *Nkx2.1* expression in the thyroid primordium is comparable to saline controls. At E10.5, the laryngotracheal groove develops normally and the expression pattern of Nkx2.1 in the groove and in the ventral prospective trachea is comparable to controls in all Adriamycin-treated embryos

Fig. 4.2 The expression pattern of the respiratory marker Nkx2.1 is not disturbed in Adriamycin-treated embryos at E10.5

Immunohistochemistry for Nkx2.1 on transverse sections from E10.5 saline-treated (a,c,e) and Adriamycin –treated embryos (b,d,f). ***(a,b)*** Expression of *Nkx2.1* in the thyroid primordium (Th), in the floor of the pharyngeal foregut (Ph), is undisturbed in Adriamycin-treated embryos. *Nkx2.1* expression in the primordium starts at E9.5 (inset). ***(c,d)*** *Nkx2.1* marks the dorsoventral boundary within the anterior foregut (Fo) (arrowheads) and is expressed in the ventral, prospective tracheal epithelium. ***(e,f)*** At more caudal levels, *Nkx2.1* is strongly expressed in the lung buds (Lb). Scale bar, 100 μm.

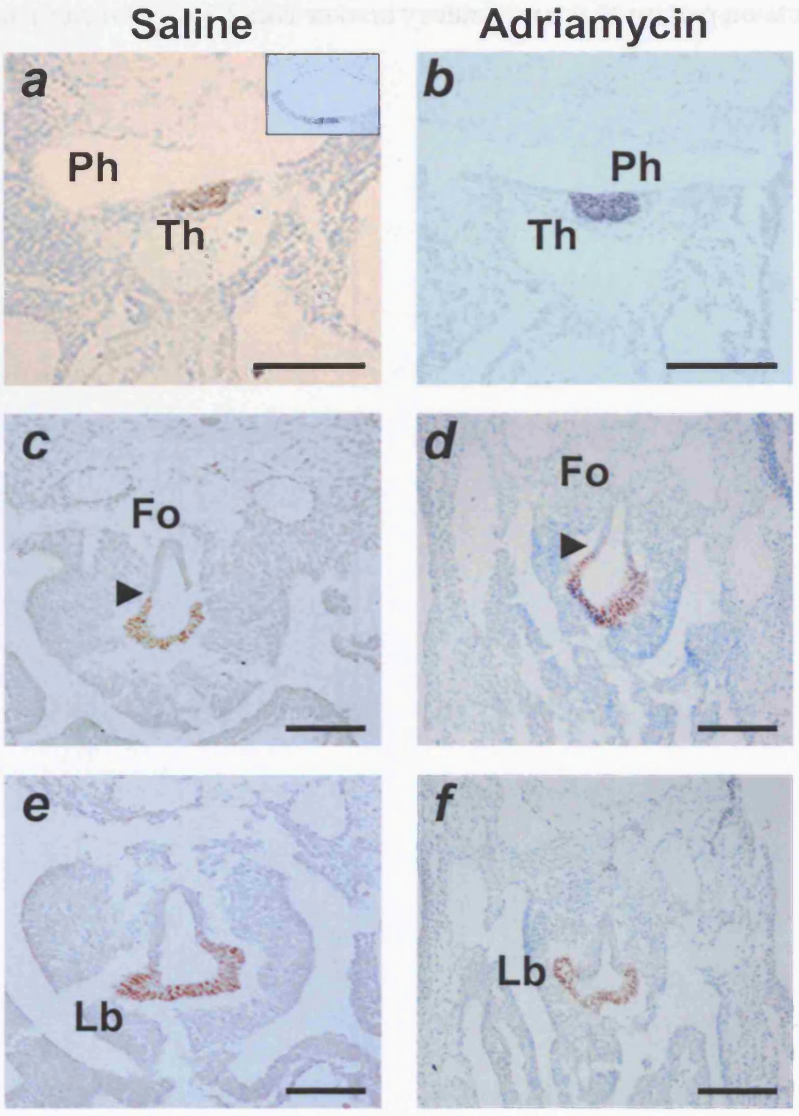
Saline
Adriamycin
a
Ph
Th
b
Ph
Th
c
Fo
d
Fo
e
Lb
f
Lb

Fig. 4.3 Failure of foregut separation in Adriamycin-treated embryos is not associated with a disturbance in the dorsoventral pattern of *Nkx2.1* expression

Immunohistochemistry for Nkx2.1 (except in *b*) on transverse sections from saline-treated (*a,b, d,e,g,h,k,l*) and Adriamycin-treated (*c,f,i,m*) E11.5 embryos. Sections in *b,e,h and l* were counterstained with PAS (Periodic Acid Schiff) which stains with magenta colour the proteoglycans produced selectively by cells of the respiratory lineage at this stage. Sections from top to bottom are from increasingly caudal levels and sections in each row are from corresponding levels. ***(a,b,c)*** Sections at the level of the laryngotracheal groove (Lt) show that Nkx2.1 expression is comparable in saline and Adriamycin-treated embryos. Note the strong PAS staining in the ventral-most part of the groove. ***(d,e,f)*** At levels just cranial to the point of tracheo-oesophageal separation, the foregut (Fo) in saline-treated embryos develops epithelial folds that coincide with the dorsoventral boundary of Nkx2.1 expression (arrowheads in *d*) as well as the dorsoventral boundary of PAS staining (arrowheads in *e*). In Adriamycin-treated embryos, the dorsoventral pattern of Nkx2.1 expression is not disturbed (arrowhead in *f*) although at this level there are no identifiable epithelial folds. ***(g,h,i)*** At more caudal levels, the Nkx2.1-positive trachea (Tr) has separated from the Nkx2.1-negative oesophagus (Oe) in saline-treated embryos (*g*) and the respiratory trachea stains strongly for PAS in contrast to the oesophagus (*h*). In the Adriamycin-treated embryo, the foregut has failed to separate and persists as an undivided oesophagotrachea (Oet) which, however, maintains the correct dorsoventral pattern of Nkx2.1 expression (arrowhead in *i*). ***(k,l,m)*** The bronchi (Br) maintain both a strong Nkx2.1 and PAS signal (*k.l*). The oesophagotrachea in Adriamycin-treated embryos ends in a trifurcation of an Nkx2.1-negative fistula and two Nkx2.1-positive bronchi. Scale bar, 100 μm.

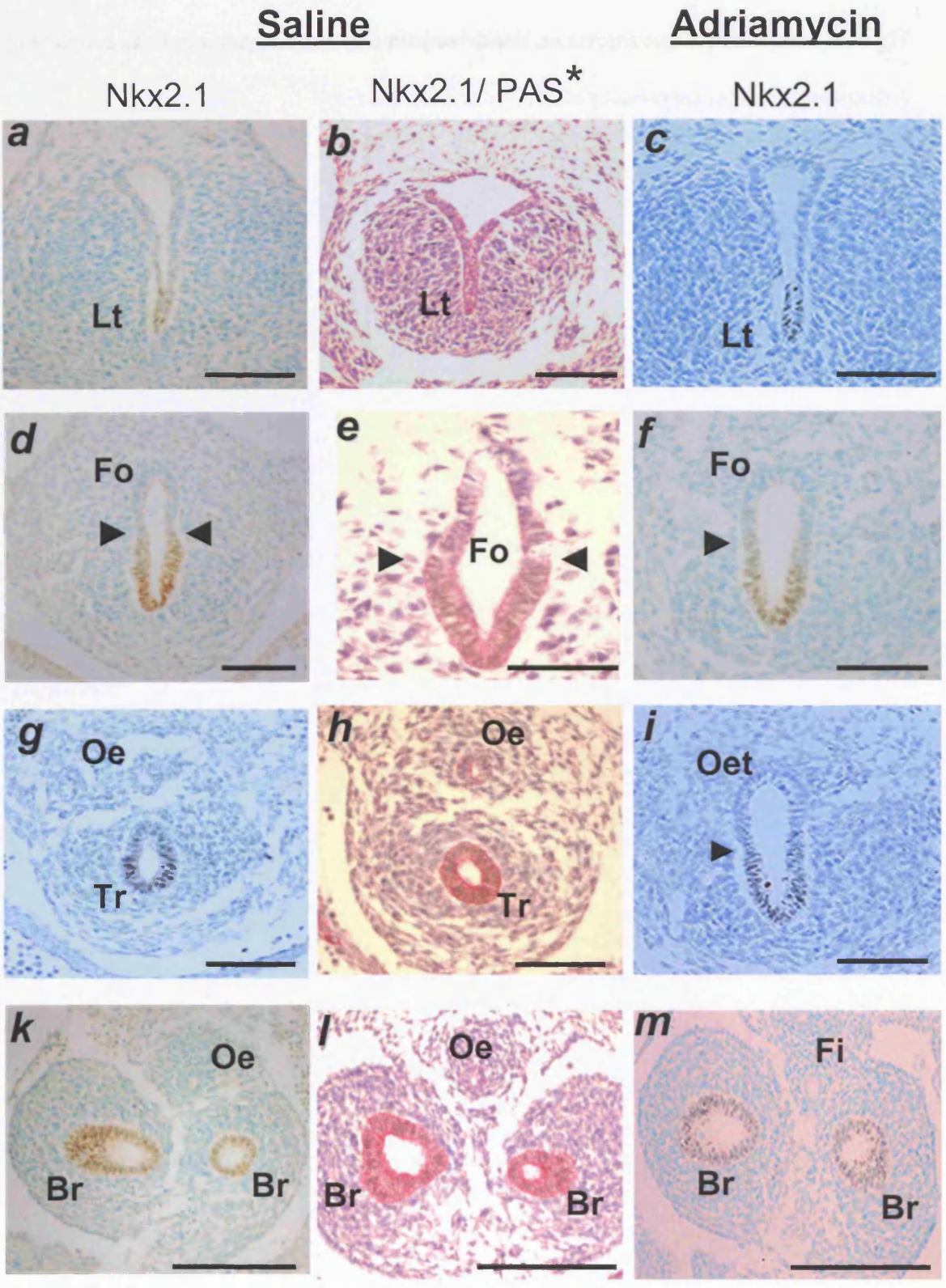

* Only PAS staining used in panel *b*

Fig. 4.4 The dorsoventral pattern of *Nkx2.1* expression is maintained in both saline- and Adriamycin-treated embryos at E12.5.

Immunohistochemistry for Nkx2.1 on transverse sections from saline-treated (*a,c,e,g*) and Adriamycin-treated (*b,d,f,h*) E12.5 embryos. **(*a-d*)** Sections at the level of the thyroid gland (Th) show comparable expression in the laryngotracheal groove (Lt) (*a,b*). At a slightly more caudal level, the Nkx2.1 positive trachea has become separated from the Nkx2.1 negative oesophagus in saline-treated embryos, in contrast to Adriamycin-treated embryos that have an undivided oesophagotrachea (Oet). The oesophagotrachea maintains the correct dorsoventral pattern of Nkx2.1 expression (arrowheads). **(*e,f*)** At the level of the heart (h), this pattern persists (arrowheads in *f*). **(*g,h*)** The branching bronchi maintain a strong Nkx2.1 signal in contrast to the oesophagus in saline-treated embryos. In Adriamycin-treated embryos, the strong bronchial signal contrasts with the lack of Nkx2.1 expression in the fistula (Fi). Scale bar, 100 μm.

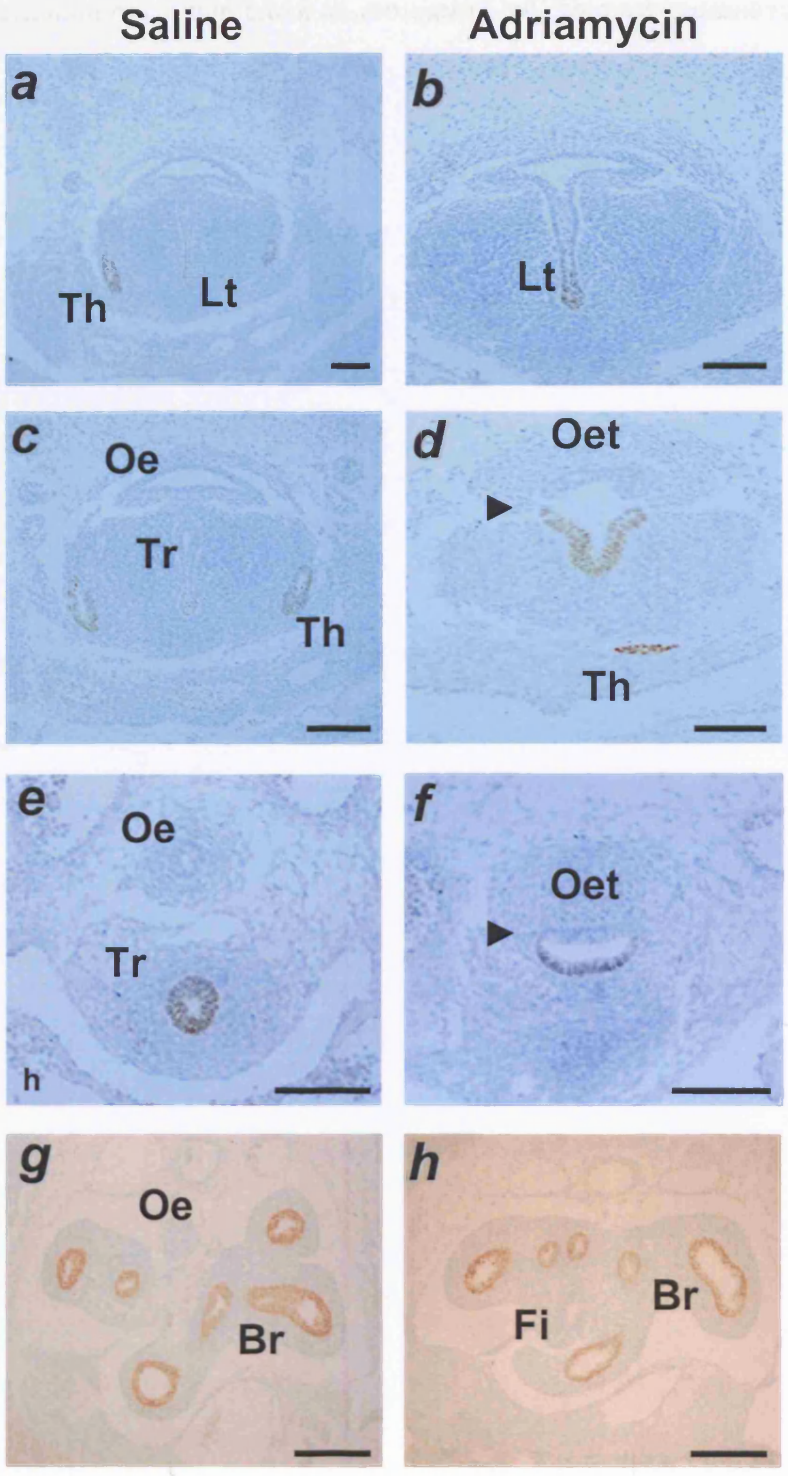
Saline
Adriamycin
a
Th
Lt
b
Lt
c
Oe
Tr
Th
d
Oet
Th
e
Oe
Tr
h
f
Oet
g
Oe
Br
h
Fi
Br

Fig. 4.5 Following tracheo-oesophageal separation, at E14.5, the trachea loses most of its Nkx2.1 expression in contrast to the lungs

Immunohistochemistry for Nkx2.1 on transverse sections from a saline-treated (*a*) and an Adriamycin-treated (*b*) E14.5 embryo taken at the level of the thyroid gland (Th). **(*a*).** In saline –treated embryos, the trachea (Tr) is weakly positive for Nkx2.1 in contrast to the thyroid gland which maintains a strong Nkx2.1 signal. The oesophagus (Oe) remains completely *Nkx2.1*-negative. The inset shows that the branching bronchi (Br) also remain strongly *Nkx2.1*-positive. **(*b*)** In Adriamycin-treated embryos that have failed to separate the trachea from the oesophagus, the undivided oesophagotrachea (Oet) also has a very weak Nkx2.1 signal in contrast to the adjacent thyroid gland. Although not immediately obvious from this section, the oesophagotrachea still maintains the dorsoventral boundary of Nkx2.1 expression at this level (arrowheads). This is confirmed by other sections (*not shown*). Scale bar, 200 μm

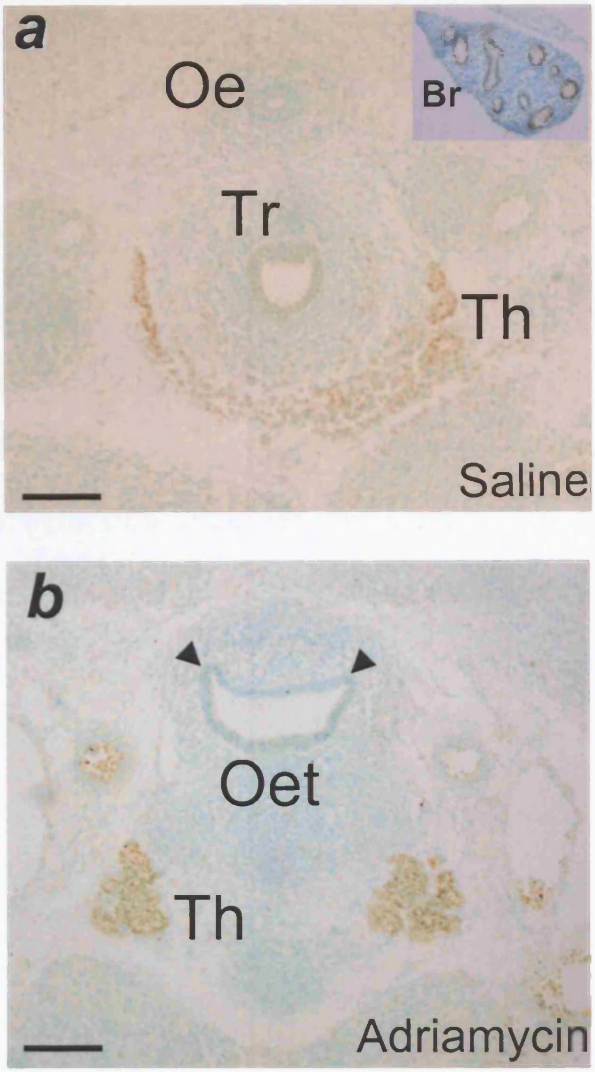
a
Oe
Br
Tr
Th
Saline
b
Oet
Th
Adriamycin

Fig. 4.6 Changes in the dorsoventral balance of *Nkx2.1* expression of the undivided foregut

Immunohistochemistry for Nkx2.1 on transverse sections from Adriamycin-treated E13.5 embryos. Section *a* is from the level of the thyroid gland and sections *b* and *c* are from progressively more caudal levels. **(*a*)** The undivided oesophagotrachea (Oet) has a clear dorsoventral boundary in *Nkx2.1* expression at the level of the thyroid gland (Th) which also has a strong *Nkx2.1* signal. Even at this level, the ventral *Nkx2.1*-positive domain has started to extend onto the dorsal foregut (arrowheads in *a*). **(*b,c*)** This encroachment becomes more pronounced in more caudal sections but the dorsal-most part of the oesophagotrachea maintains its *Nkx2.1*-negative status (arrowheads in *b* and *c*). Scale bar, 200 μm

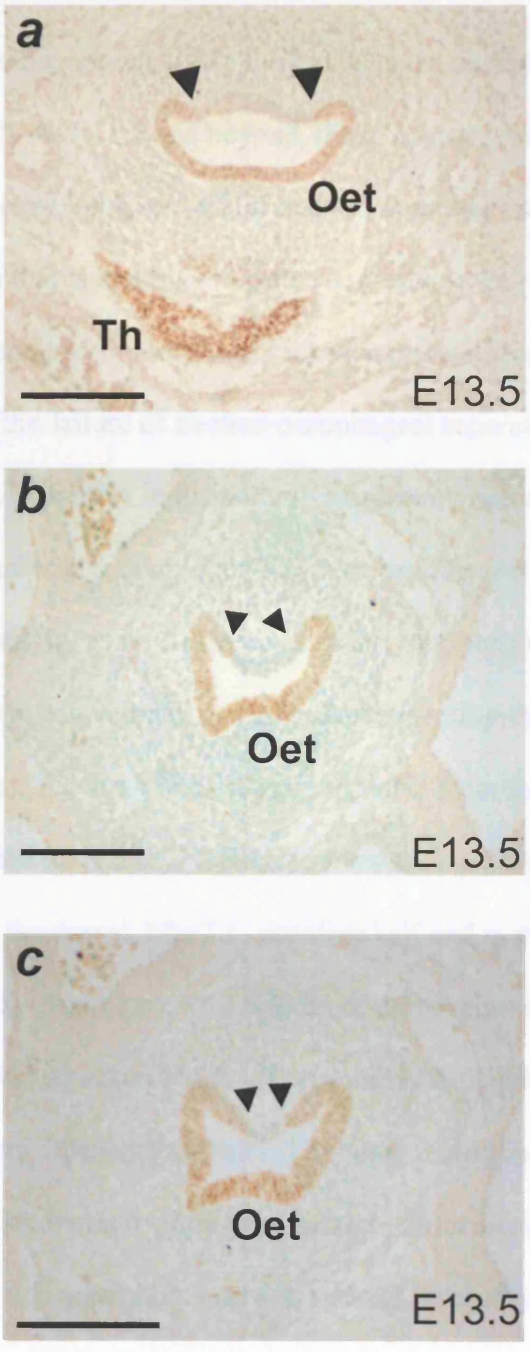
a
Oet
Th
E13.5
b
Oet
E13.5
c
Oet
E13.5

(Fig 4.2c,d). The same applies to the lung buds at the caudal end of the prospective trachea (Fig 4.2e,f). At E11.5 and beyond, those Adriamycin-treated embryos that are phenotypically normal, with successful tracheo-oesophageal separation, have an Nkx2.1 expression pattern that is identical to saline controls. In E11.5 Adriamycin-treated embryos with an undivided oesophagotrachea, expression of Nkx2.1 is not itself disturbed but rather reflects the failure of tracheo-oesophageal separation. In the E11.5 undivided foregut, Nkx2.1 is expressed in the ventral, respiratory part of the structure and is absent from the dorsal part with a sharp boundary between the two domains (Fig 4.3c,f,i). This pattern extends caudally as far as the level of the lung buds where the foregut effectively ends in a trifurcation of two buds and a fistula connecting the oesophagotrachea to the stomach (Fig 4.3m). The lung buds clearly originate from the ventral, Nkx2.1-positive half of the undivided foregut and are themselves strongly Nkx2.1-positive whereas the fistula arises from the dorsal, Nkx2.1- negative half and is itself entirely Nkx2.1-negative at this stage (E11.5) (Fig 4.3m). This pattern of dorsoventral *Nkx2.1* expression persists for both the oesophagotrachea and the fistula at E12.5 (Fig 4.4d,f,h). From E13.5 onwards, this pattern changes gradually. The foregut remains undivided, but the balance of Nkx2.1 expression along the dorsoventral axis shifts dorsally (Fig 4.6). The Nkx2.1 positive domain starts encroaching onto the dorsal foregut but does not take over the entire foregut. A small Nkx2.1 negative domain persists in the dorsal-most part of the undivided foregut. Interestingly, this encroachment becomes more evident more caudally (Fig 4.6). At later gestations (E15.5 onwards), the gradual downregulation of *Nkx2.1* expression in the cranial respiratory structures makes it difficult to comment on this balance.

4.2.2.3 - Tracheo-oesophageal fistula in the Adriamycin mouse model

As described above, the Nkx2.1 status of the trifurcation branches, with the ventral bronchi being positive and the dorsal fistula negative, reflects the dorsoventral distribution of the respiratory marker within the undivided foregut from which the trifurcation originates (Fig 4.7). As this balance changes gradually from E13.5 onwards, so does the Nkx2.1 status of the fistula. The fistula now has a mixed status with its ventral part Nkx2.1-positive and the dorsal part Nkx2.1-negative (Fig 4.7c). As the course of the fistula is followed from the trifurcation to the stomach, the fistula loses its Nkx2.1-positive domain and becomes entirely Nkx2.1-negative (Fig 4.7d). In fact, this loss of Nkx2.1-positive cells is seen within the first 40 micrometers of the length of the structure. In the case of embryos where the fistula originates from the main bronchi, rather than directly as a branch of the trifurcation, this arrangement is preserved (Fig 4.7e,f). The small residual Nkx2.1-negative domain is initially carried with the one of the two bronchi and subsequently buds off as the fistula, carrying the negative, as well as some positive, cells. As described above, these Nkx2.1-positive cells are subsequently lost within a short distance from the origin of the fistula. In summary, the fistula originates as, and essentially remains, a dorsal, Nkx2.1-negative structure despite subsequent minor alterations in gene expression profile near its origin.

4.2.2.4 - Respiratory development in the $Shh^{-/-}$ embryo

There are significant morphological differences between the foregut of CBA/Ca Adriamycin-treated embryos and that of homozygous $Shh^{-/-}$ embryos. In the $Shh^{-/-}$ embryos, the pharyngeal and post-pharyngeal foregut is abnormally shaped, there is no identifiable laryngotracheal groove and pulmonary development is grossly abnormal. Despite these differences, the *Nkx2.1* expression in the foregut of *Shh* mutant embryos is

Fig. 4.7 The origin and Nkx2.1 status of the tracheo-oesophageal fistula

Immunohistochemistry for Nkx2.1 on transverse sections from saline-treated control (*a*) and Adriamycin-treated (*b-f*) embryos. In the E12.5 control (***a***), the ventral bronchi (Br) stain strongly for Nkx2.1 whereas the oesophagus is negative. In an E11.5 Adriamycin treated embryo (***b***), the trifurcation of the oesophagotrachea produces an Nkx2.1 negative fistula (Fi) whereas the bronchi express Nkx2.1 strongly. In an E13.5 Adriamycin-treated embryo, the ventral half of the fistula stains for Nkx2.1 close to its its origin (***c***), but this staining is transient and disappears as the fistula makes its way towards the stomach (***d***). In the unusual arrangement of the fistula originating directly from the bronchi (***e,f***), the undivided foregut ends in a bifurcation of two bronchi with the *Nkx2.1*-negative domain of the oesophagotrachea being 'carried' with the right main bronchus (arrowheads in *e* and *f*). This *Nkx2.1*-negative domain will give rise to the fistula in adjacent sections. Scale bar, 50 μm.

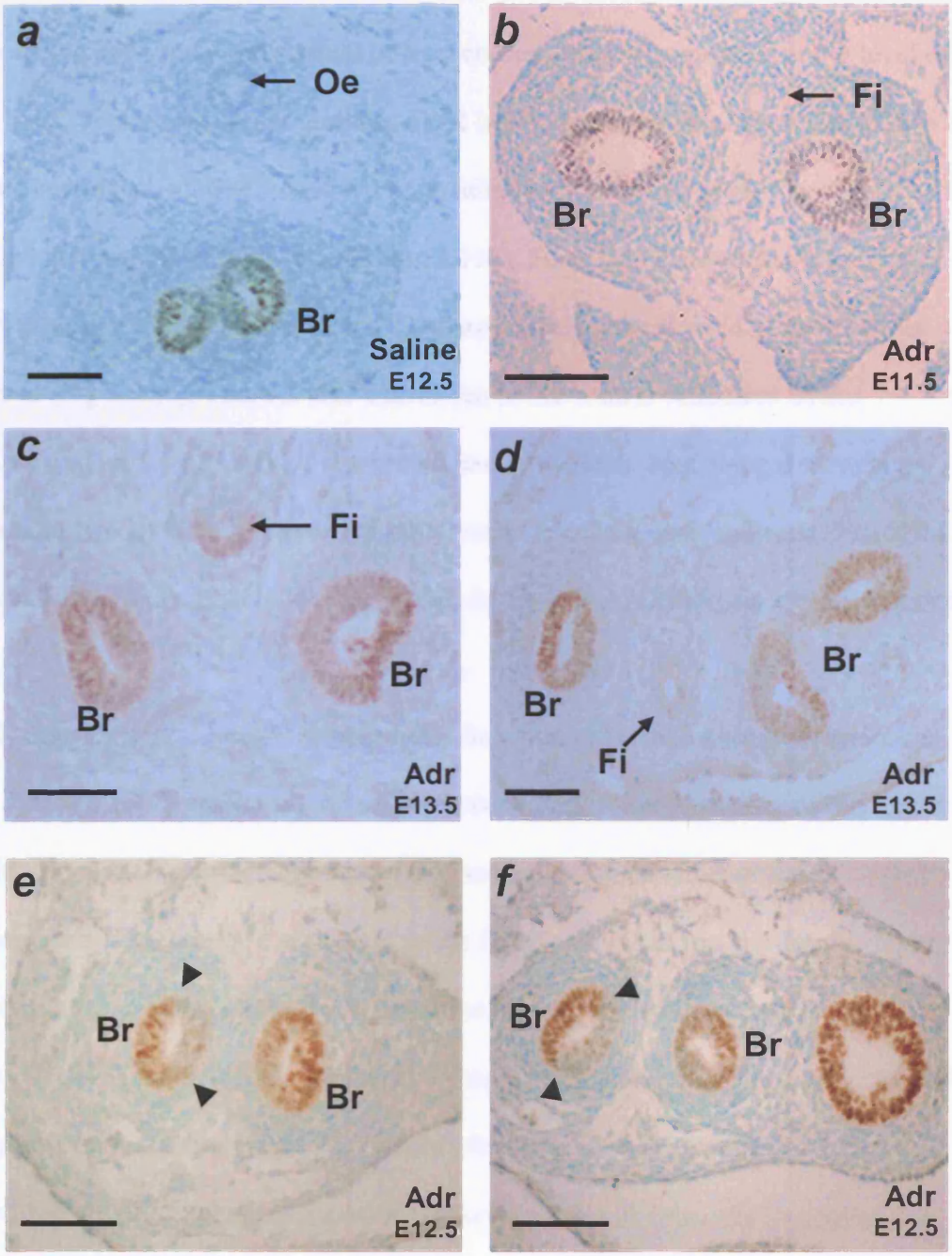
a
Oe
Br
Saline
E12.5
b
Fi
Br
Br
Adr
E11.5
c
Fi
Br
Br
Adr
E13.5
d
Br
Br
Fi
Adr
E13.5
e
Br
Br
Adr
E12.5
f
Br
Br
Adr
E12.5

similar to that of Adriamycin-treated CBA/Ca mice. At E10.5, wildtype embryos from *Shh* litters have just started the process of tracheo-oesophageal separation at the level of the lung buds (approximately six somites, or 12 hours, more advanced than CBA/Ca embryos). In contrast, all $Shh^{-/-}$ embryos have failed to start the separation process without being developmentally delayed (Fig 3.13a). Their Nkx2.1 expression pattern, however, is similar to wildtype embryos. The expression in the thyroid primordium is undisturbed (Fig 4.8c,d). There is also expression in the ventral endoderm of the prospective trachea (Fig 4.8e,f). At the caudal end of the undivided foregut there is a trifurcation of two Nkx2.1-positive lung buds and an Nkx2.1-negative fistula (Fig 4.8h). This is a similar arrangement to the trifurcation in the E11.5 Adriamycin-treated embryos.

At E11.5, the pharyngeal foregut assumes the characteristic crescent shape described in Chapter 3 and its Nkx2.1-negative status contrasts with the strong staining of the developing thyroid (Fig 4.9b,c). The foregut remains undivided but the Nkx2.1 expression pattern has changed compared to the E10.5 undivided foregut. Interestingly, these changes are in line with the findings for the post-E13.5 Adriamycin-treated embryos. The $Shh^{-/-}$ undivided foregut narrows significantly and there is no longer a well-defined prospective trachea (Fig 4.9d). Whilst Nkx2.1 is expressed in this narrow, undivided foregut, the expression signal is weaker than that in either the thyroid or the lung buds (Fig 4.9d). However, most of the endoderm of the narrow structure is Nkx2.1-positive with perhaps the exception of the dorsalmost part of the tube (Fig 4.9d). The lumen of the foregut widens and the signal becomes stronger as we move more caudally with the dorsoventral pattern of Nkx2.1 expression beginning to be re-established (Fig 4.9e). At the level of the origin of the lung buds, the dorsal *Nkx2.1*-negative domain is clearly defined (Fig 4.9f,g). This domain will give rise to the negative fistula, which is

Fig. 4.8 Expression of *Nkx2.1* is not disturbed in E10.5 *Shh*$^{-/-}$ null mutant embryos.

Photographs of whole wild type (*a*) and mutant (*b*) embryos, and immunohistochemistry for Nkx2.1 on transverse sections from E10.5 *Shh*$^{+/+}$ /*Shh*$^{+/-}$ embryos (*c,e,g*) and E10.5 *Shh*$^{-/-}$ embryos (*d,f,h*). **(*a,b*)** Mutant embryos are growth restricted, cyclopic (arrow) and have major heart (h) and limb bud (Li) abnormalities. **(*c,d*)** Expression of *Nkx2.1* in the thyroid primordium (Th) at the floor of the pharyngeal foregut (Ph) is undisturbed in mutant embryos. Note the abnormal shape of the mutant pharynx (*d*) **(*e,f*)** The undivided foregut (Fo) displays a well-defined (arrowheads) ventral expression of *Nkx2.1* in both types of embryos. **(*g,h*)** At more caudal levels, wild-type embryos have a separate oesophagus (Oe) and trachea (Tr) in contrast to mutants that have a completely undivided foregut which ends in a trifurcation of lung buds (Lb) and fistula (Fi). At that level, the original dorsoventral pattern of *Nkx2.1* expression is maintained. Scale bars: ***a,b*** - 1mm and ***c-h*** - 100μm.

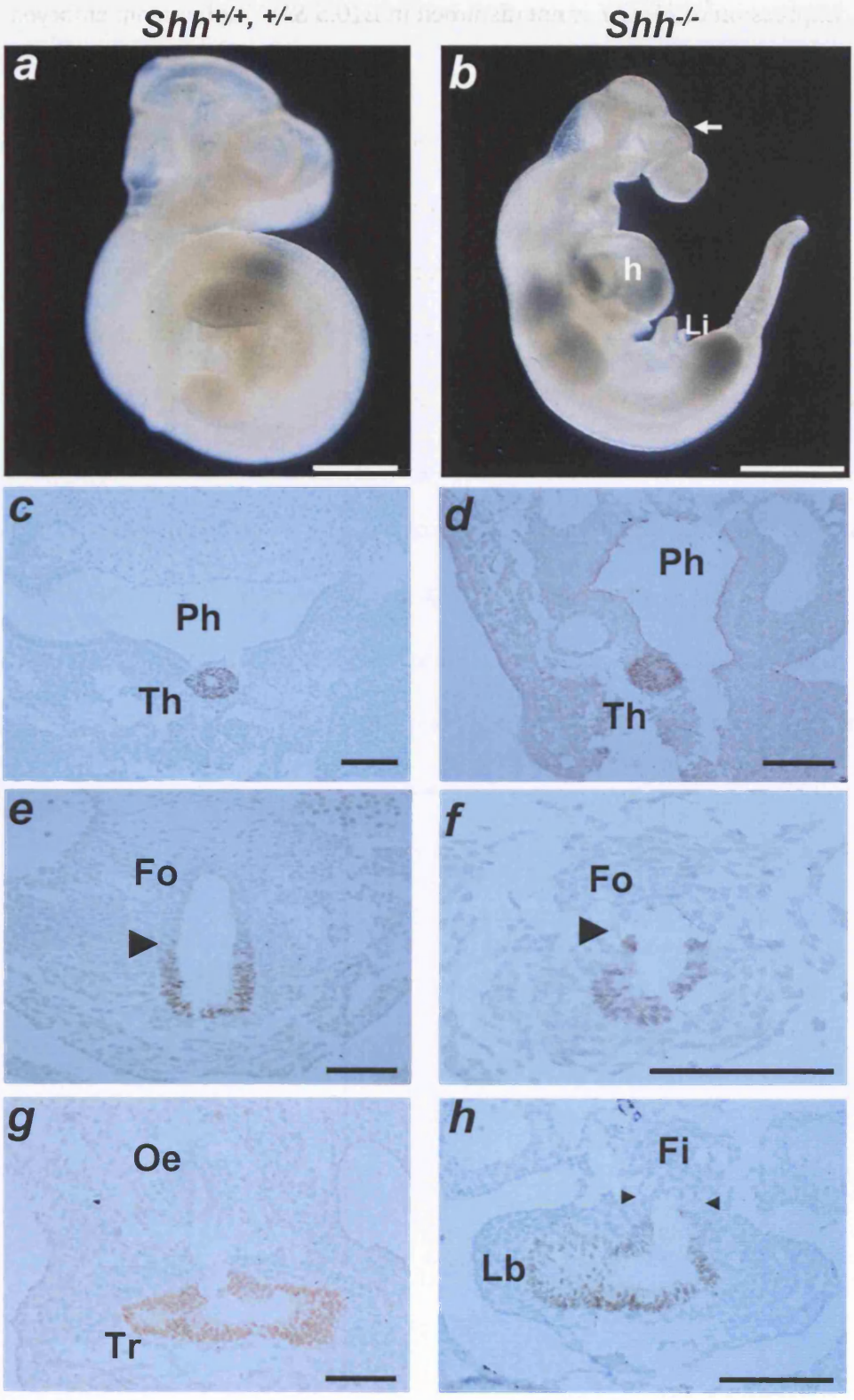
Shh+/+, +/-
Shh-/-
a
b
h
Li
c
Ph
Th
d
Ph
Th
e
Fo
f
Fo
g
Oe
Tr
h
Fi
Lb

Fig. 4.9 Expression of *Nkx2.1* in the E11.5 *Shh* null mutant embryo

Immunohistochemistry for Nkx2.1 on transverse sections from $Shh^{-/-}$ E11.5 embryos (*b-i*). Levels of sections correspond to the schematic representation of the null mutant foregut (*a*). **(*b,c*)** At the level of the pharynx (Ph), the strong signal of the thyroid gland (Th) is in sharp contrast to the lack of staining of the pharyngeal foregut which assumes the characteristic crescent shape (*c*). **(*d,e*)** As the lumen of the undivided foregut (Fo) narrows significantly, weak Nkx2.1 expression involves most of the structure with the exception of the dorsal-most endoderm (arrows in *d*). Further caudally (*e*), the lumen of the undivided foregut widens again and the dorsal, *Nkx2.1*-negative domain is better defined (arrowheads in *e*), although some *Nkx2.1*-positive cells are still found in the dorsal endoderm (arrows in *e*). **(*f,g*)** The lumen of the undivided foregut is continuous with the bronchopulmonary structures (Br) and the lungs (Lu) appear fused. The dorsal, *Nkx2.1*-negative part of the foregut is 'carried' with the bronchi (arrows in *f* and *g*) as they undergo some degree of rudimentary branching. **(*h,i*)** Further caudally, the fistula (Fi) which connects the lungs to the stomach originates from the clearly defined *Nkx2.1*-negative endoderm (arrows in *h* and *i*). Scale bar, 100 μm

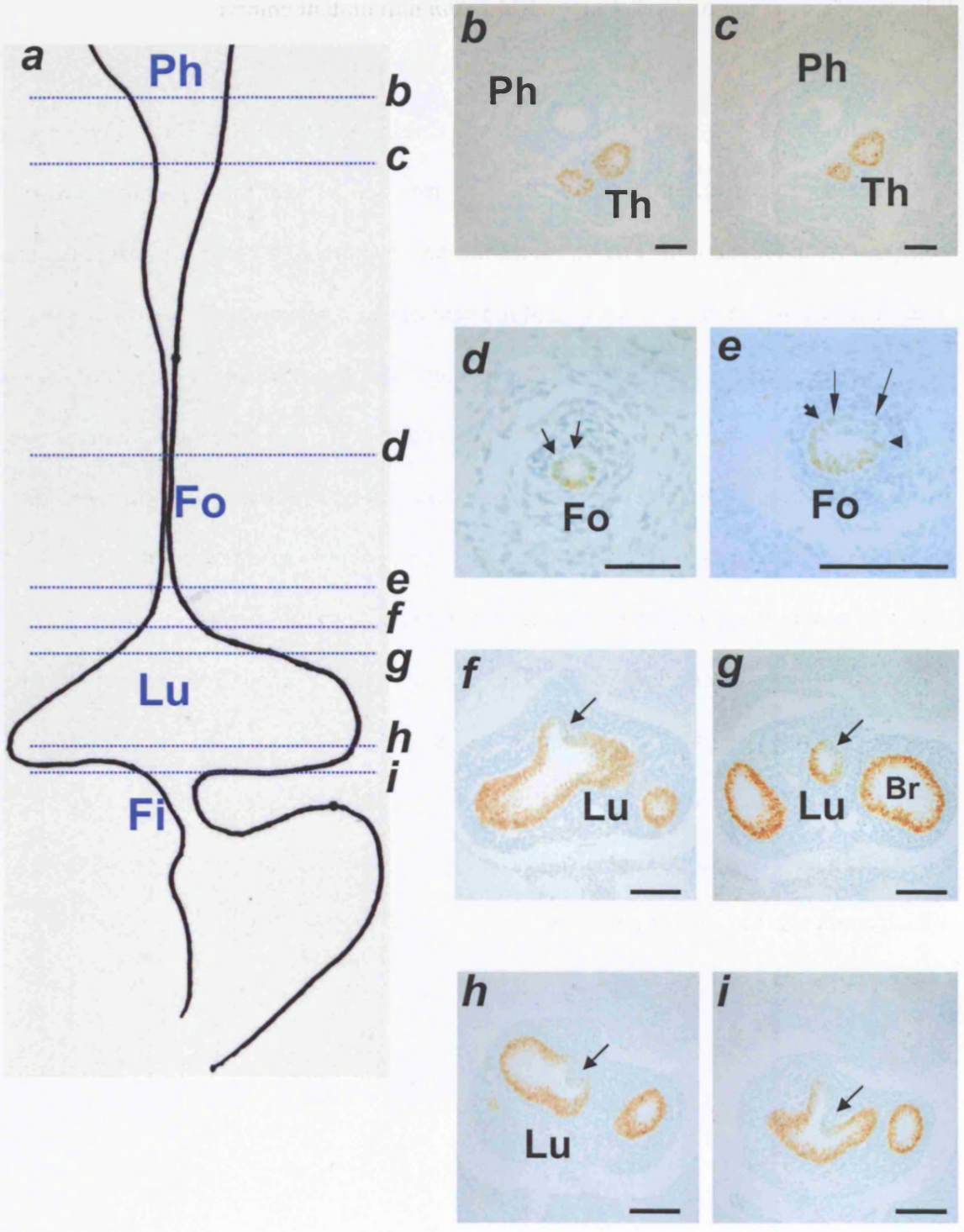
a
Ph
b
c
d
Fo
e
f
g
Lu
h
i
Fi
b
Ph
Th
c
Ph
Th
d
Fo
e
Fo
f
Lu
g
Lu
Br
h
Lu
i

Fig. 4.10 The trifurcation in E12.5 *Shh*$^{-/-}$ mutant embryos displays a distinct dorso-ventral pattern of *Nkx2.1* expression in contrast to the undivided oesophagotrachea.

(***a***). Photograph of an E12.5 mutant embryo displaying a severe forebrain malformation with a midline proboscis (Pr), abnormal limb (Lb) development and an enlarged, failing heart (h) with resulting liver (Li) congestion and severe oedema of the body wall (arrow). (***b-d***) Immunohistochemistry for Nkx2.1 on transverse sections from an E12.5 null mutant embryo. (***b***) At the level of the thyroid gland (Th), the undivided foregut (Fo) has the appearance of an oesophagus and is Nkx2.1 negative. The trachea appears not to have properly formed compared to wild-type embryos (inset). (***c***) Further caudally, the undivided oesophagotrachea (Oet) has uniform Nkx2.1 staining along the dorsoventral axis. (***d***) At the level of the trifurcation, the two lung buds (Lb) are positive for Nkx2.1 and fused, in contrast to the fistula (arrow) which is completely negative. Scale bars: ***a*** – 1 mm and ***b,c,d*** - 100 μm.

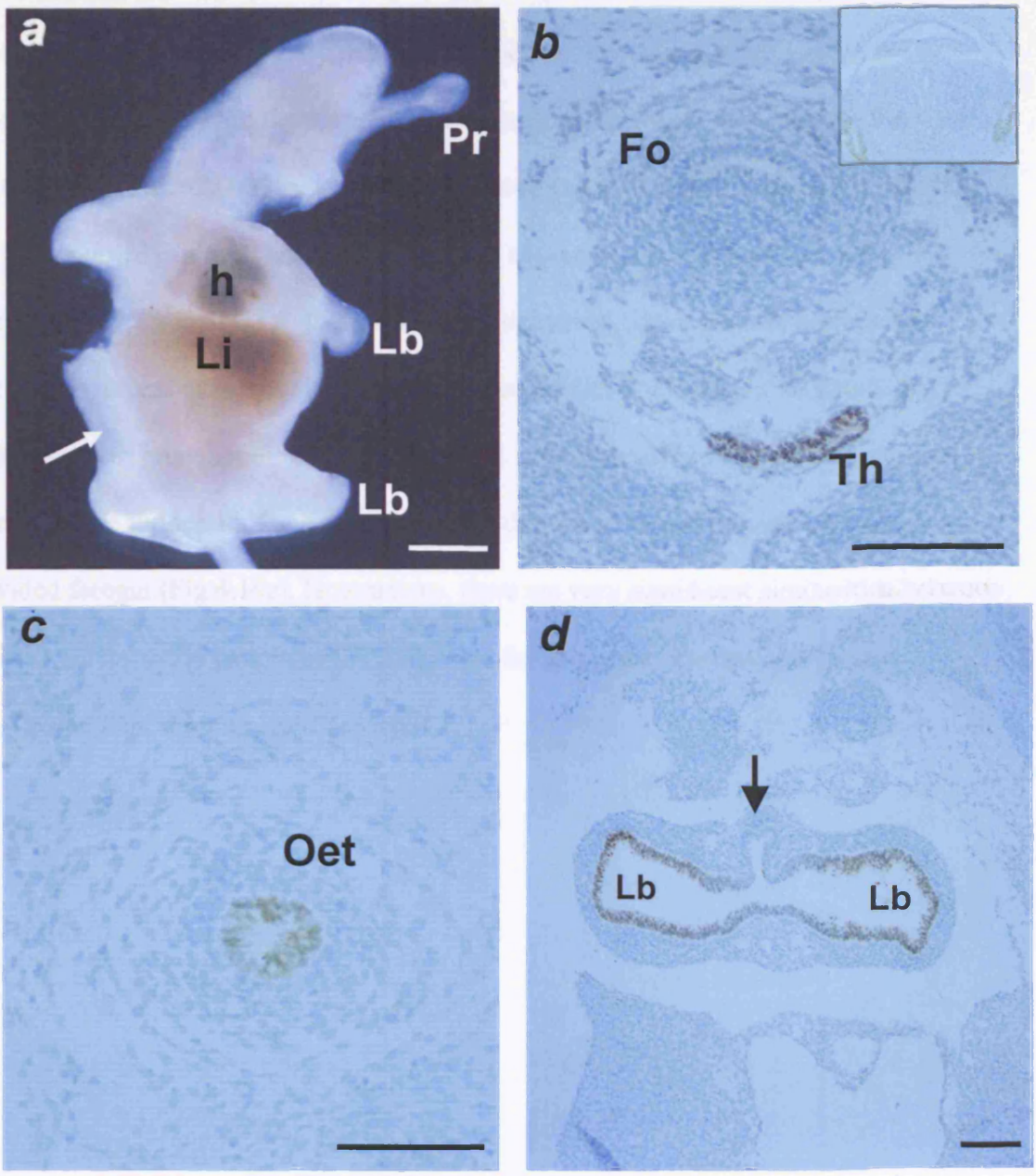
a
Pr
h
Li
Lb
Lb
b
Fo
Th
c
Oet
d
Lb
Lb

seen to originate directly from the lungs (Fig 4.9h,i). As the fused bronchopulmonary structures undergo a rudimentary degree of branching, the dorsal Nkx2.1-negative endoderm is 'carried' with the branching structures and eventually emerges as the fistula (Fig 4.9h,i). The fistula continues towards the stomach as an Nkx2.1-negative structure. This arrangement is almost identical to some of the Adriamycin-treated CBA/Ca embryos. At E12.5 and E13.5, the arrangement described above persists both in the anterior foregut and at the level of the trifurcation of the Nkx2.1-negative fistula and Nkx2.1-positive bronchopulmonary buds (Fig 4.10d). One difference is that it is no longer possible to identify the Nkx2.1-negative domain in the dorsal aspect of the undivided foregut (Fig 4.10c). In summary, there are very significant similarities between the Nkx2.1 expression pattern of the undivided foregut in the Adriamycin-treated CBA/Ca and *Shh*$^{-/-}$ homozygous embryos.

4.3 – DISCUSSION

4.3.1 – Respiratory field specification and development

One of the earliest genes expressed in the cells of the endoderm that commit to a respiratory lineage is the transcription factor *Nkx2.1* (Lazzaro et al., 1991). The upstream regulation of this expression is not known. The role of *Nkx2.1* is critical for both tracheal and pulmonary development. In my study, *Nkx2.1* expression marks a ventral territory within the undivided foregut as well as marking the developing lung buds. As a result of longitudinal growth of the anterior foregut, the *Nkx2.1*- positive domain also lengthens before the process of tracheo-oesophageal separation has started. When it does begin, separation takes place along the dorsoventral boundary of *Nkx2.1* expression. This boundary also corresponds to a cellular differentiation boundary as shown by the early distribution of proteoglycans (i.e. PAS staining) in cells of the respiratory endoderm. The role of *Nkx2.1* appears to change later in gestation. With tracheo-oesophageal separation completed, its expression is largely restricted to the pulmonary epithelial cells where it is associated with the processes of branching morphogenesis and the specification of pulmonary epithelial cells.

The study of embryos that have lost *Nkx2.1* expression as a result of targeted disruption of the *Nkx2.1* locus supports the critical role of *Nkx2.1* in respiratory development. These embryos have profoundly disturbed respiratory development with total failure of foregut separation and markedly hypoplastic lungs that cannot sustain life (Yuan et al., 2000; Minoo et al., 1999). The presence of a rudimentary respiratory system in *Nkx2.1(-/-)* embryos suggests that *Nkx2.1* is not required for the specification of the respiratory primordium. It does however control the physical separation of the tracheal and

oesophageal components of the foregut as well as the development of the phenotypic characteristics of the trachea as shown by the markedly abnormal tracheal rings found in these embryos. Since the rings are derived from the splachnic mesoderm through interactions with the developing respiratory endoderm, *Nkx2.1* is likely to play an important role in epithelial-mesenchymal interactions. In the lungs, *Nkx2.1* supports branching morphogenesis and the significantly reduced expression of *Bmp4* in the lungs of *Nkx2.1(-/-)* embryos suggests a possible mechanism based on regulation of *Bmp* signalling by *Nkx2.1* (Minoo et al., 1999). Finally, loss of Nkx2.1 function blocks pulmonary cell differentiation as shown by the absence of pulmonary surfactant protein gene expression (Minoo et al., 1999).

4.3.2 – Does Adriamycin disturb endodermal and/or respiratory development?

Whatever the nature of the effect of Adriamycin on foregut development, it does not seem to involve interference with endodermal maintenance or specification of the respiratory lineage. The transcription factor *Hnf3β* is known to play a critical role in the formation and maintenance of the foregut endoderm and endodermally-derived organs, including the trachea, lungs, oesophagus and stomach (Ang et al., 1993). In Adriamycin-treated embryos from E11.5 onwards, it is expressed uniformly in the oesophagotrachea and lung buds in a pattern comparable to saline-treated controls, where it is expressed in the endoderm of the separated respiratory and gastrointestinal organs. This suggests that the specification and maintenance of the foregut endoderm and its derivatives is not overtly disturbed during the development of OA/TOF in Adriamycin-treated embryos. The question of whether the development of the respiratory or gastrointestinal components of the foregut are specifically disturbed by Adriamycin has been addressed using the respiratory marker *Nkx2.1*. At E10.5, when embryos destined to develop OA/TOF cannot

be distinguished morphologically from controls, Adriamycin and saline-treated embryos are virtually identical in terms of Nkx2.1 expression. The conclusion is that the respiratory primordium is not only normally specified, but also grows in length appropriately.

A limitation of this study is that the conclusions are based on the study of a single respiratory marker, *Nkx2.1*. However, the respiratory expression of this transcription factor has been well documented (Lazzaro et al., 1991; Yuan et al., 2000; Minoo et al., 1999; Pera & Kessel, 1998; Small et al., 2000) and its concordance with the respiratory phenotype (early production of proteoglycans) is also demonstrated in the present study using PAS staining. The effect of Adriamycin appears, therefore, not to disturb the specification of the respiratory versus gastrointestinal parts of the foregut, but rather to inhibit the physical separation of the two components. Respiratory development continues to be undisturbed in Adriamycin-treated embryos later in gestation (E12.5 onwards), with normal levels of *Nkx2.1* expression in the developing pulmonary epithelium. One potential source of confusion is the gradual expansion of the *Nkx2.1* positive domain into the dorsal *Nkx2.1*-negative domain of the undivided foregut, which is observed from E13.5 onwards. This could give the impression that the undivided foregut is almost an entirely respiratory structure and could perhaps explain the suggestion of Crisera et al. (1999) that a respiratory structure gives rise to a fistula of respiratory origin in the Adriamycin-treated rat embryo. It would appear though that this dorsal upregulation of *Nkx2.1* is a secondary event, a response perhaps to the failure of separation. The temporal pattern of the expression shift supports this hypothesis. At E11.5, all Adriamycin-treated embryos with an undivided foregut have an identical pattern of expression with the dorsal half of the undivided structure being *Nkx2.1*-negative. The encroachment of the Nkx2.1-

positive domain can only be detected beyond E13.5. Another important observation is that the *Nkx2.1*-negative domain is never completely lost and persists, however small, in the dorsal-most part of the foregut. This late respiratory encroachment of the undivided oesophagotrachea is perhaps similar to what has been described previously as 'trachealisation' of the foregut (Merei et al., 1997b; Merei et al., 1998; Possogel et al., 1998).

4.3.3 – Does the epithelial commitment of the tracheo-oesophageal fistula provide clues to a possible underlying imbalance in cell fates during the embryogenesis of Adriamycin –induced malformations?

The fistula that connects the dorsal, oesophageal, part of the undivided foregut to the stomach has been shown in previous studies in the Adriamycin-treated rat to stain positively for Nkx2.1 along its entire length (Crisera et al., 1999b) leading to suggestions that it is of respiratory origin. A recent study of human OA/TOF (Spilde et al., 2002b) has detected the presence of Nkx2.1 in tissues taken from the fistula at the time of surgical correction of the malformation. Furthermore, studies of human embryos and neonates with OA/TOF have identified histological evidence of cartilage formation, suggestive of respiratory differentiation in the fistula (Ibrahim & Sandry, 1981; Yeung et al., 1992; Dutta et al., 2000).

The evidence provided in the present study, from the Adriamycin mouse model, appears to contradict these findings. The TOF initially appears largely or completely negative for *Nkx2.1* expression suggesting strongly that it is of gastrointestinal origin. Secondary down-regulation of *Nkx2.1* expression in the fistula in the present study is unlikely, as it was observed to be completely negative at early stages (E11.5). Furthermore, if *Nkx2.1* is

a reliable marker of the respiratory foregut component, then these results indicate that the fistula takes its origin from the dorsal part of the foregut, which is normally destined to be gastrointestinal. The observation that Nkx2.1-positve cells subsequently start to appear in the ventral half of the, originally Nkx2.1-negative, fistula, is likely to represent late alterations in gene expression patterns rather than reflect the origin of the fistula.

This apparent contradiction in findings between mouse, rat and human could be attributed to species difference but there is no evidence for this and it is very unlikely. A much more plausible explanation is that the rat study (Crisera et al., 1999b) simply did not examine the fistula at the early stages of its development and consequently cannot argue about its origin. The human studies could also mislead as far as the origin of the fistula is concerned. Intraoperative specimens of the tracheo-oesophageal fistula can only be taken from its most proximal part, near its origin, and the presence of *Nkx2.1*-positive cells at that point would be consistent with the theories described above. Furthermore, the assessment of markers at term does not necessarily reflect the embryological origin of tissues. The use of other respiratory markers in the mouse, like *Irx1* and *Irx2* (Becker et al., 2001), or markers for the oesophageal epithelium, like *Hox-3* (Geada et al., 1992), would confirm the origin of the fistula in the experimental set up.

4.3.4 – Does loss of function of *Shh* affect respiratory specification?

The precise relationship between the *Shh* and *Nkx2.1* pathways is not well understood. What is clear from the examination of mutant ($Shh^{-/-}$) embryos is that the specification of the thyroid and respiratory primordia is not overtly disturbed as indicated by *Nkx2.1* expression at E10.5. These findings suggest that *Nkx2.1* is not directly regulated by *Shh* in the foregut, in keeping with recent work showing that *Nkx2.1* expression in the

neuroectoderm, but not in mesendodermally-derived structures, depends on *Shh* (Pabst et al., 2000). The tracheo-oesophageal malformations seen in homozygous $Shh^{-/-}$ mutants are likely to result from the failure of the already specified ventral *Nkx2.1*-positive element to separate from the foregut. The picture is complicated by the fact that the development of the lungs is grossly disturbed in these embryos. However, although the developing lungs appear fused with significantly reduced branching, they still strongly express epithelial *Nkx2.1*. These observations help to separate the issue of respiratory cell fate from that of the morphogenetic effects of loss of *Shh* function.

4.3.5 – Suggested mechanisms of tracheo-oesophageal malformations

In Chapter 3, I suggested that physical failure of tracheo-oesophageal separation underlies the development of tracheo-oesophageal malformations. The aim of the present chapter, was to extend this analysis by studying the pattern of cell fate specification and development in the foregut and determine whether the respiratory and gastrointestinal components, distinguished by gene expression properties, fail to separate. During the early critical stage of the embryogenesis of tracheo-oesophageal malformations, neither the action of Adriamycin nor the loss of function of *Shh* appear to overtly disturb the development of the respiratory primordium. During subsequent stages of development, the already specified foregut elements fail to physically separate. The evidence presented in this chapter strongly supports the hypothesis that the earliest recognisable malformation is a failure of separation. The various adaptive developmental events that follow this initial failure should not distract from the simplicity of the initial defect.

Another conclusion is that the well-demarcated boundary between prospective respiratory and non-respiratory epithelium (the *Nkx2.1* expression boundary) is not by itself sufficient

to effect the separation. Additional signals must be required and it is these signals that are the likely targets of Adriamycin. It is also plausible that these signals are related to the *Shh* pathway. Finally, it may be that *Nkx2.1* (or its expression boundary) is necessary but not sufficient, as this study shows, for separation. This question has not been tackled in this chapter, but evidence from the *Nkx2.1* homozygous mutant, which exhibits an undivided foregut, would suggest that the *Nkx2.1* expression boundary is necessary for separation of the gastrointestinal and respiratory elements. It is likely that a combination of dorsoventral signals (both cell fate markers and other signalling molecules) are involved in the demarcation, initiation and execution of the separation process. The aim of the remainder of this thesis is to study these signals in greater detail.

CHAPTER 5 – ROLE OF SONIC HEDGEHOG IN FOREGUT DEVELOPMENT

5.1 – INTRODUCTION

The molecular control of separation can be considered as having three components: the molecular factors themselves that provide the positional cues for dorsoventral division, the upstream signals that determine the expression of these factors and the downstream events that contribute to the separation process. This chapter deals with the molecular factors and their control whereas the downstream events are examined in Chapter 6. The requirements for the markers controlling separation are that they are expressed in the foregut endoderm and /or the adjacent mesoderm and they have a dorsoventral expression pattern which both precedes separation and coincides with the respiratory/ gastrointestinal boundary.

The respiratory marker *Nkx2.1* satisfies these criteria. It has been shown to be necessary (Yuan et al., 2000; Minoo et al., 1999), but not sufficient (Chapter 4 data) for separation. Another candidate is the key developmental gene *Sonic hedgehog* (*Shh*). The secreted glycoprotein Shh and members of its signaling cascade are known to be involved in a wide range of morphogenetic processes in the developing embryo and have been shown to be expressed in the foregut (Riddle et al., 1993; Johnson et al., 1994; Roelink et al., 1995; Marigo et al., 1996; Litingtung et al., 1998; Motoyama et al., 1998; Chuong et al., 2000). Furthermore, tracheo-oesophageal malformations have been described in embryos with loss of function mutation for *Shh* (Litingtung et al., 1998; Pepicelli et al., 1998) and I

have specifically shown in the first two chapters that these embryos exhibit failed tracheo-oesophageal separation. Mutations in other members of the *Shh* signaling cascade have also been shown to lead to tracheo-oesophageal malformations (Motoyama et al., 1998; Mahlapuu et al., 2001). Based on these observations, I decided to study in detail the expression pattern of *Shh* and other members of its signaling cascade during tracheo-oesophageal development and in particular during the process of tracheo-oesophageal separation.

5.2 – RESULTS

5.2.1 – Expression patterns for *Shh*

5.2.1.1 - Expression of Shh in control embryos

In E10.5 saline control embryos, *Shh* is expressed in the brain, floor plate of the neural tube, notochord, limb buds, foregut and hindgut (Fig. 5.1a). At E10.5, *Shh* is weakly expressed in both the dorsal and ventral endoderm of the pharynx and is absent from the lateral endoderm of the pharyngeal pouch derivatives (Fig. 5.1c). This expression pattern persists in the E11.5 pharyngeal foregut (Fig. 5.2a). Just caudal to the pharynx, at E10.5, *Shh* is strongly expressed in the ventral endoderm of the prospective trachea with the dorsal, prospective-oesophageal endoderm lacking expression (Fig. 5.1d-g). There is a sharp boundary between expressing and non-expressing cells and this is maintained further caudally where *Shh* is strongly expressed in the lung buds but is still absent from the dorsal-most endoderm (Fig. 5.1h). At E11.5, after tracheo-oesophageal separation has started, a striking switch in dorso-ventral expression occurs. Below the level of separation, *Shh* is now expressed in the oesophagus but not in the trachea (Fig. 5.2e). Sections taken just above the level of separation also show this ventro-dorsal switch (Fig. 5.2d) whereas more cranial sections of the, as yet undivided, foregut persist in showing stronger ventral *Shh* expression, as seen in the E10.5 embryos (Fig. 5.2b,c). Strong *Shh* expression is found in the developing lung buds at E11.5 and later in gestation (Fig. 5.2f). At E12.5, the oesophagus remains strongly positive and the trachea is completely negative for *Shh* (Fig. 5.3c,e). The lung buds remain positive for *Shh* throughout this period of development.

Fig. 5.1 Expression of *Shh* and *Ptc1* in the E10.5 CBA/Ca embryo

Patterns of *Shh* expression, and complementary *Ptc1* patterns, in saline-treated E10.5 embryos. *In situ* hybridisation for *Shh* (*a,c-h*) and *Ptc1* (*b,i,j,k*): whole embryos and vibratome sections from whole-mount hybridisation experiments on E10.5 saline-treated embryos (inset in *k* Adriamycin-treated). Sections (*c*) to (*h*) and (*i*) to (*k*) form two series of progressively more caudal sections. **(*a*)** *Shh* expression is seen in ventral areas of the brain, the floor plate (Fp), the notochord (arrowhead in a), the foregut (Fo) and hindgut (Hg) endoderm, including the lung buds (arrow in a) and the limb buds (Lb). **(*b*)** *Ptc1* expression is flanking the ventral neural tube (arrow in b) and ventral midline in the brain and is also found in the somites (S), the limb buds and the mesoderm surrounding the foregut and hindgut. **(*c-k*)** *Shh* is strongly expressed in the floor plate of the neural tube (Fp) and the notochord (Nt) whereas *Ptc1* is expressed in the mesoderm adjacent to the ventral neural tube and around the notochord (arrowhead in *i*). **(*c,i*)** At the level of the pharyngeal foregut (Ph), *Shh* is expressed in both the dorsal and ventral endoderm (arrows in *c*) but is specifically absent from the endoderm of the pharyngeal pouches (arrowheads in *c*). *Ptc1* is expressed next to the *Shh*-expressing endoderm (arrows in *i*). **(*d,e,j,k*)** *Shh* is expressed in the ventral endoderm of the laryngotracheal groove (Lt) with a sharp boundary between ventral expressing and dorsal non-expressing cells (arrowheads in *d,e*). Mesodermal expression of *Ptc1* is also restricted to the ventral foregut (arrowheads in *j,k*) although the boundary is not as distinct due to adjacent perinotochordal expression. Interpretation of dorsal *Ptc1* expression in Adriamycin-treated embryos is made difficult by the proximity of the foregut to the notochord and floor plate (arrow, inset in *k*) **(*f,g*)** Further caudally, *Shh* expression is restricted to the endoderm of the prospective trachea (Tr) (arrowheads). **(*h*)** At the level of the lung buds (Lb), the *Shh* dorso-ventral boundary still exists (arrow) but appears less distinct. D – diencephalon, T – ventral telencephalon. Scale bar: ***a,b*** – 500 μm and ***c-k*** -100 μm.

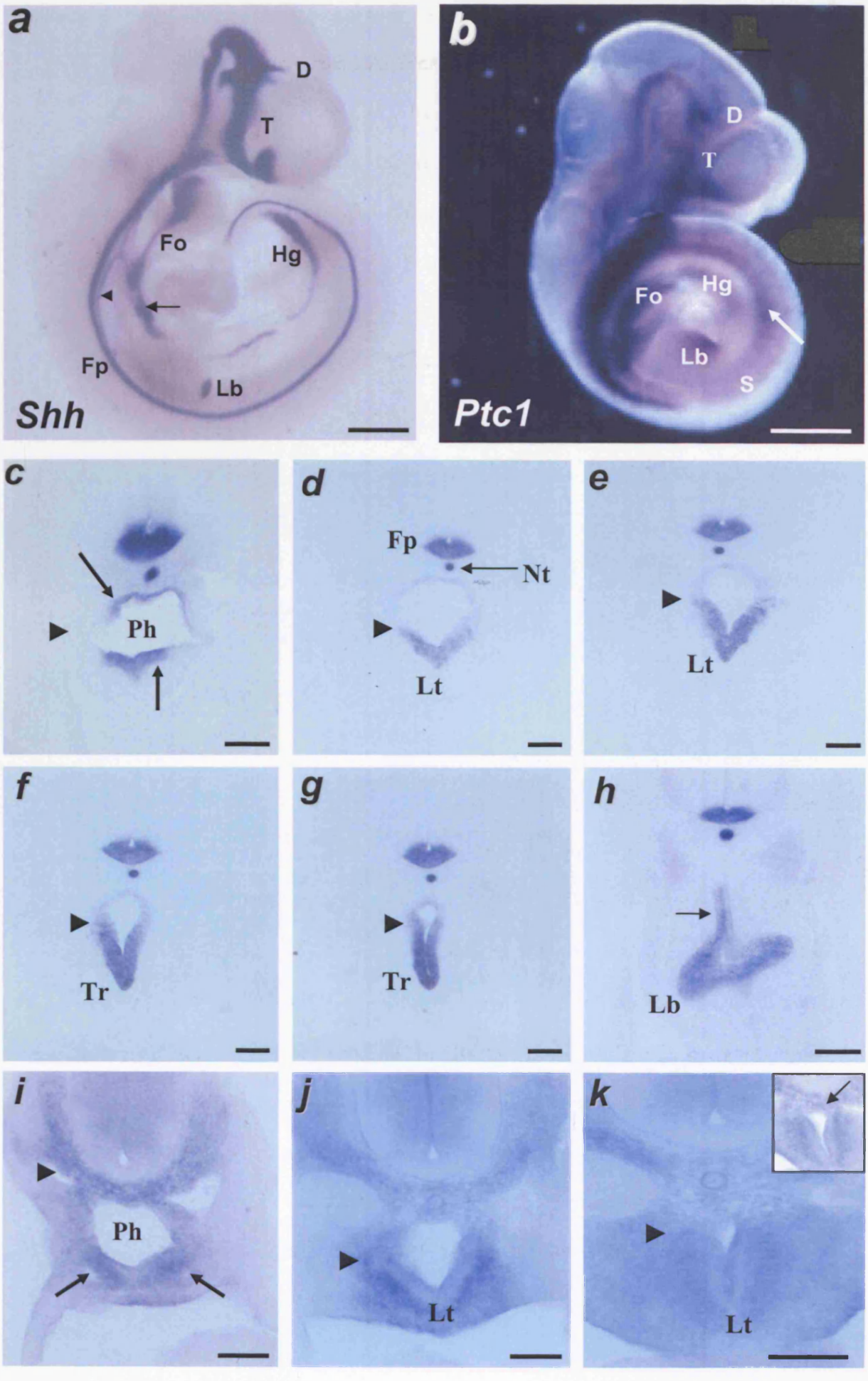
a
D
T
Fo
Hg
Fp
Lb
Shh
b
D
T
Fo
Hg
Lb
S
Ptc1
c
Ph
d
Fp
Nt
Lt
e
Lt
f
Tr
g
Tr
h
Lb
i
Ph
j
Lt
k
Lt

Fig. 5.2 Expression of *Shh* and *Ptc1* in the E11.5 CBA/Ca embryo

Changing patterns of *Shh* expression (and complementary *Ptc1* patterns) in E11.5 embryos. *In situ* hybridisation for *Shh* (*a-f*) and *Ptc1* (*g-l*) : vibratome sections from whole-mount hybridisation experiments on saline-treated embryos. *a* to *f* represent increasingly caudal levels and *g* to *l* represent corresponding levels. **(*a,g*)** In the pharyngeal foregut (Ph), *Shh* is expressed ventrally and dorsally but is absent laterally from the endoderm of the pharyngeal pouch derivatives (arrowheads in *a* mark boundary). *Ptch* is expressed adjacent to *Shh* expressing endoderm (arrow *in g*). **(*b,h*)** At the level of the laryngotracheal groove (Lt), *Shh* is expressed in a well-defined ventral domain (arrows in *b*) and *Ptch* in the adjacent mesoderm (arrow in *h*). **(*c,i*)** At a slightly more caudal level, *Shh* is still ventrally expressed (arrow in *c*) but the expression appears to be shifting dorsally. This again is reflected in mesodermal *Ptch* expression (arrow in *i*). **(*d,j*)** The pattern of *Shh* expression is now reversed with a well defined (arrowheads in *d*) dorsal *Shh* expression but weak expression ventrally. *Ptch* is expressed in the mesoderm adjacent to the dorsal foregut (Fo) (arrow in *j*). **(*e,k*)** *Shh* expression in the oesophagus (Oe) but only at low level in the trachea (Tr). *Ptch* expression is similarly confined to the peri-oesophageal mesoderm. **(*f,l*)** *Shh* is expressed in the oesophagus and lung buds (Lb). *Ptch* expression around the lung buds is stronger than the peri-oesophageal expression (asterisk in *l*). Fp - floor plate, Nt - notochord. Scale bar 100 μm.

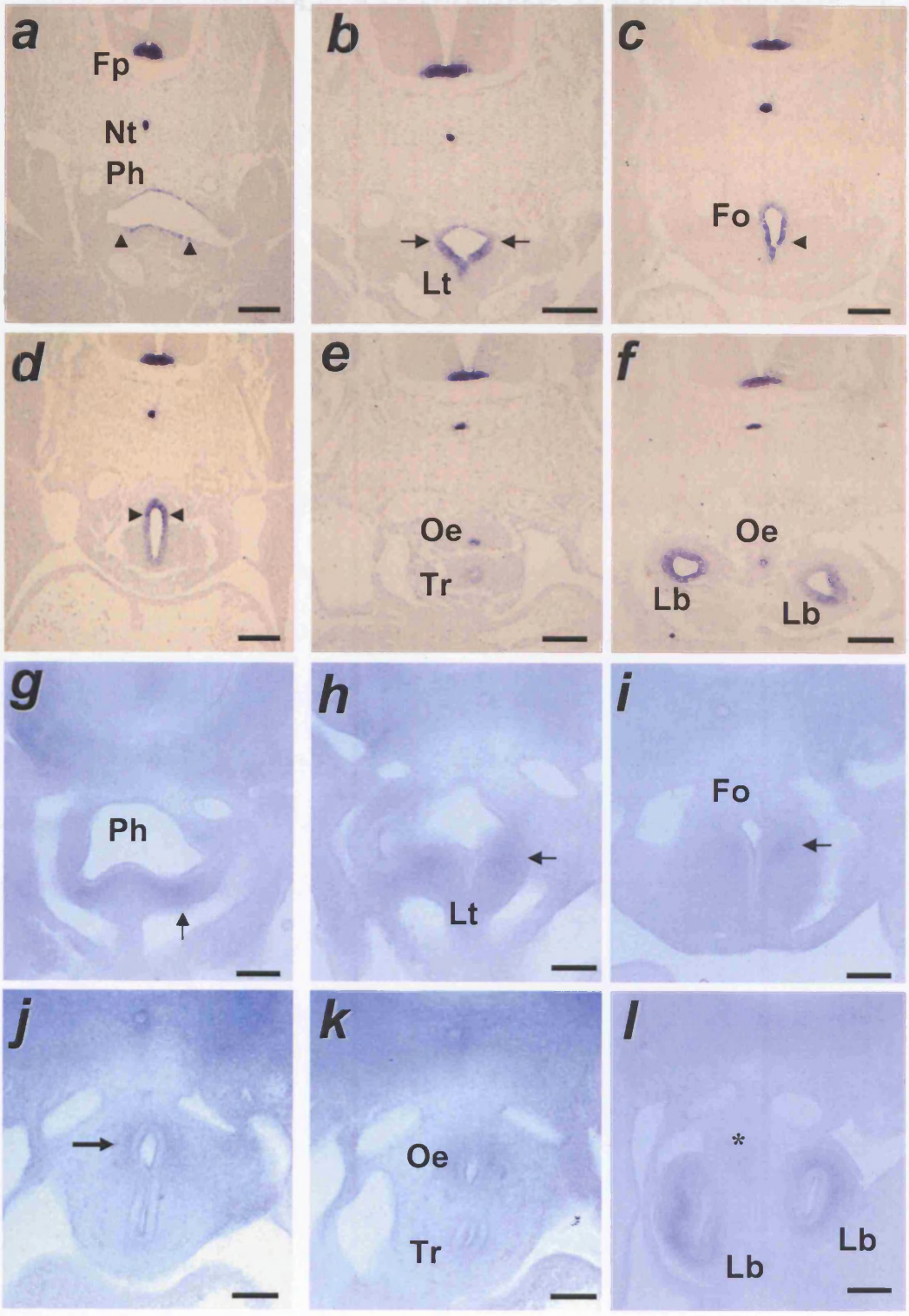
a
Fp
Nt'
Ph
b
Lt
c
Fo
d
e
Oe
Tr
f
Oe
Lb
Lb
g
Ph
h
Lt
i
Fo
j
k
Oe
Tr
l
*
Lb
Lb

Fig. 5.3 Expression of *Shh* in E12.5 saline-control and Adriamycin-treated CBA/Ca embryos

Shh expression in the oesophagotrachea of E12.5 Adriamycin-treated embryos is comparable with expression in saline-treated embryos. *In situ* hybridisation for *Shh* on transverse sections from saline- (*a,c,e*) and Adriamycin-treated (*b,d,f*) E12.5 embryos. **(*a,b*)** At E12.5, the cranial-most part of the laryngotracheal groove (Lt) has yet to separate from the oesophageal foregut. Both uniformly express *Shh* in saline- and Adriamycin-treated embryos. **(*c,d*)** At a slightly more caudal level in saline controls, the separated trachea (Tr) is completely negative for *Shh* whereas the oesophagus (Oe) retains a strong signal (*c*). In the Adriamycin-treated embryo (*d*), the undivided oesophagotrachea (Oet) reflects this dorso-ventral pattern in expression with a sharp boundary between expressing and non-expressing cells (arrows). **(*e,f*)** This dorsal-positive, ventral-negative pattern persists further caudally and is unchanged as far as the level of the trifurcation. Scale bars, 100 μm.

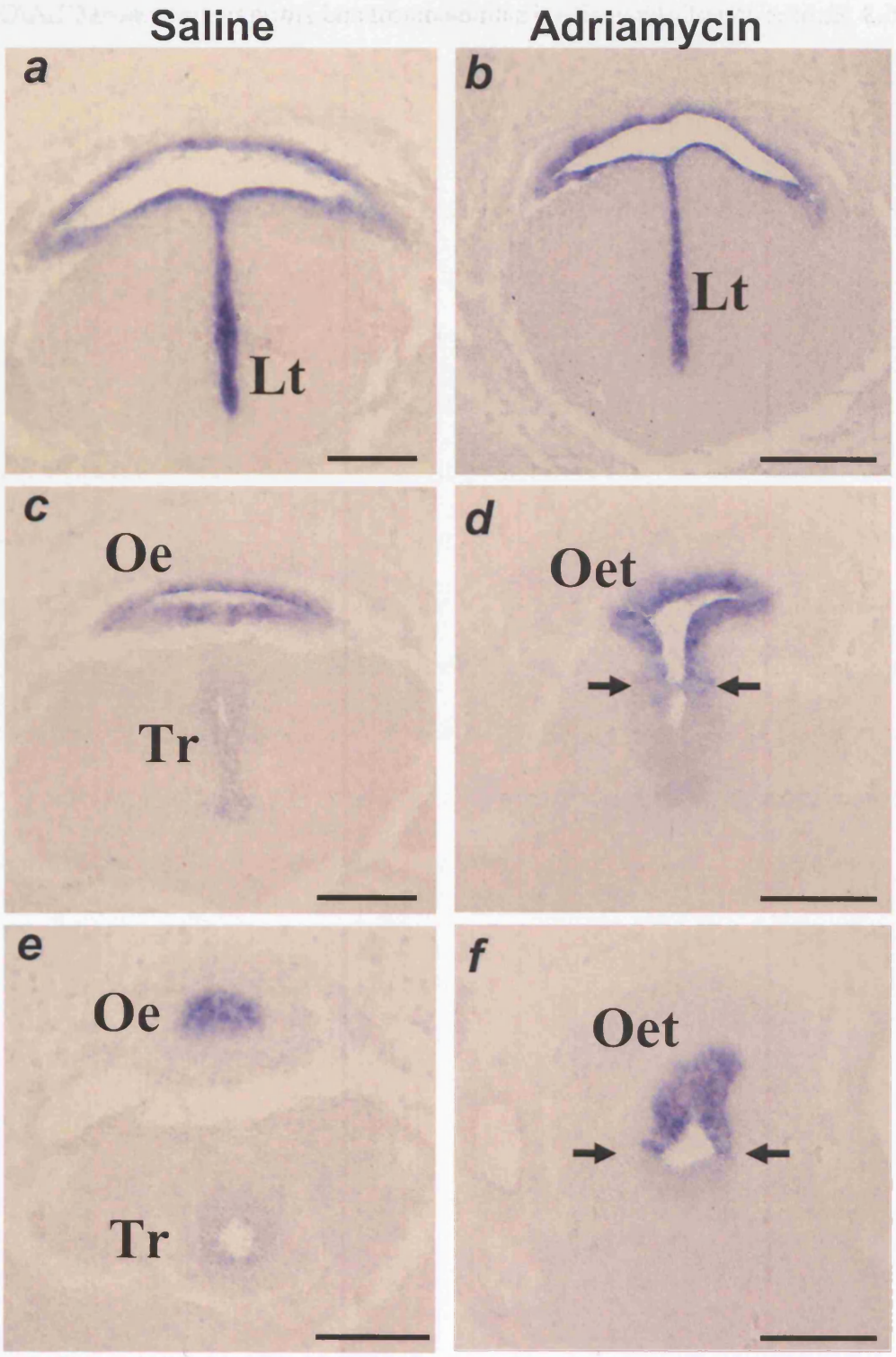
Saline
Adriamycin
a
Lt
b
Lt
c
Oe
Tr
d
Oet
e
Oe
Tr
f
Oet

Fig. 5.4 Ventro-dorsal *Shh* switch in saline-treated embryos and disturbance of this pattern in Adriamycin-treated embryos at E10.5 and E11.5

In situ hybridisation for *Shh* on saline-treated (*a.d*) and Adriamycin-treated (*b,c,e*) embryos. Vibratome sections from whole-mount experiments. ***(a,d)*** *Shh* expression shifts completely from the ventral, tracheal-prospective epithelium at E10.5 (arrowheads in *a* mark boundary), to the oesophageal epithelium at E11.5 (*d*, after tracheo-oesophageal separation). ***(b,c)*** In these two E10.5 Adriamycin-treated embryos, the undivided foregut (Fo) expresses *Shh* uniformly along the dorsoventral axis. Note *Shh* expression in part of the lung bud included in this section (arrow in *b*)***(e)*** The undivided oesophagotrachea (Oet) in this E11.5 Adriamycin-treated embryos shows diffuse staining along the dorso-ventral axis. The signal appears stronger at the two poles and contrasts sharply with the pattern seen in saline-controls (*d*). ***(inset in e)*** The split notochord seen in some Adriamycin-treated embryos exhibits an asymmetrical *Shh* signal. The ventral branch (double arrowhead) has a much stronger signal than the more normally positioned dorsal branch (arrowhead). The ventral branch is abnormally close to the undivided foregut, which itself exhibits a uniform *Shh* signal. Scale bars, 100 μm.

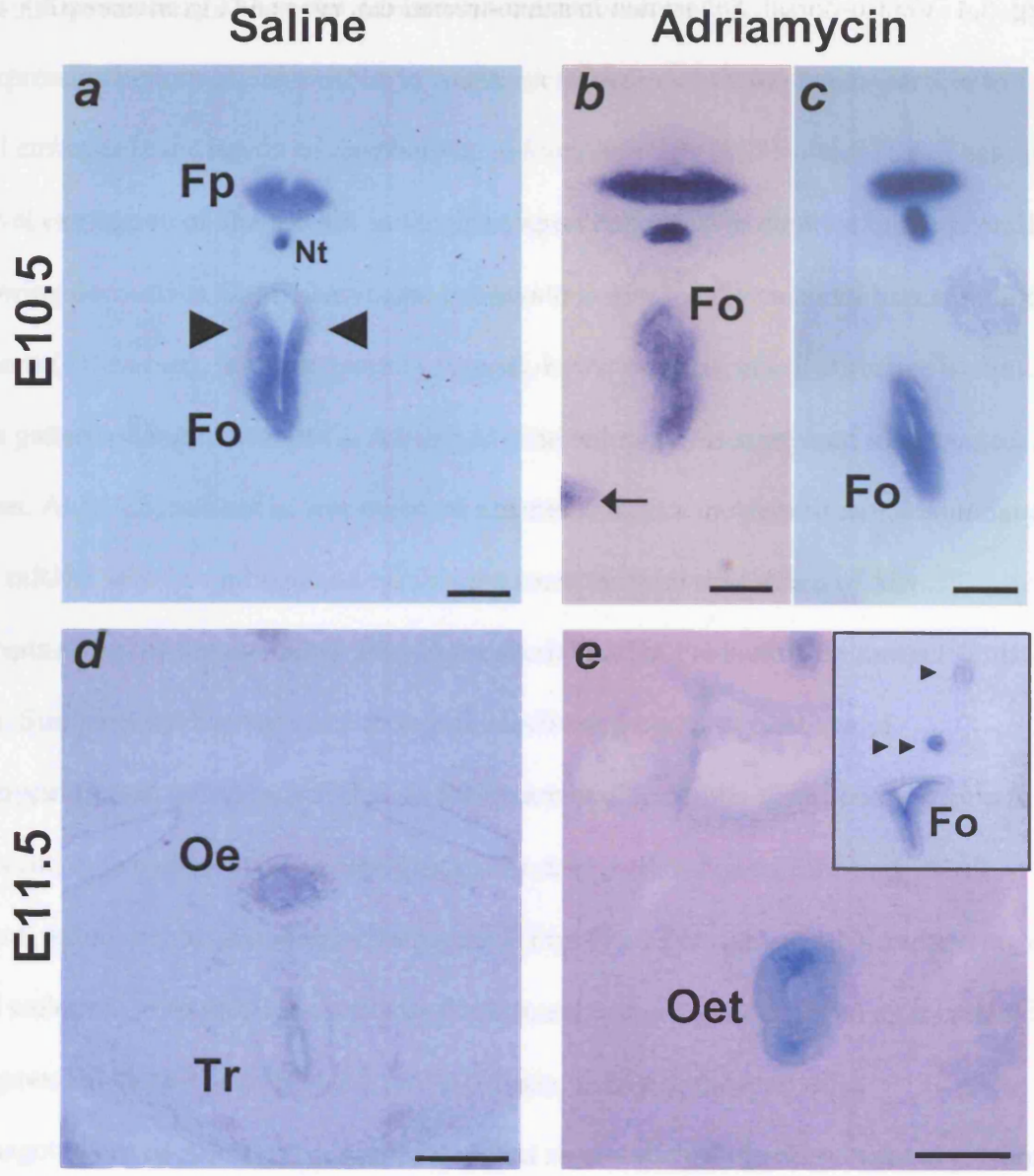
Saline
Adriamycin
a
b
c
d
e
E10.5
E11.5
Fp
Nt
Fo
Fo
Fo
Oe
Tr
Fo
Oet

5.2.1.2 - Expression of Shh in the Adriamycin-treated embryo

The expression pattern of *Shh* mRNA in Adriamycin-treated embryos is comparable to control embryos in the region of the pharyngeal foregut at both E10.5 and E11.5. There is low level expression of *Shh* mRNA in the pharyngeal endoderm in contrast to the laterally outgrowing derivatives of the pharyngeal pouches that specifically lack expression at both gestations (*not shown*). In the respiratory foregut, however, there is a disturbance in the precise pattern of *Shh* transcripts in Adriamycin-treated embryos compared to untreated embryos. At E10.5, two out of five embryos examined lacked the dorso-ventral boundary of *Shh* mRNA seen in controls, and exhibited a more uniform expression of *Shh* transcripts along the dorso-ventral axis, in the caudal part of the undivided foregut (Fig. 5.4b,c). Similar perturbations were seen in the undivided oesophagotrachea of Adriamycin-treated embryos at E11.5. In these embryos, the dorso-ventral boundary was also absent, with a more uniform signal along the dorso-ventral axis of the undivided structure, in four out of four embryos examined (Fig. 5.4e). In contrast, all Adriamycin-treated embryos (n=4) that had a separate trachea and oesophagus displayed an identical *Shh* expression pattern to saline controls. Strikingly, at E12.5, the undivided oesophagotrachea of Adriamycin-treated embryos re-established the dorso-ventral pattern of *Shh* expression seen in controls. The dorsal (oesophageal) part of the structure was strongly positive in contrast to the ventral (tracheal) part that was completely negative (Fig. 5.3d,f).

5.2.2 – Shh protein distribution in the developing mouse embryo

The validity of using the anti-Shh antibody was confirmed by the presence of Shh protein in the notochord and the floorplate of the neural tube, which are established sites of *Shh* expression, at both E10.5 and E11.5 (Fig. 5.5a,b). In the region of the notochord the

distribution of the peptide is quite distinctive, with the Shh protein found not only in the notochord itself, but also in the perinotochordal mesenchyme (Fig. 5.5a, inset). Shh protein was most abundant in the mesenchyme immediately surrounding the notochord, although Shh protein was also seen occasionally at some distance from the notochord, near the floor plate, and as far as the foregut.

At E10.5, the pattern of Shh protein distribution matches closely the pattern of expression of the *Shh* mRNA in the respiratory foregut, as shown by the *in situ* hybridisation experiments. In the E10.5 foregut, Shh protein is found in the ventral, tracheal-prospective epithelium and more caudally in the lung buds (Fig. 5.5a,b). There is a clear dorsoventral pattern of protein distribution, which matches the dorsoventral pattern of *Shh* mRNA expression (Fig. 5.5a,b). This pattern is also very similar to the *Nkx2.1* expression pattern. In sharp contrast, the Shh protein pattern differs greatly from that of the *Shh* mRNA in the pharyngeal foregut rostral to the laryngotracheal groove. Shh protein is only occasionally detected in the pharyngeal epithelium, at the boundaries of the pouch derivatives.

At E11.5, the significant discrepancy between Shh gene expression and protein distribution, seen in the E10.5 pharyngeal foregut, persists. Shh protein is found only in the ventral midline, at a point corresponding to the origin of the thyroid diverticulum (Fig. 5.5c) and laterally at the junction between the pharynx and the pharyngeal pouch epithelium (Fig. 5.5c, inset). This pattern was reproducible in all examined embryos (n=10) and might indicate a role for Shh in the budding of pharyngeal derivatives.

Fig. 5.5 Distribution of Shh protein in the developing foregut

Immunohistochemistry for Shh protein on transverse sections from saline-treated E10.5 (a,b) and E11.5 (c-h) embryos. Sections a to b and c to h are from increasingly caudal levels. ***(a,b)*** There is a strong protein signal at E10.5 in both the floor plate of the neural tube (Fp) and the notochord (Nt), both areas with established *Shh* expression. The secreted nature of the Shh glycoprotein is demonstrated by the Shh signal in the mesenchyme that surrounds the notochord (inset in a). In the E10.5 foregut (Fo), the ventral, tracheal-prospective, epithelium is Shh-positive, with clearly demarcated dorsoventral boundary (arrowheads in a). At the level of the lung buds (Lb), the ventral signal persists and the dorsoventral boundary lies dorsal to the lung bud boundary (arrowheads in b). ***(c)*** At E11.5 at the level of the pharyngeal foregut (Ph), the midline thyroid diverticulum (Th) has a strong Shh signal. The foregut epithelium generally lacks Shh signal except at the boundaries of the pharyngeal pouches (Pp) (arrowhead, inset in c). ***(d)*** At the level of the ventral laryngotracheal groove (Lt), the epithelium of the groove is Shh-positive in contrast to the dorsal epithelium that is negative. ***(e)*** Just caudal to the laryngotracheal groove, the foregut is still undivided and the Shh signal is still restricted to the ventral epithelium. ***(f)*** As the level of tracheo-oesophageal separation is approached, the signal has largely shifted dorsally, although occasional ventral cells maintain their signal (arrow in f). Despite this dorsal shift, there is little signal in the dorsalmost epithelium, and in some embryos the Shh signal is found mostly in the folding epithelial ridges that mark the separation point (arrowheads, inset in f). ***(g)*** The separated oesophagus (Oe) also has Shh-positive cells, as does the dorsal part of the trachea (Tr) (arrow in g). ***(h)*** As the trachea changes shape, and the level of tracheal bifurcation is approached, tracheal Shh signal is mostly located in the middle third of the tracheal epithelium (arrowhead in h), at the point of tracheal separation. Scale bar, 50 μm

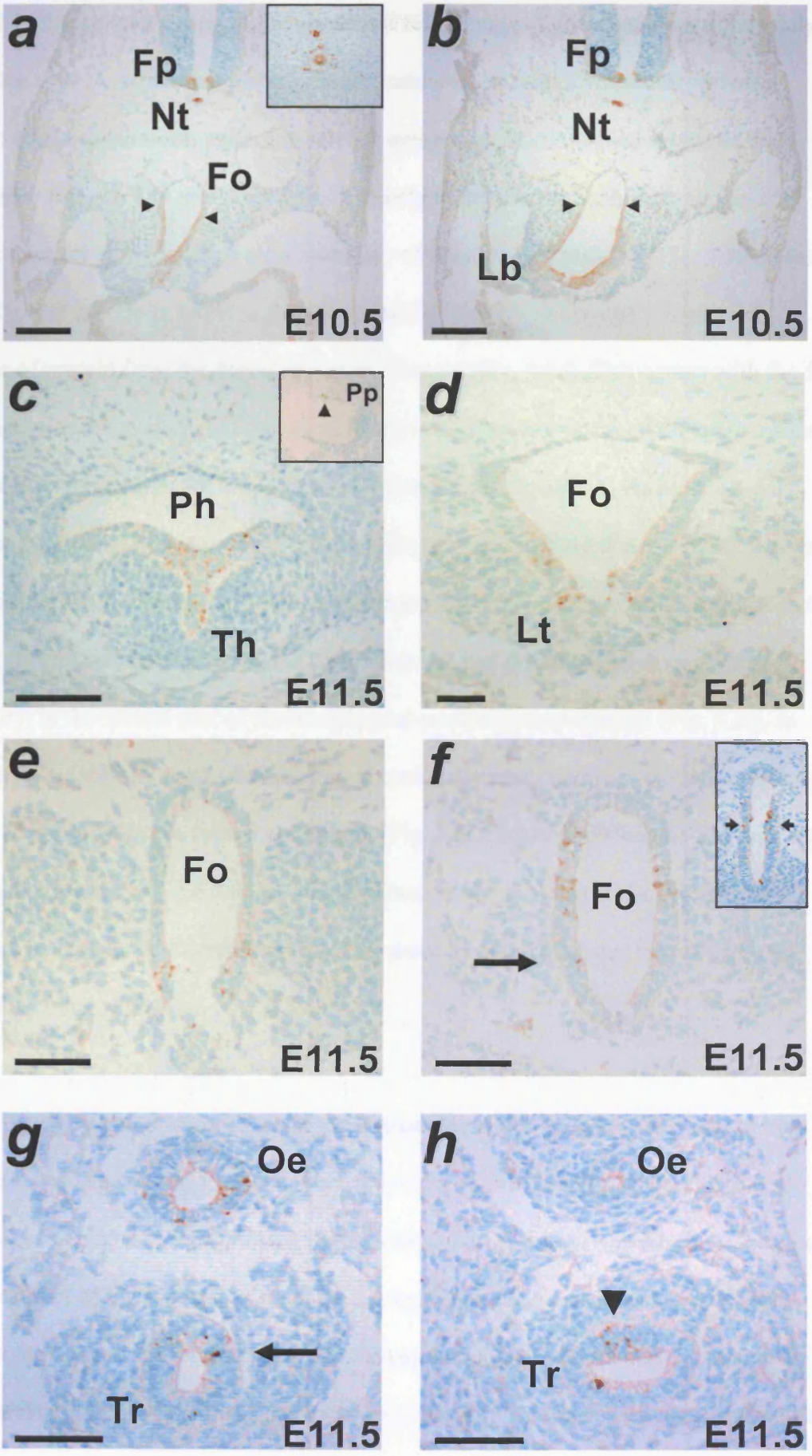
a
Fp
Nt
Fo
E10.5
b
Fp
Nt
Lb
E10.5
c
Pp
Ph
Th
E11.5
d
Fo
Lt
E11.5
e
Fo
E11.5
f
Fo
E11.5
g
Oe
Tr
E11.5
h
Oe
Tr
E11.5

In the E11.5 respiratory foregut, the pattern of Shh protein distribution does not exactly match the mRNA expression pattern. In particular, the protein distribution pattern is patchy, unlike the uniform pattern of mRNA expression. In the cranial aspect of the respiratory foregut, Shh protein is present largely in the ventral epithelium of the laryngotracheal groove, with a clear boundary of dorsoventral staining (Fig. 5.5d). More caudally, Shh protein is found in the ventral half of the still undivided foregut with absence of protein from the dorsal half of the foregut (Fig. 5.5e). This agrees with the *Shh* mRNA expression pattern, but the signal in the ventral epithelium is restricted to a small number of cells and it is not easy to define a dorsoventral boundary. As more caudal sections are examined, a dorsalward shift of the protein distribution is observed, similar to the shift in mRNA distribution at the same stage (Fig. 5.5f). Shh protein is detected in the region of future tracheo-oesophageal separation and just dorsal to this dorsoventral boundary, in the ventral part of the oesophageal-prospective epithelium (Fig. 5.5f). In contrast to the mRNA expression pattern, occasionally small numbers of cells are positive for the Shh protein in the ventral epithelium (Fig, 5.5f). Another difference between the protein distribution and the *Shh in situ* hybridisation signal is that in the dorsal, prospective-oesophageal epithelium, the Shh protein is largely absent from the dorsal-most part of this epithelium (Fig. 5.5f).

At levels just caudal to tracheo-oesophageal separation, Shh protein is detected in both the dorsal oesophagus and ventral trachea but with much more intense staining in the oesophagus (Fig. 5.5g). At this level, tracheal Shh protein is patchy and largely found in the dorsal part of the divided structure (Fig. 5.5g). The pattern changes more caudally towards the level of the bifurcation of the trachea into the two lung buds. At this level, whereas Shh protein persists in the dorsal oesophagus, it becomes more abundant in the

trachea and is present at the bifurcation (Fig. 5.5h). This pattern largely conforms to the mRNA expression pattern, where transcripts are abundant in the lung buds but absent from the trachea just caudal to the level of tracheo-oesophageal separation.

5.2.3 – Expression of mRNA for the Shh transmembrane receptor *Ptc1*

The transmembrane receptor *Ptc1* is a key downstream component of the *Shh* transduction pathway. As well as coding for the Shh receptor, *Ptc1* is a *Shh* target gene and is upregulated by *Shh* (Grindley et al., 1997). Hence, *Ptc1* serves as a useful functional 'read-out' of *Shh* activity. Whole mount *in situ* hybridisation in E10.5 saline-treated embryos, shows *Ptc1* expression in various tissues throughout the embryo including the brain, neural tube, somites and limb buds and, as a general rule, in areas immediately adjacent to *Shh* expression (Fig. 5.1b). It is found flanking *Shh* expression in the floor plate and notochord, in cells flanking the ventral midline in the brain and in the posterior part of the limb bud (Fig. 5.1b,i-k).

In the early foregut, *Ptc1* mRNA is expressed in the mesoderm adjacent to *Shh*-expressing endoderm: at E10.5, there is ventral *Ptc1* mRNA expression in the mesoderm adjacent to the ventral endoderm of the pharyngeal foregut (Fig. 5.2i). Some *Ptc1* expession is also seen in the dorsal pharyngeal mesoderm but this dorsal expression could be associated with the *Shh*-positive floor plate and notochord (Fig. 5.1i). The close proximity of the pharyngeal foregut to the neural tube makes such distinction very difficult. There is also *Ptc1* expression in the mesoderm surrounding the ventral endoderm of the prospective trachea with no expression in the mesoderm adjacent to the dorsal, oesophageal- prospective endoderm (Fig. 5.1j,k).

Expression of *Ptc1* continues to be complementary to that of *Shh* at E11.5. In the pharyngeal foregut, it is expressed in the ventral mesoderm (Fig. 5.2g). At the level of the laryngotracheal groove, the ventral mesodermal expression of *Ptc1* mRNA mirrors the persistent ventral *Shh* expression at this level (Fig. 5.2h). Further caudally, there is a definite shift in mesodermal *Ptc1* mRNA expression. In sections just caudal to the laryngotracheal groove, the strongest expression is in the 'middle' mesoderm (Fig. 5.2i). Further caudally, just cranial to tracheo-oesophageal separation, the ventral-to-dorsal switch is completed with *Ptc1* expression exclusively in the dorsal mesoderm surrounding the oesophageal-prospective endoderm (Fig. 5.2j). Caudal to the level of tracheo-oesophageal separation, *Ptc1* expression is found in the dorsal peri-oesophageal mesoderm (Fig. 5.2k). At the level of the lung buds, *Ptc1* is strongly expressed in the mesoderm surrounding the lung buds, again reflecting the pattern of *Shh* expression at this level (Fig. 5.2l).

Analysis of *Ptc1* expression in Adriamycin-treated embryos at E10.5 (n=4), shows that this is not disturbed. However, as *Ptc1* is expressed in the perinotochordal mesoderm, and as the notochord is very close to the foregut, it is difficult to comment on expression in the mesoderm surrounding the dorsal foregut (Fig. 5.1k, inset). In the E11.5 Adriamycin-treated embryo, failure of foregut separation was associated with a blurring of the mesenchymal ventral-to-dorsal shift in *Ptc1* expression, presumably reflecting the corresponding disturbance in the expression of *Shh* in Adriamycin-treated embryos.

5.3 – DISCUSSION

5.3.1 – Dynamic *Shh* expression and the separation process

The pattern of *Shh* expression gives important clues to the possible molecular mechanisms that underlie foregut development. *Shh* has important morphogenetic roles in various developmental processes. In the pharynx, *Shh* mRNA is weakly expressed in both the dorsal and ventral epithelium, but is absent from the epithelium of the pharyngeal pouch derivatives. This would be consistent with the *Shh* expression boundaries playing a role in organ budding from the epithelium of the gut tube. The evidence also suggests that boundaries between *Shh* expressing and non-expressing regions may play a role in respiratory system development. *Shh* expression is tightly regulated so that it shifts from the ventral, prospective-tracheal, epithelium (at E10.5) to the dorsal oesophageal epithelium as tracheo-oesophageal separation proceeds in a caudal to cranial direction (at E11.5). These changes in *Shh* expression are restricted to the foregut caudal to the pharynx and cranial to the lung buds. Strong ventral expression with a definite dorsoventral boundary starts at the level of the laryngo-tracheal groove. At the caudal end of the tracheal epithelium, the strong *Shh* expression in the lung buds is not downregulated even after tracheo-oesophageal separation is completed. These observations suggest that *Shh* is specifically upregulated in the ventral, prospective-tracheal epithelium and downregulated in the epithelium of the definitive trachea. Conversely, *Shh* expression appears to be downregulated in the dorsal, prospective-oesophageal epithelium and upregulated in the epithelium of the definitive oesophagus. This complete and specific ventral-to-dorsal switch that precedes tracheo-oesophageal separation suggests that *Shh* may have a role in the septation process itself. The maintenance of *Shh* in the lung buds suggests that their development is a separate process

from that of tracheo-oesophageal separation and is consistent with the known role of *Shh* in lung proliferation and branching morphogenesis (Bellusci et al., 1997b).

5.3.2 – The Shh mRNA/protein pattern difference

Whereas very little protein signal is detected in the E10.5 pharynx, the overall patterns of mRNA and protein distribution in the foregut distal to the pharynx are similar, both exhibiting a distinct dorsoventral boundary. At E11.5, the peptide and mRNA patterns remain largely concordant in parts of the foregut where the gene expression in the ventral endoderm is unchanged from E10.5 (i.e. the rostral undivided foregut and the lung buds). Between these two levels, *Shh* mRNA expression shifts from ventral to dorsal ahead of tracheo-oesophageal separation. The protein pattern also appears to shift but lags behind the mRNA shift. Specifically, at the level of separation or just cranial to it, the highest concentration of protein is in the dorsal half of the foregut but more so around the site of separation rather than in the dorsalmost foregut epithelium. Furthermore, the ventral tracheal-prospective endoderm still has some Shh-positive cells. However, patchy and inconsistent immunostaining of other tissues positive for *Shh* mRNA (e.g. pharyngeal foregut) suggests that there may be considerable variability either in *Shh* mRNA translation/stability or in protein turnover from structure to structure. This, coupled with possible differences in experimental sensitivity, particularly in relation to the Shh antibody which may be variable in its detection of the diffusible, variably modified (by cholesterol, palmitoyl residues) Shh-N peptide, could account for the discrepancies between mRNA and protein distribution patterns.

The discrepancy raises the question of validity of the technique. However, analysis of mRNA expression has been used in virtually all studies of the developmental role of *Shh*

and as my data closely agree with the findings of these other studies, the mRNA patterns described here are likely to be accurate. Shh protein was consistently detected in both the notochord and the floorplate, tissues of intense *Shh* transcription, suggesting that the immunohistochemical analysis of Shh distribution is also valid. Furthermore, the observed difference in the distribution of Shh protein and mRNA in the post-pharyngeal foregut could be attributed to the combination of shifting mRNA expression and the small temporal difference between gene transcription and protein synthesis, as well as a possible difference in mRNA and protein turnover. This explanation would be consistent with the lag observed in protein distribution. An alternative explanation for the mRNA/ protein discrepancy is that Shh is a signaling molecule and the protein may be found in cells in which it is not synthesised and lack an mRNA signal.

Overall, it could be argued that protein patterns are largely in agreement with gene expression patterns but may not be as reliable in depicting rapidly changing temporal and spatial shifts. When interpreting these patterns, however, one should bear in mind that the protein is what directs function and that the protein patterns may be more accurate from a functional point of view.

5.3.3 – How does Shh act in the foregut?

The differences described above raise the question of how exactly does Shh act to shape the foregut? Whereas the mRNA expression of *Shh* has been studied and interpreted in a number of organ-systems, it is the protein that mediates its action. The Shh protein has been shown to act both via short and long-range signaling (Drossopoulou et al., 2000; Gritli-Linde et al., 2001; Briscoe et al., 2001). The signaling capacity is restricted to the N-terminal peptide (Roelink et al., 1995) which results from autoproteolytic processing of

the Shh protein (Bumcrot et al., 1995; Ingham, 1998). As a result of this cleavage, the N-terminal peptide becomes covalently linked to cholesterol (Porter et al., 1996) and consequently the secreted protein becomes tethered to the cell surface of the *Shh* expressing cells. This mechanism provides a basis for the short-range signaling mediated by Shh (Tabin & McMahon, 1997). The Shh signal is the result of binding of Shh to its receptor complex, involving patched and smoothened protein (Marigo et al., 1996), on the cell membrane, which in turn activates an intracellular cascade which involves the *Gli* family of transcription factors. Another proposed mechanism for the short-range signaling of Shh is the role of its receptor Ptc1 acting as a sink for the Shh protein, thereby limiting its rate of diffusion. As *Ptc1* expression is upregulated by *Shh,* this would serve as a feedback mechanism to limit the range of Shh action. The recent finding that the endocytic receptor *megalin* is expressed in *Shh* expressing cells and binds the N-terminal Shh peptide, leading to its endocytosis, has suggested other mechanisms for the modulation of the range of the Shh signal. Megalin-mediated endocytosis could limit the levels of extracellular Shh protein or even mediate direct transduction of the Shh signal (McCarthy et al., 2002; McCarthy & Argraves, 2003).

There is also increasing evidence for the long-range nature of the Shh signal. In the past, this was questioned because of difficulty in demonstrating the presence of Shh peptides at a distance from its source (Marti et al., 1995). Optimised immunohistochemical techniques have demonstrated Shh signaling peptides in target tissues, away from the Shh source (Gritli-Linde et al., 2001). These studies have identified a crucial role for proteoglycans in this long-range signaling and Shh diffusion. Long –range signaling could also be mediated by the association of Shh with endocytic vesicles and recent studies suggest a possible role for *megalin* in this mechanism (Incardona et al., 2000;

McCarthy & Argraves, 2003; McCarthy et al., 2002). Evidence for long-range signaling exists in the limb (Drossopoulou et al., 2000), tooth (Gritli-Linde et al., 2001) and neural tube (Ericson et al., 1997; Ericson et al., 1996)morphogenetic systems.

In the foregut, Shh is likely to act via short-range signaling. Shh secreted by cells of the foregut endoderm is likely to influence gene transcription in cells of the adjacent mesoderm. The end result is the activation of transcription factors that regulate the transcription of target genes. This is clearly demonstrated by the expression of *Ptc1*, both a receptor and a target for *Shh*, in the mesoderm adjacent to *Shh*-expressing endoderm (this study and (Platt et al., 1997)). A number of other factors, including members of the *Gli* family of transcription factors, are also upregulated by *Shh* (Platt et al., 1997). The complementary nature of expression of Shh and its target genes (like *Ptc1*) would suggest that the expression data for *Shh* accurately represent the spatial and temporal pattern of *Shh* activity. What remains unclear is how factors expressed in the mesoderm surrounding the respiratory endoderm affect morphogenesis of the respiratory foregut and in particular tracheo-oesophageal separation. One can only speculate that mesodermal factors modify transcription of key endodermal genes that ultimately lead to morphological changes in the foregut. An alternative explanation is that Shh acts directly on adjacent endodermal cells and controls gene expression and key cellular processes. These include cell proliferation and programmed cell death, which are studied in detail in Chapters 6 and 7.

5.3.4 – Control of *Shh* expression

It is only possible to speculate as to the factors that control *Shh* expression in the foregut. Signals from the notochord could play a role in this regulation as is the case with the induction of the Shh producing cells of the floor plate (Ericson et al., 1996). There is

evidence that Shh is the signal responsible for the induction of *Shh* in the floor plate and that the induction itself is modulated by chordin, a BMP antagonist (Patten & Placzek, 2002). It is possible that Shh, produced by the notochord, regulates endodermal expression of *Shh.* Shh in the endoderm could, in turn, induce a feedback mechanism that limits the range of action of the diffusible notochordal signal. The negative feedback mechanism could be mediated by Ptc1, which is upregulated in the mesoderm adjacent to *Shh*-expressing endoderm, as seen in my experiments and in other studies (Platt et al., 1997). Ptc1 has been shown to limit the range of action of Shh during cell patterning and specification in the ventral neural tube (Briscoe et al., 2001). Another model of differential modulation of a default endodermal *Shh* pattern has been described in detail in the case of the development of the pancreas, which is also derived from the foregut. In this system, default dorsal *Shh* expression is inhibited by signals from the notochord in order to allow development of the dorsal pancreas. Conversely, ventral mesodermal signals induce *Shh* expression in the ventral endoderm and by doing so bring about development of the hepatic bud (Hebrok et al., 1998; Kim et al., 2000; Deutsch et al., 2001). Similar mechanisms could be involved in the regulation of *Shh* expression in the region of the prospective trachea and could account for the ventro-dorsal switch in its expression. According to such a model, induction of ventral *Shh* expression in the respiratory foregut could be involved in respiratory development whilst the return to a default dorsal expression could be associated with the process of tracheo-oesophageal separation.

Another potential regulator of endodermal *Shh* expression are factors originating in the foregut endoderm itself. These factors could be involved in cell specification in which case they would themselves have a dorsoventral pattern of expression. Tracheo-

oesophageal separation occurs between respiratory-specified and gastrointestinal-specified epithelium. This specification depends on the precise dorsoventral expression pattern of respiratory markers such as *Nkx2.1* (Yuan et al., 2000; Minoo et al., 1999). If it is argued that the dorsoventral *Shh* pattern somehow controls separation along the respiratory-gastrointestinal boundary, it could be hypothesised that *Nkx2.1,* or another respiratory or gastrointestinal marker, controls the *Shh* pattern. This hypothesis has a number of potential weaknesses. First, I have demonstrated that the *Shh* and *Nkx2.1* expression domains are not identical but show significant differences from each other. Second, even if *Nkx2.1* and *Shh* had identical patterns of dorsoventral expression, these could be controlled by another, as yet unidentified, factor.

5.3.5 – The *Shh* expression pattern in the Adriamycin-treated embryo

The effect of Adriamycin on the pattern of *Shh* expression suggests a possible mechanism for abnormal organogenesis in Adriamycin-treated embryos. At E10.5, some embryos lack the well-defined ventral *Shh* expression and show a more uniform pattern of expression in the caudal part of the undivided foregut. The morphological data suggest that although all Adriamycin-treated embryos appear normal at E10.5, about 40% are destined to have an undivided foregut. It seems likely that the E10.5 embryos that exhibit diffuse expression of *Shh* (also 40% of E10.5 embryos) are the ones that are destined to be abnormal. At E11.5, all Adriamycin-treated embryos that have an undivided oesophagotrachea lack the sharp dorso-ventral boundary in *Shh* expression seen in controls, exhibiting a more diffuse signal along the dorso-ventral axis of the common tube. It is not possible at this stage to rule out the possibility that the disturbance in expression is secondary to another factor that causes failure of separation. However, given the proven role of *Shh* in the separation process (i.e. $Shh^{-/-}$ has an undivided foregut)

it is reasonable to suggest that disturbance of the tightly regulated *Shh* expression expression may underlie the action of Adriamycin in disturbing foregut separation. This hypothesis is also consistent with the lack of lung malformations in Adriamycin-treated mouse embryos with OA/TOF. Whilst failure of ventral *Shh* downregulation interferes with tracheo-oesophageal separation, it should not affect branching morphogenesis as the tips of the lung buds are normally strongly *Shh* positive throughout pulmonary development (Pepicelli et al., 1998). It would also be consistent with the $Shh^{-/-}$ mice having both tracheo-oesophageal and lung malformations, as *Shh* is required in the lungs. Rather unexpectedly, the undivided oesophagotrachea in E12.5 Adriamycin-treated embryos re-establishes a dorso-ventral pattern in *Shh* expression with the dorsal epithelium positive and the ventral epithelium negative. This could indicate that the action of Adriamycin is transient and interferes with foregut expression patterns only around the time of tracheo-oesophageal separation. Once the foregut has failed to divide, the gradual re-establishment of the dorsoventral gradient may be of little consequence. A study on the Adriamycin rat model of OA/TOF has also suggested that the *Shh* expression pattern may be disturbed but the described pattern differs from my experience. Rather than a ventral-to-dorsal switch in *Shh* expression, it reports uniform expression that becomes downregulated only at the point of tracheo-oesophageal separation (Orford et al., 2001b). This downregulation is absent in the Adriamycin-treated rat embryos in which separation fails. This discrepancy could, perhaps, be explained on the basis of species differences. In contrast, a more recent study of the Adriamycin-treated rat reports a dorsoventral pattern of foregut *Shh* expression similar to the pattern described in *section 5.2.1* (Arsic et al., 2004). This study also reports that a proportion of Adriamycin-treated embryos exhibit a disturbance of this dorsoventral pattern. Further evidence of disturbance of Shh signaling in Adriamycin-treated rat embryos is provided by an organ

culture study in which the tracheo-oesophageal fistula can be induced to branch in response to exogenous Shh in contrast to the normal oesophagus (Spilde et al., 2003b). Another study in the rat used an ELISA technique to assess the quantity of Shh protein in the foregut and found this to be reduced in Adriamycin-treated embryos lacking the temporal variation seen in controls (Arsic et al., 2003).

5.3.6 – Factors underlying the disturbance of *Shh* expression in Adriamycin-treated embryos

Trying to explain the specific developmental effects of a teratogen like Adriamycin would be a speculative exercise. The actions of Adriamycin range from interference with the function of the cell membrane, mutagenic effects and interference with DNA transcription and replication to a general disturbance of cell proliferation (Ross et al., 1978). The effect on the *Shh* expression pattern could be either direct or indirect. A direct effect is unlikely as the Adriamycin-treated embryos with abnormal foreguts exhibit more diffuse *Shh* expression in the dorsoventral axis of the foregut. This would require a direct activation of the gene by Adriamycin which seems unlikely, although Adriamycin has been shown in another context to interfere with transcription in a gene-specific manner (Arai et al., 2000). Moreover, in this particular case it would be difficult to explain the restriction of the effect to the foregut. It should be pointed out, however, that detailed analysis of the *Shh* expression pattern in other organ systems, in the Adriamycin-treated mouse, was not performed in the present study, so it is not possible to rule out multi-organ effects of Adriamycin on *Shh* gene expression.

An indirect effect of Adriamycin on *Shh* expression seems more likely. Adriamycin could interfere with the expression of genes that regulate *Shh* expression. Upregulation of

activators or downregulation of inhibitors could have the effect of disrupting the fine regulation of *Shh* expression, resulting in a more diffuse pattern across the foregut endoderm. Currently, no evidence exists to support this theory. An alternative idea would be that the Adriamycin-mediated disruption of *Shh* expression is the result of a non-specific effect on the structures adjacent to the developing foregut. One such structure is the notochord. As discussed above, it could regulate *Shh* expression by the secretion of proteins that control expression in cells of the foregut endoderm. Due to the proximity between the notochord and the foregut, and the fact that both are midline structures, a secreted notochordal signal might establish a gradient resulting in a differential effect on the endodermal cells along the dorsoventral axis of the foregut. Any disturbance in the signal gradient could result in loss of the precise positional information conferred to the foregut endoderm and could disturb the spatial pattern of endodermal gene expression. The notochordal malformations noted in Adriamycin-treated embryos, which include duplication and tethering to the foregut, could provide the basis for a disturbed gradient. A split notochord can result in a ventral notochord branch that is much closer to the foregut than the notochord in control embryos. In one embryo, the *Shh* signal in the ventral branch of the notochord was much stronger than the signal from the dorsally-positioned original notochord (Fig. 5.4d inset). The resulting Shh (or other protein) gradient would be disturbed, perhaps resulting in failure of *Shh* downregulation in the ventral foregut, a blurring of the dorsoventral boundary and a failure in separation. Other studies have argued that Adriamycin disturbs mesenchymal proliferation resulting in fewer cells between the notochord and the foregut and consequently a more ventrally positioned notochord and a potentially disturbed signal gradient (Orford et al., 2001). The variability of the notochordal malformations described in Adriamycin-treated embryos would also be consistent with the variable extent of the disturbance in tracheo-

oesophageal separation. A weakness of the notochord theory, however, is that not all Adriamycin-treated embryos with undivided foreguts had malformations of the notochord. A possible explanation for this is that the abnormal ventral branches might have regressed, as demonstrated in Chapter 3, becoming undetectable just after the tracheo-oesophageal malformation was established. A related but distinct explanation is that Adriamycin might affect the notochordal signals without disturbing the structure or the position of the notochord. These various hypotheses remain to be tested.

5.4 – SUMMARY

Given that tracheo-oesophageal separation is disturbed in embryos with a loss of function mutation for *Shh*, I aimed to study the role of *Shh* in tracheo-oesophageal development and the separation process in particular. *Shh* maintained a dorsoventral pattern of expression throughout the period of normal tracheo-oesophageal development. Interestingly, there was a complete ventral-to-dorsal switch in *Shh* expression, which started at the level of the lung buds at the caudal limit of the respiratory foregut and progressed in a cranial direction just ahead of the process of tracheo-oesophageal separation. The expression of genes that are known transcriptional targets of *Shh*, like the transmembrane receptor *Ptc1*, mirrored that of *Shh* with expression in the mesoderm also exhibiting a ventral-to-dorsal switch. The pattern of distribution of the Shh protein in the respiratory foregut broadly followed the ventral-to-dorsal shift pattern but with a slight temporal delay compared to the gene expression pattern, perhaps reflecting the fact that the *Shh* expression was changing. The temporal and spatial relationship between the process of tracheo-oesophageal separation and this dynamic *Shh* expression pattern suggests that *Shh* may play an important role in the separation process itself. This hypothesis is supported by the observation that disturbance of the precise *Shh* expression pattern is associated with, and may underlie, the failure of tracheo-oesophageal separation in Adriamycin-treated embryos.

CHAPTER 6 – MECHANISMS OF TRACHEO-OESOPHAGEAL SEPARATION AND DEVELOPMENT

6.1 – INTRODUCTION

6.1.1 – Separation mechanisms in development

The reshaping of organs as a result of luminal separation is a common theme in many organ-systems during development. Traditionally, this has been associated with a process of septation in which the development of a septum completes the separation of the initial lumen. Such morphogenetic mechanisms are thought to play a role in the development of the hindgut. In this system, septation is thought to contribute to the separation of the anorectal and genitourinary tracts (de Vries & Friedland, 1974; O'Rahilly, 1983; Qi et al., 2000a). The mesenchyme that separates the two tracts is known as the urorectal septum but little is known about the mechanisms of its development, although programmed cell death has been shown to play a role in separation (Qi et al., 2000a; Qi et al., 2000b). In fact, the long held view that growth of this septum actively separates the hindgut is now being challenged by studies suggesting that it is a passive structure, simply representing a mesenchymal interposition between the two separating tracts (Paidas et al., 1999; Rogers et al., 2002). In contrast, septation in cardiac development is widely accepted as contributing to the separation of the four chambers and two outflow tracts of the heart (Icardo, 1996; Anderson et al., 2003; Moorman et al., 2003). In this system, programmed cell death has been shown to play a role in septation, in particular contributing to the completion of the process (Cheng et al., 2002; Sharma et al., 2004).

6.1.2 – Mechanisms of tracheo-oesophageal separation

The view that the foregut separates as a result of the development of a tracheo-oesophageal septum has been long held (Arey, 1966; Gray & Skandalakis, 1972). According to this theory, this septum forms when two lateral, ingrowing epithelial ridges fuse in the midline and consequently separate the lumen into the ventral trachea and the dorsal oesophagus. This process has been described as starting at the level of the lung buds and continuing in a cranial direction at the same time as the foregut gains significantly in length. Until recently however, there has been no conclusive evidence that such a septum exists (Zaw-Tun, 1982; O'Rahilly & Muller, 1984; Kluth et al., 1987). Furthermore, the contribution of the epithelial and mesenchymal elements of the foregut in its formation, or the specific cellular and molecular mechanisms that might be involved in the separation process, have not been studied in any detail. In view of this lack of solid evidence, a number of other theories have emerged to account for the development of a separate ventral trachea. Separation has been attributed to collapse of the lateral foregut walls without the formation of a septum, Kluth has described the role of epithelial folds in separation whereas others have suggested that differential growth rather than separation accounts for tracheal development (*see Chapter 3*).

The development of the Adriamycin rat model of OA/TOF has provided the opportunity to study the role of cellular and molecular mechanisms in the embryogenesis of the malformations but has also prompted a more detailed look at the mechanisms that underlie normal tracheo-oesophageal development and separation. Recent studies have focused on the role of programmed cell death (PCD) or apoptosis in the separation process and tracheo-oesophageal development in general. These studies have shown that PCD is detected in large numbers in the approximating lateral epithelial ridges at the

point of tracheo-oesophageal separation (Qi & Beasley, 1998; Zhou et al., 1999; Williams et al., 2000; Orford et al., 2001). They suggested that apoptosis plays a role in remodelling and reshaping the separating foregut. These studies have not described any PCD activity in the developing foregut at earlier stages of development, or at different levels within the developing foregut, suggesting a rather limited role for PCD in physically separating and reorganising the dividing foregut. In fact, only one of these studies (Williams et al., 2000) specifically comments about lack of PCD in the pre-separation foregut and the various levels of the foregut during tracheo-oesophageal separation, although there was no explanation of how apoptosis was detected. These same studies have confirmed that following separation, PCD is rare within the foregut, suggesting that it plays a specific role in the process. Moreover, these authors reported that Adriamycin-treated rat embryos that develop tracheo-oesophageal malformations have a different pattern of foregut PCD. The undivided foregut in these embryos had significantly reduced PCD in the region of the lateral ridges and it was suggested that this reduction was associated with the development of the malformation (Zhou et al., 1999; Williams et al., 2000; Orford et al., 2001). These studies did not address the issue of whether the reduction in PCD was a consequence rather than a cause of the failure to separate. Analysing the later stages in the abnormal Adriamycin-treated embryos, the same studies detected increased PCD in the dorsal mesenchyme of the atretic oesophagus (Zhou et al., 1999; Williams et al., 2000; Beasley et al., 2004). It is not clear from these accounts what the association is, if any, between this PCD activity and the development of the upper oesophageal pouch. Another study has failed to detect significant apoptosis in Adriamycin-treated rat embryos in the period immediately after administration of Adriamycin, suggesting that its action is not mediated by induction of PCD (Gillick et al., 2002b). In summary, existing studies have suggested a limited but specific role for PCD

in tracheo-oesophageal separation, and that reduced levels of PCD are associated with failure of separation.

6.1.3 – Questions about tracheo-oesophageal separation

In previous chapters, I have shown that tracheo-oesophageal development is likely to involve an active process of separation of two, already specified, foregut components. In this chapter, I aimed to study the mechanisms that contribute to this separation. In view of the mechanisms surrounding the notion of a tracheo-oesophageal septum, I have so far avoided mention of such a structure. My aim was to study the cellular mechanisms that effect this separation and understand its nature. In particular, I wanted to know whether programmed cell death was simply a clearing mechanism, finishing off luminal division, or whether it had an earlier, regulatory role in the separation process. Furthermore, I aimed to study the pattern of cell proliferation within the developing foregut. On one hand, this would supplement the PCD data and demonstrate whether apoptosis is simply a by-product of increased number of cells within a specific region. On the other hand, it is important to correlate morphological observations made in previous chapters with proliferation patterns. For example, I have described the development of ingrowing lateral epithelial ridges at the site of future tracheo-oesophageal separation. It is important to demonstrate whether these ridges are a result of epithelial proliferation or a consequence of proliferation of the adjacent mesenchyme. Finally, I wanted to test the hypothesis that tracheo-oesophageal separation results from differential growth of the two foregut components. Foregut length analysis in Chapter 3 suggested that this was not the case but studying levels of proliferation would address this issue directly.

6.2 – RESULTS

6.2.1 – Programmed cell death (PCD) in the developing foregut

6.2.1.1 - Patterns of programmed cell death during normal foregut development

At E10.5, the main morphogenetic event in the pharyngeal foregut is the budding of the various derivatives of the laterally-placed pharyngeal pouches. The distribution of epithelial cells undergoing PCD is precise; they are located at the junction of the epithelium of the budding organs and the pharyngeal epithelium (Fig.6.1b). At levels where these organs are separated from the pharynx, they are found in the organ epithelium. PCD is also associated with midline pharyngeal foregut derivatives. The ventral, midline-positioned, thyroid primordium is itself marked by epithelial cells undergoing PCD (Fig. 6.1b inset).

The pattern of PCD in the foregut epithelium caudal to the pharynx is dynamic and appears to be intimately linked to the process of respiratory development and tracheo-oesophageal separation. At E10.5, the stage at which respiratory tracheal specification has already taken place but tracheo-oesophageal separation has not yet started, there are three identifiable epithelial PCD patterns at different levels of the foregut. At the cranial end, PCD is localised in the ventral epithelium of the laryngotracheal groove in 6 out of 7 embryos examined (Fig. 6.1d). At more caudal levels, PCD cells are found at the dorsoventral junction of the undivided foregut in 5 out of 7 embryos examined (Fig. 6.1f). When individual sections are studied, a clear pattern emerges with foci of PCD cells located at corresponding points of the lateral foregut walls even if in some embryos the connecting imaginary line is somewhat oblique. The third level is that of the lung buds at

Fig. 6.1 PCD patterns in the E10.5 respiratory foregut (CBA/Ca embryo)

Immunohistochemistry for the PCD effector cleaved Caspase-3 on transverse sections from saline-treated (b,d,f,h) and Adriamycin-treated (c,e,g,i) E10.5 CBA/Ca embryos at levels indicated in the schematic representation of the E10.5 foregut (Fo) in (a).***(b,c)*** At the level of the pharynx (Ph), both saline and Adriamycin-treated embryos have apoptotic cells at the boundaries of the pharyngeal pouch (Pp) derivatives (arrowheads) and in the midline thyroid primordium (arrows, inset). ***(d,e)*** At the level of the laryngotracheal groove (Lt), both saline and Adriamycin-treated embryos have apoptotic cells almost exclusively in the ventral groove epithelium. ***(f,g)*** Further caudally, apoptotic cells mark the dorsoventral boundary in saline-treated embryos (arrowheads in *f*). This pattern is absent in most Adriamycin-treated embryos which exhibit apoptotic cells at various points along the dorsoventral axis of the foregut (arrowhead in *g*). ***(h,i)*** At the level of the lung buds (Lb), saline-treated embryos have apoptotic cells at the boundaries of the individual buds (arrowheads) with persistence of the cells at the dorsoventral boundary (arrow & inset). In Adriamycin-treated embryos, the marking of the lung buds by apoptosis is still seen but most embryos lack PCD at the dorsoventral boundary. Scale bar, 100 μm

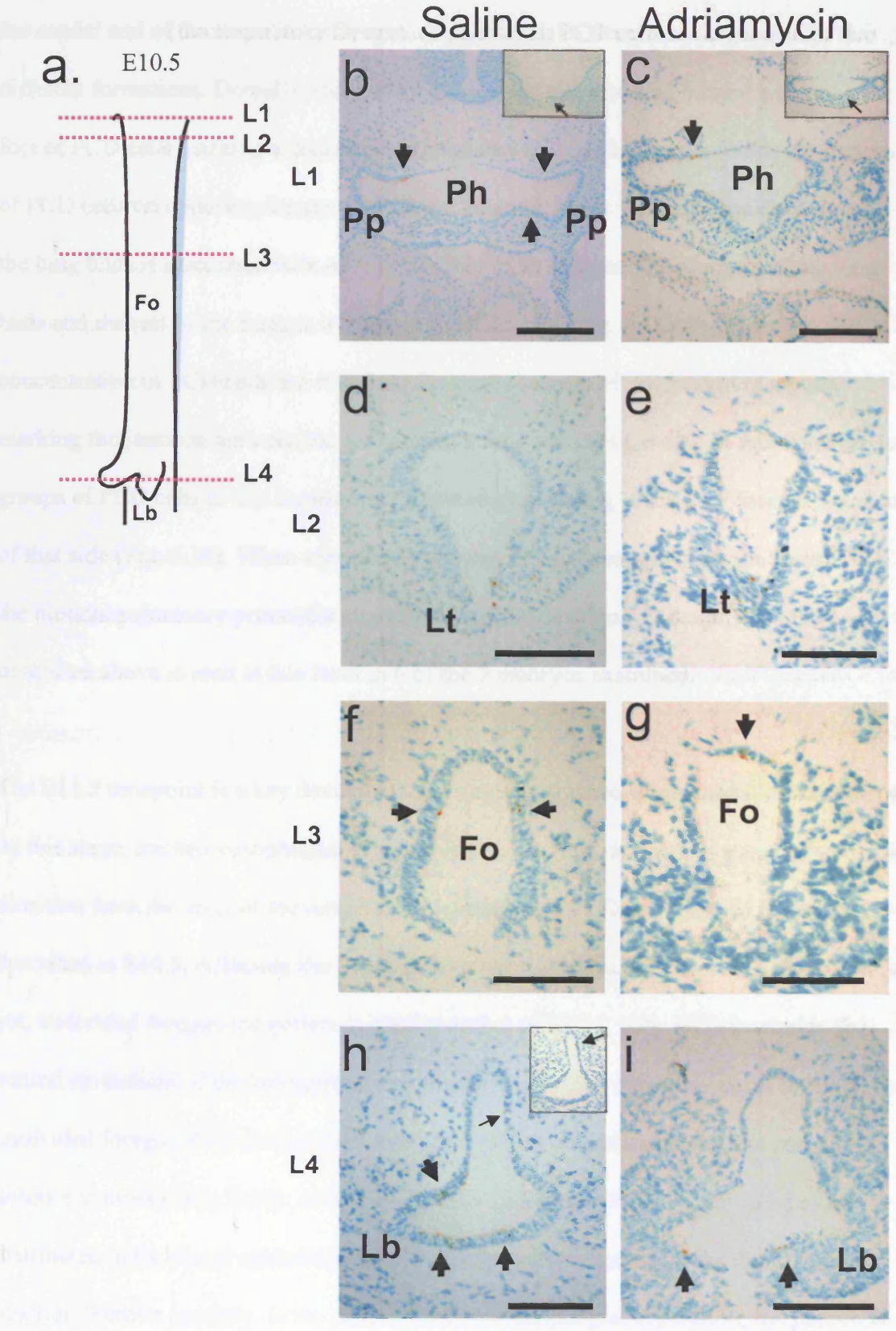
Saline
Adriamycin
a.
E10.5
L1
L2
L3
L4
Fo
Lb
b
c
Ph
Pp
Pp
Ph
Pp
L1
d
e
Lt
Lt
L2
f
g
Fo
Fo
L3
h
i
Lb
Lb
L4

the caudal end of the respiratory foregut. At that level, PCD cells are organised in two different formations. Dorsally, the pattern seen in the more cranial foregut persists with foci of PCD cells marking a dorsoventral boundary (Fig. 6.1h). At this level, the pattern of PCD cells on opposing foregut walls is maintained. More ventrally, the development of the lung buds is associated with another distinct PCD pattern. The junction of the lung buds and the rest of the foregut is marked by PCD cells (Fig. 6.1h). Furthermore, a concentration of PCD cells are found on the ventral aspect of the foregut at a point marking the junction between the left and right lung buds (Fig. 6.1h). In fact there are two groups of PCD cells at this location, each one corresponding to the bud/ foregut junction of that side (Fig. 6.1h). When viewed in this way, PCD appears to mark the budding of the bronchopulmonary primordia on each side of the developing foregut. The pattern described above is seen at this level in 6 of the 7 embryos examined.

The E11.5 timepoint is a key developmental stage for tracheo-oesophageal development. At this stage, tracheo-oesophageal separation is in progress, moving in a caudal-to-cranial direction from the level of the lung buds. The pattern of PCD has changed from that described at E10.5, reflecting the ongoing separation process. At the cranial end of the, as yet, undivided foregut, the pattern is similar to that of E10.5, with PCD located in the ventral epithelium of the laryngotracheal groove (Fig. 6.2b). At more caudal levels of the undivided foregut, PCD is now restricted to the dorsal epithelium with near-complete absence ventrally (Fig. 6.2c). At this level, cells undergoing PCD appear to be evenly distributed in the dorsal epithelium with no obvious convergence on the dorsoventral junction. Further caudally, at the point of tracheo-oesophageal separation, the pattern is somewhat different. There is still a clear dorsal distribution of PCD and an absence of PCD from the ventral epithelium, but there is an obvious increase of dying cells at and

Fig. 6.2 PCD patterns in the E11.5 respiratory foregut (CBA/Ca embryo)

Immunohistochemistry for the PCD effector cleaved Caspase-3 on transverse sections (b to f) from saline-treated E11.5 CBA/Ca embryos at levels indicated on the schematic representation of the foregut (Fo) in (a). ***(b)*** At the level of the laryngotracheal groove (Lt), PCD is seen almost exclusively in the ventral epithelium of the groove. ***(c)*** Further caudally, there is a complete reversal of this pattern with PCD concentrating in the dorsal, oesophageal-prospective, epithelium. ***(d)*** At the level of tracheo-oesophageal separation, PCD persists in the dorsal epithelium but is mostly concentrated in the folding, approximating epithelium at the separation site (arrowheads). ***(e)*** Caudal to the separation, the oesophageal epithelium maintains apoptotic cells with some apoptotic cells seen in the dorsal-most part of the separated trachea (Tr) as well as in the intervening mesenchyme (arrow). ***(f)*** As the level of tracheal bifurcation is approached, oesophageal PCD is still detected but is reduced. In contrast, apoptotic cells are concentrated in the middle third of the trachea at the site of tracheal bifurcation (arrowhead). Oe - oesophagus, Br – bronchus. Scale bar, 50 μm

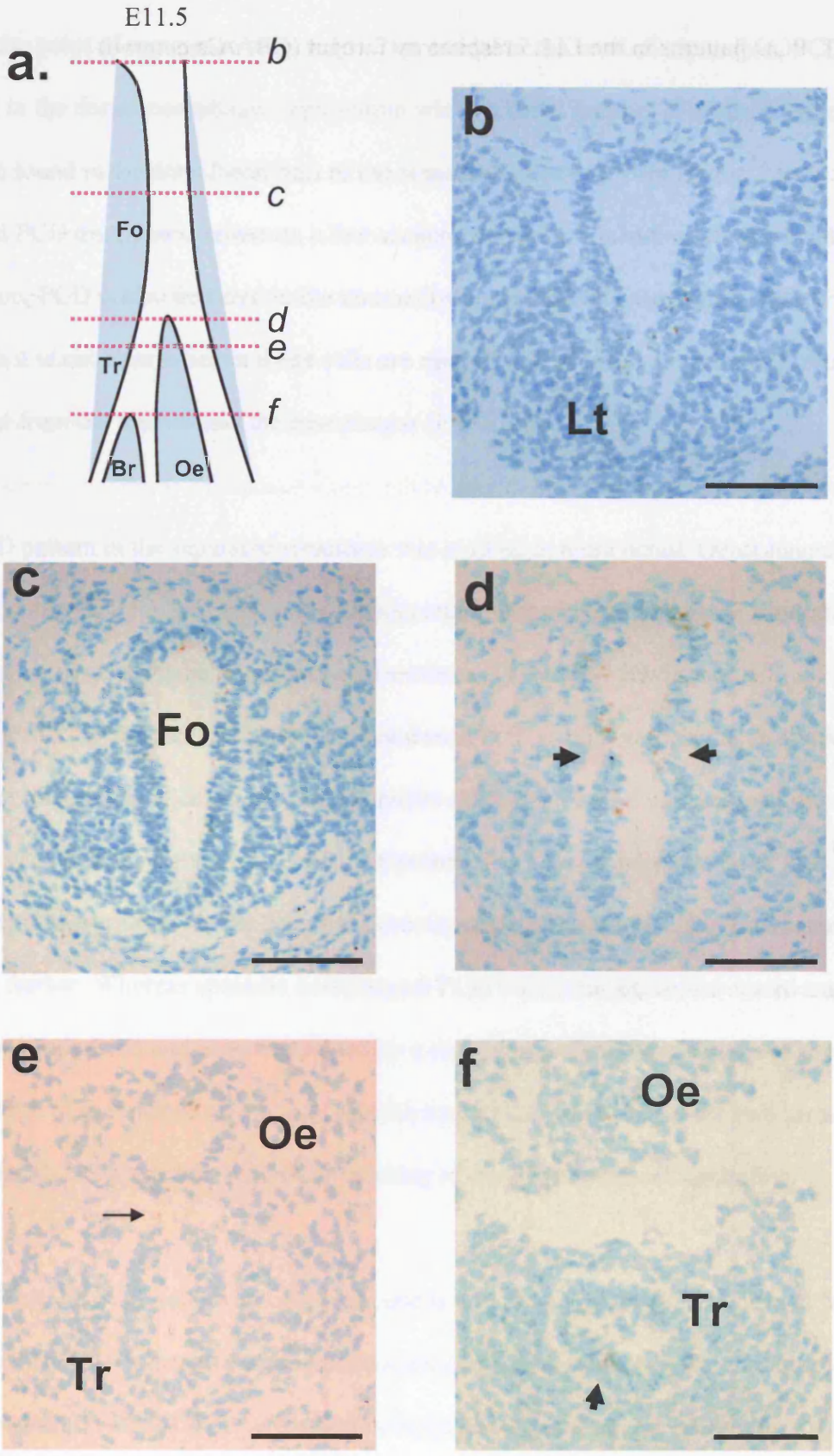
E11.5
a.
b
c
Fo
d
e
Tr
f
Br
Oe
b
Lt
c
Fo
d
e
Oe
Tr
f
Oe
Tr

around the point of separation (Fig. 6.2d). Just caudal to the level of separation, PCD remains in the dorsal oesophageal epithelium whilst a small number of cells undergoing PCD are found in the dorsalmost part of the separated ventral trachea (Fig. 6.2e). Tracheal PCD disappears, however, a few sections caudal to separation. At the level of separation, PCD is also detected in the mesenchyme between the separating structures although it is not clear whether these cells are epithelial in origin, representing those excluded from the trachea and the oesophagus (Fig. 6.2e).

The PCD pattern in the separated structures was studied in more detail. Oesophageal PCD is found consistently in sections immediately caudal to tracheo-oesophageal separation whereas it is more sporadic in more caudal sections. This initial persistence of oesophageal PCD probably reflects the clear dorsal PCD pattern seen in the undivided foregut at this gestation. Similarly, the apoptotic cells in the dorsal trachea seen in sections caudal to the separation probably represent PCD on the ventral side of the folding epithelial ridges. As the separated structures are followed caudally the pattern changes further. Whereas sporadic oesophageal PCD continues, the initial dorsal tracheal PCD has disappeared and is now replaced by a consistent pattern of apoptosis in the middle third of the trachea as we approach the tracheal bifurcation into the two bronchi (Fig.6.2f). This is consistent with PCD marking of the site of tracheal separation.

The fact that the PCD pattern is a dynamic one is underlined by the pattern seen at later gestations. By E12.5, the process of tracheo-oesophageal separation is all but completed. To emphasise the role of PCD in tracheo-oesophageal separation, the epithelium of the oesophagus shows a complete lack of PCD at this stage (Fig. 6.3c-f). In fact this is so marked that it gives the impression that the experimental technique may have not worked.

Fig. 6.3 PCD patterns in the E12.5/E13.5 respiratory foregut (CBA/Ca embryo)

Immunohistochemistry for the PCD effector cleaved Caspase-3 on transverse sections from saline-treated E12.5 (b-f) and E13.5 (inset e & f) CBA/Ca embryos at levels shown on the schematic representation of the foregut (Fo) in (a). ***(b)*** At this level, the cranialmost part of the subglottic larynx (La) is about to separate from the oesophagus (Oe) in order to complete tracheo-oesophageal separation. PCD cells (arrow) mark the point of separation. ***(c)*** The separated trachea (Tr) and oesophagus show complete lack of PCD in contrast to the high level of apoptosis in the dorsal root ganglia (Drg, inset). ***(d)*** At more caudal levels, closer to the tracheal bifurcation, some tracheal epithelial cells are Caspase-3 positive and are mostly concentrated in the middle third of the trachea (arrowhead). In contrast, no PCD is seen in the oesophagus. ***(e)*** At the level of the tracheal bifurcation, PCD cells are found primarily at the separation site (arrowheads), as well throughout the tracheal epithelium whilst the oesophagus remains completely negative. In contrast, there is no PCD in either the tracheal or oesophageal epithelium at the same level in E13.5 embryos (inset). ***(f)*** The separated bronchi (Br) maintain Caspase-3 positive cells with the oesophagus remaining entirely Caspase-3 negative. At E13.5, no PCD is found in either structure (inset). Scale bar, 50 μm

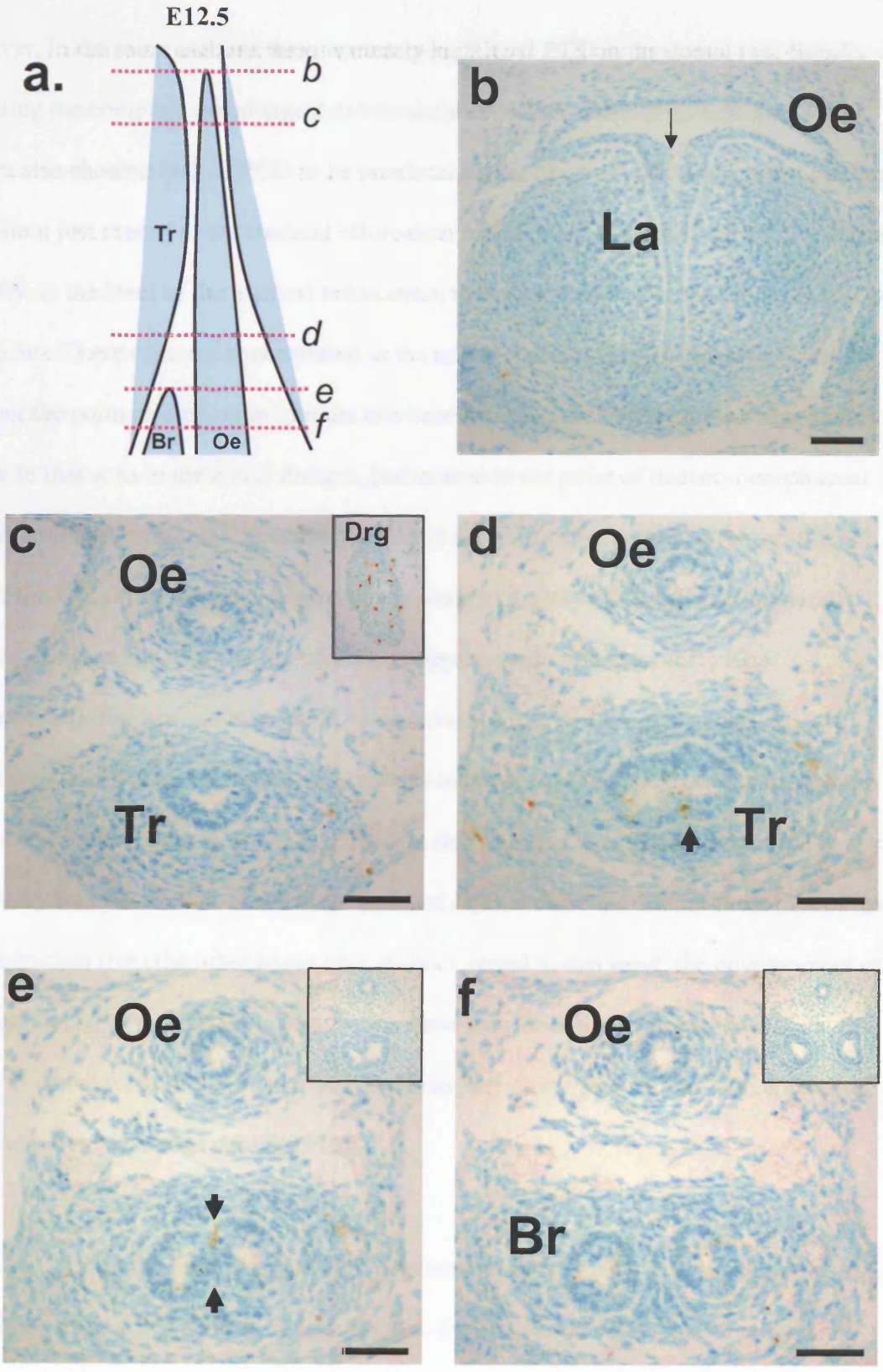
E12.5
a.
b
c
Tr
d
e
f
Br
Oe
b
Oe
La
c
Drg
Oe
Tr
d
Oe
Tr
e
Oe
f
Oe
Br

However, in the same sections there is clearly high level PCD in the dorsal root ganglia validating the complete oesophageal downregulation of cell death (Fig. 6.3c inset). The trachea also shows a lack of PCD in its proximal part although PCD is seen in the tracheal epithelium just cranial to the tracheal bifurcation into the two bronchi (Fig. 6.3c,d). More caudally, at the level of the tracheal bifurcation, there is a marked increase in PCD levels (Fig. 6.3e). These cells are concentrated in the middle third of the bifurcating trachea, marking the point of separation into the two bronchi (Fig.6.3e). This arrangement is very similar to that seen in the E11.5 foregut, just cranial to the point of tracheo-oesophageal separation. In both cases, PCD marks the site of approximating epithelial ridges; in the case of the E11.5 foregut these ridges approximate in the sagittal plane (mediolateral) whereas in the case of the E12.5 trachea they approximate in the coronal plane (ventrodorsal). Further caudally, PCD persists in the separated bronchi (Fig. 6.3f). At these levels, there is complete absence of PCD in the oesophagus in sharp contrast to the trachea and bronchi (Fig. 6.3c-f). Apoptosis is also found at the cranial limit of the respiratory foregut. PCD is found at the point of separation of the cranial-most part of the laryngotrachea from the oesophagus (Fig. 6.3b). Cranial to that level, the development of the supraglottic larynx is still ongoing with active growth of the arytenoid swellings, the fusion of which will define the entrance to the airway (laryngeal aditus). The epithelium of the arytenoid swellings exhibits PCD.

By E13.5, PCD in the foregut has all but disappeared. Specifically, there is absence of PCD in the trachea and bronchi suggesting that the process of tracheal bifurcation and shaping of the carina has been completed (Fig. 6.3e,f insets). PCD continues to be totally absent from the oesophagus (Fig. 6.3e,f insets). The lack of PCD is validated by the fact that significant apoptosis persists in the dorsal root ganglia in the same sections making it

unlikely that this is a result of experimental error. Overall, these observations indicate that if PCD does indeed play a role in the development of the respiratory foregut, this is completed by E13.5.

6.2.1.2 - Quantitation of PCD

The epithelial cells undergoing PCD at any given time are only a small proportion of the total epithelial population and are found at variable positions in the foregut. This introduces a degree of subjective interpretation when the PCD patterns are described. I reasoned that in order to substantiate and confirm the descriptive patterns of apoptosis in the developing foregut (described in the previous section) it would be important to quantify PCD in standardised segments of the foregut (dorsal or ventral) at various levels along its anteroposterior axis. This quantitation also supplements the patterns already described. It assesses the actual intensity of PCD and allows objective comparisons of PCD in different parts of the foregut, as well as with the corresponding mitotic activity in specific regions. In order to quantify PCD, the proportion of cells that stained positive for caspase-3 in a defined part of the foregut was calculated. This proportion represents the apoptotic index for that particular part of the foregut. I chose to calculate the apoptotic index at cranio-caudal levels that were relevant to the PCD patterns described above.

<u>Defining the levels for the study of the apoptotic index</u>

For the E11.5 foregut, I chose to study PCD patterns at various levels cranial to the level of separation as well as at levels of the separated trachea and oesophagus (Fig. 6.4). For each embryo, the specific section that corresponded to the specified level was studied for apoptotic activity. Levels one and five corresponded to the cranial limit of the laryngotracheal groove and the tracheo-oesophageal separation, respectively, whereas

Fig. 6.4 PCD patterns in the E11.5 respiratory foregut (CBA/Ca embryo)

Immunohistochemistry for the PCD effector Caspase-3 on transverse sections from saline-treated E11.5 CBA/Ca embryos. The level of PCD activity in the foregut epithelium was determined by calculating the PCD (or apoptotic) index for a specified region of the epithelium as defined below. The index was the proportion of epithelial cells that stained positive for the anti caspase-3 antibody. The schematic representation of the E11.5 foregut (Fo) indicates the cranio-caudal levels studied for PCD. Level 1 is the level of the laryngotracheal groove (Lt), level 5 that of the tracheo-oesophageal separation and levels 2,3 and 4 are evenly spaced between 1 and 5. Level 7 is the level of the tracheal bifurcation and level 6 is at a quarter of the distance between 5 and 7. The foregut at level 1 is divided into two equal parts (dorsal and ventral). The foregut at levels 2 to 5 is also divided in dorsal and ventral parts but the dorsal one is subdivided into middle and dorsalmost segments. Sections from level 7 show the widened trachea (Tr) at the level of its bifurcation into the bronchi (carina). The trachea is divided into three equal parts: two lateral and one middle segments. Oe - oesophagus, Br – bronchus. Scale bar, 50 μm

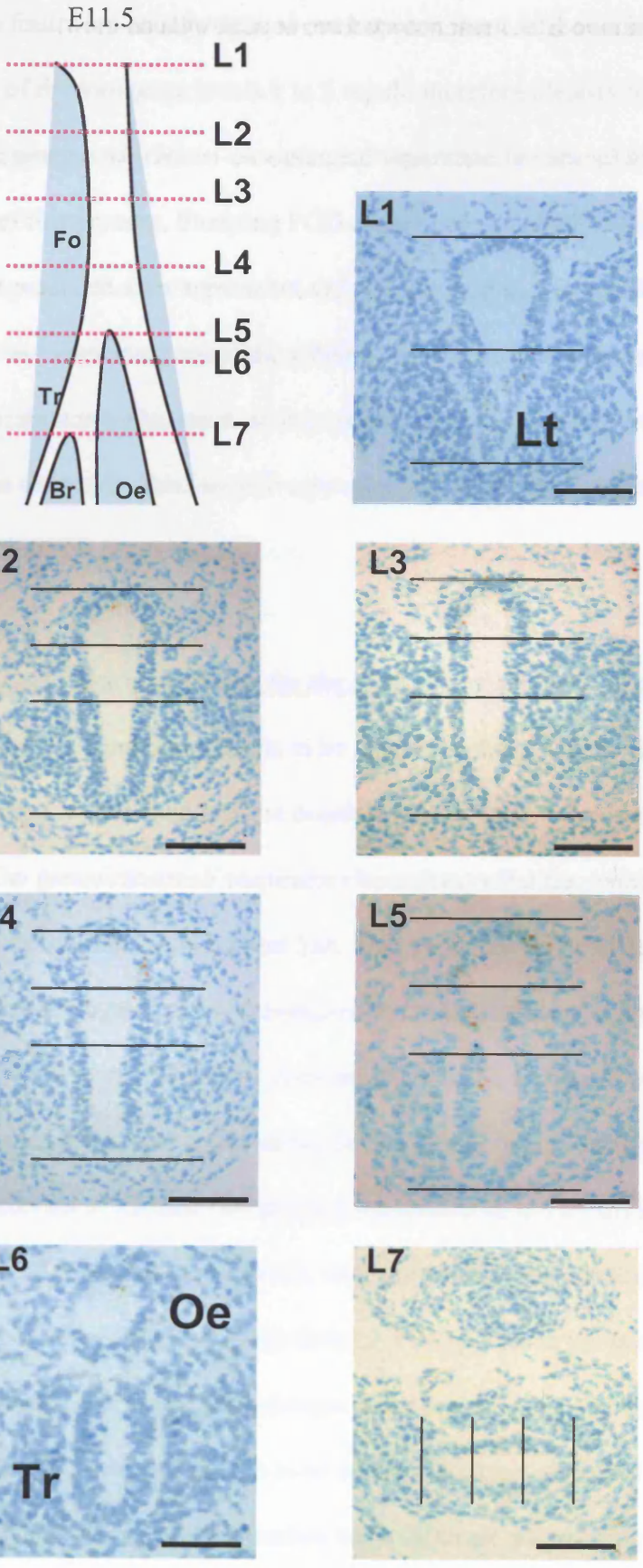
E11.5
L1
L2
L3
Fo
L4
L5
L6
Tr
L7
Br
Oe
L1
Lt
L2
L3
L4
L5
L6
Oe
Tr
L7

levels two to four were equally spaced out between them as shown in Fig.6.4. The examination of the foregut at levels 1 to 5 would therefore identify the intensity of PCD related to the process of tracheo-oesophageal separation in view of the caudocranial progression of this process. Studying PCD at more caudal levels might reveal whether such patterns persisted after separation and whether tracheal separation into the two bronchi also had associated apoptotic patterns. Level seven corresponded to the level of tracheal separation whereas level six was at a quarter of the distance from five to seven. Level six was chosen in order to pick up persistence of the pre-separation pattern in the proximal trachea and oesophagus.

Defining the dorsoventral segments for the study of the apoptotic index

The selection of the foregut segments to be studied at the individual levels also reflected the patterns already described and the possible role of PCD in tracheo-oesophageal separation. The gastrointestinal/ respiratory boundary coincides with the dorsoventral boundary of expression of *Nkx2.1* and *Shh*. This dorsoventral boundary is clearly identifiable morphologically by the presence of epithelial folds. In the majority of embryos, the dorsoventral boundary does not correspond to the midway point on the dorsoventral axis; it is closer to the dorsal limit of the foregut. For this reason, and at the levels most relevant to tracheo-oesophageal separation (2 to 5), I divided the foregut into a ventral half and two equal dorsal parts, with the middle dorsal one corresponding to the dorsoventral boundary (Fig. 6.4). This division also applied to the study of patterns of mitosis (see below). For level 1, the foregut was divided into equal dorsal and ventral components as PCD activity appears to be concentrated in the ventral laryngotracheal groove. For level 7, the separating trachea has a different shape being more flat ventrodorsally. It was divided into three equal segments: one medial segment flanked by

two lateral segments, as shown in Fig.4. The middle part corresponds to the site of separation of the trachea into the two bronchi.

Data analysis

The variation in the values of the apoptotic index suggests that there is a clear shift in apoptosis from the ventral to the dorsal epithelium as the level of separation is approached (Table 6.1, Fig.5). The level of apoptosis in the ventral half of level 1, which corresponds with cell death in the laryngotracheal groove, is high with up to 25% of cells undergoing PCD (Fig. 6.5a). The ventral index for this level is significantly higher than the ventral index for levels 3, 4 and 5 (p values of 0.003, 0.004 and 0.003). This suggests that there is very little PCD in the ventral epithelium caudal to the laryngotracheal groove. Conversely, there is significant increase in apoptotic activity in the dorsal half of the foregut (*please note that for this calculation the two dorsal segments were pooled together as the dorsal half of the foregut*) in levels 4 and 5 compared to levels 1 and 2 (p values of 0.003, 0.002, 0.004 and 0.004). At level 5, as many as 30% of dorsal epithelial cells are undergoing PCD. To emphasise the dorsoventral divide in PCD activity, the difference in the PCD index between the dorsal and ventral segments of the foregut at levels 1,4 and 5 also reaches statistical significance (p values of 0.01, 0.0001 and 0.002). In order to study PCD in the zone of tracheo-oesophageal separation, the middle section was studied separately. The index for the middle section remains low along the foregut, rising sharply at level 4 and peaking at level 5 at which up to 32% of epithelial cells are undergoing PCD (Fig.5c). This observation is consistent with a specific role of PCD at the level of tracheo-oesophageal separation. The difference is significant between levels 3 to 4 and 4 to 5 (p values of 0.02 for both comparisons), confirming the trend as the separation point is approached. However, the overall rise in dorsal PCD as we move from

cranial to caudal is not solely attributable to the gradual increase in middle segment cell death. A significant increase in PCD in the dorsal-most segment between levels 2 and 3 (p = 0.03) occurs before there is any demonstrable increase in the region of future separation (middle segment) (Fig. 6.5b). At level 3, the dorsal-most PCD index is significantly higher than both the middle and ventral indices (p values of 0.04 and 0.01). PCD in this dorsal segment remains high in levels 4 and 5. In summary, these observations suggest there are two main characteristics in the PCD pattern in the E11.5 foregut. The first is the shift of apoptotic cells to the dorsal foregut and the second is the concentration of apoptotic cells at the point of separation.

At level 6, which is nearer the tracheo-oesophageal separation than the tracheal bifurcation, there is significantly more PCD in the oesophagus than the trachea (p=0.01) (Fig. 6.5a). This appears to represent a persistence of the pattern cranial to the separation with dorsal PCD persisting in the oesophagus and a low level of tracheal PCD being contributed to by the ventral portion of the pre-separation middle segment (Fig. 6.4L5). This pattern changes in more caudal sections of the trachea and oesophagus as these structures grow and as the level of tracheal separation is approached. Oesophageal PCD falls significantly between levels 6 and 7 (p=0.03) (Fig. 6.5a) whereas the tracheal PCD becomes redistributed and is found almost exclusively in the middle part of the separating trachea (Fig. 6.5c). At level 7, middle segment tracheal PCD is significantly higher than both lateral tracheal segment and oesophageal PCD (p values of 0.008 and 0.01) with 20% (mean) of cells undergoing PCD in the middle segment. This observation would support a role for PCD in the development of the point of tracheal bifurcation.

Table 6.1. PCD patterns in the E11..5 respiratory foregut (CBA/Ca embryo)

		Mean (Standard deviation)		
		PCD cells	Total cells	PCD index (%)
Level 1 (n=5)	Dorsal half	3.8 (2.2)	90.8 (16.1)	4.2 (2)
	Ventral half	12 (12.1)	70.2 (40.8)	14.2 (6.5)
Level 2 (n=5)	Dorsal half	3.2 (2.8)	94.6 (28.1)	3.4 (2.4)
	Dorsal-most	1.8 (1.5)	47.4 (12.5)	3.9 (3.1)
	Middle	1.4 (2.1)	47.2 (21.5)	2.5 (2.8)
	Ventral half	2.6 (3.7)	48.2 (14.9)	4.9 (5.4)
Level 3 (n=6)	Dorsal half	8.5 (6.8)	87.3 (19)	9.3 (5.5)
	Dorsal-most	6.7 (5.5)	45.3 (7.4)	15.2 (9.5)
	Middle	1.8 (2.3)	44.3 (11.1)	3.7 (4.7)
	Ventral half	3 (4.1)	77.8 (42.2)	2.6 (3.1)
Level 4 (n=6)	Dorsal half	13 (4.4)	116.2 (24.5)	11.4 (3.7)
	Dorsal-most	6 (3.2)	55.8 (13.4)	8.4 (6.2)
	Middle	7 (3.4)	60.3 (15.1)	11.5 (4.8)
	Ventral half	1 (1.26)	109 (26.6)	0.8 (1)
Level 5 (n=6)	Dorsal half	17.7 (6.3)	101.8 (21)	18 (8.3)
	Dorsal-most	5.5 (4.7)	45.2 (10.2)	12.9 (11.7)
	Middle	11.8 (3.5)	56.7 (12.9)	21.6 (7.8)
	Ventral half	3.7 (1.5)	105.8 (29.6)	3.5 (1.5)
Level 6 (n=6)	Oesophagus	6.8 (3.6)	46.8 (8.7)	14.5 (7.4)
	Trachea	4.3 (3.3)	93.3 (18.5)	4.5 (3.1)
Level 7 (n=5)	Oesophagus	0.8 (1.3)	17.8 (3.8)	3.8 (6)
	Trachea	6.4 (2.5)	99.4 (18.9)	6.6 (2.9)
	Trachea middle	6 (2.3)	32.6 (12.1)	20 (9.8)
	Trachea lateral	0.2 (0.3)	33.6 (3.8)	0.6 (0.9)

Fig. 6.5 PCD quantitation in the E11.5 foregut (CBA/Ca embryo)

Apoptotic index of the foregut epithelium at different levels of the E11.5 foregut. Levels and segments are those defined in Fig. 4. (a,b,c) Vertical box plots with error bars defining the median, 10^{th}, 25^{th}, 75^{th} and 90^{th} percentile values. All outlying values are represented by individual dots. ***(a)*** In this analysis, the middle and dorsal segments in levels 2 to 5 are merged into one dorsal segment. This figure illustrates a ventral-to-dorsal shift in PCD activity as we move caudally towards the level of tracheo-oesophageal separation. Ventral PCD at level 1 is significantly higher than ventral PCD at levels 3,4 and 5 (p values of 0.003, 0.004 and 0.003). Conversely, dorsal PCD at levels 4 and 5 is significantly higher than dorsal PCD at levels 1 and 2 (p values of 0.003, 0.002, 0.004 and 0.004). Oesophageal PCD does, however, fall significantly between levels 6 and 7 (p=0.03). At levels 1,4,5 and 6 there is a significant difference between ventral and dorsal PCD (p values of 0.01, 0.0001, 0.002 and 0.01). ***(b)*** Apoptosis at the level of the tracheal bifurcation (level 7) in different segments of the trachea as defined in Fig 4. The index for the middle tracheal portion (TR/Md) is significantly higher than that for the lateral tracheal segments (TR/Lt) or the oesophagus (p values of 0.008 and 0.01). ***(c)*** This plot illustrates the sharp rise in middle segment PCD as the level of tracheo-oesophageal separation is approached. The index at level 4 is significantly higher than that at level 3 (p=0.02) and that for level 5 is significantly higher than that for level 4 (p=0.02). The index for the dorsalmost segment at level 3 is significantly higher than the middle and ventral indices for the same level (p values of 0.04 and 0.01) as well as significantly higher than the dorsalmost index for level 2 (p=0.03).

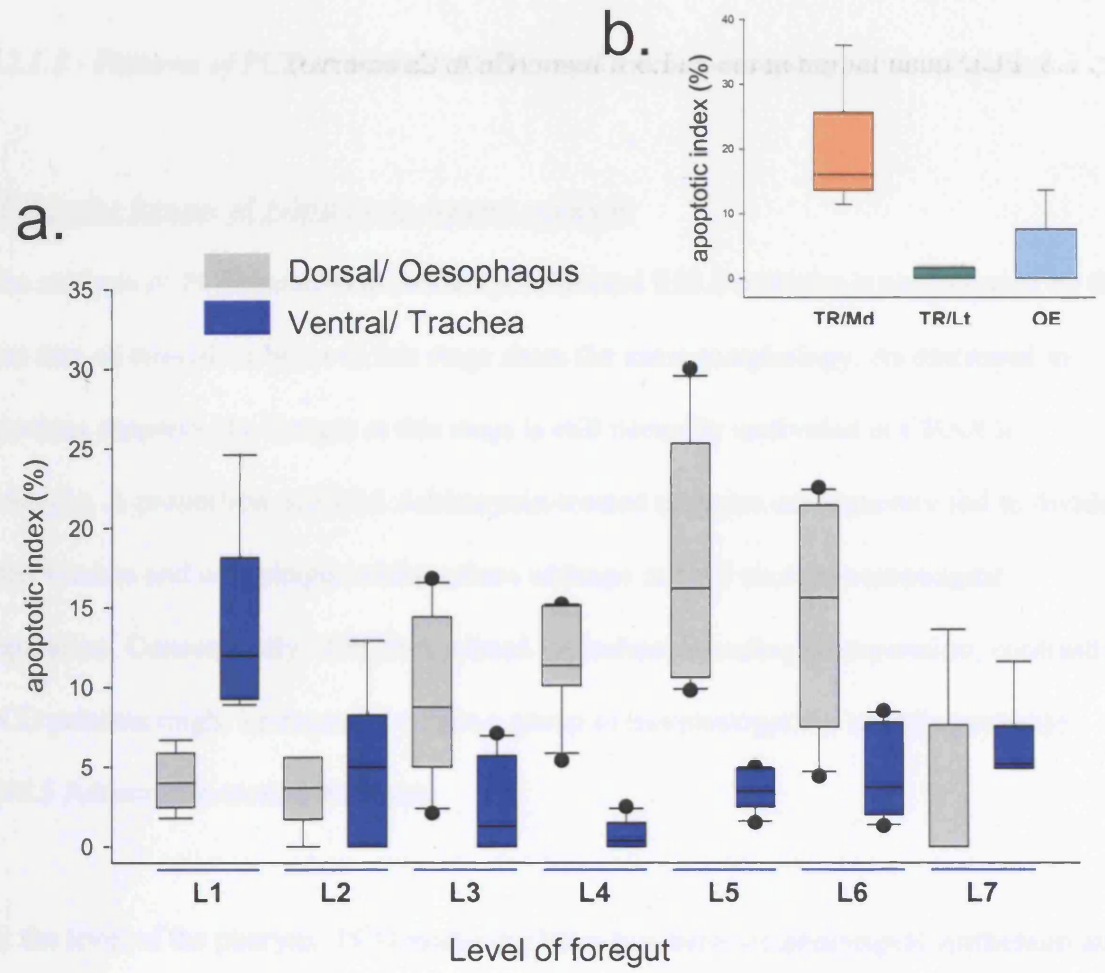
a.
b.
Dorsal/ Oesophagus
Ventral/ Trachea
apoptotic index (%)
0
5
10
15
20
25
30
35
L1
L2
L3
L4
L5
L6
L7
Level of foregut
apoptotic index (%)
0
10
20
30
40
TR/Md
TR/Lt
OE

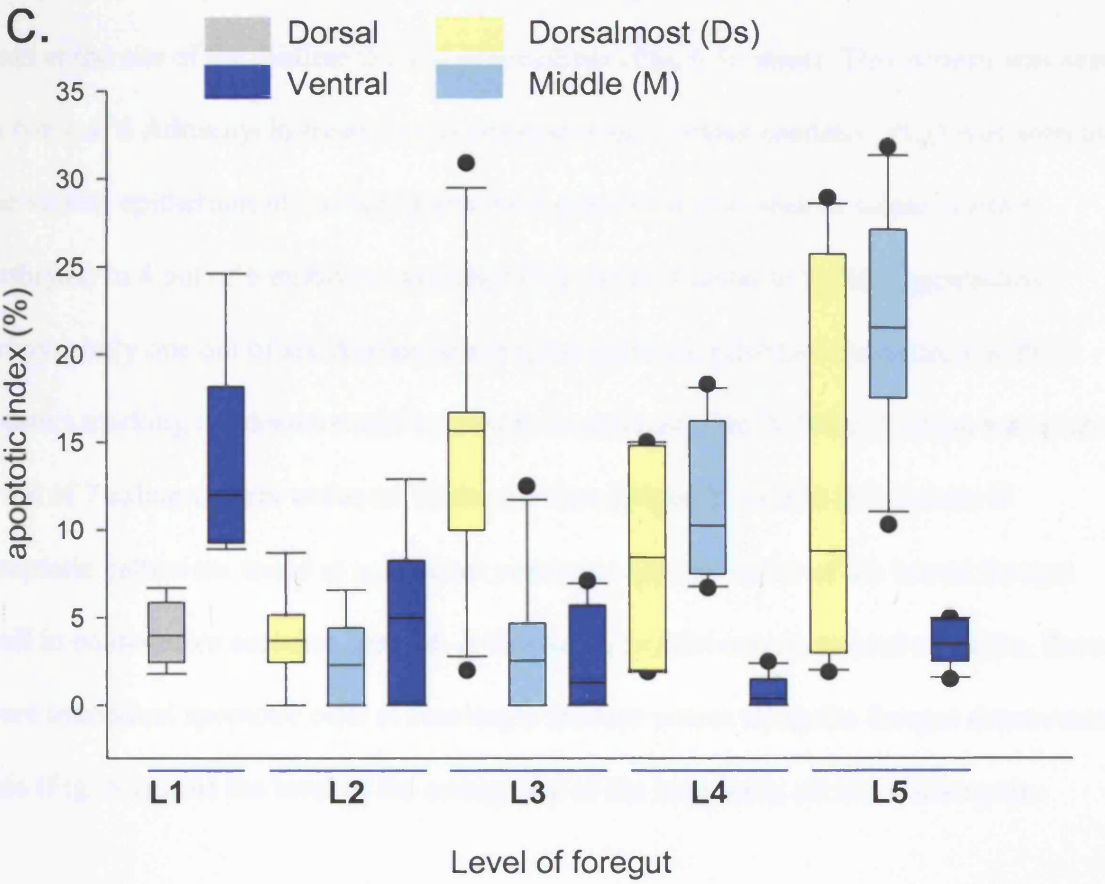
c.
Dorsal
Ventral
Dorsalmost (Ds)
Middle (M)
apoptotic index (%)
0
5
10
15
20
25
30
35
L1
L2
L3
L4
L5
Level of foregut

6.2.1.3 - Patterns of PCD in models of abnormal tracheo-oesophageal development

PCD in the foregut of Adriamycin-treated embryos

The analysis of PCD patterns in Adriamycin-treated E10.5 embryos is complicated by the fact that all treated embryos at this stage share the same morphology. As discussed in previous chapters, the foregut at this stage is still normally undivided in CBA/Ca embryos. A proportion of E10.5 Adriamycin-treated embryos subsequently fail to divide their trachea and oesophagus whilst others undergo normal tracheo-oesophageal separation. Consequently, if PCD is related to tracheo-oesophageal separation, contrasting PCD patterns might be expected within a group of morphologically indistinguishable E10.5 Adriamycin-treated embryos.

At the level of the pharynx, PCD marks the boundary between pharyngeal epithelium and the epithelium of pharyngeal pouch derivatives (Fig. 6.1c). In the same sections, PCD is seen at the site of the midline thyroid primordium (Fig. 6.1c inset). This pattern was seen in 6 out of 6 Adriamycin-treated embryos examined. Further caudally, PCD was seen in the ventral epithelium of the laryngotracheal groove (as also seen in saline-control embryos) in 4 out of 6 embryos examined (Fig. 6.1e). Caudal to the laryngotracheal groove, only one out of six Adriamycin-treated embryos exhibited the pattern of PCD clusters marking the dorsoventral boundary. In contrast, this PCD localisation was seen in 5 out of 7 saline-control embryos. Embryos were judged to exhibit this pattern if apoptotic cells were found at equivalent points on opposite sides of the lateral foregut wall in consecutive sections. Instead, at this level, in Adriamycin-treated embryos, there were individual apoptotic cells at seemingly random points along the foregut dorsoventral axis (Fig. 6.1g). At the level of the emergence of the lung buds, all six Adriamycin-

Fig. 6.6 PCD patterns in affected Adriamycin-treated E11.5 CBA/Ca embryos

PCD patterns are disturbed in Adriamycin-treated embryos in which tracheo-oesophageal separation has failed. Immunohistochemistry for the PCD effector cleaved Caspase-3 on transverse sections of Adriamycin-treated E11.5 CBA/Ca embryos. Sections are from increasingly caudal levels with (a) at the level of the laryngotracheal groove (Lt) and (d) at the level of the lung buds (Lb). ***(a)*** At the level of the laryngotracheal groove, PCD distribution is comparable to saline control embryos (see Fig. 6.2b) with apoptosis in the ventral epithelium of the groove. ***(b)*** At more caudal levels, the dorsal PCD shift seen in normal development (Fig. 2c,d) is absent and clusters of apoptotic cells are found at various points along the dorsoventral axis of the foregut (arrowheads, inset – separate embryo). ***(c)*** As the level of the lung buds is approached, apoptosis appears to be restricted to the dorsal-most part of the undivided oesophagotrachea (Oet). ***(d)*** At the level of the lung buds, the undivided foregut ends in a trifurcation of two buds and the fistula (Fi) to the stomach. At this level, epithelial PCD is found at the lung bud boundaries (arrow). A concentration of apoptotic cells is also found in the mesenchyme, dorsal to the undivided foregut and appears to be associated with an area of mesenchymal cell condensation (arrowhead). Scale bar, 50 μm

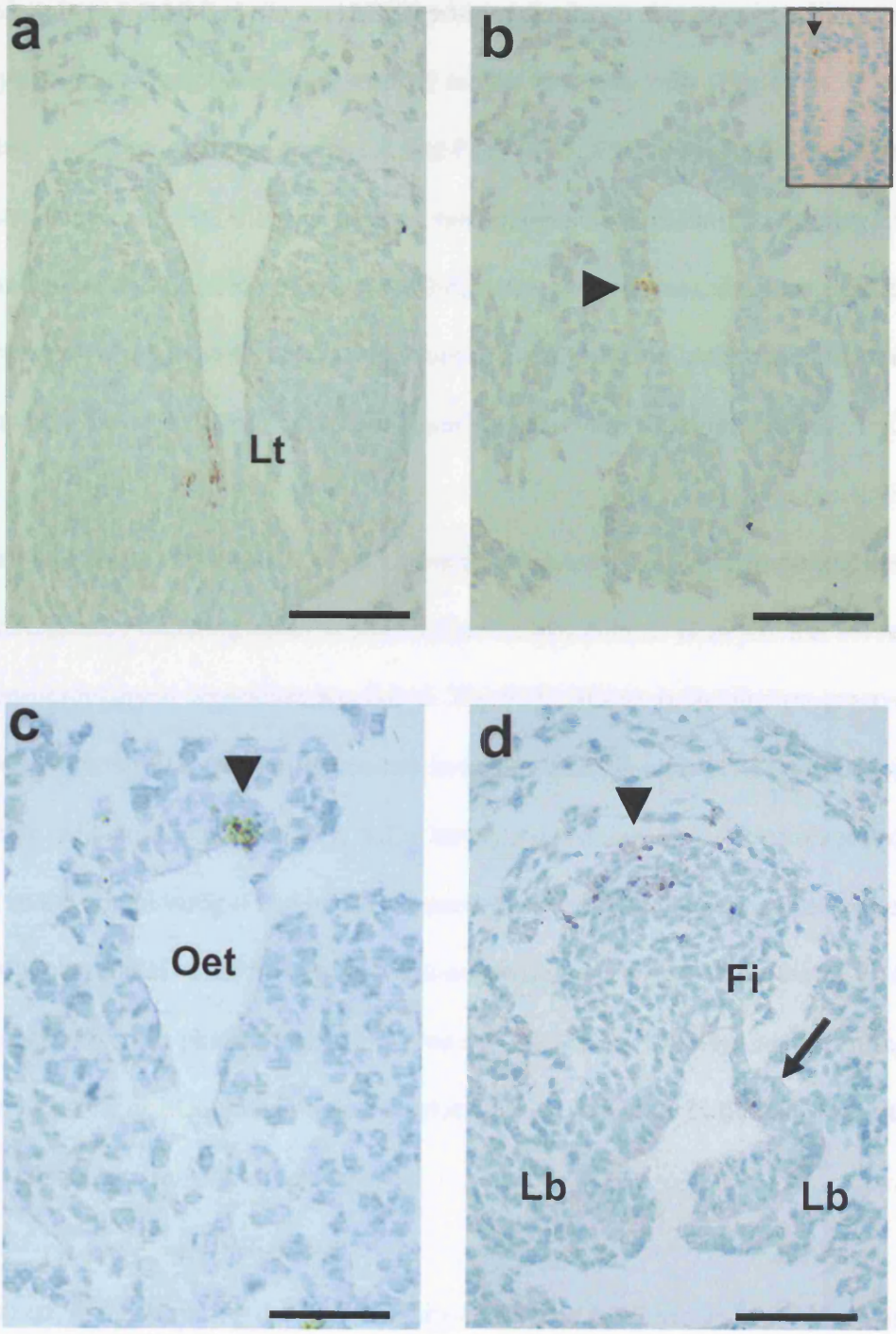
a
Lt
b
c
Oet
d
Fi
Lb
Lb

treated embryos exhibited a ventral PCD pattern similar to that seen in saline-control embryos with the lung buds being marked out by apoptotic cells (Fig. 6.1i). In contrast, only two out of six embryos examined had PCD in the dorsal foregut in a pattern similar to control embryos (Fig. 6.1h). As I have speculated above, these clusters may represent the caudal-most limit of the dorsoventral boundary. In summary, the aspect of PCD patterning affected by Adriamycin exposure appears to be the marking of the dorsoventral boundary, with the lung bud and pharyngeal patterns seemingly unaffected.

Adriamycin-treated embryos at E11.5 broadly fall into two groups; those that are morphologically indistinguishable from saline-treated control embryos and those in which tracheo-oesophageal separation has failed. The PCD pattern in the former group (*data not shown*) is very similar to the pattern seen in saline-treated controls. In the anterior foregut, apoptotic cells are found ventrally, in the laryngotracheal groove. More caudally, they are found in the dorsal foregut and become concentrated in the approximating epithelial folds immediately cranial to the level of tracheo-oesophageal separation. At more caudal levels, some apoptotic cells persist in the separated oesophagus with the trachea showing increased levels of PCD in its medial third immediately cranial to the level of bifurcation of the trachea into the two main bronchi.

In contrast, the pattern in Adriamycin-treated embryos that have an undivided foregut is disturbed compared to saline-treated control embryos and to Adriamycin-treated embryos with normal tracheo-oesophageal separation. PCD is still visible in the foregut but its spatial distribution is different. At the cranial end of the respiratory foregut, PCD is seen in the ventral epithelium of the laryngotracheal groove in a pattern similar to controls (Fig. 6.6a). Further caudally, no clear dorsal shift of apoptotic cells is seen but rather occasional PCD clusters are found at various points along the dorsoventral foregut axis

(Fig. 6.6b). Direct, level to level comparison is difficult between the undivided Adriamycin-treated foregut and the divided foregut of saline-treated controls due to the lack of a tracheo-oesophageal separation point to be used as a reference and this limitation has to be taken into account when interpreting the more caudal patterns. Further caudally, the most striking feature in the undivided foregut is the lack of PCD in the middle segment (as defined for quantitative analysis) (Fig. 6.6c). In contrast, there is a concentration of PCD clusters in the dorsal-most foregut epithelium that persists almost to the level of the trifurcation or proximal fistula formation (Fig. 6.6c). In embryos that have a proximal fistula originating from the foregut above the level of the lung buds, this cluster appears to be associated with the origin of the fistula. Another concentration of apoptotic cells is also seen in the mesenchyme dorsal to the undivided foregut (Fig. 6.6d). This cluster is associated with a distinct arrangement of mesenchymal cells I have already noted in Chapter 1. This arrangement consists of cells in concentric circles strongly resembling a structure whose lumen has become obliterated. The PCD clusters in the dorsal-most foregut epithelium and the dorsal mesenchyme do not appear to be related to one another. At the level of the trifurcation, PCD cells are found at the junction of the lung buds and the foregut. This pattern is very similar to the E10.5 PCD pattern of control embryos at the level of the physiological trifurcation. In summary, the disturbance in PCD pattern in Adriamycin-treated embryos with defective tracheo-oesophageal separation mainly affects the 'marking' of the dorsoventral boundary within the foregut.

PCD in the foregut of *Shh*$^{-/-}$ embryos

Analysis of PCD patterns in all embryos with the *Shh* background is complicated by the discrepancy in developmental stages with the CBA/Ca mice as described in previous chapters. The key gestation for the *Shh* mice, in terms of tracheo-oesophageal

Fig. 6.7 PCD patterns in the foregut of E10.5 *Shh* null-mutant embryos

PCD patterns are disturbed in the foregut of *Shh* null mutant embryos. Immunohistochemistry for the PCD effector cleaved Caspase-3 on transverse sections of E10.5 *Shh* null embryos taken at levels indicated in the schematic representation of the foregut (Fo) in (a). **(*b*)** The narrow, post-pharyngeal undivided foregut has no significant PCD in sharp contrast to the high levels of apoptosis in the ganglion-like structures in the dorsal mesenchyme. **(*c*)** At the level of emergence of the lung buds (Lb), the undivided foregut ends in a trifurcation of a fistula (Fi) and two, abnormally fused, buds. Apoptosis is absent from the foregut at this level in sharp contrast to the significant apoptotic activity seen in the neural tube (arrow, inset). Scale bar, 50 μm

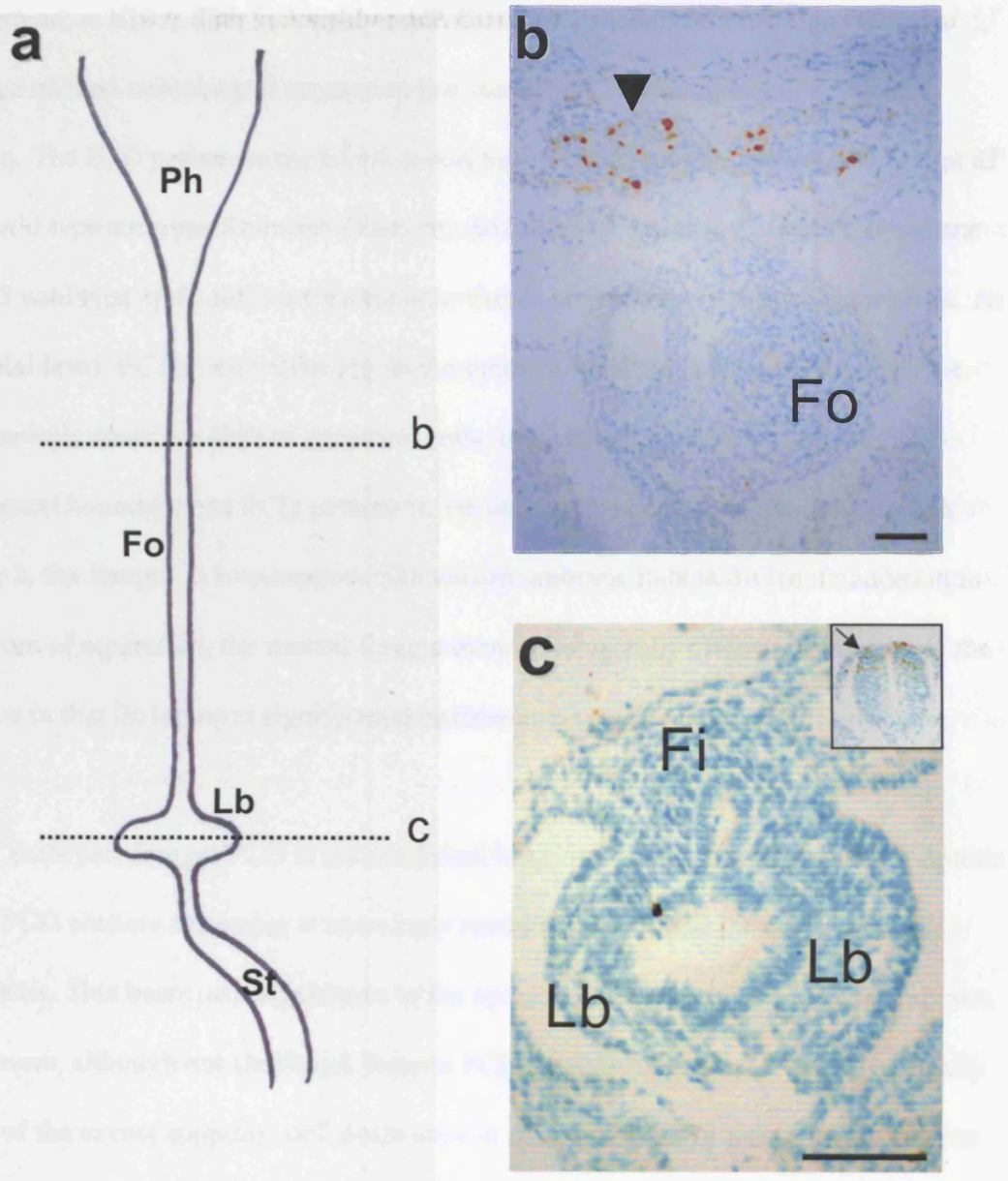
a
Ph
b
Fo
Lb
c
St
b
Fo
c
Fi
Lb
Lb

development, is E10.5. This is roughly equivalent to E11 for the CBA/Ca strain and at this stage tracheo-oesophageal separation has started and is proceeding in a cranial direction. The PCD pattern in the E10.5 homozygous mutants was contrasted with that of E10.5 wild type embryos from *Shh* litters (*pooled* $Shh^{+/+,+/-}$ embryos) . The PCD pattern of E10.5 wild type embryos is very similar to that seen in the E11.5 CBA/Ca embryos. At the cranial level, PCD is seen ventrally in the epithelium of the laryngotracheal groove. More caudally there is a shift of apoptotic cells to the dorsal epithelium and the dorsoventral boundary and PCD persists in the separated oesophagus. As discussed in Chapter 3, the foregut in homozygous *Shh* mutant embryos fails to divide. In addition to this failure of separation, the mutant foregut is morphologically different from that of the wild type in that its lumen is significantly narrower, especially in its middle part.

In $Shh^{-/-}$ embryos, foregut PCD is not abolished but is represented by occasional apoptotic cells or PCD clusters appearing at seemingly random points along the dorsoventral foregut axis. This bears no resemblance to the specific pattern seen in wild type embryos. Furthermore, although not abolished, foregut PCD appears markedly reduced, especially in view of the excess apoptotic cell death seen in other parts of the ailing $Shh^{-/-}$ embryos (Fig. 6.7b). Further caudally, the undivided foregut in null mutant embryos ends in a trifurcation of two fused bronchopulmonary buds and a fistula to the stomach. At this level, there are no PCD clusters marking the boundary between the foregut and the bronchopulmonary buds, nor are there apoptotic cells marking the boundary between the two buds (Fig. 6.7c). This contrasts not only with the pattern seen in wild type embryos and CBA/Ca saline-treated controls (at E10.5) but also with Adriamycin-treated CBA/Ca embryos. This probably reflects the extent of foregut malformations in the null mutant embryos; apart from the failure of tracheo-oesophageal separation, bronchopulmonary

development is also markedly abnormal with persistent lung fusion and persistent communication between the fused lung structures and the distal oesophagus/ fistula.

6.2.2 – Cell proliferation in the developing foregut

6.2.2.1 - Patterns of mitosis during normal foregut development

Proliferation was studied by looking at the level of mitotic activity, both in the foregut epithelium and mesenchyme. I calculated the percentage of cells staining positive for the mitotic marker phosphohistone H3 (i.e. the mitotic index).

Defining the anatomical levels for the study of mitotic index

I collected data for calculation of mitotic index from one section at each of four levels of the E10.5 foregut (Fig. 6.8) and seven levels of the E11.5 foregut (Fig. 6.9). At E10.5, the most cranial level was that of the laryngotracheal groove and the most caudal level was that of the lung buds. Two more intermediate levels were placed at regular intervals, according to number of sections and about 60 to 70 micrometres apart, along the anteroposterior axis of the foregut. . The inclusion of an additional intermediate level, compared to the PCD study, aimed to enhance the comparison between ventral and dorsal mitosis at E10.5. At E11.5, mitotic index data were collected at seven levels along the anteroposterior axis of the respiratory foregut (Fig. 6.9). Five of the seven levels used in the mitotic index study were the same as those used for the study of the apoptotic index. This allowed for direct comparison between mitotic and apoptotic activity for those levels. The difference in two of the levels reflects the fact that the two experiments address somewhat different aspects of tracheo-oesophageal development. The levels for the mitotic study were more evenly spaced along the AP axis of the respiratory foregut whereas more levels were studied for

apoptosis cranial to the point of separation, reflecting the dynamic nature of the PCD pattern in this part of the foregut.

Defining the dorsoventral segments for the study of mitotic index

At E10.5, I aimed to test the hypothesis that the respiratory part of the foregut has a higher rate of proliferation than the gastrointestinal part. Such a difference could account for the development of the trachea as a separate structure from the oesophagus (as discussed in Chapter 3). At each level, the foregut epithelium was divided for analysis into dorsal and ventral parts. At levels 1,2 and 3, this distinction corresponded to the dorsal and ventral halves of the foregut whereas at level 4, the ventral part comprised the lung buds (Fig. 6.8). At E10.5, the gastrointestinal/ respiratory boundary in the foregut roughly corresponded to the midway point along the dorsoventral axis. As there are no morphological pointers to this boundary at this gestation (no *waist*), the separate analysis of two dorsoventral halves of the foregut (*for levels 1-3*) appeared to be a satisfactory method of study.

At the E11.5 stage, I wanted to investigate whether differential epithelial proliferation contributes to tracheo-oesophageal separation. Specifically, I wanted to test the hypothesis that epithelial proliferation contributes to the appearance of the ingrowing epithelial ridges seen at levels cranial to the separation. For this reason, the foregut was divided for analysis into equal ventral and dorsal parts and the dorsal part was subdivided into two equal parts (as for the study of PCD) (Fig. 6.9). The middle part corresponded to the site of tracheo-oesophageal separation in the vast majority of sections (*see PCD section*). At the same levels (2&3), I also wanted to study the role of the mesenchyme in tracheo-oesophageal separation. I wanted to test the hypothesis that extrinsic

Fig. 6.8 Mitotic activity in the foregut of E10.5 CBA/Ca embryos

Immunohistochemistry for the mitosis marker phosphohistone H3 on transverse sections of E10.5 untreated CBA/Ca embryos. Note that epithelial cells that are H3-positive are easily identifiable in these sections. The mitotic index represents the proportion of cells in a specified part of the epithelium that are H3-positive. The schematic representation of the E10.5 foregut (Fo) indicates the levels at which sections were studied in order to calculate the epithelial mitotic index. Level 1 is at the level of the laryngotracheal groove (Lt), level 4 at the level of the emerging lung buds (Lb) and levels 2 and 3 are evenly spaced between the two. For levels 1 to 3, the mitotic index was calculated for equal dorsal and ventral segments whereas at level 4, the ventral segment comprised the lung buds. (*the oblique dividing line reflects the lung bud arrangement in this particular section)* Scale bar, 100 μm

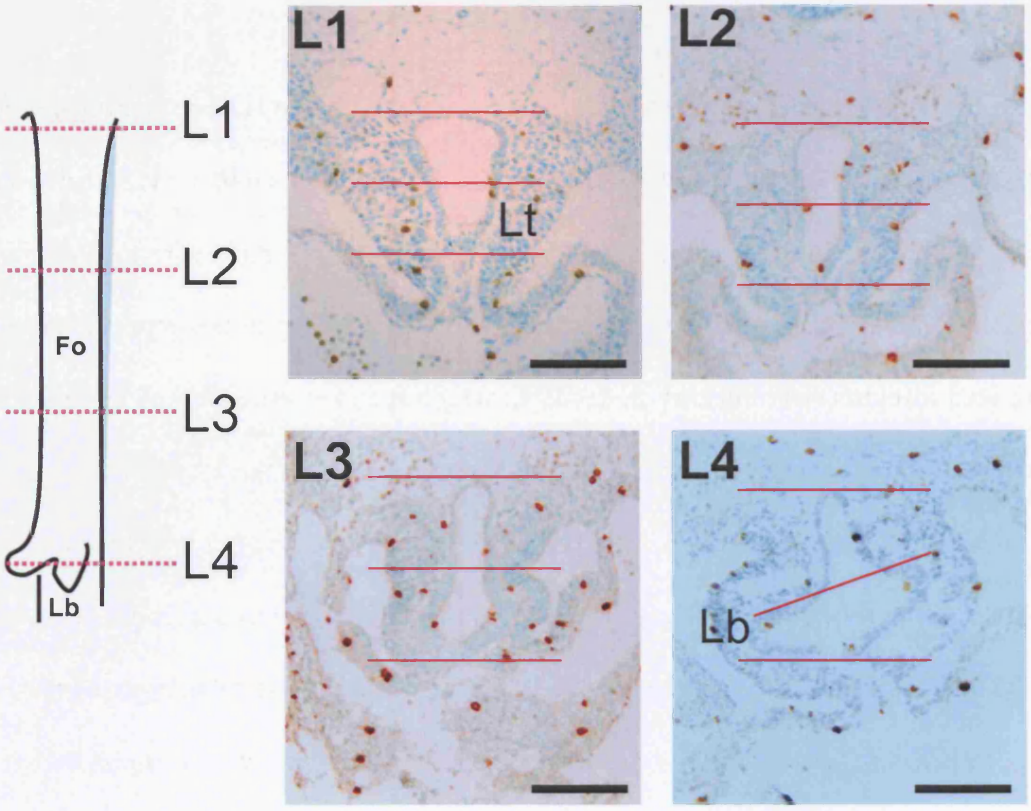
L1
L2
L3
L4
Fo
Lb
L1
Lt
L2
L3
L4
Lb

Fig. 6.9 Mitotic activity in the foregut of E11.5 CBA/Ca embryos

Immunohistochemistry for the mitosis marker phosphohistone H3 on transverse sections of E11.5 untreated CBA/Ca embryos. Note that epithelial and mesenchymal cells that are H3-positive are easily identifiable in these sections. The mitotic index represents the proportion of cells in a specified part of the epithelium or mesenchyme that are H3-positive. Schematic representation of the E11.5 foregut (Fo) indicates the levels at which sections were studied to calculate the epithelial and mesenchymal mitotic index. Level 1 is at the laryngotracheal groove (Lt), level 3 at the tracheo-oesophageal separation and level 2 is intermediate. Level 6 is at the tracheal bifurcation, level 5 is intermediate between 3 and 6 and level 4 is intermediate between 3 and 5. Finally, level 7 corresponds to the level of the separated bronchi (Br) and oesophagus (Oe). For the, as yet, undivided foregut (levels 1-3), the sections were subdivided as for the study of PCD with ventral and dorsal halves for level 1 and one ventral segment and two dorsal (one middle and one dorsalmost) segments for levels 2 and 3. For the calculation of the mitotic index in the bronchopulmonary buds (level 7), the average of the two buds was used. The surrounding mesenchyme was subdivided accordingly, with the width of each mesenchymal area corresponding to the width of the foregut as indicated by the shaded areas at level 3 (*same principle applied to level 2*). The dorsoventral division of the mesenchyme corresponds exactly to that used for the epithelial calculation. Tr – trachea. Scale bar, 50 μm

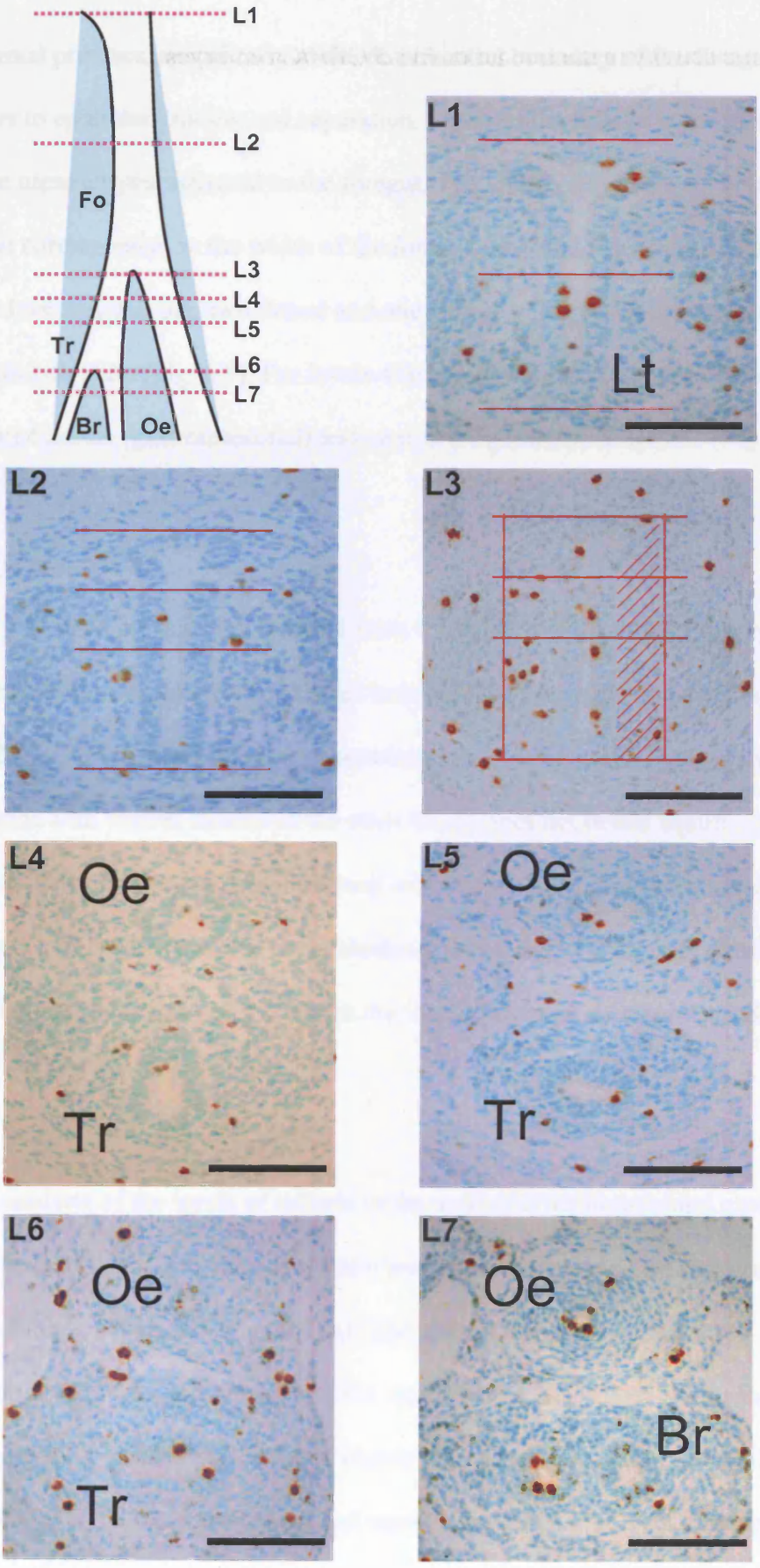
L1
L2
Fo
L3
L4
L5
Tr
L6
L7
Br
Oe
L1
Lt
L2
L3
L4
Oe
Tr
L5
Oe
Tr
L6
Oe
Tr
L7
Oe
Br

mesenchymal pressure, specifically at the dorsoventral boundary of the foregut, contributes to epithelial folding and separation. I studied the mitotic index in a defined area of the mesenchyme adjacent to the foregut. The width of this area on either side of the foregut corresponded to the width of the foregut itself and the mesenchymal area was subdivided for analysis into two dorsal and one ventral part, precisely corresponding to the epithelial division (Fig. 6.9). For levels 4 to 7, I compared the mitotic index between the separated dorsal (gastrointestinal) and ventral (respiratory) structures (Fig. 6.9).

Data analysis

At E10.5, the mean mitotic index ranged from 7% to 14 % with no statistically significant differences between the ventral and dorsal halves of the foregut at all levels studied (Table 6.2, Fig. 6.10). Furthermore, comparison between ventral mitosis at the level of the lung buds with ventral mitosis at the other levels does not reveal significant differences. This observation is inconsistent with the notion of the ventral foregut growing at a higher rate resulting in the trachea developing as a separate structure. The dorsal mitotic index is also comparable at the four levels with no significant difference detected.

At E11.5, analysis of the levels of mitosis in the separated respiratory and gastrointestinal structures reveals that this is increased compared to the corresponding sections of the undivided foregut (Table 6.3, Fig. 6.11a). The mitotic index at levels 6 and 7 is as high as 42% for the oesophagus and as high as 36% and 38% for the trachea and bronchi. The respiratory mitotic index is significantly higher at levels 6 and 7 compared to level 2 (p values of 0.002 and 0.02 respectively) and significantly higher at level 6 compared to level 1 (p=0.02). The dorsal mitotic index at levels 6 and 7 is significantly higher than the index at both level 1 (p values of 0.002 and 0.007 respectively) and level 2 (p values of

0.002 and 0.007 respectively). On the other hand, there is no significant difference in mitotic index between the trachea/ bronchi and the oesophagus, or between the ventral and dorsal halves of the undivided foregut, at any of the levels studied (Fig. 6.11a). These observations suggest that following separation, increased proliferation could account for the rapid longitudinal growth of both the trachea and the oesophagus, although the two structures appear to grow at comparable rates. Mitosis in the middle foregut section at levels 2 and 3 (undivided) is not significantly different from either the dorsal-most or ventral sections (Table 6.3, Fig. 6.11b). This suggests that localised peaks of proliferation are unlikely to account for the infolding epithelium at the site of future tracheo-oesophageal separation. However, mitotic index in the middle section was significantly greater at the level of separation (level 3) compared to level 2 (p=0.049). This could reflect the general trend of increase in epithelial proliferation at increasingly posterior levels (Fig. 6.11a).

The study of mesenchymal proliferation revealed no significant differences between the index for the middle segment and either the dorsal-most or ventral parts at both levels 2 and 3 (Table 6.3, Fig. 6.12). This observation does not support the notion that differential mesenchymal proliferation could account for the change in the configuration of the foregut (infolding/ waist formation) at the different levels. The mesenchymal mitotic index is, however, significantly increased in the middle segment at level 3 compared to level 2 (p=0.045), mirroring the epithelial proliferation for that segment.

Table 6.2. Numbers of mitotic (H3 positive cells), total cells and mitotic index in the normal E10.5 CBA/Ca foregut

		Mean (Standard deviation)		
		H3-positive cells	Total cells	Mitotic index (%)
Level 1 (n=9)	Dorsal	7.2 (4.5)	58.7 (13.9)	13.7 (11.9)
	Ventral	9.1 (2.8)	74.7 (16.8)	13.0 (5.6)
Level 2 (n=9)	Dorsal	5.9 (3.4)	65.8 (14.7)	9.5 (6.2)
	Ventral	5.7 (3.4)	72.8 (20.6)	8.6 (6.8)
Level 3 (n=9)	Dorsal	5.6 (2.9)	70.8 (15.5)	7.2 (3.4)
	Ventral	10.0 (4.6)	109.1 (20.1)	8.3 (2.3)
Level 4 (n=8)	Dorsal	7.0 (3.2)	78.5 (29.2)	10.3 (5.1)
	Ventral	11.1 (3.2)	122.5 (28.6)	10.2 (3.7)

Table 6.3. Levels of mitosis (H3 positive cells) in the normal E11.5 CBA/Ca foregut

			Mean (Standard Deviation)		
			H3-positive cells	Total cells	Mitotic index (%)
Level 1	Epithelium	Dorsal half	6.1 (3.3)	72.5 (26)	8.6 (4.1)
(n=10)		Ventral half	7.3 (10)	68.2 (27.8)	9 (7.5)
Level 2	Epithelium	Dorsal half	5.6 (4)	92.5 (18.1)	6.6 95.8)
(n=10)		Dorsal-most	3.1 (2.5)	45.7 (11.8)	7.5 (7.1)
		Middle	2.5 (1.6)	45.8 (8.1)	5.7 (4.8)
		Ventral half	4.6 (3)	80.1 (21)	6.7 (5.8)
	Mesenchyme	Dorsal-most	5 (3.6)	82.2 (31.1)	7.2 (5.3)
		Middle	5.9 (5.7)	110.1 (56)	5 94.2)
		Ventral half	16.3 (12.2)	273.9 (129.4)	5.7 (2.3)
Level 3	Epithelium	Dorsal half	13.1 (10.1)	102.2 (21.9)	12.9 (8.5)
(n=10)		Dorsal-most	6.8 (5)	53 (16.6)	13.1 (9.5)
		Middle	6.5 (5.4)	48.2 (9.1)	12.9 (9)
		Ventral half	11.8 (9.6)	97.3 (31.8)	11.5 (6.7)
	Mesenchyme	Dorsal-most	5.8 (4.6)	104.9 (46.3)	6.3 (5.6)
		Middle	9.2 (5.3)	104.6 (40.1)	9.7 (7.2)
		Ventral half	18.2 (13.3)	277.2 (103.3)	6.1 (3)
Level 4	Epithelium	Oesophagus	9.4 (5)	55.6 (15.6)	18.1 (9.3)
		Trachea	9.8 (4.3)	83.3 (46.7)	13.8 (8.3)
Level 5	Epithelium	Oesophagus	7.7 (3.5)	52.3 (14.6)	14.7 (5.4)
		Trachea	8.5 (5.4)	70.8 (18.1)	11.6 (6)
Level 6	Epithelium	Oesophagus	4.4 (1.4)	21.5 (8.3)	22.4 (10.6)
		Trachea	15.5 (10.2)	78.2 (21.5)	20.4 (11.7)
Level 7	Epithelium	Oesophagus	3.9 (2)	18.8 (5.9)	23.5 (13.6)
		Buds, average	10.3 (7)	59.3 (19.5)	19 (14.1)

Fig. 6.10 Dorsoventral distribution of mitosis in E10.5 control CBA/Ca embryos

Mitotic index for the dorsal and ventral segments of the E10.5 foregut. Levels and segments are defined in Fig. 8. There is no significant difference between the index of the dorsal and ventral segments at any of the four levels. Furthermore, there is no significant difference between the ventral index at the level of the lung buds and that of the other three levels.

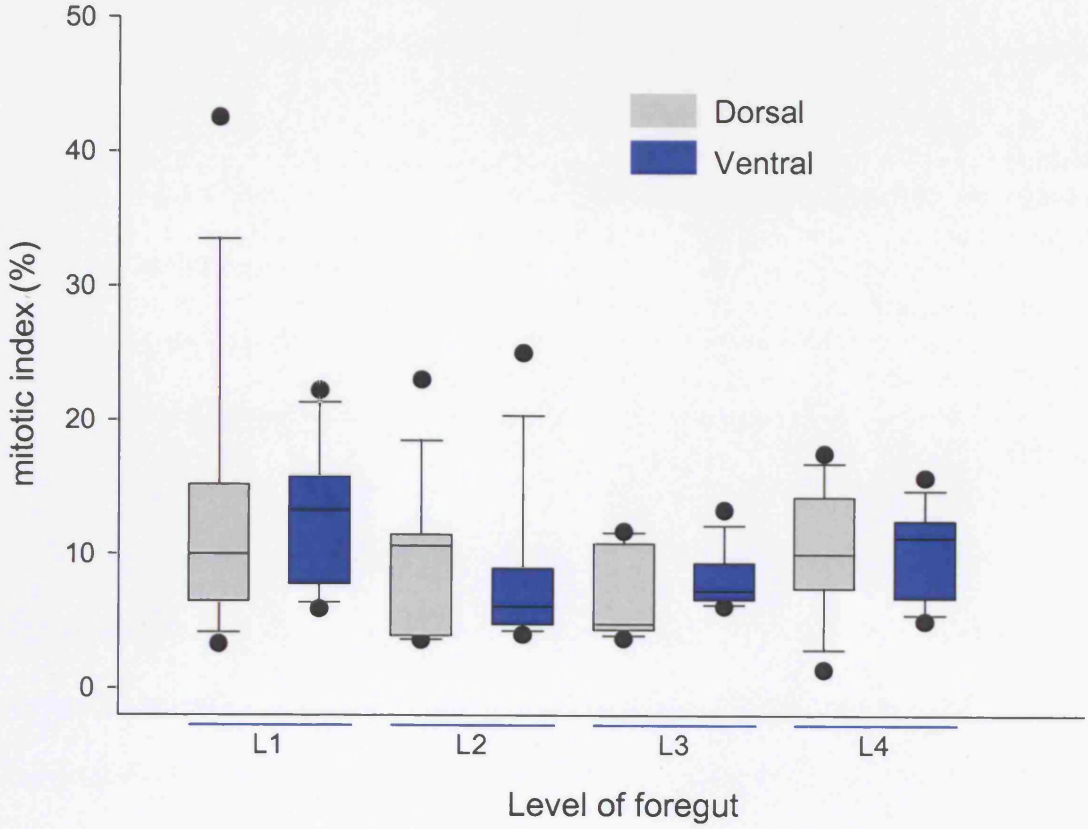
50
40
30
20
10
0
mitotic index (%)
Dorsal
Ventral
L1
L2
L3
L4
Level of foregut

Fig. 6.11 Dorsoventral distribution of epithelial mitosis in E11.5 control CBA/Ca embryos

Mitotic activity in the E11.5 foregut with levels as defined in Figure 9. ***(a)*** In this graph, the mitotic index was calculated separately for the ventral and dorsal halves at all levels, not taking into account the subdivision of the dorsal segment. There is no significant difference between the ventral and dorsal mitosis at each of the seven levels. There is, however, a gradual increase in mitotic index in more caudal sections and the separated structures have significantly higher mitotic indices than the corresponding segments of the undivided foregut. The tracheal index (level 6) is significantly higher than the ventral index for both levels 1 and 2 (p values of 0.02 and 0.002) and the bronchial index (level 7) is significantly higher than the ventral index for level 2 (p=0.02). The oesophageal index for levels 6 and 7 is higher than the dorsal index for levels 1 and 2 (p values of 0.002, 0.002, 0.007 and 0.007). ***(b)*** In this analysis, the dorsal half is represented by equal dorsalmost (L2Ds & L3Ds) and middle segments (L2M & L3M) as described in Figure 9. At each of the two levels, middle segment mitotic indices did not differ significantly from either dorsal or ventral ones. The middle segment index was higher at the level of separation (level 3) than at level 2 (p=0.049). The higher mitotic rate at this level is in keeping with the general trend of increase in mitotic index at more caudal levels as shown in (a).

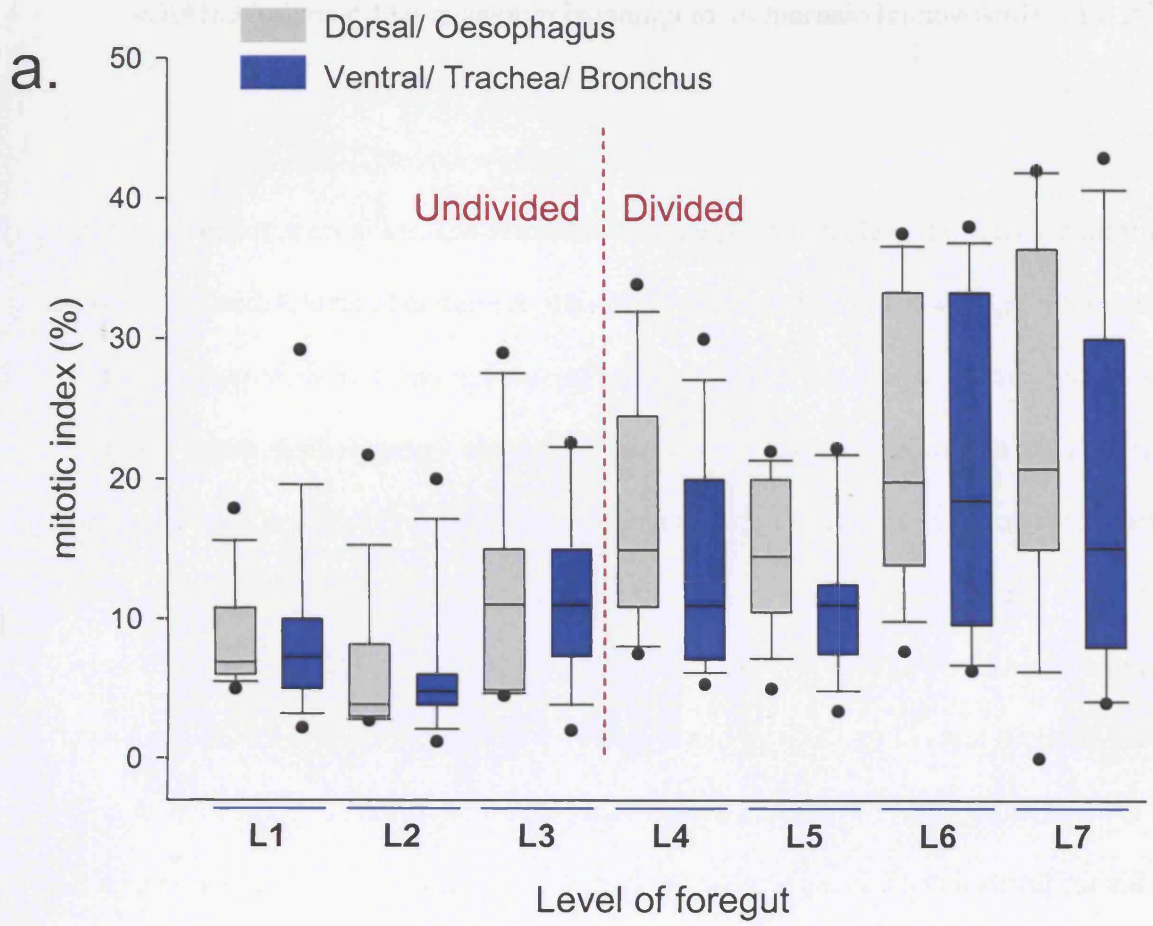
a.
Dorsal/ Oesophagus
Ventral/ Trachea/ Bronchus
Undivided
Divided
mitotic index (%)
0
10
20
30
40
50
L1
L2
L3
L4
L5
L6
L7
Level of foregut

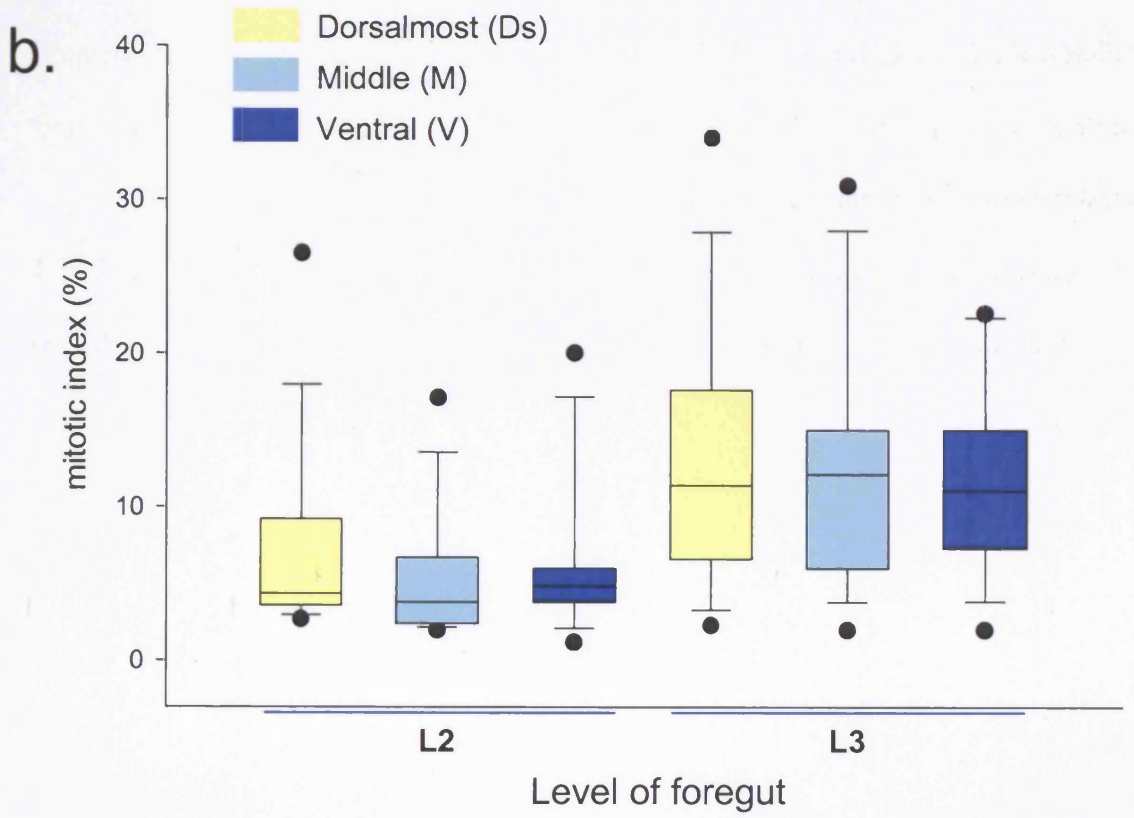
b.
Dorsalmost (Ds)
Middle (M)
Ventral (V)
mitotic index (%)
0
10
20
30
40
L2
L3
Level of foregut

Fig. 6.12 Mesenchymal mitosis in E11.5 control CBA/Ca embryos

Mitotic activity in the foregut mesenchyme at or above the level of tracheo-oesophageal separation. Levels as for figure 9 with the dorsal segments being represented here by both dorsalmost (L2Ds & L3Ds) and middle (L2M & L3M) subdivisions as shown in figure 9. At each of the two levels, the mitotic index of the middle segment is not significantly different from either the dorsalmost or ventral segments. The middle segment mesenchymal mitosis is, however, significantly higher at level 3 than at level 2 (p=0.045).

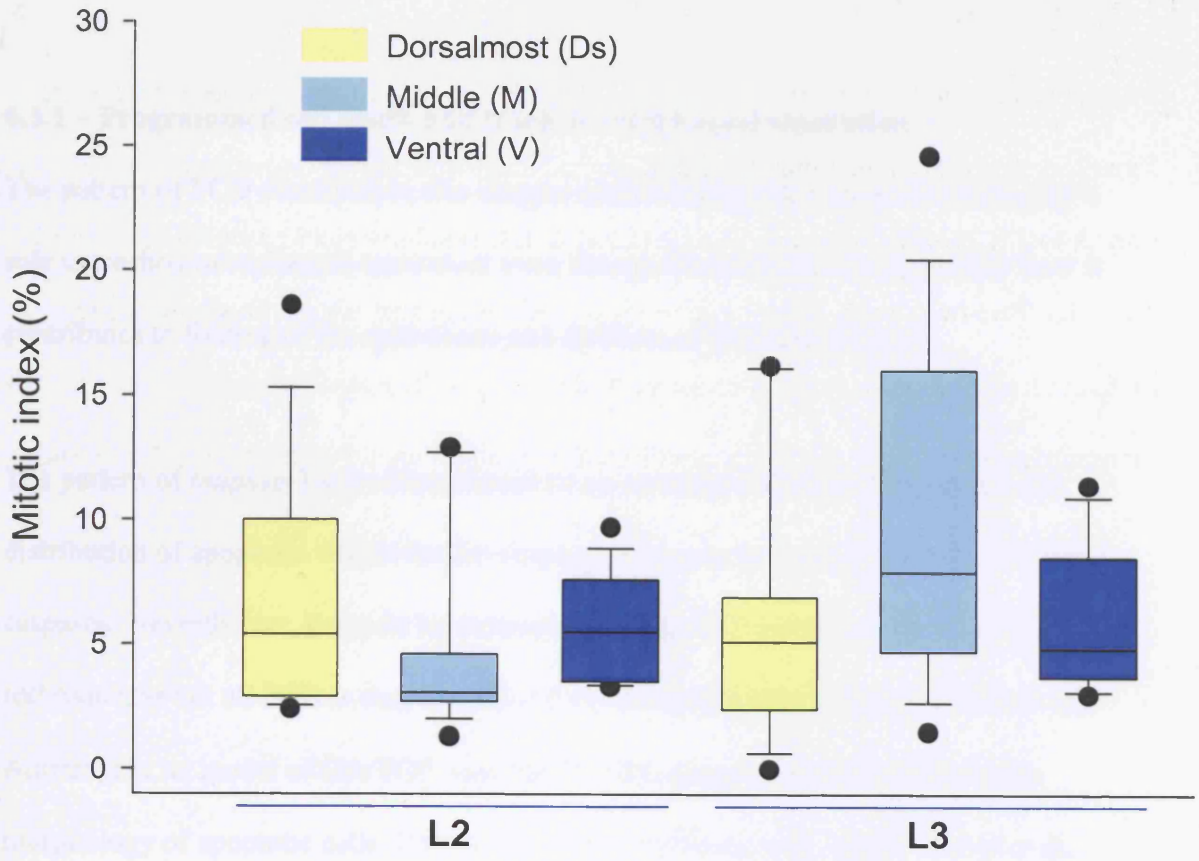
Dorsalmost (Ds)
Middle (M)
Ventral (V)
Mitotic index (%)
30
25
20
15
10
5
0
L2
L3

6.3 – DISCUSSION

6.3.1 – Programmed cell death and tracheo-oesophageal separation

The pattern of PCD described in this chapter makes it likely that apoptosis does play a role in tracheo-oesophageal separation even though it remains unclear precisely how it contributes to folding of the epithelium and division of the foregut lumen.

The pattern of caspase-3 activation should be an accurate reflection of the level and distribution of apoptosis within the developing foregut as it is one of the key effector caspases. Nevertheless, it would be desirable to study PCD patterns with a different technique, as not all PCD is caspase-dependent. Several studies of foregut PCD in the Adriamycin rat model of OA/TOF used the TUNEL assay or simply identified the morphology of apoptotic cells (Zhou et al., 1999; Williams et al., 2000; Orford et al., 2001b). These studies identified only a limited role for PCD, finding apoptotic cells solely in the epithelial ridges of the separating foregut in saline-treated embryos. The fact that the caspase-3 assay has identified a more extensive pattern of PCD makes it very unlikely that it is missing any significant number of apoptotic cells. The difference between PCD detected by TUNEL and caspase-3 could be attributed to a species difference (all previous studies were of rat) in overall level of PCD. A difference in sensitivity between TUNEL and caspase-3 is an unlikely explanation as TUNEL detects DNA fragmentation and should show more PCD than caspase-3 immunohistochemistry. Another possible explanation is that the majority of rat studies investigate PCD only at the time of tracheo-oesophageal separation and at the site of separation. The only rat study that specifically comments on PCD patterns in pre-separation gestations and at anatomical levels other than that of the separation, does not even explain how apoptosis

was detected making it difficult to assess the findings and compare the patterns (Williams et al., 2000).

6.3.1.1 – PCD and tracheo-oesophageal separation in the E11.5 foregut

According to the rat studies, the localisation of PCD in the approximating epithelial folds is an indication that it is contributing to the division and reshaping of the foregut. As these ridges come together at the point of separation, some of the apoptotic cells from the original undivided foregut would then become localised in the intervening mesenchyme. Such cells are also demonstrated in the present study and could correspond to apoptotic cells seen at the folding epithelial ridges, at levels cranial to the point of separation.

Whilst PCD is likely to contribute to the remodelling of the separated trachea and oesophagus, its role may be more complicated as suggested by the extensive PCD pattern in this study. An observation that is perhaps difficult to explain is the dorsal predominance of PCD in the foregut cranial and caudal to the separation point in the E11.5 foregut. Apoptotic cells in the folding epithelial ridges at the point of separation are associated in the same sections with apoptotic cells in the dorsal, prospective-oesophageal foregut but not in the ventral, prospective-tracheal foregut. Dorsal PCD cannot be simply explained on the basis of cell loss leading to reorganisation and separation, as perhaps is the case for apoptosis at the dorsoventral boundary. This dorsal predominance appears to occur in an organised manner in the E11.5 mouse foregut. Just caudal to the laryngotracheal groove, PCD in the dorsal epithelium clearly predominates with PCD in the ridge epithelium becoming more prominent as we approach the separation level. It appears that in this context, PCD is somehow marking the dorsal foregut components just as the separation process is progressing in a cranial direction. Much more than just finishing off separation, PCD would appear to correlate with the process and its progress.

The persistence of PCD in the separated oesophagus for some distance caudal to separation, is consistent with this notion. Tracheo-oesophageal separation would seem to be a process of separating the PCD-marked dorsal foregut from the largely PCD-free ventral foregut. Such a notion would perhaps require PCD to be able to alter the shape of the foregut or to lead to epithelial folding, in preparation for separation. Folding would be equivalent to a change in the shape of a number of cells in a specific part of the epithelial layer of the foregut. These cells are likely to be those at, and adjacent to, the site of future separation. Shape change is likely to depend on a change in the ratio between the basal and luminal diameters of the cell and this in turn would require a rearrangement of the cytoskeleton. There has been a recent report linking cells in the early stages of PCD with signals to neighbouring cells that cause changes in the arrangement of actin microfilaments (Rosenblatt et al., 2001). If this was the case in the foregut, it would imply that PCD has, at least at the initial stages, a signaling role. This notion could help explain the paradox of accumulation of PCD in the dorsal, oesophageal-prospective endoderm well away from the site of separation. A change in the shape of cells in the shorter dorsal part might contribute more effectively to folding. I have yet to demonstrate such a change in epithelial cell shape; electron microscopy assessment would be useful in this aspect.

6.3.1.2 - PCD in the caudal foregut at E11.5

The role of PCD in foregut morphogenesis is further illustrated at more caudal levels of the E11.5 foregut. The dorsal pattern described above gradually gives way to a specific tracheal pattern of apoptosis. The trachea changes shape as the tracheal bifurcation is approached, becoming narrow dorsoventrally and wider form side to side. There is increasing PCD in the mid-portion of the trachea at the point where the epithelium appears to fold leading to the eventual separation into the two bronchi. This arrangement is similar to that associated with tracheo-

oesophageal separation and provides further evidence of the role of PCD in the processes of luminal separation in the respiratory tract. This pattern of PCD at the site of tracheal separation remains prominent at E12.5, but then becomes significantly downregulated with almost no PCD in the E13.5 foregut. One important distinction should be made, however. The pattern seen in the caudal trachea is specific to the point of tracheal bifurcation into the bronchi in contrast to the undivided foregut where it involves the whole dorsal foregut cranial to the separation. Furthermore, there is no evidence that tracheal separation is progressing cranially in any way similar to tracheo-oesophageal separation. Besides, the two lung buds are distinct structures as early as E10.5. In this case, PCD is likely to be involved in the process of shaping the area of the tracheal carina (tracheal bifurcation) as well as the separation of the cranial end of the bronchi. At the same time, longitudinal growth of the bronchopulmonary buds is likely to be the major contributor to bronchial lengthening.

6.3.1.3 - PCD in the pre-separation foregut (E10.5)

A major difference between the present study and previous PCD studies in the rat is that the latter did not demonstrate an apoptotic pattern in the pre-tracheo-oesophageal separation foregut (Qi & Beasley, 1998; Zhou et al., 1999; Williams et al., 2000; Orford et al., 2001b). It should be noted that only one of these studies includes an assessment of the relevant pre-separation gestations (Williams et al., 2000). The present study has identified a distinct pattern in the E10.5 foregut. At that gestation, the ventral part of the foregut has already been specified as respiratory epithelium and is already expressing different markers (e.g. *Nkx2.1*) from the dorsal epithelium. The foregut has, however, not started to divide

physically. At this stage, PCD becomes organised in clusters on the lateral walls of the foregut and on many occasions these clusters are found on corresponding positions on the opposing walls. It is likely these are marking the foregut dorsoventral boundary although more detailed double labelling studies are required to confirm this. It should be noted that at this gestation there is no demonstrable change in foregut shape, and no formation of a waist to indicate the precise dorsoventral or oesophageal-respiratory boundary. This concentration of apoptotic cells would suggest that PCD plays an early role in marking the site of tracheo-oesophageal separation, well before any morphological evidence of epithelial folding or separation.

This principle is clearly demonstrated in the sections from the level of the lung buds. At that level, there is a reproducible pattern of PCD, which marks the junction between the lung buds and the foregut as well as the junction between the two lung buds. This PCD pattern reflects the development of the lung buds. The lung bud level is also the level at which tracheo-oesophageal separation will start. The apoptotic cells that are involved in tracheo-oesophageal definition and separation are likely to fall into two categories. Firstly, in some embryos at the level of the lung buds, the respiratory epithelium (as judged by *Nkx2.1* expression – Chapter 4) does not extend more dorsally than the junction between the lung buds and the foregut itself. It would seem logical that tracheo-oesophageal separation would start at that point and the PCD activity at that junction could be involved in this process. Secondly, the foregut specification in some embryos is such that respiratory epithelium does extend more dorsally and consequently the respiratory/ gastrointestinal junction is shifted more dorsally due to natural variation. This could account for the dorsal PCD clusters seen in some embryos in

addition to the ones related to the lung buds (Fig. 6.1h arrows). It could also be significant that the more consistent PCD pattern is seen at the lung bud level where the process of tracheo-oesophageal separation is starting. In summary, the E10.5 PCD pattern in the foregut is consistent with the notion of the apoptotic cells defining the borders between developing foregut components and derivatives, well before these structures start the process of separating from each other. This argument raises the possibility of PCD being involved in the initiation of the separation process. This question will be addressed in the next chapter.

Cranial to the laryngotracheal groove, the pharynx is characterised by the development of the pharyngeal pouches and their derivatives. PCD is associated with these processes in the present study. Apoptotic cells mark the junction between pharyngeal epithelium and that of the pharyngeal pouches. One explanation is that it could represent the boundary between two epithelial populations that are growing at different rates. Another explanation is that these PCD clusters might be contributing to the separation of these derivatives from the pharyngeal lumen; organs like the thymus and the parathyroids become detached from the pharynx to assume their position in the neck. If that is the case then this would be another example of separation. Epithelial PCD in the third pharyngeal pouch has been shown to be regulated by thymic and parathyroid endodermal transcription factors (*Hoxa3* & *Pax1*) and *Hoxa3*(+/-)*Pax1*(-/-) compound mutants exhibit delayed separation of the thymic and parathyroid primordia from the pharynx (Su et al., 2001). A similar mechanism is possibly involved in the development of the thyroid. The thyroid diverticulum is a ventral, midline outgrowth from the floor of the pharyngeal foregut. As the thyroid gland develops and descends to its final position in the neck, it initially remains attached to the

pharyngeal floor by the thyroglossal duct that subsequently regresses. Apoptosis seen at the site of the thyroid primordium in the present study may be contributing to this separation. Apoptosis in the thyroid primordium during the period thyroid organogenesis has been previously described and is likely to be regulated by the Bax/Bcl-2 system (Sun et al., 2002). Ventral PCD is also detected more caudally in the laryngotracheal groove. It is not clear what morphogenetic process this apoptotic activity might be contributing to. It might reflect an initial burst of proliferation at the early stages of the development of the respiratory primordium (E9.5) even though no such difference in mitotic activity was detected at E10.5.

6.3.1.4 - Defining the PCD pattern

I have already concluded from data in this chapter that the precise temporospatial pattern of PCD in the foregut between E10.5 and E12.5 could play a role in the marking, initiation and execution of tracheo-oesophageal separation, as well as other processes including tracheobronchial development and pharyngeal pouch development. Assuming this is so, we need to understand what cellular/ molecular mechanisms could regulate the PCD pattern and lie upstream to apoptosis in this complex developmental cascade. As apoptotic cells are found in significant numbers at the boundary between two distinct epithelial populations, it would be logical to examine the case for gene expression patterns to be involved in PCD regulation. I have already shown that *Nkx2.1* and *Shh*, genes involved in fate specification and foregut morphogenesis, are both expressed in distinct dorsoventral patterns in the developing foregut. The expression boundary of such genes could provide positional cues to cells committing to the apoptotic process. PCD patterns are dynamic and it seems unlikely that its induction will be associated solely with an expression pattern that does not change during development (e.g. *Nkx2.1*). *Sonic hedgehog*, on the other hand, has a dynamic pattern of expression with a complete

dorsoventral switch in expression between E10.5 and E11.5. Interestingly, the foregut maintains a *Shh* boundary despite the expression reversal. Interestingly, recent studies have linked the induction of PCD with disruptions in gene expression gradients and have called this morphogenetic apoptosis (Adachi-Yamada & O'Connor, 2002). It could also be argued that the PCD pattern broadly follows that of *Shh* expression in the E11.5 foregut. Cranially, the laryngotracheal groove PCD coincides with ventral *Shh* expression. Moving caudally, there is a gradual increase in both dorsal PCD and dorsal *Shh* expression. As discussed in Chapter 5, this reversal of the E10.5 *Shh* pattern appears to be propagated ahead of tracheo-oesophageal separation in a cranial direction. In an analogous, but by no means identical pattern, the pattern of PCD is restricted to the dorsal foregut and the lateral epithelial folds at the dorsoventral junction. It could be argued that *Shh* expression provides positional cues for the activation of the PCD process. This notion would of course imply that *Shh* has a pro-apoptotic role in this particular developmental system. A review of the literature reveals that *Shh* is involved in PCD regulation in a number of systems having either a pro or anti-apoptotic role, depending on cellular context (Oppenheim et al., 1999; Sanz-Ezquerro & Tickle, 2000; Charrier et al., 2001; Yamamoto et al., 2004; Sacedon et al., 2005). Other genes could be involved in PCD regulation and Bax and Bcl-2 expression in the foregut has been shown to be associated with epithelial PCD (Sun et al., 2002).

An alternative explanation is that PCD is not under the precise control of pro-apoptotic signals but rather is the result of mechanical stresses developing at the junction between various parts of the developing foregut that may be growing at different rates. This mechanism could contribute to the separation of foregut components. This could explain the presence of apoptotic cells at the junction between the proliferating epithelium of the pharyngeal pouch derivatives and the epithelium of the pharynx. Whilst this concept

could account for some of the PCD observed in the developing foregut, it cannot explain the presence of apoptosis in the dorsal foregut at E11.5, nor does it explain the clusters of PCD marking the dorsoventral boundary at E10.5, a time when the two parts of the foregut do not differ as far as gross morphology and mitotic index are concerned.

6.3.1.5 - PCD in models of abnormal tracheo-oesophageal separation

The models of abnormal foregut development further highlight the important role of PCD. In both the Adriamycin-treated mouse and *Shh* homozygous mutant models, abnormal development, and failure of tracheo-oesophageal separation in particular, is associated with a disturbed pattern of PCD. Apoptosis still takes place in the abnormally developing foregut in both models but its precise temporospatial pattern is disturbed. At E10.5, the aspect of PCD mostly affected is the marking of the dorsoventral boundary. In the affected E11.5 Adriamycin-treated mouse, there appears to be a shift in the concentration of PCD in the caudal foregut. This results in apoptotic cells concentrating in the dorsalmost part of the foregut, as well as the dorsal mesenchyme, whereas at equivalent levels in the control embryo, PCD is concentrated at the tracheo-oesophageal junction, where separation is occurring. This raises the question whether the fundamental developmental disturbance in the Adriamycin-treated embryos is in the positional information for PCD induction. One previous suggestion is that PCD occurs more dorsally and the result of this is the formation of the atretic upper oesophageal segment (Qi & Beasley, 2000). Some theories suggest that the concentration of apoptotic cells in the mesoderm, dorsal to the undivided foregut in Adriamycin-treated embryos, actually represents the atretic oesophageal segment (Zhou et al., 1999). Other theories suggest that mesodermal apoptosis may be associated with degenerating ectopic notochord and that the fundamental tracheo-oesophageal defect is caused by generally reduced foregut apoptosis (Williams et al., 2000). The findings of my work confirm that the PCD pattern

seen in the Adriamycin-treated mouse embryos undergoes a dorsalward shift but that this is unlikely to be related to the upper oesophageal pouch. This pattern is identified at E11.5 in the mouse whereas the upper oesophageal segment starts developing at E12.5 as a result of reshaping of the cranial foregut. This temporal relationship makes it unlikely that the dorsal mesenchymal apoptosis represents the atretic oesophagus. In the case of the Adriamycin-treated mouse, it is possible that the dorsal PCD shift results in failure of separation at the dorsoventral junction. The hypothesis is that a disturbance in the normal dorsoventral pattern of PCD along the entire length of the respiratory foregut would result in total failure of tracheo-oesophageal separation and the development of an undivided oesophagotrachea ending in a trifurcation of two bronchi and a fistula. On the other hand, a dorsalward shift of PCD activity affecting only part of the respiratory foregut would allow partial tracheo-oesophageal separation and result in the fistula originating from the foregut cranial to the point of origin of the bronchi.

In the case of *Shh* homozygous mutant embryos, there is again loss of the temporospatial PCD pattern seen in controls. The mutant foregut lacks a recognisable PCD pattern with a seemingly random distribution of PCD clusters in the foregut endoderm. The reduced PCD activity in the mutant foregut endoderm is in contrast with increased apoptosis in other areas of the embryo like the neural tube. This high level of neural tube apoptosis could be attributed to the fact that the homozygous mutant embryos do not fare very well and exhibit generalised oedema. However, clearly loss of *Shh* function does not interfere with the ability of cells to undergo PCD in these non-gut regions. By the same logic, the downgrading and loss of pattern of foregut PCD could be secondary to local molecular disturbances related to the specific disturbance of the *Shh* signaling in the foregut. Alternatively, *Shh* might be proapoptotic specifically in the context of foregut development so that *Shh* loss of function leads directly to reduced PCD. *Shh* is known to

have different effects on PCD depending on the cell/tissue context (Oppenheim et al., 1999; Sanz-Ezquerro & Tickle, 2000; Charrier et al., 2001; Yamamoto et al., 2004; Sacedon et al., 2005).

Therefore, the patterns of PCD are disturbed in both models of failed tracheo-oesophageal separation. Both models are characterised by loss of the precise temporospatial pattern of *Shh* expression. The disturbance in the gene expression is however very different between the two models. The Adriamycin model is characterised by a more diffuse expression whereas the null mutant by lack of expression of a functioning gene. The feature shared by the two models is the loss of the dorsoventral *Shh* boundary. If, as discussed above, induction of PCD is linked to this boundary, the loss of PCD at the dorsoventral boundary can be explained.

6.3.2 – Proliferation and separation

Cell proliferation undoubtedly plays an important role in the development of the foregut, as the embryo is growing rapidly at this stage of development. The question that this study attempted to answer was whether differential rates of mitosis in specific components of the foregut may contribute to foregut morphogenesis. The respiratory system develops as a ventral outgrowth from the foregut. The mesenchyme that surrounds the respiratory (ventral) component of the foregut is well organised and has a higher cell density than the dorsal mesenchyme. There is, however, no evidence that the rate of mitosis in the mesenchyme adjacent to the epithelial tracheo-oesophageal ridge contributes to epithelial folding or that it exerts some sort of external pressure on the foregut. Neither was the ridge epithelium found to proliferate more rapidly, which could have contributed to its fusion in the midline forming a separating septum. These

observations do not support a specific role for differential cell proliferation in the process of tracheo-oesophageal separation. Neither do the proliferation patterns support the hypothesis, developed in Chapter 3, that the tracheal primordium outgrows the oesophageal foregut resulting in the trachea being a distinct structure from the outset. The oesophageal foregut is proliferating at least as rapidly as the tracheal component. Differential growth of the trachea could be primarily driven by the caudolaterally growing lung buds, as the most distal part of the respiratory system but, again, the mitotic activity in the lung buds is not higher than in the dorsal foregut at that level. There is, however, one significant difference in epithelial proliferation and that is between mitotic index of the separated structures (both respiratory and gastrointestinal) at E11.5 and the undivided foregut at more cranial levels. The epithelia of the trachea and oesophagus have a higher rate of proliferation than the undivided foregut. This observation could suggest that, once separated, the foregut components gain in length by proliferating at a significantly higher rate. Even if separation itself may not require regional proliferation peaks, longitudinal growth of the individual respiratory and gastrointestinal structures is likely to involve increased mitotic activity. Finally, the temporospatial pattern of mitosis does not correspond to the PCD pattern making it very unlikely that PCD is simply a balancing of increased proliferation in specific parts of the foregut.

6.3.3 – Mechanisms of separation

It seems likely that a number of mechanisms interact to bring about the successful separation of the ventral trachea from the dorsal oesophagus. I have already shown that the undivided foregut grows and gains in length between E10 and E11, with its ventral part already specified as trachea. The subsequent growth of the foregut structures is coupled with another process, that of separation of this ventral respiratory component from the dorsal oesophageal segment. The traditional view has been that this separation is

the result of the medial growth of an intervening septum, the components of which fuse in the midline and divide the foregut into dorsal and ventral parts. However, the concept of septation, although a popular theme in developmental biology, is not always supported by convincing evidence. In the case of hindgut development, the idea of an actively growing urorectal septum that separates the urogenital from the gastrointestinal tubes is now disputed with an alternative mechanism based on passive mesenchymal interposition between the two proliferating tracts being suggested (Paidas et al., 1999; Rogers et al., 2002). On the other hand, cardiac septation as an active infolding process is a much more established developmental concept (Anderson et al., 2003; Moorman et al., 2003). In the case of the foregut, PCD appears to play a role in this process from its early stages to its completion. In the early stages, PCD may bring about folding of the foregut epithelium as a precursor to fusion and separation. Folding is likely to involve changes in the shape of epithelial cells as a result of rearrangement of their cytoskeleton. Different mechanisms are likely to be involved in the later stages of separation. Whilst folding approximates opposing epithelial layers, the actual separation process would involve opposing cells of the same respiratory/gastrointestinal specification to come into contact with each other and eventually lead to the separation of the two structures. The mechanism that could be involved in this process is cell adhesion. In summary, tracheo-oesophageal separation is a complex process likely to involve a precise choreography of cellular processes including programmed cell death, cell proliferation, cell adhesion and changes in the cellular cytoskeleton. In the next chapter, I will test the hypothesis that PCD is a requirement, and not simply an association, of tracheo-oesophageal separation.

6.4 – SUMMARY

In previous chapters, a tentative conclusion was drawn that separation of the foregut lumen into a ventral trachea and a dorsal oesophagus is an active process. In this chapter, I studied the nature of this separation and in particular the roles of programmed cell death (PCD) and cell proliferation in this process. PCD occurs in reproducible patterns in both the E10.5 and the E11.5 foregut. Significantly, it is present in the foregut at a stage when tracheo-oesophageal separation has not yet started, suggesting that it may play a role in the marking and initiation of this process. Furthermore, the PCD pattern at E11.5 suggests that it does not simply appear at the site of tracheo-oesophageal separation in order to complete luminal division but is distributed in the whole dorsal foregut. This raises the possibility that it is involved in the process that underlies the change of shape of the foregut, which precedes separation. The importance of PCD in the process of tracheo-oesophageal separation is highlighted by the disturbance of its pattern in both the Adriamycin-treated embryo and the *Shh* homozygous mutant which are two models of failed tracheo-oesophageal separation. The study of cell proliferation suggests that this process is likely to contribute to the lengthening of the foregut structures following separation but does not appear to contribute to separation itself. It is likely that tracheo-oesophageal separation is a complex process requiring the precise interplay of a number of morphogenetic events.

CHAPTER 7 – IN VITRO MODEL OF TRACHEO-OESOPHAGEAL DEVELOPMENT

7.1 – INTRODUCTION

7.1.1 – Testing the hypothesis

I have so far identified a key role for the morphogenetic process of tracheo-oesophageal separation in both normal development and the embryogenesis of tracheo-oesophageal malformations. I have also identified a close association between separation and the temporospatial pattern of expression of sonic hedgehog and the pattern of programmed cell death. It would clearly be desirable to study this morphogenetic process more directly and to further investigate the role of gene expression and cell death in its initiation and execution. Specifically, the aim of studies in the present chapter was to test hypotheses formulated on the basis of previous observations. One such hypothesis is that a disturbance in the pattern of programmed cell death would lead to tracheo-oesophageal defects. In order to test this hypothesis, I reasoned that I needed to develop an appropriate experimental system that would allow a close study of tracheo-oesophageal separation and also direct interference with programmed cell death. One such system would be embryo culture during an appropriate embryological window.

7.1.2 – The use of whole-embryo culture

Whereas it is possible to expose embryos to a variety of agents in utero (as is the case with Adriamycin), the precise level of exposure of the embryos cannot be easily controlled. Furthermore, the effects of these agents on the mother has to be taken into account and are difficult to quantify. Another problem with experimental analysis of

embryos *in utero* is a relative lack of access and the difficulty of performing surgical manipulations of the embryos. For these reasons, the technique of *in vitro* embryo culture has been established as an invaluable experimental technique. Embryos have been shown to grow apparently normally *in vitro* for a period of up to 48 hours and the system allows precise control of the culture conditions, composition of the culture medium and concentration of additives and readily allows surgical manipulation (New et al., 1976). It should be noted that culture of embryos during this relatively 'late' period of embryogenesis involves exteriorisation from the yolk sac, a modification of the standard whole-embryo culture procedure (Cockcroft, 1990). Details of the procedure are described in Chapter 2 (section 2.5).

7.1.3 – Interfering with programmed cell death

The embryo culture system allows the possibility of interfering with programmed cell death by the addition of specific inhibitors to the culture medium. One such widely used PCD inhibitor is z-vad-FMK, a protease inhibitor which inhibits the cleavage and activation of several key components of the caspase pathway (Slee et al., 1996; Susin et al., 1996; Marchetti et al., 1996). Although not all PCD is caspase-dependant, caspase inhibition significantly reduces levels of apoptosis and z-vad-FMK has proved to be an invaluable scientific tool when studying the complex mechanisms of PCD activation (Susin et al., 1997; Coin et al., 2000; Fauvel et al., 2001). Several studies have shown that the agent could provide a novel therapeutic approach to diseases characterised by apoptosis-mediated tissue damage (Cook et al., 1996; Cheng et al., 1998; Li et al., 2000b; DeBiasi et al., 2004).

7.2 – RESULTS

7.2.1 – Establishing the *in vitro* model

7.2.1.1 - The design of the culture period

The time parameters of the culture experiment targeted the process of tracheo-oesophageal separation. It has already been shown in Chapter 3 that at E10.5 the foregut is still undivided and that the separation process starts at about E11 and is still in progress at E11.5. For this reason, the embryos were incubated from E10.5 for a period of 18 hours, in order to focus on the separation process. During this time window, it is possible to directly interfere with the cellular/molecular processes involved in tracheo-oesophageal division. The size of embryos at this developmental stage makes them easy to manipulate, thus increasing the options for intervention.

7.2.1.2 - Choice of culture medium

Embryos that developed *in utero* for the same period as the duration of the culture (18 hours) served as controls, both with regard to embryo growth and development as well as tracheo-oesophageal development. The first aim was to establish an *in vitro* model of tracheo-oesophageal development. In order to optimise conditions to allow foregut development to proceed as normally as possible, an established culture medium was used. As described by Cockroft (1999), and previously used in our lab by P. Sharma and V. Reed, 25% rat serum in culture solution was used. Another aim of this chapter was to test the hypothesis that PCD is required for tracheo-oesophageal separation and development. In order to test the hypothesis, a specific PCD inhibitor (Z-vad FMK), dissolved in the chemical DMSO, was added to the culture serum in concentrations successfully used in

this laboratory by P.Sharma (200 μM). In order to assess the effect of DMSO on the development of the embryos, this was added to the culture medium alone as a control. Previous studies have identified potential toxic effects of DMSO on embryo growth and development (Noel et al., 1975).

7.2.1.3 - Assessment of cultured embryos and embryo survival

Cultured embryos were judged to be alive and were included in the study if they satisfied certain criteria at the 18-hour assessment. These were: the presence of a regular and vigorous heartbeat with a minimum rate of 60 beats per minute and the presence of blood flow in the umbilical, the head and neck vessels. Embryos that showed some early signs of ill health, for example a mild degree of oedema, but satisfied the criteria described above, were judged to be alive and were included in the study. The overall survival rate was 87.7 % and the rates were comparable between the different groups of cultured embryos (Tab. 1).

Table 7.1 Summary of cultured embryos and their treatment

	Total cultured	Alive at 18hrs	% survival
Serum only*	16	14	87.5
DMSO in serum	18	15	83.3
z-vad (in DMSO) in serum, 200 μM	23	21	91.2
Total	57	50	87.7

* Serum was diluted 1:4 with culture solution in all groups

7.2.1.4 - Growth and development of cultured embryos

The development and growth characteristics of cultured embryos are summarised in Fig. 7.1. It appears that development as judged by somite number, and growth as judged by crown-rump length of cultured embryos are comparable to control embryos growing in utero for an equivalent time period. The *in utero* embryos used in this comparison were harvested at the same time as the termination of culture of the experimental embryos (about 9.00 AM on E11.5). For somite numbers, there is no statistically significant difference between the groups. The crown-rump lengths appear shorter in the *in utero* embryos and there is a significant difference between the *in utero* and z-vad-treated groups. This greater crown-rump length in cultured embryos is difficult to explain. It may reflect the slight loss of fetal curvature that is seen in culture, perhaps owing to removal of the amnion. This yields a larger crown –rump length without reflecting an increased embryonic body mass. Nevertheless, the fact that embryos develop normally in culture from E10.5 for 18 hours suggests that the various developmental processes are unlikely to be non-specifically influenced by growth restriction, and hence increasing the usefulness of the *in vitro* model for studying mechanisms of organogenesis.

7.2.2 – Foregut development in cultured embryos

7.2.2.1 - Tracheo-oesophageal development in cultured embryos

Tracheo-oesophageal morphology

Tracheo-oesophageal development proceeds normally in embryos cultured both in serum only and those cultured in the presence of DMSO (Fig. 7.2). In fact, the trachea and oesophagus separate even in embryos that showed significant signs of ill health (which

Fig. 7.1 Summary of developmental and growth data for embryos *in utero* and following culture for 18 hours from E10.5

Box plots summarise somite numbers (a) and crown-rump (CR) length (b) data. The numbers above the vertical boxes denote the number of embryos examined for each group. ***(a)*** Somite numbers are comparable between the four groups with no statistically significant differences detected (unpaired t-test). ***(b)*** Crown-rump (CR) lengths are also comparable although the lengths in the z-vad-treated embryos are significantly longer than those of the *in utero* embryos (p=0.0016, unpaired t-test). Overall, these observations suggest no developmental or growth restriction in cultured embryos versus those *in utero*. Moreover, cultured embryos of the different treatment groups are comparable. It should be noted that at the beginning of the culture period (at E10.5), the mean CR length was 3.73 mm and the median somite number was 28.

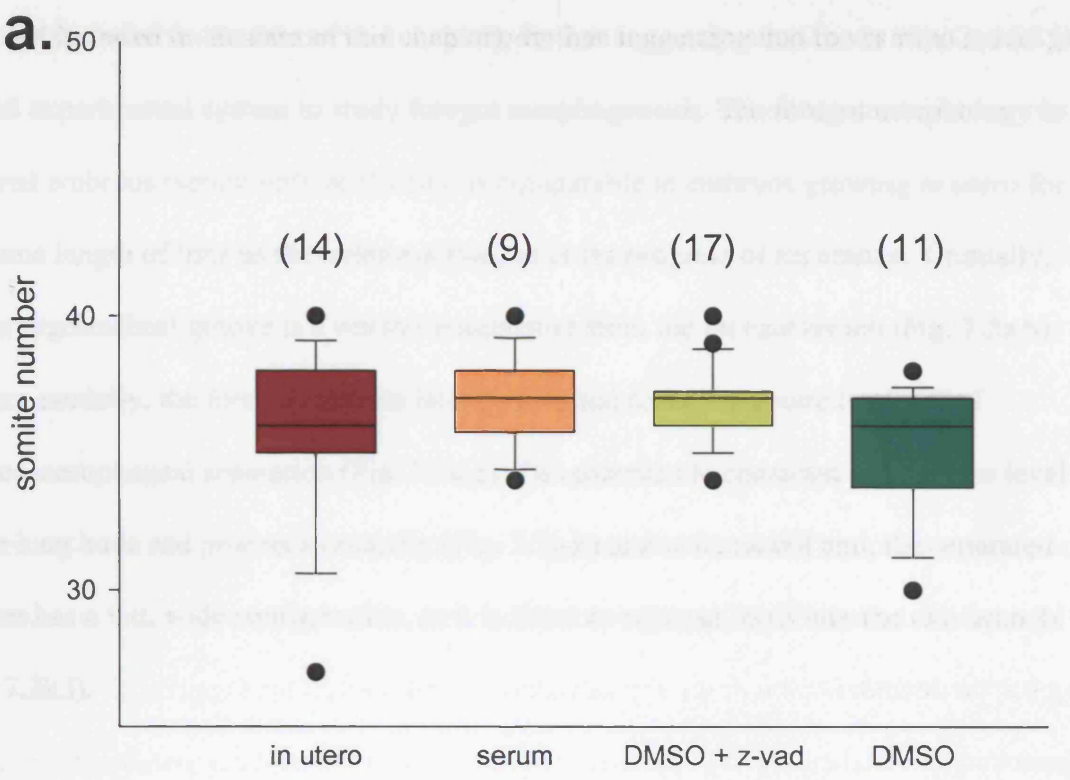
a.
50
40
30
somite number
(14)
(9)
(17)
(11)
in utero
serum
DMSO + z-vad
DMSO

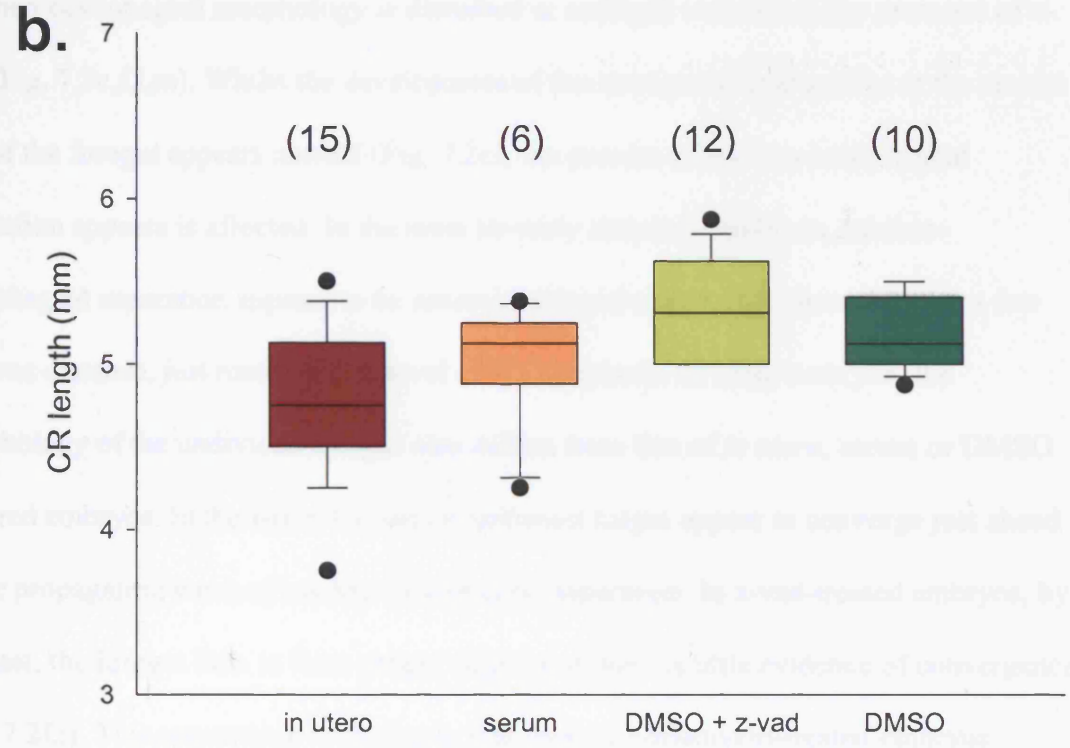
b.
7
6
5
4
3
CR length (mm)
(15)
(6)
(12)
(10)
in utero
serum
DMSO + z-vad
DMSO

were not included in the data of this chapter), further suggesting that the *in vitro* model is a good experimental system to study foregut morphogenesis. The foregut morphology in cultured embryos (serum only & DMSO) is comparable to embryos growing *in utero* for the same length of time as the culture period, as is the progress of separation. Cranially, the laryngotracheal groove is a ventral evagination from the foregut lumen (Fig. 7.2a,b). Further caudally, the foregut exhibits lateral epithelial folds just above the level of tracheo-oesophageal separation (Fig. 7.2d,e). The process of separation starts at the level of the lung buds and proceeds cranially (Fig. 7.2g,h) and at its caudal end, the separated trachea has a flat, wide configuration, as it is about to separate itself into the two bronchi (Fig. 7.2k,l).

Tracheo-oesophageal morphology is disturbed in embryos cultured in the presence of z-vad (Fig. 7.2c,f,i,m). Whilst the development of the laryngotracheal groove at the cranial end of the foregut appears normal (Fig. 7.2c), the process of tracheo-oesophageal separation appears is affected. In the most severely abnormal embryos, tracheo-oesophageal separation appears to be severely delayed and is only observed over a few microns distance, just rostral to the level of the lung buds. In these embryos, the morphology of the undivided foregut also differs from that of *in utero*, serum or DMSO cultured embryos. In the latter, the lateral epithelial ridges appear to converge just ahead of the propagating wave of tracheo-oesophageal separation. In z-vad-treated embryos, by contrast, the foregut fails to form proper ridges and there is little evidence of convergence (Fig. 7.2f,i). This appearance is similar to that seen in Adriamycin-treated embryos (compare Figs. 7.2i and 3.6h). More subtle defects are seen in other z-vad-treated embryos. Here, tracheo-oesophageal separation has started at the level of the lung buds

Fig. 7.2 Tracheo-oesophageal morphology in cultured embryos

Transverse sections, stained with Methyl Green, from embryos harvested at E10.5 and cultured for 18 hours either in culture serum only (a,d,g,k), DMSO in culture serum (b,e,h,l) or in z-vad-FMK (diluted in DMSO) in culture serum (c,f,i,m). Sections are taken from four equivalent and progressively more caudal levels starting at the level of the laryngotracheal groove (Lt) down to the level of the emergence of the bronchopulmonary buds (Br). ***(a,b,c,)*** The development of the laryngotracheal groove is comparable between the three culture groups. ***(d,e,f)*** More caudally, the undivided foregut (Fo) in serum only and DMSO-treated embryos exhibits approximating epithelial folds at the site of tracheo-oesophageal separation (arrowheads in d and e). In contrast, no clear evidence of epithelial folding or approximation is seen in the foregut of z-vad-treated embryos at an equivalent level (f). ***(g,h,i)*** Further caudally, the trachea (Tr) and oesophagus (Oe) are separate structures in serum only and DMSO-treated embryos. In contrast, tracheo-oesophageal separation has been disturbed in z-vad-treated embryos. Despite the failure of separation, some epithelial approximation occurs at this level (arrow in i), although the widening shape of the ventral foregut suggests this is just cranial to the emergence of the bronchopulmonary buds. ***(k,l,m)*** In serum only and DMSO-treated embryos, the trachea has become wide and flat ventro-dorsally, where it is about to separate into the bronchopulmonary buds. Invagination occurs in the sagittal plane in the middle third of the trachea (arrows in k). In z-vad-treated embryos, the foregut almost ends in a trifurcation of oesophagus and two buds although the trachea does become separated from the oesophagus, about 15 micrometers rostral to the origin of the bronchopulmonary buds even in the worst affected embryos (inset in m). It should be noted that tracheo-oesophageal separation is variable in z-vad-treated embryos (Fig. 7.3b). Scale bar, 100 μm

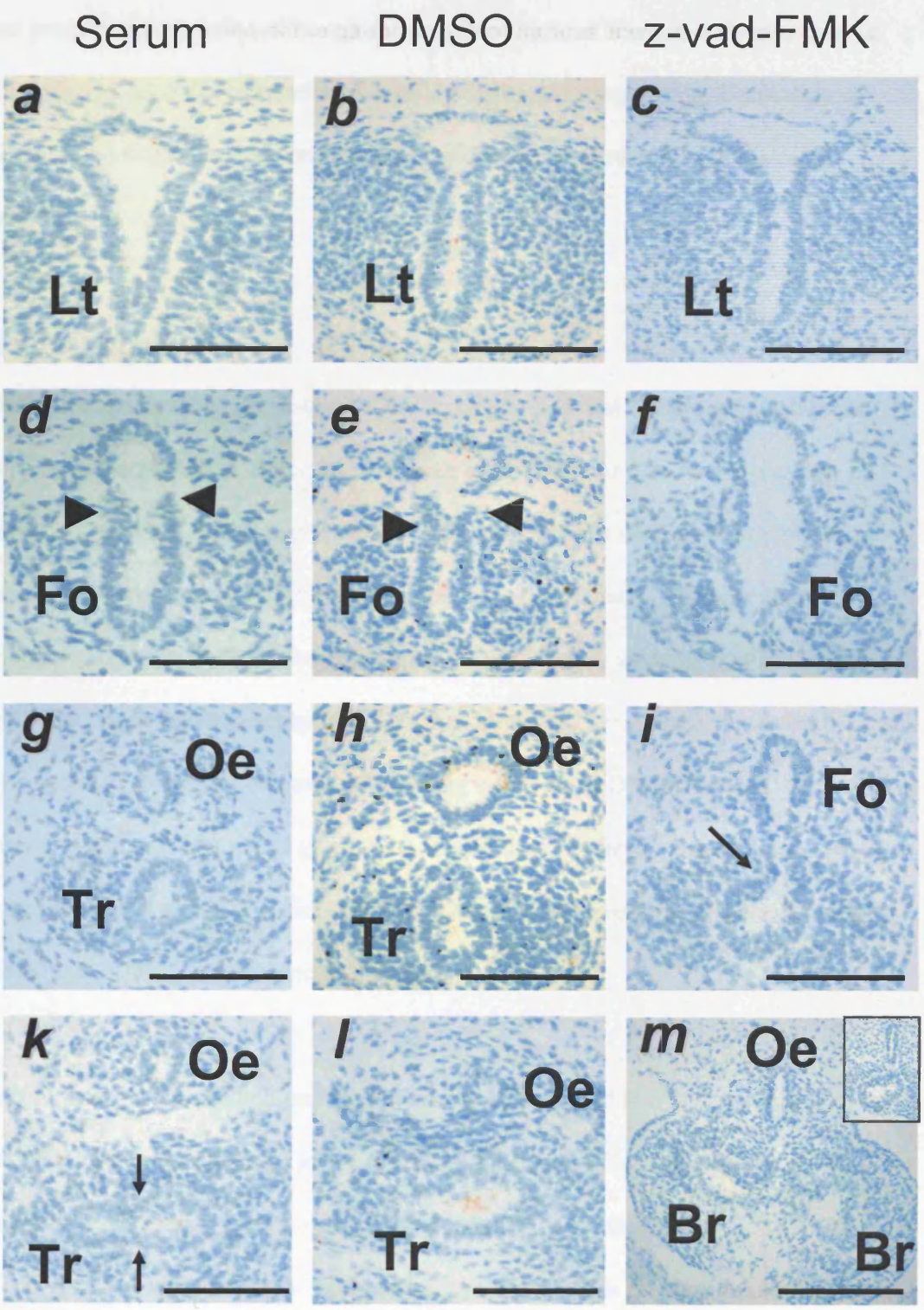
Serum
DMSO
z-vad-FMK
a
Lt
b
Lt
c
Lt
d
Fo
e
Fo
f
Fo
g
Oe
Tr
h
Oe
Tr
i
Fo
k
Oe
Tr
l
Oe
Tr
m
Oe
Br
Br

and has progressed cranially, although the length of divided foregut is shorter than in control embryos, as if the separation process had stopped progressing. Formation of lateral epithelial ridges in these embryos was also abnormal rostral to the level of separation.

Quantitative analysis

Morphological analysis of z-vad-treated embryos showed that the process of tracheo-oesophageal separation had either failed almost completely or else its progression had been arrested. To further document the variation occurring in tracheo-oesophageal separation, following z-vad treatment, I studied the contribution of the divided and undivided segments to the total length of respiratory foregut, as described in Chapter 3. I reasoned that, since tracheo-oesophageal morphology was comparable between the three groups of control embryos (*in utero*, serum only culture and DMSO-treated), it would be acceptable to compare the z-vad group with the cultured embryos. Furthermore, given that z-vad is diluted in DMSO, and that DMSO can itself have toxic effects, it would be desirable to use DMSO controls in the analysis.

When comparing z-vad-treated embryos with serum only and DMSO-treated controls, there is no significant difference in the total foregut length (Fig. 7.3a). In the z-vad-treated embryos, the undivided length is significantly longer than the divided length ($p < 0.0001$) (Fig. 7.3b) whereas in the two control groups, there is no significant difference between divided and undivided segments (Fig. 7.3b). In contrast, the divided segment was significantly shorter (p values of 0.0004 and < 0.0001) and the undivided segment significantly longer (p values of 0.0004 and < 0.0001) in z-vad embryos compared to serum only and DMSO embryos respectively (Fig. 7.3b). Hence, the foregut in z-vad

Fig. 7.3 Quantitative analysis of foregut components in E10.5 embryos cultured for 18 hours

Box plots show (a) total respiratory foregut length and (b) divided and undivided lengths separately. The numbers above the vertical boxes denote the number of embryos examined for each group. **(*a*)** There is no statistically significant difference in total foregut length between serum only, DMSO and z-vad-treated embryos. **(*b*)** In serum only and DMSO-treated embryos, the divided segment is of a similar length to the undivided segment showing that control embryos had reached approximately the midpoint of the tracheo-oesophageal separation process. In contrast, the undivided segment is significantly longer in z-vad-treated embryos compared to the divided segment ($p < 0.0001$). Furthermore, the undivided segment is significantly longer in z-vad-treated embryos compared to both serum only cultured embryos ($p = 0.0004$) and DMSO-treated embryos ($p = 0.0001$). Conversely, the divided segment is significantly longer in both the serum only group ($p = 0.0004$) and the DMSO-treated group ($p < 0.0001$) when compared to z-vad-treated embryos.

a.

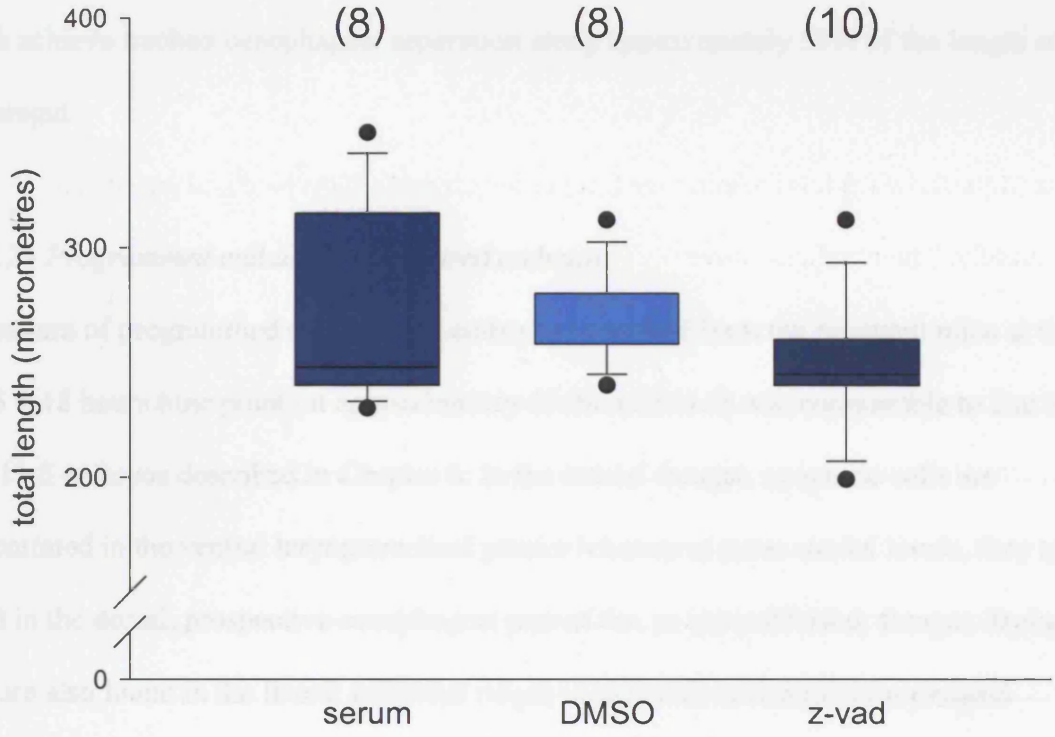
(8)
(8)
(10)
400
300
200
0
total length (micrometres)
serum
DMSO
z-vad

b.

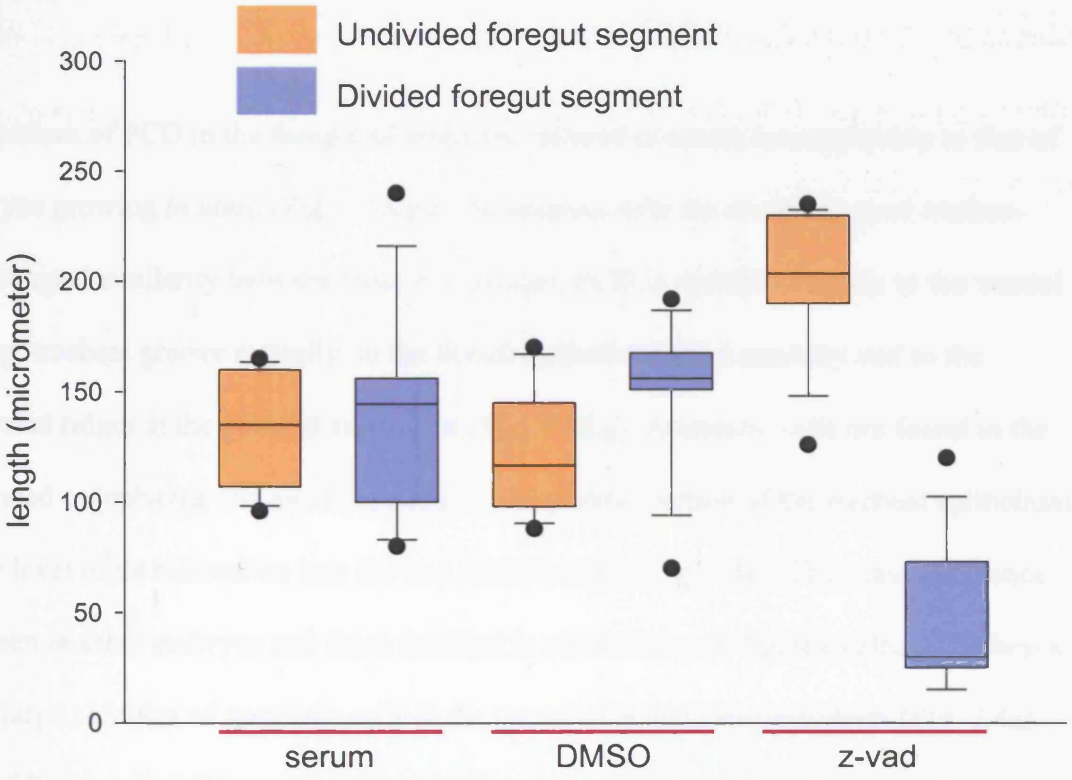
Undivided foregut segment
Divided foregut segment
300
250
200
150
100
50
0
length (micrometer)
serum
DMSO
z-vad

treated embryos lengthens but remains largely undivided, in contrast to controls embryos which achieve tracheo-oesophageal separation along approximately 50% of the length of the foregut.

7.2.2.2 - Programmed cell death in cultured embryos

The pattern of programmed cell death in embryos harvested from the pregnant mice at the E10.5 + 18 hours time point (at approximately 09:00 on E11.5) was comparable to that in the E11.5 embryos described in Chapter 6. In the cranial foregut, apoptotic cells are concentrated in the ventral laryngotracheal groove whereas at more caudal levels, they are found in the dorsal, prospective-oesophageal part of the, as yet undivided, foregut. Dying cells are also found in the lateral epithelial ridges at the point of tracheo-oesophageal separation and, more caudally, small numbers persist in the separated oesophagus *(data not shown).*

The pattern of PCD in the foregut of embryos cultured in serum is comparable to that of embryos growing *in utero* (Fig. 7.4d,g,k). In keeping with the morphological tracheo-oesophageal similarity between these two groups, PCD is found to localise to the ventral laryngotracheal groove rostrally, to the dorsal epithelium more caudally and to the epithelial ridges at the point of separation (Fig. 7.4d,g). Apoptotic cells are found in the separated oesophagus and more caudally, in the middle portion of the tracheal epithelium, at the level of its bifurcation into the two main bronchi (Fig. 7.4k). The main difference between *in utero* embryos and those cultured in serum alone is that the cultured embryos have large numbers of apoptotic cells in the neural tube and neuroectoderm (Fig. 7.4a). This difference is striking, and is likely to be a consequence of the culture conditions.

Fig. 7.4 Programmed cell death in cultured embryos

Immunohistochemistry for the PCD mediator cleaved caspase 3 on transverse sections from serum only, DMSO and z-vad-treated cultured embryos (harvested at E10.5 and cultured for 18 hours). Sections were counterstained with methyl green. Sections are from equivalent levels for each culture group. ***(a,b,c)*** The neural tube (Nt) shows high levels of PCD in both serum and DMSO cultured embryos. The neural tube in embryos growing in utero has almost no PCD activity (data not shown) suggesting that the increased incidence of cell death in neural tubes of cultured embryos relates to the culture conditions. In sharp contrast, PCD is abolished in the neural tube of z-vad-treated embryos with the exception of occasional caspase 3 - stained cells (arrow in c). ***(d,e,f)*** The epithelium of the laryngotracheal groove (Lt) is marked by caspase 3-positive cells (arrows in d and e) in sharp contrast to the laryngotracheal groove of z-vad-treated embryos (*f*) that lacks PCD completely. ***(g,h,i)*** More caudally, PCD localises to the dorsal, oesophageal-prospective part of the undivided foregut (Fo) (arrows in g and h). At the level of tracheo-oesophageal separation, PCD is prominent at the approximating epithelial ridges (arrowheads, inset in g). There is no detectable PCD in the undivided foregut of z-vad-treated embryos. ***(k,l,m)*** At the level of the origin of the bronchopulmonary buds (Br), PCD marks the site of tracheal separation (arrows in k and l) in serum and DMSO-treated embryos. The 'near trifurcation' into oesophagus (Oe) and bronchopulmonary buds (Br) seen in some z-vad treated embryos is completely devoid of PCD (*m*). Scale bar, 100 μm

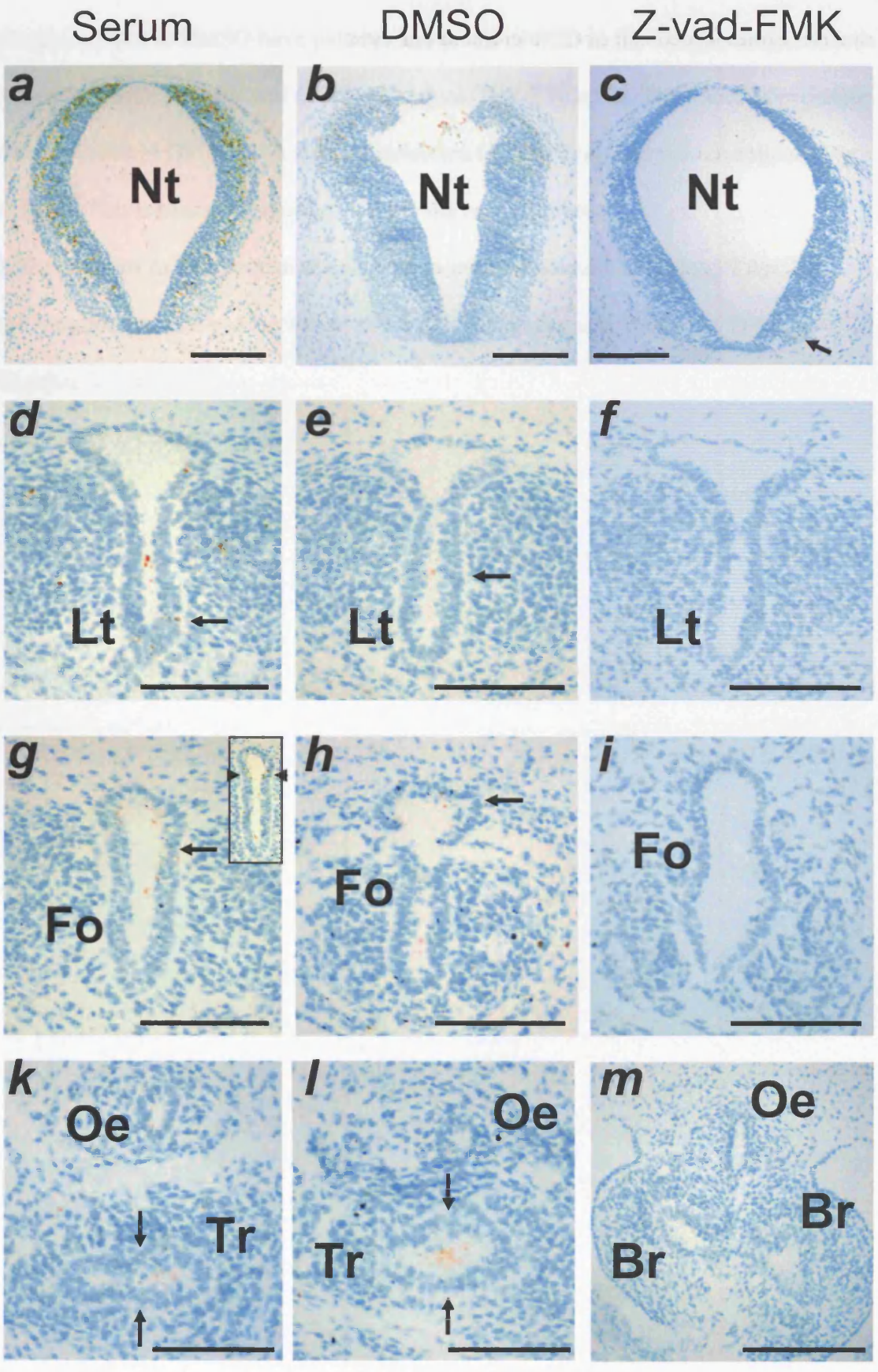
Serum
DMSO
Z-vad-FMK
a
Nt
b
Nt
c
Nt
d
Lt
e
Lt
f
Lt
g
Fo
h
Fo
i
Fo
k
Oe
Tr
l
Oe
Tr
m
Oe
Br
Br

Embryos cultured in DMSO have patterns and levels of PCD in the foregut comparable to serum-only culture controls and *in utero* embryos (Fig. 7.4b,e,h,l). The effect of exposure to z-vad (diluted in DMSO) is a striking reduction in PCD in all embryos examined (Fig. 7.4c,f,i,m). This inhibition is most striking in the regions where cultured embryos exhibit excessive cell death, namely the neural tube (Fig. 7.4c). The developing foregut of z-vad treated embryos exhibits a complete lack of PCD (Fig. 7.4f,i,m).

7.3 – DISCUSSION

7.3.1 – Is the in vitro model reliable for the study of tracheo-oesophageal development?

The first priority in this chapter was to establish that the process of tracheo-oesophageal separation proceeds normally during the time window of the embryo culture period. The somite and crown-rump length data suggest that growth and development of cultured embryos is comparable to that of embryos growing *in utero* for the same time period. This finding is consistent with many other studies describing the technique of culture of post-implantation embryos for between 24 and 48 hours (New et al., 1976) and confirms that even relatively advanced embryos, e.g E10.5, can be cultured successfully (Cockcroft, 1990). Loss of fetal curvature in cultured embryos could explain the observation that CR lengths appear longer in z-vad-treated embryos compared to embryos growing in utero. Whatever the mechanism, the finding reinforces the argument that the cultured embryos are not growth restricted. In addition to normal growth, tracheo-oesophageal development appears to proceed normally in cultured embryos. The morphology of the foregut is comparable to that of embryos growing *in utero*, and specifically, the process of tracheo-oesophageal separation progresses apparently normally. It should be noted that even in embryos that exhibited increasing signs of ill health, for example general and pericardial oedema, tracheo-oesophageal separation appeared to proceed normally. These observations suggest that tracheo-oesophageal separation is a process that lends itself to study via the in vitro embryo culture system. The period of the culture encompasses the critical point of initiation of separation and an overnight (18 h) culture period is sufficient for tracheo-oesophageal separation to progress to approximately 50% completion, while allowing overall satisfactory growth and development of the embryos.

7.3.2 – Can we be confident about the inhibitory effect of z-vad?

The pan-caspase inhibitor z-vad has been an invaluable tool for the study of caspase-dependant programmed cell death in many organ systems (Susin et al., 1997; Coin et al., 2000; Fauvel et al., 2001). It has been shown to inhibit apoptosis assessed by flow cytometry, DNA proteolysis and nucleosomal fragmentation, as well as block all the classical ultrastructural features of apoptosis including chromatin condensation, nucleolar disintegration and cytoplasmic vacuolation (Fearnhead et al., 1995). In the specific culture system studied, the effect of 200 μM of the inhibitor abolished PCD as revealed by immunohistochemistry for cleaved caspase-3. This observation is most striking when z-vad-treated embryos are compared to other cultured embryos. In the latter group, the culture procedure appears to induce high levels of PCD in the more exposed organ-systems of the embryos, as is the case for the neural tube. This may be a direct effect of the culture medium on the embryo. In sharp contrast, z-vad-treated embryos show no evidence of PCD in these organ systems. Similarly, z-vad-treated embryos show no evidence of PCD in the developing foregut in contrast to control cultured embryos in which foregut PCD patterns conform to the pattern seen in the *in utero* embryos. These observations suggest that treatment with z-vad affects both physiological and culture-induced PCD. I conclude that the use of z-vad is an effective and reliable method to inhibit PCD in the midgestation embryo, enabling study of the effect of such inhibition on the development of the foregut.

One potential weakness of this inhibitory system is the fact that although most PCD depends on activation of the caspase pathway of cell death mediators, not all PCD is caspase dependent (Didenko et al., 2002; Jaattela, 2002; Donovan & Cotter, 2004; Bursch, 2004). This raises the possibility that PCD may still be occurring in cells that are

negative for cleaved caspase 3. In order to address this question, I would need to study PCD using an alternative technique. For example, the use of TUNEL staining should pick up all the cells that are caspase 3 positive as well as cells in which an alternative apoptotic pathway is used. The advantage of TUNEL would be that it actually demonstrates apoptosis by staining DNA strand breaks of the dying cells. Whereas it would clearly be desirable to run concurrent TUNEL studies, or other methods, to supplement and consolidate the caspase 3 data, it is likely that the cleaved caspase 3 distribution is a reliable marker for PCD. There are a number of reasons for this. There is no doubt that cells that stain positively for cleaved caspase 3 are in the process of undergoing PCD. Caspase 3 is an effector caspase and is found downstream in the pathway of caspase activation (Kumar & Harvey, 1995; Orth et al., 1996; Alnemri, 1997; Susin et al., 1997). Furthermore, there have been a number of studies reporting very good correlation between patterns of TUNEL and caspase 3 activation (Hoshi et al., 1998; Duan et al., 2003; Sharma et al., 2004; Arai et al., 2005). These studies also suggest that there is no significant difference in the number of TUNEL-positive and caspase 3-positive cells in many organ systems, including the midgestation mouse embryo.

7.3.3 – What is the significance of the effect of z-vad on foregut morphology?

When considering the effect of caspase inhibition on the development of the foregut and on tracheo-oesophageal separation and development, we should consider the role of PCD during normal development. The temporospatial pattern of PCD within the developing foregut is consistent with a role for PCD in marking the site of tracheo-oesophageal separation and, perhaps, playing a key role in effecting this process. From E10.5 onwards, cells undergoing PCD are found at the dorsoventral boundary in the caudal end of the, as yet undivided, foregut and at the boundary between the separating lung buds and the

foregut. During the next twelve hours, PCD changes dynamically and shifts exclusively to the dorsal foregut just ahead of the progressing front of tracheo-oesophageal separation whilst at the same time concentrating on the converging epithelial ridges at the very point of separation. Hence, there is a close correlation between the spatial localisation of PCD and tracheo-oesophageal separation, raising the real possibility of a causal connection. If the latter is correct, with PCD participating in the mechanism of epithelial separation, then one might expect that tracheo-oesophageal separation would be adversely affected, or abolished, by PCD inhibition. My results support this idea. In some embryos, virtually no separation takes place, whilst in others, separation is initiated but does not progress normally. The conclusion is that without PCD the process of tracheo-oesophageal separation cannot be maintained confirming the impression that it is required for the execution of epithelial separation.

Z-vad treated embryos with almost total failure of separation have a foregut that, whilst growing normally in length, fails to show the morphological evidence of converging epithelial ridges. This evidence supports a role of PCD in marking the site of epithelial folding and initiation of separation. Other z-vad treated embryos, however, showed a degree of separation, clearly demonstrating that the process was initiated. A plausible explanation for this is the timing of PCD inhibition. The findings of Chapter 6 showed that, at E10.5, cells undergoing PCD are already localised within the foregut. The application of a caspase inhibitor at E10.5 would have no effect on cells already far advanced in the apoptotic process, as they have already activated the downstream caspase 3 effector and are destined to undergo PCD. Hence, such embryos would succeed in the early stages of separating their foregut. Once the z-vad is applied to these embryos, the epithelial separation process is arrested, in contrast to control cultured embryos which continue to separate their foregut. In contrast, embryos that are somewhat less advanced

at the beginning of the experiment are the ones that are most likely to fail entirely in the separation process as z-vad is present prior to the onset of separation and so can prevent its initiation.

This explanation could form the basis of a model for the phenotypic variation of tracheo-oesophageal malformations. If we assume that interference with PCD in the foregut play a role in the embryogenesis of tracheo-oesophageal malformations, then the timing of this interference provides the key to the type of malformation. If an anti-apoptotic insult is applied early, it will result in complete failure of separation. If the insult is applied later, this will result in the separation process being arrested at a variable distance from the level of the lung buds resulting in variations of the 'proximal fistula' phenotype described in Chapter 3. In order to further support this hypothesis, culture experiments could apply z-vad at an earlier stage or allow the culture to proceed for longer periods. These are interesting experiments for future research.

7.3.4 – How specific is the effect of z-vad?

It is logical to attribute the effect of z-vad on foregut morphology to inhibition of PCD. It is important, however, to consider the possibility that z-vad may influence other cellular and molecular processes which, in turn, have a bearing on the process of separation. One such process is cell proliferation. This seems unlikely in view of the lack of any detectable foregut or general growth impairment in z-vad treated embryos. Furthermore, a non-specific interference with cell proliferation would not be expected to affect separation based on the evidence described in Chapter 6, which showed that cell proliferation is comparable between the dorsal and ventral parts of the foregut and the separated trachea and oesophagus. Nevertheless, it would be useful to study cell

proliferation in the cultured embryos, to exclude this hypothetical mode of action of z-vad although this has been ruled out in previous studies (Weil et al., 1997).

It would also be important to establish whether z-vad has any effect, directly or indirectly, on the temporospatial expression of foregut patterning genes, in particular *Shh*. I have already established that both PCD and *Shh* expression are disturbed during failure of tracheo-oesophageal separation in Adriamycin-treated embryos. Furthermore, I have already shown that loss of *Shh* function in homozygous mutants results in a disturbed PCD pattern as well as failure of separation. Whilst it is clear that a complex interplay exists between gene expression and cell death, the overwhelming evidence of past studies suggests that cell death is controlled by gene expression, rather the other way round. The most parsimonious explanation, therefore, for the effect of z-vad on tracheo-oesophageal development is that PCD is necessary for epithelial separation. It remains to be determined whether PCD is also sufficient, *per se*, at the dorsoventral boundary of the foregut for physical separation of the tracheal and oesophageal components. Further experimental studies will be needed to test this idea.

PCD is involved in a number of similar morphogenetic systems. Whether PCD drives these morphogenetic processes, or is simply a necessary condition for them, is a matter of debate. During development of the palate, PCD in the medial edge epithelia is activated by contact of the palatal shelves and appears to be the primary process required for palatal fusion (Cuervo et al., 2002). PCD is also required for epithelial fusion during neural tube closure as shown by the failure of fusion of the neural folds in embryos treated with z-vad (Weil et al., 1997). Moreover, it has been suggested that PCD plays a role in the bending and rolling up of the neural folds as indicated by the failure of coming together of the folds in z-vad-treated embryos (Weil et al., 1997). This would suggest a more

central role for PCD in this morphogenetic process. During cardiac development, PCD is associated with morphological remodeling and contributes to the fusion of the outflow tract ridges and the formation of the aortopulmonary septum (Sharma et al., 2004). Finally, PCD is required for the conversion of solid primordia into hollow tubes (Coucouvanis & Martin, 1995). In this system, however, PCD is the direct result of proapoptotic signals from neighbouring epithelial cells and its role is simply in cell removal and sculpting of these structures.

7.4 – SUMMARY

Tracheo-oesophageal development and separation can be reliably studied in embryos growing *in vitro* during the narrow embryological window between E10.5 and E11.5. The pattern of developmental processes, including PCD, is comparable between embryos growing *in vitro* and *in utero*, making the *in vitro* model a useful tool to further study these processes in tracheo-oesophageal development. The addition of the pan-caspase inhibitor z-vad to the culture medium effectively abolishes caspase-dependent PCD. Embryos growing in the presence of the inhibitor grow normally compared to controls but have disturbed tracheo-oesophageal development. Whilst total foregut length in these embryos is comparable to controls, tracheo-oesophageal separation appears to become arrested, with most of the foregut length remaining undivided. This result supports the hypothesis that PCD is necessary for the initiation and execution of tracheo-oesophageal separation.

CHAPTER 8 – GENERAL DISCUSSION

8.1 – GENERAL REMARKS

The study of the events that underlie the development of OA/TOF has been hampered by persisting controversies over the mechanisms of normal organogenesis. In this study, the development of a new model of tracheo-oesophageal malformations has focused attention on one aspect of foregut morphogenesis, namely tracheo-oesophageal separation. Through the parallel study of normal and abnormal foregut development, tracheo-oesophageal separation was studied in detail. It was shown that the foregut does indeed separate along the dorsoventral boundary between two different cell populations (respiratory and gastrointestinal). Separation was intricately linked to the dorsoventral expression pattern of the key developmental gene *Sonic hedgehog*. The manner in which the temporospatial pattern of expression of foregut patterning genes could influence separation is unclear but could include programmed cell death (PCD). The separating foregut exhibits a dorsoventral pattern of PCD consistent with it being a mediator of separation and, more importantly, separation was shown to be arrested when PCD was inhibited.

One of the most striking findings of this study was the repeated finding of failed separation in the various models of tracheo-oesophageal malformations. Treatment with the teratogen Adriamycin, loss of function of *Shh* and inhibition of PCD in cultured embryos had an easily identifiable and specific effect on the developing foregut: the persistence of an undivided foregut having a respiratory (ventral) and a gastrointestinal

(dorsal) component. The study of these models could allow us to start putting together a plausible mechanism for tracheo-oesophageal separation.

8.2 – POTENTIAL PITFALLS/ POSSIBLE IMPROVEMENTS

8.2.1. – Experimental techniques

8.2.1.1 - Genotyping of Shh mice

In this study, genotyping was not routinely used because of time constraints. Mice that were homozygous for the *Shh* mutation were distinguished from heterozygous or wild type *Shh* mice only on the basis of their gross morphology. This approach can be justified from previous studies, including work by others in my own lab, that have described gross morphological abnormalities in $Shh^{-/-}$ mice. In contrast, $Shh^{+/-}$ heterozygous mice are morphologically normal and indistinguishable from genotypically normal mice (Chiang et al., 1996). The problem with the use of morphology alone to identify $Shh^{-/-}$ embryos, is that $Shh^{+/-}$ and $Shh^{+/+}$ embryos were pooled together and subtle differences that might exist in foregut morphology between the two groups could not be assessed. Furthermore, even genotyping of the grossly abnormal $Shh^{-/-}$ embryos would be desirable for reasons of scientific completeness. Nevertheless, all control embryos in the Shh studies had a foregut morphology indistinguishable from CBA/Ca control embryos. Moreover, the abnormalities of foregut development in *Shh* null mutants, as described in this study, are consistent with previous work on the knockout (Litingtung et al., 1998; Chiang et al., 1996) and almost certainly reflect the true effect of *Shh* null status on foregut development.

8.2.1.2 - Immunohistochemistry controls

For all immunohistochemical studies, the validity of the findings was tested by using a secondary antibody without a primary antibody, in order to assess non-specific staining. A more appropriate negative control would have been the use of a non-specific antibody raised against the host tissue. Nevertheless, all antibodies had been previously used and validated in other published studies and the patterns of antibody staining are consistent with those obtained previously.

8.2.2 – Interpretation of findings

8.2.2.1 - Interpreting tracheo-oesophageal malformations in the mouse

Whereas it is reported that the majority of Adriamycin-treated rat embryos with tracheo-oesophageal malformations have defects closely matching the human ones, the Adriamycin-treated mice had more severe malformations with only a small minority conforming to the classic oesophageal atresia and distal tracheo-oesophageal fistula phenotype. One interpretation is that the mouse malformations resemble the rare human condition known as laryngotracheo-oesophageal cleft, whereas the rat malformation more closely corresponds to OA/TOF. It could be argued, therefore, that any comparisons between the two models (mouse and rat) and any conclusions derived from the study of the mouse model on the embryogenesis of OA/TOF, are not valid. However, irrespective of the differences in the near term phenotype between the two models, foregut morphology in the early stages of tracheo-oesophageal development is almost identical in the rat and mouse. An undivided foregut forms the basis of both rat and mouse malformations with, during subsequent development, the formation of a spectrum of tracheo-oesophageal malformations some of which closely resemble OA/TOF. Hence, by

inference, human OA/TOF probably also forms as part of a spectrum of defects, the more severe of which might be lost *in utero*. Therefore, the Adriamycin-treated mouse appears to offer a satisfactory model for the study of the early events of faulty organogenesis that lead to OA/TOF and other tracheo-oesophageal malformations.

8.2.2.2 - Describing morphogenetic events

The mechanisms of development that are discussed in this thesis are based on interpretation of foregut morphology at specific time points in development, as derived from 'still images'. In other words, inferences are drawn about continuous developmental processes based on 'snapshots' of these processes. Furthermore, interpretation of 'still images' could be misleading unless it is fully appreciated that embryos, and specifically the foregut, alter structurally in a continuous manner throughout development, so that the spatial relationship between different structures does not remain constant. This is a particularly relevant consideration for the study of foregut lengths where the distance between specific reference points was used to assess foregut/tracheal length at different gestations. Admittedly, there are potential pitfalls if solely morphological data are used to describe developmental processes. However, in this particular study, every effort was made to standardise the different experiments. In other words, the developmental stages of embryos used in different experiments were comparable and consequently morphological observations could be checked against antibody or gene expression data from other stage-matched embryos. One example of this is the assessment of the length of the different foregut segments during development. In addition to the chosen reference points being easily reproducible (laryngotracheal groove, tracheal bifurcation), these were verified by contrasting with the Nkx2.1 data that confirmed the extent of the respiratory endoderm.

8.3 – FUTURE WORK

Future work could build upon the findings of this study and concentrate on the molecular and cellular mechanisms of foregut separation. Although this would primarily involve the study of tracheo-oesophageal separation, it would have implications for other organ systems where similar morphogenetic processes take place. One such system is the hindgut where a similar separation takes place between the anorectal and genitourinary tracts. Moreover, defects in this process yield clinically important malformations including anorectal malformations (Kluth & Lambrecht, 1997b; Qi et al., 2002; Bai et al., 2004). The mechanisms underlying this hindgut separation process remain controversial (Kluth & Lambrecht, 1997b; Paidas et al., 1999; Qi et al., 2000b; Rogers et al., 2002).

In order to enable experimental hypothesis-testing in future work, tracheo-oesophageal separation could be studied in appropriate culture systems that would allow relatively direct access to the foregut. This would provide the opportunity to alter molecular signals that are likely to contribute to separation. The present study has shown that tracheo-oesophageal separation can be reliably studied in whole embryos grown *in vitro*. The same *in vitro* model could be used to study other aspects of the separation process (*see below*). A major additional undertaking would be to develop of an organ culture model of foregut development, in order to allow a very close study of the events that underlie separation, as well as to offer opportunities for specific manipulation of the morphogenetic process.

Experiments that would appear to have high priority in future work might include the role of the notochord in tracheo-oesophageal separation. Using the whole embryo culture

system, it might be possible to surgically remove or ablate the notochord in order to assess the effect on both foregut folding and separation as well as the effect on gene expression in the foregut. I would plan to specifically study *Shh* expression in view of the proven association of *Shh* with separation, the known role of the notochord as a source of a diffusible Shh signal, and evidence from other culture systems suggesting repression of endodermal *Shh* expression by the notochord (Hebrok et al., 2000; Hebrok et al., 1998). If the foregut could be itself cultured successfully *in vitro*, it would be possible to recombine the notochord with the endoderm and study the pattern of endodermal gene expression and foregut morphogenesis. Alternatively, beads impregnated with diffusible signals could be placed near the developing foregut in intact embryos. In preliminary experiments, I have successfully placed beads around the foregut at the start of the whole embryo culture without interfering with embryo development or tracheo-oesophageal separation.

The changes in foregut configuration, with the development of converging epithelial ridges rostral to the level of tracheo-oesophageal separation, have been previously described and are well documented in the present study. Future work could study the cellular events that mediate this folding at the dorsoventral junction of the foregut. I have already demonstrated that increased levels of PCD occur at that point and that PCD is required for separation to proceed. One option would be to use electron microscopy to study any configurational change in the epithelial cells at that dorsoventral junction. One possibility is that changes in the ratio of basal to luminal diameter of epithelial cells could cause a change in the shape of the foregut bringing about epithelial folding. Such a change in cell shape could be caused by local changes in cell cycle as the basal localisation of S phase nuclei would lead to expansion of that part of the cell, as has been postulated for neuroepithelial bending at hinge points (Smith & Schoenwolf, 1987;

Gerrelli & Copp, 1997). However, the lack of differential mitotic activity along the dorsoventral axis of the foregut in this study would not support this notion. Alternatively, it could be mediated by rearrangements of the cellular cytoskeleton, as has been demonstrated in single layer epithelium growing in culture (Graebert et al., 1997). One possibility would be to study the distribution of actin microfilaments using Phalloidin and the effect of disruption of microfilaments (e.g. using Cytochalasin D) on foregut development. Alternatively, I could use inhibitors of the Rho GTPase-dependant pathways to interfere with the arrangement and function of the actin filament systems during whole embryo or organ culture. Such a specific inhibitor is the exoenzyme C3 from *Clostridium botulinum* (Kobayashi et al., 2001).

8.4 – CONCLUSION

Within the constraints of experimental technique, this thesis has demonstrated that separation of the foregut along its dorsoventral boundary is a critical step in the development of the trachea and the oesophagus and that disturbance of this process leads to tracheo-oesophageal malformations. This work provides insight into both normal foregut development and pathogenesis of tracheo-oesophageal malformations and points the way to further experimental studies to elucidate molecular and cellular mechanisms that could ultimately identify targets for therapeutic intervention to prevent OA/TOF.

BIBLIOGRAPHY

Abu-Hijleh, G., Qi, B. Q., Williams, A. K., & Beasley, S. W. (2000) Development of the bones and synovial joints in the rat model of the VATER association. *J.Orthop.Sci.* **5**, 390-396.

Adachi-Yamada, T. & O'Connor, M. B. (2002) Morphogenetic apoptosis: a mechanism for correcting discontinuities in morphogen gradients. *Dev.Biol.* **251**, 74-90.

Ahlgren, U., Jonsson, J., & Edlund, H. (1996) The morphogenesis of the pancreatic mesenchyme is uncoupled from that of the pancreatic epithelium in IPF1/PDX1-deficient mice. *Development* **122**, 1409-1416.

Alexander, J., Rothenberg, M., Henry, G. L., & Stainier, D. Y. (1999) casanova plays an early and essential role in endoderm formation in zebrafish. *Dev.Biol.* **215**, 343-357.

Alnemri, E. S. (1997) Mammalian cell death proteases: a family of highly conserved aspartate specific cysteine proteases. *J.Cell Biochem.* **64**, 33-42.

Anderson, R. H., Webb, S., Brown, N. A., Lamers, W., & Moorman, A. (2003) Development of the heart: (2) Septation of the atriums and ventricles. *Heart* **89**, 949-958.

Ang, S. L., Wierda, A., Wong, D., Stevens, K. A., Cascio, S., Rossant, J., & Zaret, K. S. (1993) The formation and maintenance of the definitive endoderm lineage in the mouse: involvement of HNF3/forkhead proteins. *Development* **119**, 1301-1315.

Apelqvist, A., Ahlgren, U., & Edlund, H. (1997) Sonic hedgehog directs specialised mesoderm differentiation in the intestine and pancreas. *Curr.Biol.* **7**, 801-804.

Arai, M., Sasaki, A., Saito, N., & Nakazato, Y. (2005) Immunohistochemical analysis of cleaved caspase-3 detects high level of apoptosis frequently in diffuse large B-cell lymphomas of the central nervous system. *Pathol.Int.* **55**, 122-129.

Arai, M., Yoguchi, A., Takizawa, T., Yokoyama, T., Kanda, T., Kurabayashi, M., & Nagai, R. (2000) Mechanism of doxorubicin-induced inhibition of sarcoplasmic reticulum Ca(2+)-ATPase gene transcription. *Circ.Res.* **86**, 8-14.

Arcamone, F., Cassinelli, G., Fantini, G., Grein, A., Orezzi, P., Pol, C., & Spalla, C. (1969) Adriamycin, 14-hydroxydaunomycin, a new antitumor antibiotic from S. peucetius var. caesius. *Biotechnol.Bioeng.* **11**, 1101-1110.

Arey, L.B. (1966) In: *Developmental Anatomy* (ed 7). Philadelphia, PA, Saunders, 263-265

Arsic, D., Cameron, V., Ellmers, L., Quan, Q. B., Keenan, J., & Beasley, S. (2004) Adriamycin disruption of the Shh-Gli pathway is associated with abnormalities of foregut development. *J.Pediatr.Surg.* **39**, 1747-1753.

Arsic, D., Keenan, J., Quan, Q. B., & Beasley, S. (2003) Differences in the levels of Sonic hedgehog protein during early foregut development caused by exposure to Adriamycin give clues to the role of the Shh gene in oesophageal atresia. *Pediatr.Surg.Int.* **19**, 463-466.

Ashcraft, K. W. & Holder, T. M. (1969) The story of esophageal atresia and tracheoesophageal fistula. *Surgery* **65**, 332-340.

Aubin, J., Lemieux, M., Tremblay, M., Berard, J., & Jeannotte, L. (1997) Early postnatal lethality in Hoxa-5 mutant mice is attributable to respiratory tract defects. *Dev.Biol.* **192**, 432-445.

Bai, Y., Chen, H., Yuan, Z. W., & Wang, W. (2004) Normal and abnormal embryonic development of the anorectum in rats. *J.Pediatr.Surg.* **39**, 587-590.

Barde, Y. A. (1989) Trophic factors and neuronal survival. *Neuron* **2**, 1525-1534.

Beasley, S. W., Allen, M., & Myers, N. (1997) The effects of Down syndrome and other chromosomal abnormalities on survival and management in oesophageal atresia. *Pediatr.Surg.Int.* **12**, 550-551.

Beasley, S. W., Diez, P. J., Qi, B. Q., Tovar, J. A., & Xia, H. M. (2000) The contribution of the adriamycin-induced rat model of the VATER association to our understanding of congenital abnormalities and their embryogenesis. *Pediatr.Surg.Int.* **16**, 465-472.

Beasley, S. W., Williams, A. K., Qi, B. Q., & Vleesch, D., V (2004) The development of the proximal oesophageal pouch in the adriamycin rat model of oesophageal atresia with tracheo-oesophageal fistula. *Pediatr.Surg.Int.* **20**, 548-550.

Beck, F., Erler, T., Russell, A., & James, R. (1995) Expression of Cdx-2 in the mouse embryo and placenta: possible role in patterning of the extra-embryonic membranes. *Dev.Dyn.* **204**, 219-227.

Becker, M. B., Zulch, A., Bosse, A., & Gruss, P. (2001) Irx1 and Irx2 expression in early lung development. *Mech.Dev.* **106**, 155-158.

Bellusci, S., Furuta, Y., Rush, M. G., Henderson, R., Winnier, G., & Hogan, B. L. (1997b) Involvement of Sonic hedgehog (Shh) in mouse embryonic lung growth and morphogenesis. *Development* **124**, 53-63.

Bellusci, S., Grindley, J., Emoto, H., Itoh, N., & Hogan, B. L. (1997a) Fibroblast growth factor 10 (FGF10) and branching morphogenesis in the embryonic mouse lung. *Development* **124**, 4867-4878.

Bienz, M. (1997) Endoderm induction in Drosophila: the nuclear targets of the inducing signals. *Curr.Opin.Genet.Dev.* **7**, 683-688.

Bilder, D. & Scott, M. P. (1998) Hedgehog and wingless induce metameric pattern in the Drosophila visceral mesoderm. *Dev.Biol.* **201**, 43-56.

Biller, J. A., Allen, J. L., Schuster, S. R., Treves, S. T., & Winter, H. S. (1987) Long-term evaluation of esophageal and pulmonary function in patients with repaired esophageal atresia and tracheoesophageal fistula. *Dig.Dis.Sci.* **32**, 985-990.

Bonadonna, G., Monfardini, S., De Lena, M., & Fossati-Bellani, F. (1969) Clinical evaluation of adriamycin, a new antitumour antibiotic. *Br.Med.J.* **3**, 503-506.

Bostrom, H., Gritli-Linde, A., & Betsholtz, C. (2002) PDGF-A/PDGF alpha-receptor signaling is required for lung growth and the formation of alveoli but not for early lung branching morphogenesis. *Dev.Dyn.* **223**, 155-162.

Bostrom, H., Willetts, K., Pekny, M., Leveen, P., Lindahl, P., Hedstrand, H., Pekna, M., Hellstrom, M., Gebre-Medhin, S., Schalling, M., Nilsson, M., Kurland, S., Tornell, J., Heath, J. K., & Betsholtz, C. (1996) PDGF-A signaling is a critical event in lung alveolar myofibroblast development and alveogenesis. *Cell* **85**, 863-873.

Breitschopf, H., Suchanek, G., Gould, R. M., Colman, D. R., & Lassmann, H. (1992) In situ hybridization with digoxigenin-labeled probes: sensitive and reliable detection method applied to myelinating rat brain. *Acta Neuropathol.(Berl)* **84**, 581-587.

Brewer, C., Holloway, S., Zawalnyski, P., Schinzel, A., & FitzPatrick, D. (1998) A chromosomal deletion map of human malformations. *Am.J.Hum.Genet.* **63**, 1153-1159.

Briscoe, J., Chen, Y., Jessell, T. M., & Struhl, G. (2001) A hedgehog-insensitive form of patched provides evidence for direct long-range morphogen activity of sonic hedgehog in the neural tube. *Mol.Cell* **7**, 1279-1291.

Brown, A. K., Roddam, A. W., Spitz, L., & Ward, S. J. (1999) Oesophageal atresia, related malformations, and medical problems: a family study. *Am.J.Med.Genet.* **85**, 31-37.

Brunner, H. G. & Winter, R. M. (1991) Autosomal dominant inheritance of abnormalities of the hands and feet with short palpebral fissures, variable microcephaly with learning disability, and oesophageal/duodenal atresia. *J.Med.Genet.* **28**, 389-394.

Bumcrot, D. A., Takada, R., & McMahon, A. P. (1995) Proteolytic processing yields two secreted forms of sonic hedgehog. *Mol.Cell Biol.* **15**, 2294-2303.

Bursch, W. (2004) Multiple cell death programs: Charon's lifts to Hades. *FEMS Yeast Res.* **5**, 101-110.

Celli, J., van Beusekom, E., Hennekam, R. C., Gallardo, M. E., Smeets, D. F., de Cordoba, S. R., Innis, J. W., Frydman, M., Konig, R., Kingston, H., Tolmie, J., Govaerts, L. C., van Bokhoven, H., & Brunner, H. G. (2000) Familial syndromic esophageal atresia maps to 2p23-p24. *Am.J.Hum.Genet.* **66**, 436-444.

Charrier, J. B., Lapointe, F., Le Douarin, N. M., & Teillet, M. A. (2001) Anti-apoptotic role of Sonic hedgehog protein at the early stages of nervous system organogenesis. *Development* **128**, 4011-4020.

Cheng, G., Wessels, A., Gourdie, R. G., & Thompson, R. P. (2002) Spatiotemporal and tissue specific distribution of apoptosis in the developing chick heart. *Dev.Dyn.* **223**, 119-133.

Cheng, Y., Deshmukh, M., D'Costa, A., Demaro, J. A., Gidday, J. M., Shah, A., Sun, Y., Jacquin, M. F., Johnson, E. M., & Holtzman, D. M. (1998) Caspase inhibitor affords neuroprotection with delayed administration in a rat model of neonatal hypoxic-ischemic brain injury. *J.Clin.Invest* **101**, 1992-1999.

Chetcuti, P., Phelan, P. D., & Greenwood, R. (1992) Lung function abnormalities in repaired oesophageal atresia and tracheo-oesophageal fistula. *Thorax* **47**, 1030-1034.

Chiang, C., Litingtung, Y., Lee, E., Young, K. E., Corden, J. L., Westphal, H., & Beachy, P. A. (1996) Cyclopia and defective axial patterning in mice lacking Sonic hedgehog gene function. *Nature* **383**, 407-413.

Chittmittrapap, S., Spitz, L., Kiely, E. M., & Brereton, R. J. (1989) Oesophageal atresia and associated anomalies. *Arch.Dis.Child* **64**, 364-368.

Chuong, C. M., Patel, N., Lin, J., Jung, H. S., & Widelitz, R. B. (2000) Sonic hedgehog signaling pathway in vertebrate epithelial appendage morphogenesis: perspectives in development and evolution. *Cell Mol.Life Sci.* **57**, 1672-1681.

Ciruna, B. G., Schwartz, L., Harpal, K., Yamaguchi, T. P., & Rossant, J. (1997) Chimeric analysis of fibroblast growth factor receptor-1 (Fgfr1) function: a role for FGFR1 in morphogenetic movement through the primitive streak. *Development* **124**, 2829-2841.

Clarke, A. R., Purdie, C. A., Harrison, D. J., Morris, R. G., Bird, C. C., Hooper, M. L., & Wyllie, A. H. (1993) Thymocyte apoptosis induced by p53-dependent and independent pathways. *Nature* **362**, 849-852.

Clementi, M., Di Gianantonio, E., Pelo, E., Mammi, I., Basile, R. T., & Tenconi, R. (1999) Methimazole embryopathy: delineation of the phenotype. *Am.J.Med.Genet.* **83**, 43-46.

Cockroft, D.L. (1990) Dissection and culture of postimplantation embryos. In *Postimplantation Mammalian Embryos – A Practical Approach,* eds: A.J. Copp and D.L.Cockcroft – Oxford University Press

Coin, R., Kieffer, S., Lesot, H., Vonesch, J. L., & Ruch, J. V. (2000) Inhibition of apoptosis in the primary enamel knot does not affect specific tooth crown morphogenesis in the mouse. *Int.J.Dev.Biol.* **44**, 389-396.

Cook, G., Sharp, R. A., Tansey, P., & Franklin, I. M. (1996) A phase I/II trial of Z-Dex (oral idarubicin and dexamethasone), an oral equivalent of VAD, as initial therapy at diagnosis or progression in multiple myeloma. *Br.J.Haematol.* **93**, 931-934.

Copp, A.J., Cogram, P., Fleming, A., Gerelli, D., Henderson, D.J., Hynes, A., Kolatsi-Joannou, M., Murdoch, J.M. and Ybot-Gonzalez, P. (1999) Neurulation and neural tube closure defects. In: *Developmental Biology Protocols, Volume 1,* eds: R.S. Tuan and C.W. Lo – Academic Press: New York

Costa, R. H., Kalinichenko, V. V., & Lim, L. (2001) Transcription factors in mouse lung development and function. *Am.J.Physiol Lung Cell Mol.Physiol* **280**, L823-L838.

Coucouvanis, E. & Martin, G. R. (1995) Signals for death and survival: a two-step mechanism for cavitation in the vertebrate embryo. *Cell* **83**, 279-287.

Courtens, W., Levi, S., Verbelen, F., Verloes, A., & Vamos, E. (1997) Feingold syndrome: report of a new family and review. *Am.J.Med.Genet.* **73**, 55-60.

Crisera, C. A., Connelly, P. R., Marmureanu, A. R., Colen, K. L., Rose, M. I., Li, M., Longaker, M. T., & Gittes, G. K. (1999a) Esophageal atresia with tracheoesophageal fistula: suggested mechanism in faulty organogenesis. *J.Pediatr.Surg.* **34**, 204-208.

Crisera, C. A., Connelly, P. R., Marmureanu, A. R., Li, M., Rose, M. I., Longaker, M. T., & Gittes, G. K. (1999b) TTF-1 and HNF-3beta in the developing tracheoesophageal fistula: further evidence for the respiratory origin of the distal esophagus'. *J.Pediatr.Surg.* **34**, 1322-1326.

Crisera, C. A., Grau, J. B., Maldonado, T. S., Kadison, A. S., Longaker, M. T., & Gittes, G. K. (2000b) Defective epithelial-mesenchymal interactions dictate the organogenesis of tracheoesophageal fistula. *Pediatr.Surg.Int.* **16**, 256-261.

Crisera, C. A., Maldonado, T. S., Longaker, M. T., & Gittes, G. K. (2000a) Defective fibroblast growth factor signaling allows for nonbranching growth of the respiratory-derived fistula tract in esophageal atresia with tracheoesophageal fistula. *J.Pediatr.Surg.* **35**, 1421-1425.

Cuervo, R., Valencia, C., Chandraratna, R. A., & Covarrubias, L. (2002) Programmed cell death is required for palate shelf fusion and is regulated by retinoic acid. *Dev.Biol.* **245** , 145-156.

Curry, C. J., Jensen, K., Holland, J., Miller, L., & Hall, B. D. (1984) The Potter sequence: a clinical analysis of 80 cases. *Am.J.Med.Genet.* **19**, 679-702.

Czeizel, A. (1981) Schisis-association. *Am.J.Med.Genet.* **10**, 25-35.

de Vries, P. A. & Friedland, G. W. (1974) The staged sequential development of the anus and rectum in human embryos and fetuses. *J.Pediatr.Surg.* **9**, 755-769.

DeBiasi, R. L., Robinson, B. A., Sherry, B., Bouchard, R., Brown, R. D., Rizeq, M., Long, C., & Tyler, K. L. (2004) Caspase inhibition protects against reovirus-induced myocardial injury in vitro and in vivo. *J.Virol.* **78**, 11040-11050.

Deutsch, G., Jung, J., Zheng, M., Lora, J., & Zaret, K. S. (2001) A bipotential precursor population for pancreas and liver within the embryonic endoderm. *Development* **128**, 871-881.

Didenko, V. V., Ngo, H., Minchew, C. L., Boudreaux, D. J., Widmayer, M. A., & Baskin, D. S. (2002) Caspase-3-dependent and -independent apoptosis in focal brain ischemia. *Mol.Med.* **8**, 347-352.

Diez-Pardo, J. A., Baoquan, Q., Navarro, C., & Tovar, J. A. (1996) A new rodent experimental model of esophageal atresia and tracheoesophageal fistula: preliminary report. *J.Pediatr.Surg.* **31**, 498-502.

Digilio, M. C., Marino, B., Bagolan, P., Giannotti, A., & Dallapiccola, B. (1999) Microdeletion 22q11 and oesophageal atresia. *J.Med.Genet.* **36**, 137-139.

Donovan, M. & Cotter, T. G. (2004) Control of mitochondrial integrity by Bcl-2 family members and caspase-independent cell death. *Biochim.Biophys.Acta* **1644**, 133-147.

Drossopoulou, G., Lewis, K. E., Sanz-Ezquerro, J. J., Nikbakht, N., McMahon, A. P., Hofmann, C., & Tickle, C. (2000) A model for anteroposterior patterning of the vertebrate limb based on sequential. *Development* **127**, 1337-1348.

Duan, W. R., Garner, D. S., Williams, S. D., Funckes-Shippy, C. L., Spath, I. S., & Blomme, E. A. (2003) Comparison of immunohistochemistry for activated caspase-3 and cleaved cytokeratin 18 with the TUNEL method for quantification of apoptosis in histological sections of PC-3 subcutaneous xenografts. *J.Pathol.* **199**, 221-228.

Dutta, H. K., Mathur, M., & Bhatnagar, V. (2000) A histopathological study of esophageal atresia and tracheoesophageal fistula. *J.Pediatr.Surg.* **35**, 438-441.

Edlund, H. (1998) Transcribing pancreas. *Diabetes* **47**, 1817-1823.

Ericson, J., Morton, S., Kawakami, A., Roelink, H., & Jessell, T. M. (1996) Two critical periods of Sonic Hedgehog signaling required for the specification of motor neuron identity. *Cell* **87**, 661-673.

Ericson, J., Rashbass, P., Schedl, A., Brenner-Morton, S., Kawakami, A., van, H., V, Jessell, T. M., & Briscoe, J. (1997) Pax6 controls progenitor cell identity and neuronal fate in response to graded Shh signaling. *Cell* **90**, 169-180.

Fauvel, H., Marchetti, P., Chopin, C., Formstecher, P., & Neviere, R. (2001) Differential effects of caspase inhibitors on endotoxin-induced myocardial dysfunction and heart apoptosis. *Am.J.Physiol Heart Circ.Physiol* **280**, H1608-H1614.

Fearnhead, H. O., Dinsdale, D., & Cohen, G. M. (1995) An interleukin-1 beta-converting enzyme-like protease is a common mediator of apoptosis in thymocytes. *FEBS Lett.* **375**, 283-288.

Feingold, M., Hall, B. D., Lacassie, Y., & Martinez-Frias, M. L. (1997) Syndrome of microcephaly, facial and hand abnormalities, tracheoesophageal fistula, duodenal atresia, and developmental delay. *Am.J.Med.Genet.* **69**, 245-249.

Geada, A. M., Gaunt, S. J., Azzawi, M., Shimeld, S. M., Pearce, J., & Sharpe, P. T. (1992) Sequence and embryonic expression of the murine Hox-3.5 gene. *Development* **116**, 497-506.

Gerrelli, D. & Copp, A. J. (1997) Failure of neural tube closure in the loop-tail (Lp) mutant mouse: analysis of the embryonic mechanism. *Brain Res.Dev.Brain Res.* **102**, 217-224.

Gillick, J., Giles, S., Bannigan, J., & Puri, P. (2002b) Cell death in the early adriamycin rat model. *Pediatr.Surg.Int.* **18**, 576-580.

Gillick, J., Giles, S., Bannigan, S., & Puri, P. (2002a) Midgut atresias result from abnormal development of the notochord in an Adriamycin rat model. *J.Pediatr.Surg.* **37**, 719-722.

Gillick, J., Mooney, E., Giles, S., Bannigan, J., & Puri, P. (2003) Notochord anomalies in the adriamycin rat model: A morphologic and molecular basis for the VACTERL association. *J.Pediatr.Surg.* **38**, 469-473.

Goldin, G. V., Hindman, H. M., & Wessells, N. K. (1984) The role of cell proliferation and cellular shape change in branching morphogenesis of the embryonic mouse lung: analysis using aphidicolin and cytochalasins. *J.Exp.Zool.* **232**, 287-296.

Goldin, G. V. & Wessells, N. K. (1979) Mammalian lung development: the possible role of cell proliferation in the formation of supernumerary tracheal buds and in branching morphogenesis. *J.Exp.Zool.* **208**, 337-346.

Graebert, K. S., Bauch, H., Neumuller, W., Brix, K., & Herzog, V. (1997) Epithelial folding in vitro: studies on the cellular mechanism underlying evagination of thyrocyte monolayers. *Exp.Cell Res.* **231**, 214-225.

Grapin-Botton, A. & Melton, D. A. (2000) Endoderm development: from patterning to organogenesis. *Trends Genet.* **16**, 124-130.

Gray, S.W. & Scandalakis, J.E. (1972) *Embryology for surgeons.* Philadelphia, PA, Saunders, 63-100

Grindley, J. C., Bellusci, S., Perkins, D., & Hogan, B. L. (1997) Evidence for the involvement of the Gli gene family in embryonic mouse lung development. *Dev.Biol.* **188**, 337-348.

Gritli-Linde, A., Lewis, P., McMahon, A. P., & Linde, A. (2001) The whereabouts of a morphogen: direct evidence for s. *Dev.Biol.* **236**, 364-386.

Gualdi, R., Bossard, P., Zheng, M., Hamada, Y., Coleman, J. R., & Zaret, K. S. (1996) Hepatic specification of the gut endoderm in vitro: cell signaling and transcriptional control. *Genes Dev.* **10**, 1670-1682.

Hancock, J. M. (2004) A bigger mouse? The rat genome unveiled. *Bioessays* **26**, 1039-1042.

Have-Opbroek, A. A. (1981) The development of the lung in mammals: an analysis of concepts and findings. *Am.J.Anat.* **162**, 201-219.

Hebrok, M., Kim, S. K., & Melton, D. A. (1998) Notochord repression of endodermal Sonic hedgehog permits pancreas development. *Genes Dev.* **12**, 1705-1713.

Hebrok, M., Kim, S. K., St Jacques, B., McMahon, A. P., & Melton, D. A. (2000) Regulation of pancreas development by hedgehog signaling. *Development* **127**, 4905-4913.

Henry, G. L. & Melton, D. A. (1998) Mixer, a homeobox gene required for endoderm development. *Science* **281**, 91-96.

Hoshi, T., Sasano, H., Kato, K., Yabuki, N., Ohara, S., Konno, R., Asaki, S., Toyota, T., Tateno, H., & Nagura, H. (1998) Immunohistochemistry of Caspase3/CPP32 in human stomach and its correlation with cell proliferation and apoptosis. *Anticancer Res.* **18**, 4347-4353.

Hudson, C., Clements, D., Friday, R. V., Stott, D., & Woodland, H. R. (1997) Xsox17alpha and -beta mediate endoderm formation in Xenopus. *Cell* **91**, 397-405.

Ibrahim, N. B. & Sandry, R. J. (1981) Congenital oesophageal stenosis caused by tracheobronchial structures in the oesophageal wall. *Thorax* **36**, 465-468.

Icardo, J. M. (1996) Developmental biology of the vertebrate heart. *J.Exp.Zool.* **275**, 144-161.

Incardona, J. P., Lee, J. H., Robertson, C. P., Enga, K., Kapur, R. P., & Roelink, H. (2000) Receptor-mediated endocytosis of soluble and membrane-tethered Sonic hedgehog by Patched-1. *Proc.Natl.Acad.Sci.U.S.A* **97**, 12044-12049.

Ingham, P. W. (1998) Transducing Hedgehog: the story so far. *EMBO J.* **17**, 3505-3511.

Ishii, Y., Fukuda, K., Saiga, H., Matsushita, S., & Yasugi, S. (1997) Early specification of intestinal epithelium in the chicken embryo: a study on the localization and regulation of CdxA expression. *Dev.Growth Differ.* **39**, 643-653.

Ishii, Y., Rex, M., Scotting, P. J., & Yasugi, S. (1998) Region-specific expression of chicken Sox2 in the developing gut and lung epithelium: regulation by epithelial-mesenchymal interactions. *Dev.Dyn.* **213**, 464-475.

Iuchtman, M., Brereton, R., Spitz, L., Kiely, E. M., & Drake, D. (1992) Morbidity and mortality in 46 patients with the VACTERL association. *Isr.J.Med.Sci.* **28**, 281-284.

Jaattela, M. (2002) Programmed cell death: many ways for cells to die decently. *Ann.Med.* **34**, 480-488.

Jacobson, M. D., Weil, M., & Raff, M. C. (1997) Programmed cell death in animal development. *Cell* **88**, 347-354.

Johnson, R. L., Riddle, R. D., Laufer, E., & Tabin, C. (1994) Sonic hedgehog: a key mediator of anterior-posterior patterning of the limb and dorso-ventral patterning of axial embryonic structures. *Biochem.Soc.Trans.* **22**, 569-574.

KALTER, H. & WARKANY, J. (1957) Congenital malformations in inbred strains of mice induced by riboflavin-deficient, galactoflavin-containing diets. *J.Exp.Zool.* **136**, 531-565.

Kang, H. C., Ohmori, M., Harii, N., Endo, T., & Onaya, T. (2001) Pax-8 is essential for regulation of the thyroglobulin gene by transforming growth factor-beta1. *Endocrinology* **142**, 267-275.

Kang, S., Graham, J. M., Jr., Olney, A. H., & Biesecker, L. G. (1997) GLI3 frameshift mutations cause autosomal dominant Pallister-Hall syndrome. *Nat.Genet.* **15**, 266-268.

Kashuk, J. L. & Lilly, J. R. (1983) Esophageal atresia in father and son. *J.Pediatr.Surg.* **18**, 621-622.

Kim, P. C., Mo, R., & Hui, C. C. (2001) Murine models of VACTERL syndrome: Role of sonic hedgehog signaling pathway. *J.Pediatr.Surg.* **36**, 381-384.

Kim, S. K., Hebrok, M., Li, E., Oh, S. P., Schrewe, H., Harmon, E. B., Lee, J. S., & Melton, D. A. (2000) Activin receptor patterning of foregut organogenesis. *Genes Dev.* **14**, 1866-1871.

Kim, S. K., Hebrok, M., & Melton, D. A. (1997) Notochord to endoderm signaling is required for pancreas development. *Development* **124**, 4243-4252.

Kleckner, S. C., Pringle, K. C., & Clark, E. B. (1984) The effect of chick embryo hyperflexion on tracheoesophageal development. *J.Pediatr.Surg.* **19**, 340-344.

Kluth, D. & Fiegel, H. (2003) The embryology of the foregut. *Semin.Pediatr.Surg.* **12**, 3-9.

Kluth, D. & Lambrecht, W. (1997a) Applied embryology in pediatric surgery. *Eur.J.Pediatr.Surg.* **7**, 196-203.

Kluth, D. & Lambrecht, W. (1997b) Current concepts in the embryology of anorectal malformations. *Semin.Pediatr.Surg.* **6**, 180-186.

Kluth, D., Steding, G., & Seidl, W. (1987) The embryology of foregut malformations. *J.Pediatr.Surg.* **22**, 389-393.

Kobayashi, M., Azuma, E., Ido, M., Hirayama, M., Jiang, Q., Iwamoto, S., Kumamoto, T., Yamamoto, H., Sakurai, M., & Komada, Y. (2001) A pivotal role of Rho GTPase in the regulation of morphology and function of dendritic cells. *J.Immunol.* **167**, 3585-3591.

Koivusalo, A., Pakarinen, M. P., Turunen, P., Saarikoski, H., Lindahl, H., & Rintala, R. J. (2005) Health-related quality of life in adult patients with esophageal atresia-a questionnaire study. *J.Pediatr.Surg.* **40**, 307-312.

Koletzko, B. & Majewski, F. (1984) Congenital anomalies in patients with choanal atresia: CHARGE-association. *Eur.J.Pediatr.* **142**, 271-275.

Kolker, A. R., Coombs, C. J., Meara, J. G., Bates, D., Rowler, D. K., & Hutson, J. M. (2000) Patterns of radial dysmorphology with the VACTERL association in the adriamycin-exposed prenatal rat. *Ann.Plast.Surg.* **45**, 525-530.

Kotsios, C., Merei, J., Hutson, J. M., & Graham, H. K. (1998) Skeletal anomalies in the adriamycin-exposed prenatal rat: a model for VATER association. *J.Orthop.Res.* **16**, 50-53.

Kumar, S. & Harvey, N. L. (1995) Role of multiple cellular proteases in the execution of programmed cell death. *FEBS Lett.* **375**, 169-173.

Kuo, C. T., Morrisey, E. E., Anandappa, R., Sigrist, K., Lu, M. M., Parmacek, M. S., Soudais, C., & Leiden, J. M. (1997) GATA4 transcription factor is required for ventral morphogenesis and heart tube formation. *Genes Dev.* **11**, 1048-1060.

Lawson, K. A., Meneses, J. J., & Pedersen, R. A. (1986) Cell fate and cell lineage in the endoderm of the presomite mouse embryo, studied with an intracellular tracer. *Dev.Biol.* **115**, 325-339.

Lawson, K. A., Meneses, J. J., & Pedersen, R. A. (1991) Clonal analysis of epiblast fate during germ layer formation in the mouse embryo. *Development* **113**, 891-911.

Lawson, K. A. & Pedersen, R. A. (1987) Cell fate, morphogenetic movement and population kinetics of embryonic endoderm at the time of germ layer formation in the mouse. *Development* **101**, 627-652.

Lazzaro, D., Price, M., De Felice, M., & Di Lauro, R. (1991) The transcription factor TTF-1 is expressed at the onset of thyroid and lung morphogenesis and in restricted regions of the foetal brain. *Development* **113**, 1093-1104.

LeSouef, P. N., Myers, N. A., & Landau, L. I. (1987) Etiologic factors in long-term respiratory function abnormalities following esophageal atresia repair. *J.Pediatr.Surg.* **22**, 918-922.

Levi, G., Gumbiner, B., & Thiery, J. P. (1991) The distribution of E-cadherin during Xenopus laevis development. *Development* **111**, 159-169.

Li, C., Cai, J., Pan, Q., & Minoo, P. (2000a) Two functionally distinct forms of NKX2.1 protein are expressed in the pulmonary epithelium. *Biochem.Biophys.Res.Commun.* **270**, 462-468.

Li, H., Colbourne, F., Sun, P., Zhao, Z., Buchan, A. M., & Iadecola, C. (2000b) Caspase inhibitors reduce neuronal injury after focal but not global cerebral ischemia in rats. *Stroke* **31**, 176-182.

Lin, T. P., Labosky, P. A., Grabel, L. B., Kozak, C. A., Pitman, J. L., Kleeman, J., & MacLeod, C. L. (1994) The Pem homeobox gene is X-linked and exclusively expressed in extraembryonic tissues during early murine development. *Dev.Biol.* **166**, 170-179.

Lipson, A. H. & Berry, A. B. (1984) Oesophageal atresia in father and daughter. *Aust.Paediatr.J.* **20**, 329.

Litingtung, Y., Lei, L., Westphal, H., & Chiang, C. (1998) Sonic hedgehog is essential to foregut development. *Nat.Genet.* **20**, 58-61.

Liu, M. I. & Hutson, J. M. (2000) Cloacal and urogenital malformations in adriamycin-exposed rat fetuses. *BJU.Int.* **86**, 107-112.

Mahlapuu, M., Enerback, S., & Carlsson, P. (2001a) Haploinsufficiency of the forkhead gene Foxf1, a target for sonic hedgehog signaling, causes lung and foregut malformations. *Development* **128**, 2397-2406.

Marchetti, P., Castedo, M., Susin, S. A., Zamzami, N., Hirsch, T., Macho, A., Haeffner, A., Hirsch, F., Geuskens, M., & Kroemer, G. (1996) Mitochondrial permeability transition is a central coordinating event of apoptosis. *J.Exp.Med.* **184**, 1155-1160.

Marigo, V., Laufer, E., Nelson, C. E., Riddle, R. D., Johnson, R. L., & Tabin, C. (1996) Sonic hedgehog regulates patterning in early embryos. *Biochem.Soc.Symp.* **62**, 51-60.

Marsh, A. J., Wellesley, D., Burge, D., Ashton, M., Browne, C., Dennis, N. R., & Temple, K. (2000) Interstitial deletion of chromosome 17 (del(17)(q22q23.3)) confirms a link with oesophageal atresia. *J.Med.Genet.* **37**, 701-704.

Marti, E., Takada, R., Bumcrot, D. A., Sasaki, H., & McMahon, A. P. (1995) Distribution of Sonic hedgehog peptides in the developing chick and mouse embryo. *Development* **121**, 2537-2547.

Martinez, L., Ceano-Vivas, M. D., Gonzalez-Reyes, S., Hernandez, F., Fernandez-Dumont, V., Calonge, W. M., Ruiz, E., Rodriguez, J. I., & Tovar, J. A. (2004) Decrease of parafollicular thyroid C-cells in experimental esophageal atresia: further evidence of a neural crest pathogenic pathway. *Pediatr.Surg.Int.*

Matsushita, S. (1999) Fate mapping study of the endoderm in the posterior part of the 1.5-day-old chick embryo. *Dev.Growth Differ.* **41**, 313-319.

McCarthy, R. A. & Argraves, W. S. (2003) Megalin and the neurodevelopmental biology of sonic hedgehog and retinol. *J.Cell Sci.* **116**, 955-960.

McCarthy, R. A., Barth, J. L., Chintalapudi, M. R., Knaak, C., & Argraves, W. S. (2002) Megalin functions as an endocytic sonic hedgehog receptor. *J.Biol.Chem.* **277**, 25660-25667.

Merei, J., Batiha, A., Hani, I. B., & El Qudah, M. (2001) Renal anomalies in the VATER animal model. *J.Pediatr.Surg.* **36**, 1693-1697.

Merei, J., Hasthorpe, S., Farmer, P., & Hutson, J. M. (1998) Relationship between esophageal atresia with tracheoesophageal fistula and vertebral anomalies in mammalian embryos. *J.Pediatr.Surg.* **33**, 58-63.

Merei, J., Hasthorpe, S., Farmer, P., & Hutson, J. M. (1999) Visceral anomalies in prenatally adriamycin-exposed rat fetuses: a model for the VATER association. *Pediatr.Surg.Int.* **15**, 11-16.

Merei, J., Kotsios, C., Hutson, J. M., & Hasthorpe, S. (1997a) Histopathologic study of esophageal atresia and tracheoesophageal fistula in an animal model. *J.Pediatr.Surg.* **32**, 12-14.

Merei, J. M. (2004) Notochord-gut failure of detachment and intestinal atresia. *Pediatr.Surg.Int.* **20**, 439-443.

Merei, J. M., Farmer, P., Hasthorpe, S., Qi, B. Q., Beasley, S. W., Myers, N. A., & Hutson, J. M. (1997b) Timing and embryology of esophageal atresia and tracheo-esophageal fistula. *Anat.Rec.* **249**, 240-248.

Methot, N. & Basler, K. (2001) An absolute requirement for Cubitus interruptus in Hedgehog signaling. *Development* **128**, 733-742.

Millar, A. J., Forootan, H., & Rode, H. (2001) An adriamycin experimental rat model inducing a wide variety of abnormalities similar to VACTERL association in humans is now well established. *Pediatr.Surg.Int.* **17**, 502.

Milligan, C. E., Prevette, D., Yaginuma, H., Homma, S., Cardwell, C., Fritz, L. C., Tomaselli, K. J., Oppenheim, R. W., & Schwartz, L. M. (1995) Peptide inhibitors of the ICE protease family arrest programmed cell death of motoneurons in vivo and in vitro. *Neuron* **15**, 385-393.

Ming, J. E., Kaupas, M. E., Roessler, E., Brunner, H. G., Golabi, M., Tekin, M., Stratton, R. F., Sujansky, E., Bale, S. J., & Muenke, M. (2002) Mutations in PATCHED-1, the receptor for SONIC HEDGEHOG, are associated with holoprosencephaly. *Hum.Genet.* **110**, 297-301.

Ming, J. E., Roessler, E., & Muenke, M. (1998) Human developmental disorders and the Sonic hedgehog pathway. *Mol.Med.Today* **4**, 343-349.

Minoo, P. (2000) Transcriptional regulation of lung development: emergence of specificity. *Respir.Res.* **1**, 109-115.

Minoo, P., Su, G., Drum, H., Bringas, P., & Kimura, S. (1999) Defects in tracheoesophageal and lung morphogenesis in Nkx2.1(-/-) mouse embryos. *Dev.Biol.* **209**, 60-71.

Molkentin, J. D., Lin, Q., Duncan, S. A., & Olson, E. N. (1997) Requirement of the transcription factor GATA4 for heart tube formation and ventral morphogenesis. *Genes Dev.* **11**, 1061-1072.

Moorman, A., Webb, S., Brown, N. A., Lamers, W., & Anderson, R. H. (2003) Development of the heart: (1) formation of the cardiac chambers and arterial trunks. *Heart* **89**, 806-814.

Mortell, A., O'Donnell, A. M., Giles, S., Bannigan, J., & Puri, P. (2004) Adriamycin induces notochord hypertrophy with conservation of sonic hedgehog expression in abnormal ectopic notochord in the adriamycin rat model. *J.Pediatr.Surg.* **39**, 859-863.

Motoyama, J., Liu, J., Mo, R., Ding, Q., Post, M., & Hui, C. C. (1998) Essential function of Gli2 and Gli3 in the formation of lung, trachea and oesophagus. *Nat.Genet.* **20**, 54-57.

Muller, B. & Basler, K. (2000) The repressor and activator forms of Cubitus interruptus control Hedgehog target genes through common generic gli-binding sites. *Development* **127**, 2999-3007.

New, D. A., Coppola, P. T., & Cockroft, D. L. (1976) Comparison of growth in vitro and in vivo of post-implantation rat embryos. *J.Embryol.Exp.Morphol.* **36**, 133-144.

Niswander, L. & Martin, G. R. (1992) Fgf-4 expression during gastrulation, myogenesis, limb and tooth development in the mouse. *Development* **114**, 755-768.

Noel, P. R., Barnett, K. C., Davies, R. E., Jolly, D. W., Leahy, J. S., Mawdesley-Thomas, L. E., Shillam, K. W., Squires, P. F., Street, A. E., Tucker, W. C., & Worden, A. N. (1975) The toxicity of dimethyl sulphoxide (DMSO) for the dog, pig, rat and rabbit. *Toxicology* **3**, 143-169.

O'Rahilly, R. (1983) The timing and sequence of events in the development of the human reproductive system during the embryonic period proper. *Anat.Embryol.(Berl)* **166**, 247-261.

O'Rahilly, R. & Muller, F. (1984) Chevalier Jackson lecture. Respiratory and alimentary relations in staged human embryos. New embryological data and congenital anomalies. *Ann.Otol.Rhinol.Laryngol.* **93**, 421-429.

Oostlander, A. E., Meijer, G. A., & Ylstra, B. (2004) Microarray-based comparative genomic hybridization and its applications in human genetics. *Clin.Genet.* **66**, 488-495.

Oppenheim, R. W., Homma, S., Marti, E., Prevette, D., Wang, S., Yaginuma, H., & McMahon, A. P. (1999) Modulation of early but not later stages of programmed cell death in embryonic avian spinal cord by sonic hedgehog. *Mol.Cell Neurosci.* **13**, 348-361.

Orford, J., Glasson, M., Beasley, S., Shi, E., Myers, N., & Cass, D. (2000) Oesophageal atresia in twins. *Pediatr.Surg.Int.* **16**, 541-545.

Orford, J., Manglick, P., Cass, D. T., & Tam, P. P. (2001) Mechanisms for the development of esophageal atresia. *J.Pediatr.Surg.* **36**, 985-994.

Orth, K., O'Rourke, K., Salvesen, G. S., & Dixit, V. M. (1996) Molecular ordering of apoptotic mammalian CED-3/ICE-like proteases. *J.Biol.Chem.* **271**, 20977-20980.

Otten, C., Migliazza, L., Xia, H., Rodriguez, J. I., Diez-Pardo, J. A., & Tovar, J. A. (2000) Neural crest-derived defects in experimental esophageal atresia. *Pediatr.Res.* **47**, 178-183.

Pabst, O., Herbrand, H., Takuma, N., & Arnold, H. H. (2000) NKX2 gene expression in neuroectoderm but not in mesendodermally derived structures depends on sonic hedgehog in mouse embryos. *Dev.Genes Evol.* **210**, 47-50.

Paidas, C. N., Morreale, R. F., Holoski, K. M., Lund, R. E., & Hutchins, G. M. (1999) Septation and differentiation of the embryonic human cloaca. *J.Pediatr.Surg.* **34**, 877-884.

Patten, I. & Placzek, M. (2002) Opponent activities of Shh and BMP signaling during floor plate induction in vivo. *Curr.Biol.* **12**, 47-52.

Pepicelli, C. V., Lewis, P. M., & McMahon, A. P. (1998) Sonic hedgehog regulates branching morphogenesis in the mammalian lung. *Curr.Biol.* **8**, 1083-1086.

Pera, E. M. & Kessel, M. (1998) Demarcation of ventral territories by the homeobox gene NKX2.1 during early chick development. *Dev.Genes Evol.* **208**, 168-171.

Peters, H., Neubuser, A., Kratochwil, K., & Balling, R. (1998) Pax9-deficient mice lack pharyngeal pouch derivatives and teeth and exhibit craniofacial and limb abnormalities. *Genes Dev.* **12**, 2735-2747.

Platt, K. A., Michaud, J., & Joyner, A. L. (1997) Expression of the mouse Gli and Ptc genes is adjacent to embryonic sources of hedgehog signals suggesting a conservation of pathways between flies and mice. *Mech.Dev.* **62**, 121-135.

Porter, J. A., Young, K. E., & Beachy, P. A. (1996) Cholesterol modification of hedgehog signaling proteins in animal development. *Science* **274**, 255-259.

Possoegel, A. K., Diez-Pardo, J. A., Morales, C., & Tovar, J. A. (1999) Notochord involvement in experimental esophageal atresia. *Pediatr.Surg.Int.* **15**, 201-205.

Possogel, A. K., Diez-Pardo, J. A., Morales, C., Navarro, C., & Tovar, J. A. (1998) Embryology of esophageal atresia in the adriamycin rat model. *J.Pediatr.Surg.* **33**, 606-612.

Qi, B. Q. & Beasley, S. W. (1998) Preliminary evidence that cell death may contribute to separation of the trachea from the primitive foregut in the rat embryo. *J.Pediatr.Surg.* **33**, 1660-1665.

Qi, B. Q. & Beasley, S. W. (1999) Relationship of the notochord to foregut development in the fetal rat model of esophageal atresia. *J.Pediatr.Surg.* **34**, 1593-1598.

Qi, B. Q. & Beasley, S. W. (2000) Stages of normal tracheo-bronchial development in rat embryos: resolution of a controversy. *Dev.Growth Differ.* **42**, 145-153.

Qi, B. Q., Beasley, S. W., & Frizelle, F. A. (2002) Clarification of the processes that lead to anorectal malformations in the ETU-induced rat model of imperforate anus. *J.Pediatr.Surg.* **37**, 1305-1312.

Qi, B. Q., Beasley, S. W., Williams, A. K., & Fizelle, F. (2000b) Apoptosis during regression of the tailgut and septation of the cloaca. *J.Pediatr.Surg.* **35**, 1556-1561.

Qi, B., Diez-Pardo J.A., Navarro C. & Tovar J.A. (1996) Narrowing the embryologic window of the adriamycin-induced fetal rat model of esophageal atresia and tracheoesophageal fistula. *Pediatr.Surg.Int.* **11**, 444-447

Qi, B. Q., Merei, J., Farmer, P., Hasthorpe, S., Hutson, J. M., Myers, N. A., & Beasley, S. W. (1997b) Tracheomalacia with esophageal atresia and tracheoesophageal fistula in fetal rats. *J.Pediatr.Surg.* **32**, 1575-1579.

Qi, B. Q., Merei, J., Farmer, P., Hasthorpe, S., Myers, N. A., Beasley, S. W., & Hutson, J. M. (1997a) Cardiovascular malformations in rat fetuses with oesophageal atresia and tracheo-oesophageal fistula induced by adriamycin. *Pediatr.Surg.Int.* **12**, 556-564.

Qi, B. Q., Williams, A., Beasley, S., & Frizelle, F. (2000a) Clarification of the process of separation of the cloaca into rectum and urogenital sinus in the rat embryo. *J.Pediatr.Surg.* **35**, 1810-1816.

Rhinn, M., Dierich, A., Shawlot, W., Behringer, R. R., Le Meur, M., & Ang, S. L. (1998) Sequential roles for Otx2 in visceral endoderm and neuroectoderm for forebrain and midbrain induction and specification. *Development* **125**, 845-856.

Riddle, R. D., Johnson, R. L., Laufer, E., & Tabin, C. (1993) Sonic hedgehog mediates the polarizing activity of the ZPA. *Cell* **75**, 1401-1416.

Roberts, D. J., Smith, D. M., Goff, D. J., & Tabin, C. J. (1998) Epithelial-mesenchymal signaling during the regionalization of the chick gut. *Development* **125**, 2791-2801.

Robertson, D. F., Mobaireek, K., Davis, G. M., & Coates, A. L. (1995) Late pulmonary function following repair of tracheoesophageal fistula or esophageal atresia. *Pediatr.Pulmonol.* **20**, 21-26.

Roelink, H., Porter, J. A., Chiang, C., Tanabe, Y., Chang, D. T., Beachy, P. A., & Jessell, T. M. (1995) Floor plate and motor neuron induction by different concentrations of the amino-terminal cleavage product of sonic hedgehog autoproteolysis. *Cell* **81**, 445-455.

Roessler, E., Belloni, E., Gaudenz, K., Jay, P., Berta, P., Scherer, S. W., Tsui, L. C., & Muenke, M. (1996) Mutations in the human Sonic Hedgehog gene cause holoprosencephaly. *Nat.Genet.* **14**, 357-360.

Rogers, D. S., Paidas, C. N., Morreale, R. F., & Hutchins, G. M. (2002) Septation of the anorectal and genitourinary tracts in the human embryo: crucial role of the catenoidal shape of the urorectal sulcus. *Teratology* **66**, 144-152.

Romeo, G., Zuccarello, B., Proietto, F., & Romeo, C. (1987) Disorders of the esophageal motor activity in atresia of the esophagus. *J.Pediatr.Surg.* **22**, 120-124.

Rosenblatt, J., Raff, M. C., & Cramer, L. P. (2001) An epithelial cell destined for apoptosis signals its neighbors to extrude it by an a. *Curr.Biol.* **11**, 1847-1857.

Ross, W. E., Glaubiger, D. L., & Kohn, K. W. (1978) Protein-associated DNA breaks in cells treated with adriamycin or ellipticine. *Biochim.Biophys.Acta* **519**, 23-30.

Sacedon, R., Diez, B., Nunez, V., Hernandez-Lopez, C., Gutierrez-Frias, C., Cejalvo, T., Outram, S. V., Crompton, T., Zapata, A. G., Vicente, A., & Varas, A. (2005) Sonic hedgehog is produced by follicular dendritic cells and protects germinal center B cells from apoptosis. *J.Immunol.* **174**, 1456-1461.

Sakiyama, J., Yamagishi, A., & Kuroiwa, A. (2003) Tbx4-Fgf10 system controls lung bud formation during chicken embryonic development. *Development* **130**, 1225-1234.

Sanz-Ezquerro, J. J. & Tickle, C. (2000) Autoregulation of Shh expression and Shh induction of cell death suggest a mechanism for modulating polarising activity during chick limb development. *Development* **127**, 4811-4823.

Sasaki, T., Kusafuka, T., & Okada, A. (2001) Analysis of the development of normal foregut and tracheoesophageal fistula in an adriamycin rat model using three-dimensional image reconstruction. *Surg.Today* **31**, 133-139.

Sekine, K., Ohuchi, H., Fujiwara, M., Yamasaki, M., Yoshizawa, T., Sato, T., Yagishita, N., Matsui, D., Koga, Y., Itoh, N., & Kato, S. (1999) Fgf10 is essential for limb and lung formation. *Nat.Genet.* **21**, 138-141.

Sharma, P. R., Anderson, R. H., Copp, A. J., & Henderson, D. J. (2004) Spatiotemporal analysis of programmed cell death during mouse cardiac septation. *Anat.Rec.A Discov.Mol.Cell Evol.Biol.* **277**, 355-369.

Slee, E. A., Zhu, H., Chow, S. C., MacFarlane, M., Nicholson, D. W., & Cohen, G. M. (1996) Benzyloxycarbonyl-Val-Ala-Asp (OMe) fluoromethylketone (Z-VAD.FMK) inhibits apoptosis by blocking the processing of CPP32. *Biochem.J.* **315 (Pt 1)**, 21-24.

Small, E. M., Vokes, S. A., Garriock, R. J., Li, D., & Krieg, P. A. (2000) Developmental expression of the Xenopus Nkx2-1 and Nkx2-4 genes. *Mech.Dev.* **96**, 259-262.

Smith, J. L. & Schoenwolf, G. C. (1987) Cell cycle and neuroepithelial cell shape during bending of the chick neural plate. *Anat.Rec.* **218**, 196-206.

Somppi, E., Tammela, O., Ruuska, T., Rahnasto, J., Laitinen, J., Turjanmaa, V., & Jarnberg, J. (1998) Outcome of patients operated on for esophageal atresia: 30 years' experience. *J.Pediatr.Surg.* **33**, 1341-1346.

Spilde, T., Bhatia, A., Ostlie, D., Marosky, J., Holcomb, G., III, Snyder, C., & Gittes, G. (2003c) A role for sonic hedgehog signaling in the pathogenesis of human tracheoesophageal fistula. *J.Pediatr.Surg.* **38**, 465-468.

Spilde, T. L., Bhatia, A. M., Marosky, J. K., Hembree, M. J., Kobayashi, H., Daume, E. L., Prasadan, K., Manna, P., Preuett, B. L., & Gittes, G. K. (2002a) Complete discontinuity of the distal fistula tract from the developing gut: direct histologic evidence for the mechanism of tracheoesophageal fistula formation. *Anat.Rec.* **267**, 220-224.

Spilde, T. L., Bhatia, A. M., Marosky, J. K., Preuett, B., Kobayashi, H., Hembree, M. J., Prasadan, K., Daume, E., Snyder, C. L., & Gittes, G. K. (2003a) Fibroblast growth factor signaling in the developing tracheoesophageal fistula. *J.Pediatr.Surg.* **38**, 474-477.

Spilde, T. L., Bhatia, A. M., Mehta, S., Ostlie, D. J., Hembree, M. J., Preuett, B. L., Prasadan, K., Li, Z., Snyder, C. L., & Gittes, G. K. (2003b) Defective sonic hedgehog signaling in esophageal atresia with tracheoesophageal fistula. *Surgery* **134**, 345-350.

Spilde, T. L., Bhatia, A. M., Miller, K. A., Ostlie, D. J., Chaignaud, B. E., Holcomb, G. W., III, Snyder, C. L., & Gittes, G. K. (2002b) Thyroid transcription factor-1 expression in the human neonatal tracheoesophageal fistula. *J.Pediatr.Surg.* **37**, 1065-1067.

Spitz, L. (1993) Esophageal atresia and tracheoesophageal fistula in children. *Curr.Opin.Pediatr.* **5**, 347-352.

Spitz, L. (1996) Esophageal atresia: past, present, and future. *J.Pediatr.Surg.* **31**, 19-25.

Spitz, L., Kiely, E. M., Morecroft, J. A., & Drake, D. P. (1994) Oesophageal atresia: at-risk groups for the 1990s. *J.Pediatr.Surg.* **29**, 723-725.

Su, D., Ellis, S., Napier, A., Lee, K., & Manley, N. R. (2001) Hoxa3 and pax1 regulate epithelial cell death and proliferation during thymus and parathyroid organogenesis. *Dev.Biol.* **236**, 316-329.

Sun, F., Akazawa, S., Sugahara, K., Kamihira, S., Kawasaki, E., Eguchi, K., & Koji, T. (2002) Apoptosis in normal rat embryo tissues during early organogenesis: the possible involvement of Bax and Bcl-2. *Arch.Histol.Cytol.* **65**, 145-157.

Susin, S. A., Zamzami, N., Castedo, M., Daugas, E., Wang, H. G., Geley, S., Fassy, F., Reed, J. C., & Kroemer, G. (1997) The central executioner of apoptosis: multiple connections between protease activation and mitochondria in Fas/APO-1/. *J.Exp.Med.* **186**, 25-37.

Susin, S. A., Zamzami, N., Castedo, M., Hirsch, T., Marchetti, P., Macho, A., Daugas, E., Geuskens, M., & Kroemer, G. (1996) Bcl-2 inhibits the mitochondrial release of an apoptogenic protease. *J.Exp.Med.* **184**, 1331-1341.

Tabin, C.J. & McMahon, A.P. (1997) Recent advances in Hedgehog signalling. *Trends in Cell Biol.* **7**, 442-446

Temelcos, C. & Hutson, J. M. (2004b) Ontogeny of the VATER kidney in a rat model. *Anat.Rec.A Discov.Mol.Cell Evol.Biol.* **278**, 520-527.

Temelcos, C. & Hutson, J. M. (2004a) Renal abnormalities in rat fetuses exposed to doxorubicin. *J.Urol.* **171**, 877-881.

Thiery, J. P., Delouvee, A., Gallin, W. J., Cunningham, B. A., & Edelman, G. M. (1984) Ontogenetic expression of cell adhesion molecules: L-CAM is found in epithelia derived from the three primary germ layers. *Dev.Biol.* **102**, 61-78.

Thomas, P. & Beddington, R. (1996) Anterior primitive endoderm may be responsible for patterning the anterior neural plate in the mouse embryo. *Curr.Biol.* **6**, 1487-1496.

Thomas, P. Q., Brown, A., & Beddington, R. S. (1998) Hex: a homeobox gene revealing peri-implantation asymmetry in the mouse embryo and an early transient marker of endothelial cell precursors. *Development* **125**, 85-94.

Thompson, D. J., Molello, J. A., Strebing, R. J., & Dyke, I. L. (1978) Teratogenicity of adriamycin and daunomycin in the rat and rabbit. *Teratology* **17**, 151-157.

Trahair, J. F., Wing, S. J., & Horn, J. L. (1995) Failure of short-term luminal IGF-I to protect against atrophy in a model of fetal esophageal atresia. *J.Pediatr.Surg.* **30**, 1564-1570.

Van Staey, M., De Bie, S., Matton, M. T., & De Roose, J. (1984) Familial congenital esophageal atresia. Personal case report and review of the literature. *Hum.Genet.* **66**, 260-266.

Vleesch, D., V, Quan, Q. B., Beasley, S. W., & Williams, A. (2002) Abnormal branching and regression of the notochord and its relationship to foregut abnormalities. *Eur.J.Pediatr.Surg.* **12**, 83-89.

Warburton, D., Schwarz, M., Tefft, D., Flores-Delgado, G., Anderson, K. D., & Cardoso, W. V. (2000) The molecular basis of lung morphogenesis. *Mech.Dev.* **92**, 55-81.

Warga, R. M. & Nusslein-Volhard, C. (1999) Origin and development of the zebrafish endoderm. *Development* **126**, 827-838.

Weil, M., Jacobson, M. D., & Raff, M. C. (1997) Is programmed cell death required for neural tube closure? *Curr.Biol.* **7**, 281-284.

Weinstein, M., Xu, X., Ohyama, K., & Deng, C. X. (1998) FGFR-3 and FGFR-4 function cooperatively to direct alveogenesis in the murine lung. *Development* **125**, 3615-3623.

Wells, J. M. & Melton, D. A. (1999) Vertebrate endoderm development. *Annu.Rev.Cell Dev.Biol.* **15**, 393-410.

Wesson, D. E., Muraji, T., Kent, G., Filler, R. M., & Almalchi, T. (1984) The effect of intrauterine esophageal ligation on growth of fetal rabbits. *J.Pediatr.Surg.* **19**, 398-399.

Wilding, L. & Gannon, M. (2004) The role of pdx1 and HNF6 in proliferation and differentiation of endocrine precursors. *Diabetes Metab Res.Rev.* **20**, 114-123.

Williams, A. K., Qi, B. Q., & Beasley, S. W. (2000) Temporospatial aberrations of apoptosis in the rat embryo developing esophageal atresia. *J.Pediatr.Surg.* **35**, 1617-1620.

Williams, A. K., Qi, B. Q., & Beasley, S. W. (2001) Demonstration of abnormal notochord development by three-dimensional reconstructive imaging in the rat model of esophageal atresia. *Pediatr.Surg.Int.* **17**, 21-24.

Williams, A. K., Quan, Q. B., & Beasley, S. W. (2003) Three-dimensional imaging clarifies the process of tracheoesophageal separation in the rat. *J.Pediatr.Surg.* **38**, 173-177.

WILSON, J. G., ROTH, C. B., & WARKANY, J. (1953) An analysis of the syndrome of malformations induced by maternal vitamin A deficiency. Effects of restoration of vitamin A at various times during gestation. *Am.J.Anat.* **92**, 189-217.

Wolfson, P. J., Schloss, M. D., Guttman, F. M., & Nguyen, L. (1984) Laryngotracheoesophageal cleft. An easily missed malformation. *Arch.Surg.* **119**, 228-230.

Xia, H., Migliazza, L., Montedonico, S., Rodriguez, J. I., Diez-Pardo, J. A., & Tovar, J. A. (1999a) Skeletal malformations associated with esophageal atresia: clinical and experimental studies. *J.Pediatr.Surg.* **34**, 1385-1392.

Xia, H., Otten, C., Migliazza, L., Diez-Pardo, J. A., & Tovar, J. A. (1999b) Tracheobronchial malformations in experimental esophageal atresia. *J.Pediatr.Surg.* **34**, 536-539.

Yamamoto, Y., Stock, D. W., & Jeffery, W. R. (2004) Hedgehog signalling controls eye degeneration in blind cavefish. *Nature* **431**, 844-847.

Yeung, C. K., Spitz, L., Brereton, R. J., Kiely, E. M., & Leake, J. (1992) Congenital esophageal stenosis due to tracheobronchial remnants: a rare but important association with esophageal atresia. *J.Pediatr.Surg.* **27**, 852-855.

Yuan, B., Li, C., Kimura, S., Engelhardt, R. T., Smith, B. R., & Minoo, P. (2000) Inhibition of distal lung morphogenesis in Nkx2.1(-/-) embryos. *Dev.Dyn.* **217**, 180-190.

Zaret, K. (1998) Early liver differentiation: genetic potentiation and multilevel growth control. *Curr.Opin.Genet.Dev.* **8**, 526-531.

Zaw-Tun, H. A. (1982) The tracheo-esophageal septum--fact or fantasy? Origin and development of the respiratory primordium and esophagus. *Acta Anat.(Basel)* **114**, 1-21.

Zhou, B., Hutson, J. M., Farmer, P. J., Hasthorpe, S., Myers, N. A., & Liu, M. (1999) Apoptosis in tracheoesophageal embryogenesis in rat embryos with or without adriamycin treatment. *J.Pediatr.Surg.* **34**, 872-875.